A Transcriptomic Approach to Pigs at Weaning: A role for *Saccharomyces cerevisiae boulardii*?

By

Oliver Watts

BSc (Hons)

Thesis Submitted to the University of Nottingham for the Degree of Doctor of Philosophy

April 2018

Supervisors: Prof. David Haig, Dr. Kenneth Mellits, Dr. Sabine Tötemeyer

Dedicated to:



Brian Charles Watts

21st February 1950- 4th April 2016

Table of Contents

Table of Contents i
List of Figures viii
List of Tables xi
Additional Files xii
Abstract xv
Acknowledgements xvii
Abbreviations xx
1 **CHAPTER 1: INTRODUCTION** 24
1.1 **Gut Structure & Function** 25
1.1.1 Intestinal Tissues 30
1.1.2 Tight Junctions 35
1.2 **Intestinal Immunity** 37
1.2.1 Innate Immunity 40
1.2.2 Cells of the Innate Immune System 40
1.2.3 Cytokines and Chemokines 45
1.2.4 Pattern Recognition in the Innate Immune System 52
1.2.5 Immunoglobulins 57
1.2.6 Colostrum and Milk Intake by Piglets 61
1.3 **Pigs at Weaning** 63
1.4 **Stress and the Hypothalamic-Pituitary-Adrenal (HPA) Axis** 74
1.4.1 Cortisol and Immunity 77
1.4.2 Cortisol and Circadian Rhythm 77
1.4.3 CRF as an Effector of Stress 78
1.4.4 The Role of Mast Cell Granules 86

1.4.5 Mast Cells in Tissue Remodelling, Repair and Fibrosis 88
1.5 **Stress & the Enteric Nervous System** 90
1.6 **Probiotics Overview** 93
1.7 **Probiotics in Health** 95
1.8 **Probiotics and Infectious Disease** 102
1.9 ***Saccharomyces cerevisiae boulardii*** 106
1.10 **Next Generation Sequencing** 112
1.10.1 Transcriptome Profiling 115
1.11 **General Hypothesis and Aims** 121
2 **CHAPTER 2: MATERIALS AND METHODS** 122
2.1 **Sample Set** 122
2.2 **Colon Sample Collection and RNA Extraction** 130
2.2.1 RNA Extraction 131
2.2.2 RNA Quality Control 133
2.3 **Transcriptomics** 135
2.3.1 Library Preparation for Next Generation Sequencing Technology 135
2.3.2 Sample Purification and mRNA Selection 136
2.3.3 First-Strand Synthesis 139
2.3.4 Second Strand Synthesis 140
2.3.5 End Repair 142
2.3.6 Adenylate 3’ Ends 144
2.3.7 Adapter Ligation 145
2.3.8 DNA Fragment Enrichment 148
2.3.9 Library Validation 150
2.3.10 Normalization and Library Pooling 150
2.3.11 Cluster Generation 152
2.3.12 Sequencing 152

2.3.13 Preparation of Sequencing Data for Bioinformatic Analysis 152

2.3.14 Quality Filtering and Adaptor Removal 153

2.3.15 Quality Metrics 153

2.3.16 Mapping of Illumina Sequence Data 154

2.3.17 Differential Gene Expression..... 155

2.3.18 Gene Ontology and Gene Pathway Enrichment 156

2.4 **Graphics and Statistical Analysis**..... 157

3 **CHAPTER 3: THE TRANSCRIPTIONAL EFFECT OF WEANING ON THE PORCINE COLON OBSERVED AFTER HISAT2 MAPPING**..... 159

3.1 **Introduction** 159

3.2 **Results**..... 162

3.2.1 Raw Transcriptomic Reads 162

3.2.2 Overview of Read Usage 162

3.2.3 Principal Component Analysis of FPKM Profiles 165

3.2.4 Overview of Weaning Related Differential Gene Expression 170

3.2.5 Comparison of Differential Gene Expression between One, Four and 14 days Post-Weaning 172

3.2.6 Differentially Expressed Transcripts 175

3.3 **Discussion**..... 178

3.4 **Conclusion**..... 186

4 **CHAPTER 4: THE TRANSCRIPTIONAL EFFECT OF WEANING ON THE PORCINE COLON OBSERVED BY A PSEUDOALIGNMENT TECHNIQUE** 187

4.1 **Introduction** 187

4.2 **Results**..... 190

4.2.1 Overview of RNA-seq Mapping using Kallisto..... 190

4.2.2 Comparison of Global Expression between Weaned and Suckling Pigs at 22, 25 and 35 Days of Age (Weaning at 21 days of age) 192

4.2.3 Overview of Differential Gene Expression in the Porcine Colon at Weaning Observed using a Pseudo-alignment Method 195

4.2.4 Comparison between Differential Expression Observed Using Conventional and Pseudo-alignment Methods 199

4.2.5 Inter-Sample Expression Variation in Differentially Expressed Transcripts 202

4.2.6 Gene Ontology Analysis of Differentially Expressed Genes to Characterise the Transcriptomic Differences between Colon Samples Obtained from Weaned and Suckling Pigs 207

4.3 **Discussion** 228

4.3.1 The Transcriptomic Effect of Weaning in the Porcine Colon 231

4.3.2 The Transcriptional Effect of Weaning in the Colon of 22 Day Old Pigs (One Day Post-Weaning) 236

4.3.3 The Transcriptional Effect of Weaning in 25 Day Old Pigs (4 Days Post-Weaning) 240

4.4 **Conclusion** 245

5 **CHAPTER 5: THE TRANSCRIPTIONAL EFFECT OF DIETARY INTAKE OF SACCHAROMYCES CEREVISIAE BOULARDII IN THE COLON OF WEANING PIGS** 247

5.1 **Introduction** 247

5.2 **Results** 249

5.2.1 The Effect of Oral *Saccharomyces cerevisiae boulardii* Supplementation on the Colon of Suckling Pigs 249

5.2.2 The Effect of Oral *Saccharomyces cerevisiae boulardii* Supplementation in the Colon of Weaned Pigs 268

5.3 **Discussion** 287

5.3.1 The Effect of *Saccharomyces cerevisiae boulardii* in Suckling Pigs 287

5.3.2 The Effect of *Saccharomyces cerevisiae boulardii* in Weaned Pigs 291

5.4 **Conclusion** 294

6 **CHAPTER 7: THE EFFECT OF DIETARY SACCHAROMYCES CEREVISIAE BOULARDII ON WEANING INDUCED TRANSCRIPTION IN THE PORCINE COLON** 296

6.1 **Introduction** 296

6.2 **Results** 297

6.2.1 Comparison of Global Gene Expression in Suckling Control and SCB Supplemented Weaned Colon Samples 297

6.2.2 Overview of Differential Transcript Expression Between Colon Tissue Extracted from Suckling Control and SCB Supplemented Weaned Pigs. 299

6.2.3 Comparison of the Transcriptional Effect of Weaning (Suckling Control vs Weaned Control) and Weaning with SCB Supplemented Weaned Animals (Suckling Control vs Weaned SCB). 303

6.2.4 Gene Ontology Analysis of Genes Exclusive to the Suckling Control vs SCB Supplemented Weaned Comparison 305

6.2.5 Comparison of Differentially Expressed Gene Sets to Identify a Common Effect of *Saccharomyces cerevisiae boulardii* 311

6.2.6 Comparison of Expression Values for Differentially Expressed Transcripts Across all Samples 316

6.3 **Discussion** 327

6.4 **Conclusion** 333

7 **GENERAL DISCUSSION** 334

7.1 **Results Summary** 334

7.2 **Limitations of the Current Study** 340

7.3 **Future Perspectives** 345

7.4 **Conclusion** 348

References 349

Appendix 1: Creep Feed Composition 404

Appendix 2: Sample Concentration and Sequencing Information 405

Appendix 3: Benchmarking of 50 and 100bp Reads 406

Appendix 4: Sample Treatment Information 417

Appendix 5: Read Usage Numbers and Percentages 418

Appendix 6: Hierarchical clustering of FPKM Profiles Without FPKM Cutoff 420

Appendix 7: PCA Plots Comparing Transcript Expression Profiles Between Treatments when Applying HiSat2 and Kallisto Mapping Methodologies. 421

Appendix 8: Biological Process Gene Ontology Terms Enriched in Genes Up and Downregulated by Weaning at One Day Post-Weaning 423

Appendix 9: Cellular Component Gene Ontology Terms Enriched in Genes Up and Downregulated by Weaning at One Day Post-Weaning 426

Appendix 10: Molecular Function Gene Ontology Terms Enriched in Genes Up and Downregulated by Weaning at One Day Post-Weaning 429

Appendix 11: Biological Process Gene Ontology Terms Enriched in Genes Up and Downregulated by Weaning at Four Days Post-Weaning 431

Appendix 12: Cellular Component Gene Ontology Terms Enriched in Genes Up and Downregulated by Weaning at Four Days Post-Weaning 432

Appendix 13: Molecular Function Gene Ontology Terms Enriched in Genes Up and Downregulated by Weaning at Four Days Post-Weaning 433

Appendix 14: Biological Process Gene Ontology Terms Enriched in Genes Differentially Expressed in Suckling Pigs by SCB Supplementation at 22 Days of Age 434

Appendix 15: Cellular Component Gene Ontology Terms Enriched in Genes Differentially Expressed in Suckling Pigs by SCB Supplementation at 22 Days of Age 437

Appendix 16: Molecular Function Gene Ontology Terms Enriched in Genes Differentially Expressed in Suckling Pigs by SCB Supplementation at 22 Days of Age..... 441

Appendix 17: Biological Process Gene Ontology Terms Enriched in Genes Differentially Expressed in Weaned Pigs by SCB Supplementation at 25 Days of Age..... 443

Appendix 18: Cellular Component Gene Ontology Terms Enriched in Genes Differentially Expressed in Weaned Pigs by SCB Supplementation at 25 Days of Age..... 447

Appendix 19: Molecular Function Gene Ontology Terms Enriched in Genes Differentially Expressed in Weaned Pigs by SCB Supplementation at 25 Days of Age..... 449

Appendix 20: Biological Process Gene Ontology Enrichment of Genes Exclusive to Suckling Control vs Weaned SCB Comparison when Compared to Suckling Control vs Weaned Control (1-day post weaning) 451

Appendix 21: Biological Process Gene Ontology Enrichment of Genes Exclusive to Suckling Control vs Weaned SCB Comparison when Compared to Suckling Control vs Weaned Control (4 days post weaning) 454

List of Figures

Figure 1-1: Comparison of sections of human and porcine large intestines.. 29
Figure 1-2: Schematic of intestinal structure and epithelial cells. 34
Figure 1-3: Cross-sectional view of a mouse Peyer's patch showing the main anatomical compartments.. 35
Figure 1-4: Tight junction structure. 37
Figure 1-5: Delivery of luminal antigens to dendritic cells by M cells.. 42
Figure 1-6: Distribution and function of DC subsets within Peyer's Patches. 44
Figure 1-7: IL-1 signal transduction of NF-kB activation.. 47
Figure 1-8: Schematic of signalling induced by TLR molecules. 56
Figure 1-9: Two-dimensional schematic of immunoglobulins.. 58
Figure 1-10: Impact of early weaning on the development of the GI Barrier. 67
Figure 1-11: The CRF-mast cell axis. Stressors such as weaning, social stress and infectious disease trigger activation of intestinal CRF and its receptors.. 72
Figure 1-12: The hypothalamic-pituitary-adrenal axis.. 76
Figure 1-13: CRF receptor sensitivity.. 81
Figure 1-14: Central and peripheral actions of CRF. 86
Figure 1-15: Enteric nervous system and gut breakdown 91
Figure 1-16: Interaction between mast cells and enteric nerve endings 93
Figure 1-17: Illumina sequencing: A diagram to show the process of sequencing DNA fragments using Illumina sequencing. 115
Figure 2-1: Trial timeline. 125
Figure 2-2: Random allocation of experimental and control sows to pens in wean trial. 125
Figure 2-3: The weaning process. 126
Figure 2-4: The one day post weaning slaughter point.. 127
Figure 2-5: The four days post weaning slaughter point. 128
Figure 2-6: The 14 days post weaning slaughter point. 129
Figure 2-7: Tissue collection at slaughter 131
Figure 2-8: Example of Agilent 2100 Bioanalyzer output at RNA integrity number (RIN) of 6. 135
Figure 3-1: Percentages of RNAseq datasets mapped uniquely, unmapped and removed by quality filtering. 164
Figure 3-2: Box plots to show the number of raw RNAseq reads, reads removed by trimming, reads which were unmapped and reads which mapped successfully.. 165
***Fi*gure 3-3: PCA of FPKM profiles coloured by slaughter point. 167**
Figure 3-4: PCA of FPKM profiles coloured by weaning status. 168
Figure 3-5: PCA of FPKM profiles coloured by probiotic status. 169
Figure 3-6: Volcano Plots to show differential gene expression when comparing weaned and suckling control pigs at one, four and 14 days post-weaning. 171
Figure 3-7: Venn diagrams to show differentially expressed transcripts shared between timepoints.. 174
Figure 4-1: Percentages of RNA-seq datasets pseudo-aligned, unmapped and quality filtered when using the Kallisto methodology.. 191
Figure 4-2: PCA plots to show similarity in global expression pattern between weaned and suckling control colon samples at 22, 25 and 35 days of age. 194

Figure 4-3: Volcano plots to show differential expression of transcripts in the porcine colon at one, four and 14 days post-weaning.. 197
Figure 4-4: Venn diagram to display differentially expressed transcripts observed at one, four and 14 days post-weaning.. 198
Figure 4-5: Venn diagrams to show significantly differentially expressed transcripts shared between the HiSat2/Ballgown and Kallisto/Sleuth methodologies.. 201
Figure 4-6: Heatmap to show variation in sample TPM values for transcripts identified as differentially expressed at one-day post-weaning.. 204
Figure 4-7: Heatmap to show variation in sample TPM values for transcripts identified as differentially expressed at four days post-weaning.. 205
Figure 4-8: Heatmap to show variation in Sample TPM values for transcripts identified as differentially expressed at 14 days post-weaning.. 206
Figure 4-9: Enrichment of biological process terms in genes identified as up and downregulated in colon tissue at one-day post-weaning 212
Figure 4-10: Enrichment of cellular compartment terms in genes identified as up and downregulated in colon tissue at one-day post-weaning..... 215
Figure 4-11: Enrichment of molecular function terms in genes identified as up and downregulated in colon tissue at one-day post weaning. 219
Figure 4-12: Enrichment of biological process terms in genes identified as up and downregulated in colon tissue at four days post-weaning.. 222
Figure 4-13: Enrichment of cellular compartment terms in genes identified as up and downregulated in colon tissue at four days post-weaning..... 224
Figure 4-14: Enrichment of molecular function terms in genes identified as up and downregulated in colon tissue at four days post-weaning..... 226
Figure 5-1: Principal component analysis to compare the global expression pattern of suckling pig colon samples with and without SCB supplementation at 22, 25 and 35 days of age. 251
Figure 5-2: Volcano plots to show differential expression of transcripts in the colon of suckling pigs in response to SCB supplementation.. 253
Figure 5-3: Venn diagram to demonstrate differential expression observed between suckling pigs with and without SCB supplementation at 22, 25 and 35 days of age. 254
Figure 5-4: Heatmap to show TPM expression values for transcripts identified as differentially expressed in pigs of 22 days of age. 256
Figure 5-5: Enrichment of biological process terms in genes identified as up and downregulated by SCB in the colon tissue of suckling pigs at 22 days of age..... 260
Figure 5-6: Enrichment of cellular component terms in genes identified as up and downregulated by SCB in the colon tissue of suckling pigs at 22 days of age. 263
Figure 5-7: Enrichment of molecular function terms in genes identified as up and downregulated by SCB in the colon tissue of suckling pigs at 22 days of age.. 266
Figure 5-8: PCA to compare the global expression pattern of weaned pig colon samples with and without SCB supplementation at 22, 25 and 35 days of age. 270
Figure 5-9: Volcano plots to show differential expression of transcripts in the colon of weaned pigs in response to SCB supplementation.. 272
Figure 5-10:Venn diagram to demonstrate differential expression observed between suckling pigs with and without SCB supplementation at 22, 25 and 35 days of age. 273
Figure 5-11: Heatmap to show TPM expression values for transcripts identified as differentially expressed in weaned pigs of 25 days of age.. 275
Figure 5-12: Enrichment of biological process terms in genes identified as up and downregulated by SCB in the colon tissue of weaned pigs at 25 days of age.. 279
Figure 5-13: Enrichment of cellular component terms in genes identified as up and downregulated by SCB in the colon tissue of weaned pigs at 25 days of age 282

Figure 5-14: Enrichment of molecular function terms in genes identified as up and downregulated by SCB in the colon tissue of weaned pigs at 25 days of age.. 285
Figure 6-1: PCA to compare the global expression pattern of suckling pig colon samples with and without SCB supplementation at 22, 25 and 35 days of age..... 298
Figure 6-2: Volcano plots to show differential expression of transcripts in the colon of suckling pigs in response to SCB supplementation.. 301
Figure 6-3: Venn diagram to demonstrate differential expression observed between suckling control pigs with and SCB supplemented weaned pigs at 22, 25 and 35 days of age. 302
Figure 6-4: Venn Diagrams to show differentially expressed transcripts shared between (suckling control vs weaned control) and (suckling control vs weaned SCB).. 304
Figure 6-5: Enrichment of biological process terms in up and downregulated genes exclusive to the suckling control vs SCB supplemented weaned comparison when compared to differential gene expression observed between suckling control and weaned control samples at one day post-weaning..... 308
Figure 6-6: Enrichment of biological process terms in up and downregulated genes exclusive to the suckling control vs SCB supplemented weaned comparison when compared to differential gene expression observed between suckling control and weaned control samples at four days post-weaning..... 310
Figure 6-7: Comparison of differentially expressed transcripts to identify a common effect of oral SCB supplementation in the colon of 22 day old pigs.. 313
Figure 6-8: Comparison of differentially expressed transcripts to identify a common effect of oral SCB supplementation in the colon of 25 day old pigs.. 314
Figure 6-9: Comparison of differentially expressed transcripts to identify a common effect of oral SCB supplementation in the colon of 25 day old pigs. 315
Figure 6-10: PCA to explain the relationship of sample expression patterns across all differentially expressed transcripts identified between 22 day old pig colon samples.. 319
Figure 6-11: Heatmap to explain the relationship of sample expression patterns across all differentially expressed transcripts identified between 22 day old pig colon samples..... 320
Figure 6-12: PCA to explain the relationship of sample expression patterns across all differentially expressed transcripts identified between 25 day old pig colon samples. 322
Figure 6-13: Heatmap to explain the relationship of sample expression patterns across all differentially expressed transcripts identified between 25 day old pig colon samples..... 323
Figure 6-14: PCA to explain the relationship of sample expression patterns across all differentially expressed transcripts identified between 35-day old pig colon samples.. 325
Figure 6-15: Heatmap to explain the relationship of sample expression patterns across all differentially expressed transcripts identified between 35-day old pig colon samples.. 326

List of Tables

Table 1-1: Cells of the innate immune system 41
Table 4-1: Differentially expressed transcripts (q <0.1) identified using Ballgown 177

Additional Files

Additional File 1	Suckling Control vs Weaned Control D1 Differential Expression (q < 0.1, FC >2)
Additional File 2	Suckling Control vs Weaned Control D4 Differential Expression (q < 0.1, FC >2)
Additional File 3	Suckling Control vs Weaned Control D14 Differential Expression (q < 0.1, FC >2)
Additional File 4	Suckling Control vs Suckling Probiotic D1 Differential Expression (q < 0.1, FC >2)
Additional File 5	Suckling Control vs Suckling Probiotic D4 Differential Expression (q < 0.1, FC >2)
Additional File 6	Suckling Control vs Suckling Probiotic D14 Differential Expression (q < 0.1, FC >2)
Additional File 7	Weaned Control vs Weaned Probiotic D1 Differential Expression (q < 0.1, FC >2)
Additional File 8	Weaned Control vs Weaned Probiotic D4 Differential Expression (q < 0.1, FC >2)
Additional File 9	Weaned Control vs Weaned Probiotic D14 Differential Expression (q < 0.1, FC >2))
Additional File 10	Suckling Control vs Weaned Probiotic D1 Differential Expression (q < 0.1, FC >2)
Additional File 11	Suckling Control vs Weaned Probiotic D4 Differential Expression (q < 0.1, FC >2)
Additional File 12	Suckling Control vs Weaned Probiotic D14 Differential Expression (q < 0.1, FC >2)

Additional File 13	Comparison of Differential Expression between Suckling Control vs Weaned Probiotic and Suckling Control vs Weaned Control
Additional File 14	Comparison of Differential Expression between (SCB Associated Suckling Control vs Weaned Probiotic), (Suckling Control vs Suckling Probiotic) and (Weaned Control vs Weaned Probiotic) D1
Additional File 15	Comparison of Differential Expression between (SCB Associated Suckling Control vs Weaned Probiotic), (Suckling Control vs Suckling Probiotic) and (Weaned Control vs Weaned Probiotic) D4
Additional File 16	Comparison of Differential Expression between (SCB Associated Suckling Control vs Weaned Probiotic), (Suckling Control vs Suckling Probiotic) and (Weaned Control vs Weaned Probiotic) D14
Additional File 17	Suckling Probiotic vs Weaned Probiotic D1 Differential Expression ($q < 0.1$, FC >2)
Additional File 18	Suckling Probiotic vs Weaned Probiotic D4 Differential Expression ($q < 0.1$, FC >2)
Additional File 19	Suckling Probiotic vs Weaned Probiotic D14 Differential Expression ($q < 0.1$, FC >2)
Additional File 20	TPM Values for Transcripts Differentially Expressed in Comparisons at D1
Additional File 21	TPM Values for Transcripts Differentially Expressed in Comparisons at D4

Additional File 22	TPM Values for Transcripts Differentially Expressed in Comparisons at D14

Abstract

Weaning is a stressful period in the early life of a pig. This stress manifests as immediate weight loss coinciding with increases in intestinal transepithelial resistance. This study aims to identify the transcriptional differences in the colon between suckling and weaned animals over this period using RNA-seq. This approach identified the maximal transcriptional differences at one-day post-weaning with 353 transcripts differentially expressed compared to 78 and three transcripts at four and fourteen days post weaning respectively (q<0.1, FC>2). This work identified increased transcription of pro-inflammatory cytokine genes including *IL1A* (FC=2.63) and *IL1B2* (FC = 2.98) in the colon of weaned animals at one-day post weaning, suggesting activation of the immune system. The same time points at one, four and 14 days post weaning was used to assess the transcriptional effect of supplementation with probiotic *Saccharomyces cerevisiae boulardii* (4.43 Log_{10} CFU per day from seven days of age) on the colon. A distinct effect of probiotic yeast supplementation on transcription in the colon was identified in both weaned and suckling pigs. One, 77 and one transcripts were affected by the probiotic in weaned animals at the

three time points respectively compared to 197, six and two in suckling animals. However, evidence of an anti-inflammatory effect (including increased expression of *IL10*, FC = 2.88) was identified in weaned animals at four days post-weaning. The clear distinction between differential expression in weaned and suckling animals suggests that the transcriptional effect of *Saccharomyces cerevisiae boulardii* supplementation may depend on the physiological state of the host. These differences may be due to the interaction of the probiotic with the host immune system as a result of weaning related bowel disruption.

Acknowledgements

I would firstly like to acknowledge the work and academic support of my supervisory team (Prof. David Haig, Dr Kenneth Mellits and Dr Sabine Tötemeyer) during this project. I am also extremely grateful for the advice of Prof. Richard Emes for his extreme patience with me concerning bioinformatics matters.

I would also like to thank Lallemand, the industrial sponsor for this work for the funding and opportunity to pursue this interesting field of study.

I would particularly like to thank Dr Melanie Le Bon who provided the basis for this work and provided RNA and paraffin-embedded tissue samples for this study from trials she conducted before my arrival. What is presented here is very much a continuation of her efforts. Also, Siyu Wu for her unlimited patience and expertise in the extraction of RNA from tissue samples which were subsequently used for RNA-sequencing.

I am very grateful to the technical teams in both the school of biosciences (David Fowler, Wendy Fielder, and Lorraine Gillet) and the

school of veterinary science and medicine (Scott Hulmes and Ceri Allen) for their expertise and assistance.

I am deeply thankful to thank the staff at the bio-research unit (Dave Edwards, Mick Baker, Deborah Surgay) for their endless help and knowledge during the Wean trials. Also, to Mick Watson at Ark Genomics, Edinburgh for his advice and assistance in the analysis of large datasets.

My thanks also go to fellow PhD students, all of whom have since graduated including Dr Melanie Le Bon, Dr Laura Hancox, Dr Rebecca Chandler-Bostock, Dr Helen Davies, Elizabeth King and Dr Nathan Meade for providing moral support, a sense of humour and a pleasant working environment during these years. A mention to Dr Andy Timms, Dr Steven Hooton and Phil Richards for your support when times were at their darkest, and Dr Julia Kydd for the pastoral support you provided over this period.

On a more personal note, I would like to thank my father Alan, my grandfather John Bennett, his partner Margaret Webb and my grandmother Maureen Bennett for their support (both financial and moral) during these years. My thoughts are particularly drawn to my uncle, Brian, who sadly passed during my period of study and to whom

this thesis is dedicated and without the huge financial and moral support of whom, none of this would have been possible.

Finally, I would like to thank my partner Jennifer Dean who has been there for me through thick and thin and for which I am eternally grateful.

Abbreviations

18S rRNA	18S ribosomal RNA subunit
28s rRNA	28s Ribosomal RNA subunit
5s rRNA	5s Ribosomal RNA subunit
ALR	AIM2-like receptor
APC	Antigen-presenting cell
ATCH	Adrenocorticotropic hormone
AVP	Arginine vasopressin
BAM	Binary alignment map
bp	Base pair
BP	Biological process
CC	Cellular component
CD	Cluster of differentiation
cDNA	Copy DNA
CDR	Complementarity determining region
CFU	Colony forming unit
CLR	C-type lectin receptor
CNS	Central nervous system
CRF	Corticotropin-releasing factor
CRFR	Corticotropin-releasing factor receptor
Ct	Crossing threshold
CTL	Control
DC	Dendritic cell
DEG	Differentially expressed genes
DNA	Deoxyribonucleic acid
DNase	Deoxyribonuclease
dNTP	Deoxyribonucleotide
DPW	Days post weaning
ECM	Extracellular matrix
EDTA	Ethylenediaminetetraacetic acid
EHEC	Enterohemorrhagic *E.coli*
ELISA	Enzyme-linked immunosorbent assay
ENS	Enteric nervous system
EST	Expressed sequence tag

ETEC	Enterotoxigenic *Escherichia coli*
FAE	Follicle associated epithelium
FC	Fold change
FDR	False detection rate
FMT	Faecal microbiota transplantation
FPKM	Fragments per kilobase of exon model per million reads
FR	Framework region
GALT	Gut-associated lymphoid tissue
GI	Gastrointestinal
GO	Gene ontology
HEV	High endothelial venule
HPA	Hypothalamic-pituitary-adrenal
HVAC	Heating, ventilation and air conditioning
IEC	Intestinal epithelial cell
IFN	Interferon
IFR	Inter-follicular region
Ig	Immunoglobulin
IKK	IκB kinase
IL	Interleukin
IM	Intramuscular
IMS	Industrial methylated spirit
IP	Intra-peritoneal
IRAK	IL-1 receptor-associated kinase
KEGG	Kyoto encyclopaedia of genes and genomes
LPS	Lipopolysaccharide
MALT	Mucosal-associated lymphoid tissue
MAMP	Microbe associated molecular pattern
MAPK	Mitogen-activated protein kinase
MC	Mast cell
MF	Molecular function
M-MLV	Moloney murine leukaemia virus
MP	Myenteric plexus
mRNA	Messenger RNA
NCBI	National centre for biotechnology information
NF-κB	Nuclear factor kappa B
NGS	Next-generation sequencing
NK	Natural killer

NLR	NOD like receptor
PCR	Polymerase chain reaction
PFTS	Peri-weaning failure to thrive syndrome
PLAU	Plasminogen activating factor
PLAUR	Plasminogen activating factor receptor
PM	Pathogenic microorganism
PP	Peyer's patch
PRR	Pattern recognition receptor
PVN	Paraventricular nucleus
q value	False detection rate corrected p value
qPCR	Quantitative polymerase chain reaction
RIN	RNA integrity number
RLR	RIG-I-like receptor
RNA	Ribonucleic acid
RNAi	Interference RNA
RNAse	Ribonuclease
RNA-seq	RNA sequencing
RPKM	Reads per kilobase of exon model per million reads
RT	Reverse transcription
SAGE	Serial analysis of gene expression
SAM	Sequence alignment map
SCB	*Saccharomyces cerevisiae boulardii* CNCM I-1079
SD	Standard deviation
SE	Standard error
SED	Sub-epithelial dome
SI	Small intestine
SMP	Sub mucosal plexus
SMRT	Single molecule real time
TACE	TNFα converting metalloprotease
TAMRA	Tetramethyl-6-Carboxyrhodamine
Taq	*Thermus aquaticus* heat stable DNA polymerase
TGF-β	Transforming growth factor β
Th	T helper
TIMP	Tissue inhibitor of metalloprotease
TIR	Toll/IL1 receptor domain
TJ	Tight junction
TLR	Toll-like receptor

TNFR	Tumour necrosis factor receptor
TNF-α	Tumour necrosis factor α
TPM	Transcripts per million
Treg	T regulatory
TRIF	TIR domain-containing adaptor-inducing Interferon-β
UV	Ultra-violet

1 Chapter 1: Introduction

The gut epithelium of any animal represents an essential element in the barrier between the animal, and pathogens which may contaminate dietary intake. As the gut is the point at which dietary nutrients are absorbed, careful and delicate regulation of passage across the intestinal barrier is essential. However, harmful bacteria and antigens are normally prevented from crossing the epithelial barrier where they could cause inflammation or disease. The maintenance of homeostasis in the gut will be reviewed in this section using knowledge of human, porcine and rodent gastrointestinal models.

During stress, such as the weaning stress experienced by pigs, the delicate balance of permeability in the gut can be disturbed via the action of both endocrine and nervous mechanisms (Kelly *et al.*, 2015; Mereu *et al.*, 2015; Moussaoui *et al.*, 2017). Activation of the hypothalamic-pituitary-adrenal (HPA) axis and activation of the enteric nervous system are both able to contribute to loss of barrier function. Both mechanisms will be discussed with a view to both function and dysregulation.

Probiotics will be introduced with a view to their function in both health and disease, detailing their activity in helping to maintain the gut epithelial barrier. A particular focus will be made on *Saccharomyces cerevisiae boulardii*, the probiotic used in the current study, and the potential health benefits which may result from administration of this probiotic to early weaning pigs.

1.1 Gut Structure & Function

The lower gastrointestinal tract is the segment of the intestinal tract from the pyloric sphincter of the stomach to the anus; this consists of two main parts, the small and large intestines. The small intestine of a fully grown adult pig is 16-21 meters in length (Lewis and Southern, 2000).This can be divided into three sections. The duodenum is a short section constituting 4-5% of the length of the small intestine (Lewis and Southern, 2000), and which functions to neutralise the acidity of stomach acid thereby protecting the rest of the lower GI tract from damage (Allen *et al.*, 1986). The jejunum, which composes 88-91% of the porcine small intestine (Lewis and Southern, 2000), has a large folded surface area formed of villi and microvilli (Herich *et al.*, 2004) which enable efficient uptake of sugars, amino acids and fatty acids

(Radloff *et al.*, 2017). The concluding section of the small intestine is the ileum which constitutes 4-5% of the length of the adult pig small intestine (Lewis and Southern, 2000), and has a similar structure to the jejunum in that it has villi to increase surface area. The main function of the ileum is to absorb vitamin B12 and bile acids, as well as any remaining nutrients (Aldini *et al.*, 1995). The most obvious difference between adult human and adult pig intestines is the length. The total small intestine length in pigs ranges from 16 to 22 meters (2110g). Whereas in humans this range is 4 to 6 meters (1040g) (Mosenthin 1998; Patterson *et al.*, 2008; Gonzalez *et al.*, 2015). When the higher body weight of adult pigs (200 to 300kg in pigs compared to 60-100kg in adult humans) is considered, both humans and pigs average around 0.1 meters of intestine per kilogram of body weight. Anatomically the gastrointestinal tract of pigs is similar to that of humans. However, the demarcation between the duodenum, jejunum and ileum is not as distinct in the porcine small intestine as they are in the human small intestine (Patterson *et al.*, 2008).

The large intestine consists of the cecum, colon, rectum and anal canal and is mainly responsible for water uptake (Stevens *et al.*, 1986). In adult pigs, the large intestine is between 4 and 6 meters in length

compared to 1.5 meters in humans (Patterson *et al.*, 2008). This disparity in length is reflected in the weight which is approximately 590g in human adults compared to 1970g in adult pigs (Gonzalez *et al.*, 2015). A distinct difference between the two gastrointestinal tracts is the spatial arrangement of the intestine in the abdominal cavity. In humans the large intestine is arranged in a square formation. Whereas in pigs the majority of the large intestine consisting of the cecum, proximal (ascending), mid (transverse) and most of the distal (descending) colon, forms a spiral conformation beginning in the mid abdomen and spiralling toward the left upper part of the abdomen in a series of clockwise and counterclockwise turns. The remainder of the distal colon passes along the left abdominal wall to the rectum (Figure 1-1) (Patterson *et al.*, 2008). A particular focus will be made on the ascending colon as it is the site of investigation in the present study. This location was selected to match existing research on the effects of weaning in the porcine colon (Moeser *et al.*, 2007a; Moeser *et al.*, 2007b; Moeser *et al.*, 2017).

As the large intestine in pigs forms a spiral, the sections are identified differently to those of humans, with the transverse section forming a short juncture between the ascending and descending sections.

Another notable difference is that the descending colon is of smaller diameter and is located within the spiral formed of the ascending colon. Additionally, the porcine cecum is larger and more clearly delineated compared to that of humans, and pigs lack an appendix (Figure 1-1) (Gonzalez *et al.*, 2015).

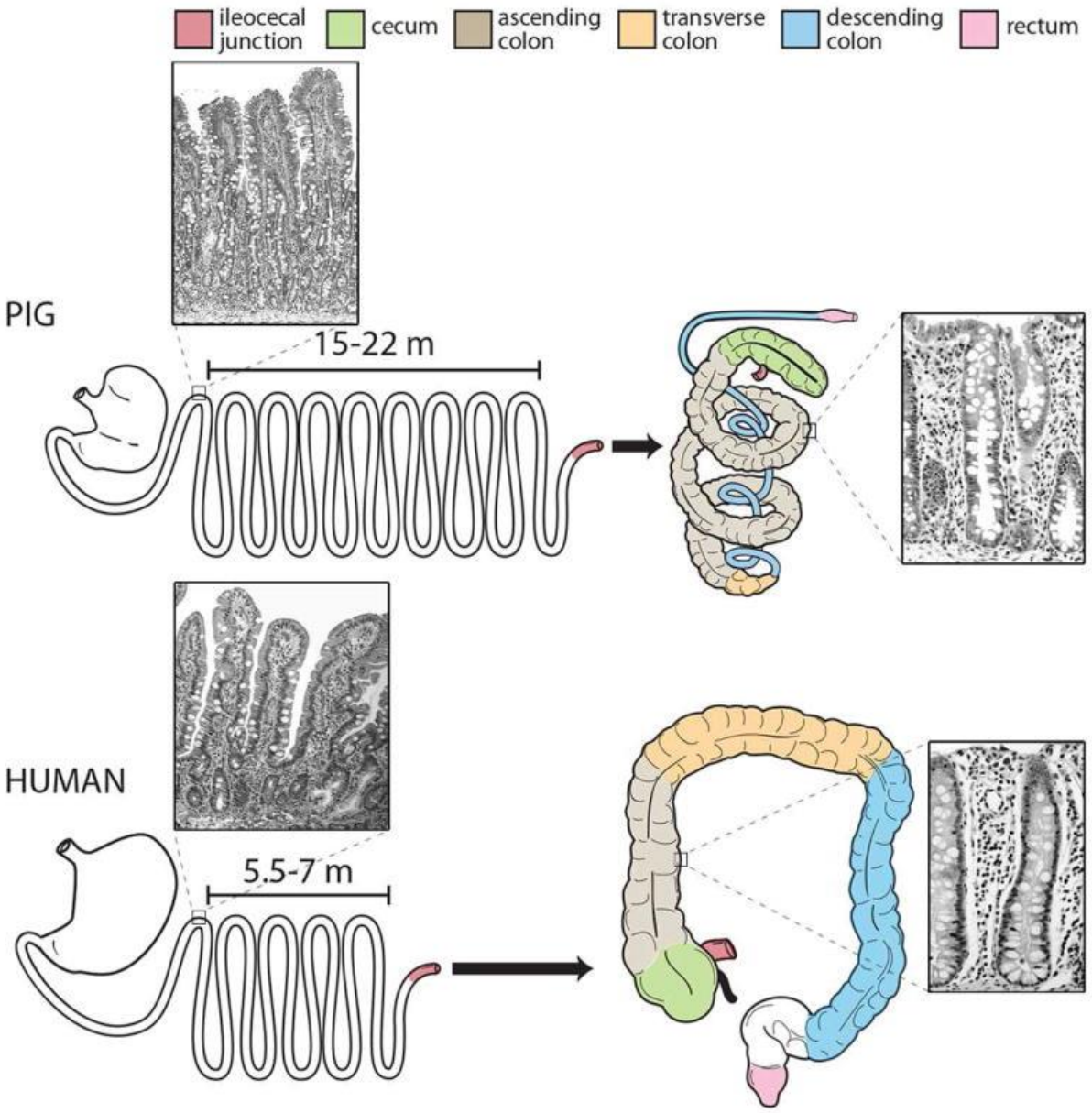


Figure 1-1: Comparison of sections of human and porcine large intestines. The porcine large intestine consists mainly of ascending colon with the concluding section constituting a transverse section and descending colon of smaller diameter than the other sections. This contrasts with the human large intestine which shows defined ascending, transverse and descending sections (Gonzalez *et al.*, 2015).

1.1.1 Intestinal Tissues

The organisation of intestinal tissues is complex and consists of multiple layers with distinct functions (Figure 1-2). These include longitudinal musculature and circular musculature which are responsible for peristalsis (Howell and Wells, 2011; Mittal, 2016) and the muscularis mucosa, the contractility of which is closely linked with mucosal secretory function (Uchida and Kamikawa, 2007). Other layers include; the serosa, which constitutes a continuous sheet of mesothelium and forms a natural barrier from the spread of inflammatory and malignant processes (Rao and Wang, 2010); The submucosa, a collagen-based extracellular matrix layer (Lin *et al.*, 2014) and finally the epithelial layer. Also present are neurons of the myenteric plexus and submucosal plexus (Brugmann and Wells, 2013) which will be described in more detail in later sections. A cross-section of the intestinal structure can be found in Figure 1-2a.

The Intestinal epithelial cells (IECs) of the epithelial layer form a single cell layer with each cell joined by a tight junction (Crawford and Dagnino, 2017). To this extent, the intestinal epithelium is a selectively permeable barrier which prevents pathogens crossing into the host. Specialised cells reside in the intestinal epithelial layer and include;

enterocytes, which are the most common and are mainly responsible for absorption of nutrients and water via active and passive transport (Howell and Wells, 2011). Goblet cells are responsible for mucin production (Birchenough *et al.*, 2015) and Paneth cells secrete lysozyme to prevent bacterial infection (Howell and Wells, 2011). Enteroendocrine cells comprise only 1% of the epithelium and include approximately ten subtypes which secrete a variety of hormones that participate in glucose homeostasis, satiety, pH balance, gallbladder contraction, gut motility and the regulation of pancreatic and pituitary hormone secretion. However, subtypes are often confined to specific gut compartments (Howell and Wells, 2011) (Figure 1-2b). Intestinal mesenchymal cells (IMCs) also exist within the gut; this term encompasses a spectrum of cell types which are similar in origin, function and molecular markers (Koliaraki *et al.*, 2017). In the bowel, the phenotype of mesenchymal cells overlaps with myofibroblasts, lining the bottom walls of the intestinal crypts or interspersed within intestinal submucosa (Messina *et al.*, 2017). Lamina propria mesenchymal cells are critical to the instruction of intestinal morphogenesis and regulation of epithelial proliferation and differentiation in the stem cell niche (Pinchuk *et al.*, 2010).

In the small intestine, villi and microvilli projections into the intestinal lumen increase the surface area available for nutrient absorption whereas these are absent in the colon (Moon, 1972; Lewis and Southern, 2000; Wiese *et al.*, 2003; Howell and Wells, 2011).

Gut-associated lymphoid tissue (GALT) consists of isolated or aggregated lymphoid follicles forming Peyer's patches (PPs). As PPs can transport luminal antigens and bacteria, they can be considered the immune sensors of the intestine (Jung *et al.*, 2010). Within a Peyer's patch, antigens are delivered by microfold epithelial cells (M cells) where they may be captured by resident dendritic cells (Reboldi and Cyster, 2016). PPs are organised into three main regions, a series of large B cell follicles; the overlying follicle-associated epithelium (FAE) and associated sub-epithelial dome (SED) which lie between the follicles and the FAE; and the small T cell zones which are situated adjacent to the B cell follicles (Figure 1-3) (Reboldi and Cyster, 2016).

PPs are not present in the colon. However, two distinct lymphoid tissues have been identified: colonic patches and colonic solitary intestinal lymphoid tissues (SILT), (Baptista *et al.*, 2013). Colonic patches are in the submucosa between the external longitudinal and circular muscular layers and the *muscularis mucosae.* At the sites of colonic

patches, the *muscularis mucosae* is disrupted allowing contact of the colonic patch with the colonic epithelia which allows sampling of antigen-presenting cells within the colonic patch to access the contents of the colonic lumen (Baptista *et al.*, 2013). This is compared to SILTs which are positioned in the lamina propria of the colon and so are in direct contact with the colonic epithelia (Baptista *et al.*, 2013). As colonic lymphoid tissues are not as well studied as PPs, PPs will be used as an example of an intestinal immune inducible site (Bloom and Boedeker, 1996).

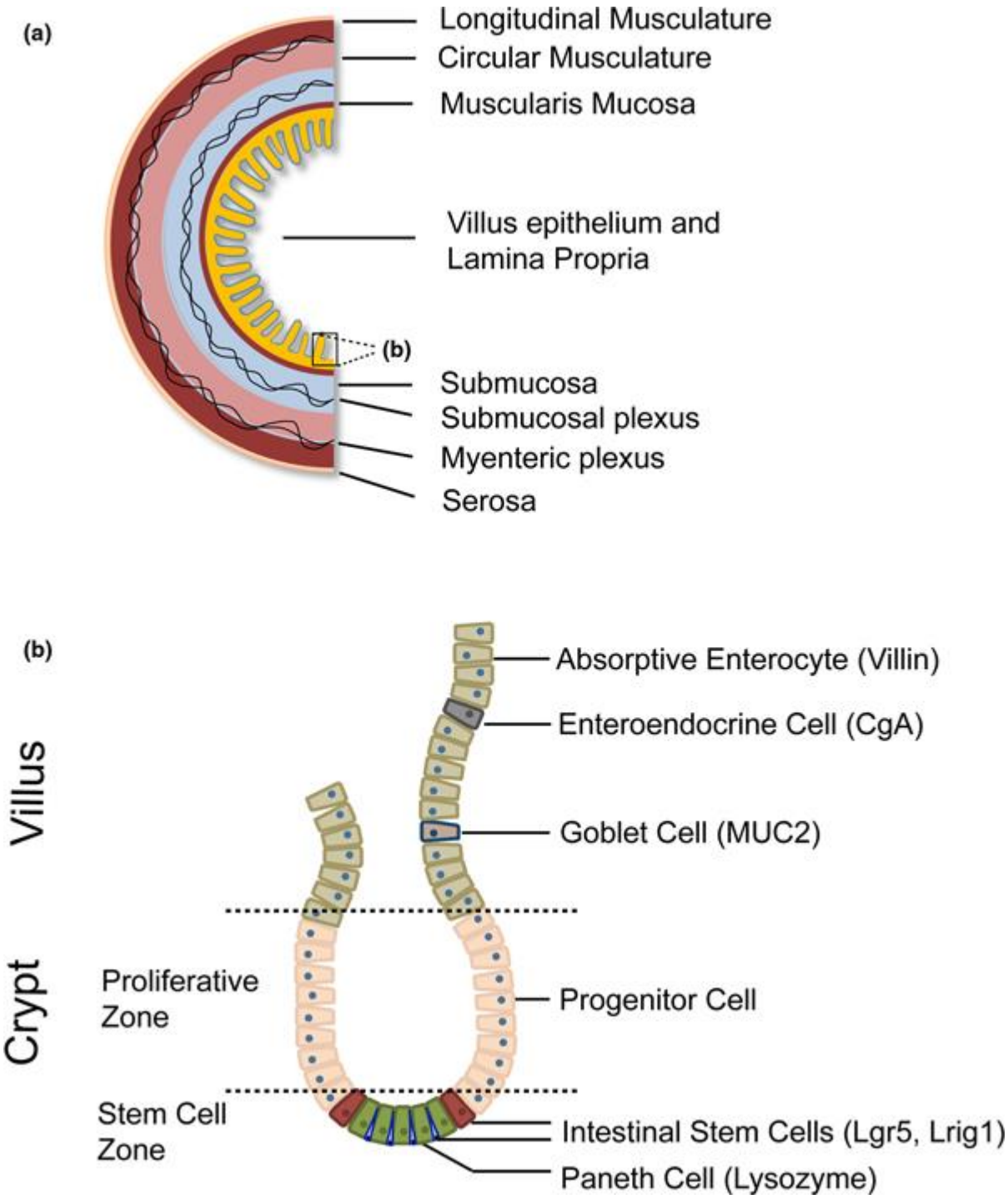


Figure 1-2: Schematic of intestinal structure and epithelial cells. (a) The layers of the intestine of an adult showing circular and smooth muscle layers in addition to submucosal and mucosal layers. The enteric nervous system is comprised of the submucosal and myenteric neural plexus. (b) Cell types of the intestinal epithelium, markers for each cell type are shown in parentheses. Stem cells and Paneth cells are found in the crypt whereas enterocytes including goblet cells and enteroendocrine cells are found in the villus. Figure from (Brugmann and Wells, 2013).

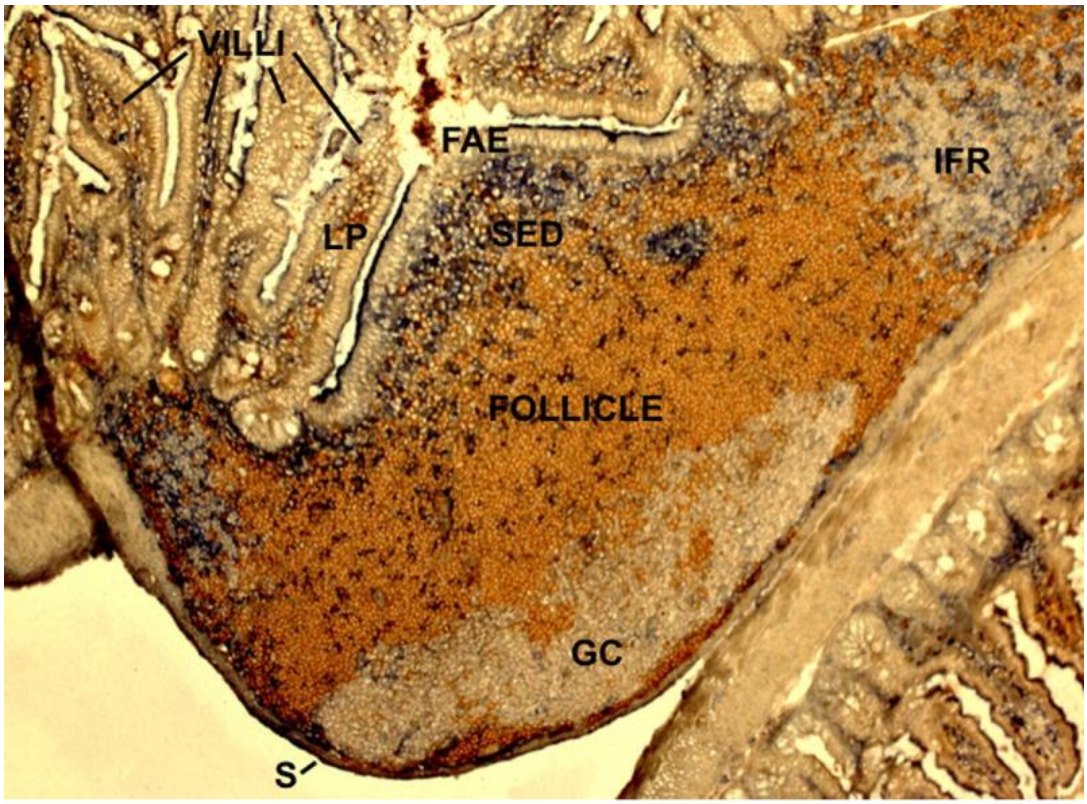


Figure 1-3: Cross-sectional view of a mouse Peyer's patch showing the main anatomical compartments. The section has been stained to detect naïve B cells (IgD, brown) and dendritic cells (CD11c, blue). FAE, follicle-associated epithelium, SED, subepithelial drome; GC, germinal centre; IFR, interfollicular region (T cell zone); LP, lamina propria; S, serosa. Also present is another loop of small intestine (bottom right of the image) which became juxtaposed during preparation (Reboldi and Cyster, 2016).

1.1.2 Tight Junctions

In the gut, epithelial tight junctions are the key structures which regulate paracellular trafficking of macromolecules, and forms a selectively permeable seal between adjacent epithelial cells (Lee, 2015).

Tight junctions are multiple protein complexes located at the apical ends of the lateral membranes of intestinal epithelial cells (Lee, 2015). Four integral transmembrane protein elements of tight junctions have

been identified, these include occludin (Furuse *et al.*, 1993), claudins (Furuse *et al.*, 1998), junctional adhesion molecules (JAMs) (Martin-Padura *et al.*, 1998) and tricellulin (Ikenouchi *et al.*, 2005) (Figure 1-4). The intracellular domains of these transmembrane proteins interact with cytosolic scaffold proteins, such as zonula occludens (ZO) proteins, which in turn anchor the transmembrane proteins to the actin cytoskeleton (Lee, 2015). The interaction of tight junction proteins with the actin cytoskeleton is integral to the maintenance of tight junction structure, and allows cytoskeletal regulation of tight junction barrier integrity (Gonzalez-Mariscal *et al.*, 2003). The intestinal tight junction barrier is dynamically regulated by cytokines and pathogens (Lee, 2015).

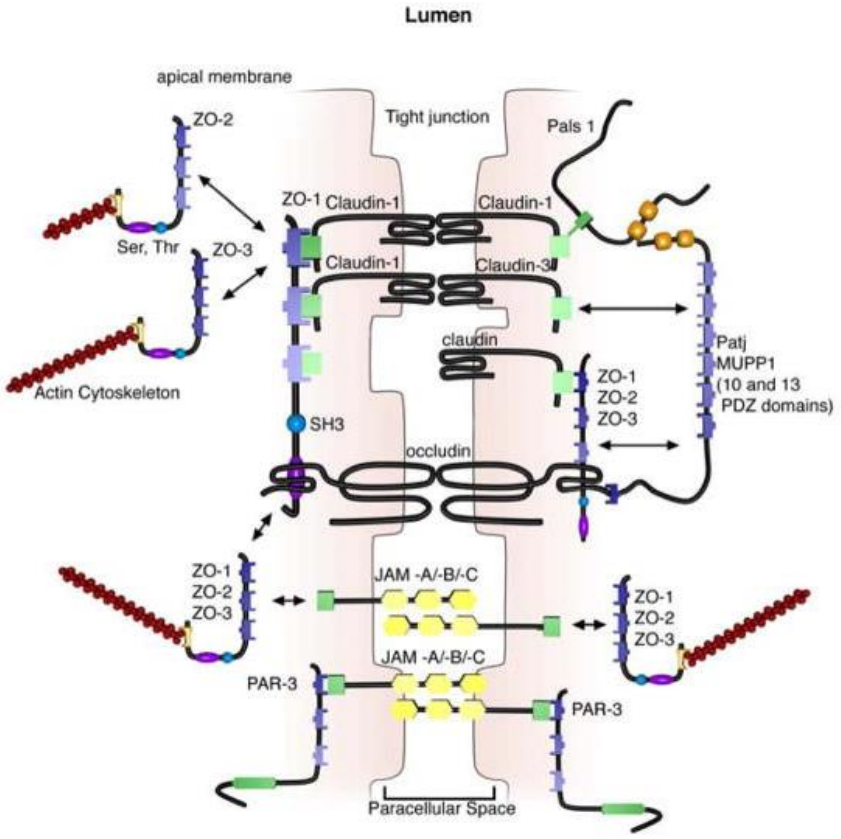


Figure 1-4: Tight junction structure. The tight junction consists of four transmembrane protein families: claudins, occludin, junctional adhesion molecules (JAMs) and tricellulin (not shown). These proteins form a selectively permeable seal between adjacent epithelial cells. The intracellular domains of these proteins interact with zonula occludens (ZO) proteins, which in turn interact with the actin cytoskeleton, forming an anchored structural barrier between epithelial cells. Image adapted from (Groschwitz and Hogan, 2009)

1.2 Intestinal Immunity

The gut and associated immune organs represent a substantial proportion of the total immune system in the body with GALT, being a prominent element of MALT. Indeed, it represents 70% of the immune system, with around 80% of plasma cells (mainly immunoglobulin A

bearing cells) residing within GALT (Kuvaeva *et al.*, 1980; Nogaller and Abdeeva, 1991; Vighi *et al.*, 2008; Burkey *et al.*, 2009).

The immune system consists of two distinct elements, the innate immune system and the adaptive immune system. Innate immunity is the first line of defence against the intrusion of pathogens and antigens into tissues and is non-antigen specific, fast acting and short lasting (Scanzano and Cosentino, 2015; Riera Romo *et al.*, 2016). In contrast, adaptive immunity is antigen-specific, requiring recognition of 'non-self' antigens via the process of antigen presentation (Flori *et al.*, 2011). The activation of adaptive immunity leads to immunological memory which provides protection and enables the organism to benefit from experiences with its antigenic environment (Mackay, 1993). Phagocytic cells, including macrophages, play a significant role in the cross-talk between the innate and adaptive immune system as they serve as antigen presenting cells in the recruitment of the adaptive immune system (Kyrova *et al.*, 2014).

The intestinal tract is host to a diverse population of 100 trillion bacteria (Rolhion and Chassaing, 2016). These bacteria shed microbe-associated molecular patterns (MAMPs) such as β- glucans, flagellin and polysaccharide A (PSA) which interact with the innate immune system.

Interaction of these molecules is important for distinguishing between pathogens and commensal microorganisms, and is also essential in the development of the immune system and maintenance of mucosal barrier function (Hooper *et al.*, 2002; Pamer, 2007; Round and Mazmanian, 2009; Hill and Artis, 2010).

Pathogenic (and non-pathogenic) microorganisms can gain entry via the gastrointestinal tract, and therefore once the intestinal barrier is breached, a fast and proportional innate immune response is necessary for response to an invasion across the epithelial barrier. This is followed by a specific and tailored response to the invasion by the adaptive immune system to control the infection. However, an inappropriately vigorous innate immune responses can result in severe tissue damage (Kinnebrew and Pamer, 2012). This can lead to increased penetration of bacteria and antigens past the epithelial barrier, therefore prolonging intestinal inflammation.

1.2.1 Innate Immunity

1.2.2 Cells of the Innate Immune System

Many cell types are involved in the innate immune response. These include; phagocytes (macrophages and neutrophils), dendritic cells, mast cells, basophils, eosinophils, natural killer (NK) cells and T lymphocytes (Table 1-1)(Warrington *et al.*, 2011; Kawakami, 2016). Phagocytes are divided into two main subtypes: neutrophils and macrophages. These two cell types share a similar function in that they engulf (phagocytose) microbes. The differences between the two cell types are that neutrophils contain granules which when released, assist in the elimination of pathogenic bacteria (Medeiros *et al.*, 2017). Unlike neutrophils which are relatively short-lived (6 hours to a few days), macrophages are long-lived and are involved in antigen presentation to T cells (Warrington *et al.*, 2011).

Table 1-1: Cells of the innate immune system

Cell Type	Nucleus	Functions	Lifespan	Main Targets	Reference
Macrophage	Varies	• Phagocytosis • Antigen Presentation to T cells	Months-Years	• various	(Murphy *et al.*, 2007)
Neutrophil	Multi-lobed	• Phagocytosis • Degranulation (Discharge of cell contents	6 hours-few days	• Bacteria • fungi	(Murphy *et al.*, 2007; Oakes *et al.*, 2009)
Eosinophil	Bi-lobed	• Degranulation • Release of enzymes, growth factors, cytokines	8-12 days (circulate for 4-5 hours)	• Parasites • Various allergic tissues	(Murphy *et al.*, 2007)
Basophil	Bi or Tri-lobed	• Degranulation • Release of histamine, enzymes, cytokines	Lifetime uncertain; likely a few hours-few days	• Various allergic tissues	(Murphy *et al.*, 2007)
Monocytes	Kidney-shaped	• Differentiate into macrophages and dendritic cells to elicit an immune response	Hours-days	• Various • Inflammatory sites	(Murphy *et al.*, 2007; Qu *et al.*, 2014)
Dendritic cells	Oval or kidney-shaped	• Antigen presentation • Lymphocyte activation • Produce large quantities of pro-inflammatory cytokines	days	• Various • Body's sentinels	(Hardin, 2005; Summerfield and McCullough, 2009)

Table adapted from (Warrington *et al.*, 2011)

Dendritic cells (DCs) also phagocytose microbes and function as antigen presenting cells, DCs also function as important messengers between innate and adaptive immunity. DCs are the most potent antigen-presenting cells and are efficient at generating a robust immune response (Constantino *et al.*, 2017). In PPs, DCs reside just beneath the SED underlying the FAE (Sato and Iwasaki, 2005). In the intestine, DCs

can sense antigens which have been transported across the epithelium through various routes (Coombes and Powrie, 2008). Firstly, specialised M cells (microfold cells) which are present in PPs, can transcytose luminal antigen which is then taken up by nearby DCs (Figure 1-5) (Coombes and Powrie, 2008). DCs can also sample antigens directly from the intestinal lumen by forming tight junction-like structures with IECs, and projecting dendrites through the epithelial layer into the intestinal lumen (Rescigno *et al.*, 2001; Coombes and Powrie, 2008).

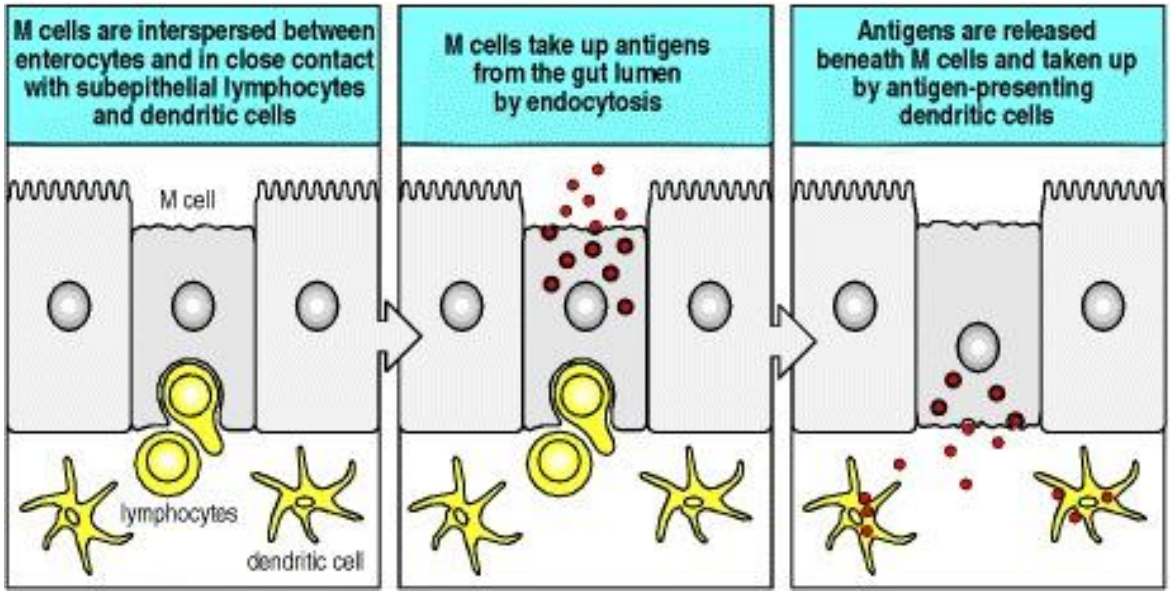


Figure 1-5: Delivery of luminal antigens to dendritic cells by M cells. Antigens from the gut lumen are transported through M cells for release and uptake by dendritic cells (Janeway, 2001).

DCs are often classified based on cell surface receptor expression. In PPs, DCs are predominately of the $CD11c^{hi}CD11b^{+}CD8\alpha^{-}$, $CD11c^{hi}CD11b^{-}$

$CD8\alpha^+$ and $CD11c^{hi}CD11b^-CD8\alpha^-$ subtypes, each with unique functional properties and anatomical localisation (Figure 1-6) (Iwasaki and Kelsall, 2000; Iwasaki and Kelsall, 2001). DCs from PPs can also be distinguished regarding their expression of the chemokine receptors, CX_3C-chemokine receptor 1 (CX_3CR1) and CC-chemokine receptor 6 (CCR6) (Niess *et al.*, 2005; Salazar-Gonzalez *et al.*, 2006). In the colon, DCs appear to be concentrated within isolated lymphoid follicles, with very few present in the lamina propria under steady-state conditions (conditions where no infection or inflammation is present) (Karlis *et al.*, 2004; Niess *et al.*, 2005).

DCs are integral to ensuring that pathological immune responses to harmless antigens do not develop. DCs that have migrated to the mesenteric lymph nodes during steady-state conditions can interact with B and T cells to initiate responses aimed at maintaining a non-inflammatory state in the intestine (Coombes and Powrie, 2008).

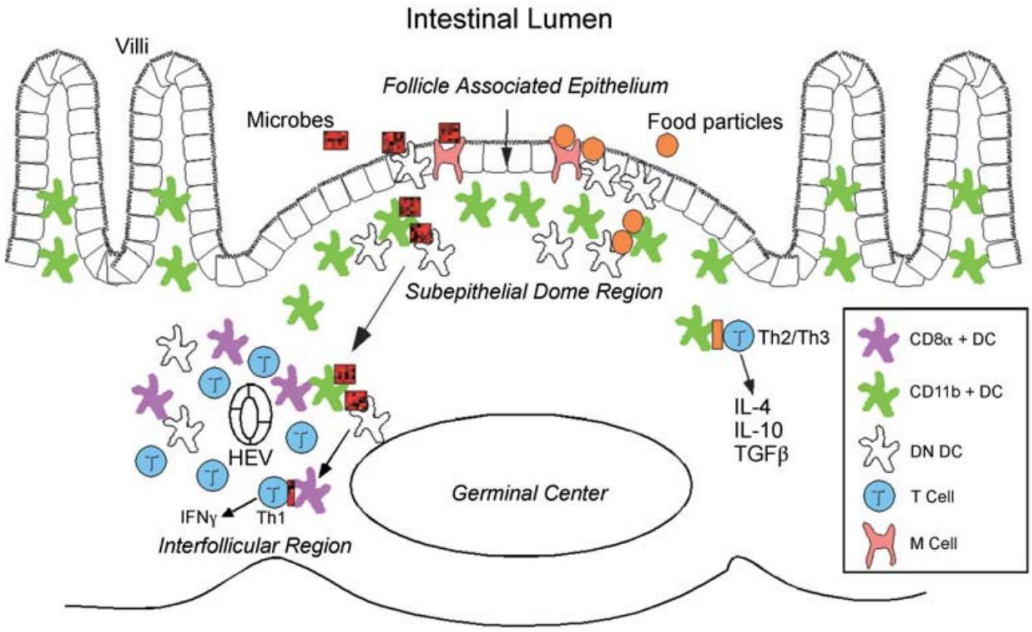


Figure 1-6: Distribution and function of DC subsets within Peyer's Patches. Antigens within the intestinal mucosa are transferred to the PP via M cells where DCs acquire them. DCs residing in the subepithelial dome (SED) mainly express the CD11b molecule whereas those residing in the interfollicular region (IFR) express CD8α. A subset of DCs localised in the SED, IFR and follicle-associated epithelium (FAE) lack expression of either surface receptors and are termed double negative DCs (DN DCs). These three DC subsets have distinct abilities to induce CD4+ T cell differentiation. HEV, high endothelial venule; IFNγ, interferon γ; IL interleukin; TGF-β, transforming growth factor β; Th, T helper (Sato and Iwasaki, 2005).

Appropriate activation of $CD4^+$ T cell responses is important for a variety of immune responses against intestinal pathogens and antigens. Depending on the context of the antigen encountered, a range of $CD4^+$ T cell responses are induced following oral antigen exposure (Sato and Iwasaki, 2005). These include the responses of the Th1 (Interferon γ, IFNγ), Th2 (Interleukin-4 (IL-4), Interleukin-13(IL-13)), Th3 (Transforming

growth factor-β, TGF-β),Tr-1 (Interleukin-10 (IL-10)) and Treg ($CD25^{+}Foxp3^{+}$) phenotypes (Sato and Iwasaki, 2005).

In the absence of pathogenic microorganisms, antigens give orally normal results in suppressive immune responses. Th3, Tr-1 and Treg can suppress responses to ingested antigens and are likely responsible for mediating tolerance (Daynes *et al.*, 1990; Weiner, 2001). Th1 responses are observed in PP T cells particularly after infection with pathogenic microorganisms, an example of which would be the secretion of IFNγ by PP T cells after gastrointestinal infection with *Salmonella typhimurium* (George, 1996; Karem *et al.*, 1996).

1.2.3 Cytokines and Chemokines

Cytokines are small proteins or glycoproteins whereas chemokines form a group of smaller cytokines with chemotactic properties that are produced in a variety of cells (Kwak *et al.*, 2014).

It is possible to classify cytokines by the nature of the immune response, with individual cytokines performing specific roles. Key pro-inflammatory cytokines include interleukin-1 (IL-1) and tumour necrosis factor (TNFα) (Turner *et al.*, 2014), whereas anti-inflammatory cytokines

include transforming growth factor-β (TGF-β) and interleukin 10 (IL-10) (Su *et al.*, 2012).

The IL-1 family includes 11 members: IL-1α, IL-1β, the IL-1 receptor antagonist (IL-1Ra), IL-18, IL-33, IL-36α, IL-36β, IL-36γ, IL-36Ra, IL-37 and IL-1Hy2 (Boraschi *et al.*, 2011). These include both pro and inflammatory cytokines and are expressed in a number of cell types including macrophages and monocytes (Boraschi *et al.*, 2011).

IL-1α and IL-1β are synthesised in multiple cell types including monocytes, macrophages and neutrophils (Arend *et al.*, 2008). IL-1α is constitutively expressed in many cell types whereas IL-1β expression is mainly induced in response to microbial molecules, although it can stimulate its own expression (Dinarello, 2009). The functional receptor for IL-1 consists of a heterodimeric complex of IL-1 receptor 1 (IL-1R1) and the IL-1R accessory protein (IL-1RAcP) (O'Neill, 2008).

Il-1R1 belongs to the IL-1R/TLR (Toll Like Receptor) family due to the presence of a conserved cytoplasmic Toll/IL-1R (TIR) domain (O'Neill, 2008). Signal transduction leads to activation of both mitogen-activated protein kinases (MAPKs) and the transcription factor nuclear factor κB (NF-κB), resulting in pro-inflammatory cytokine expression (Figure 1-7) (Turner *et al.*, 2014).

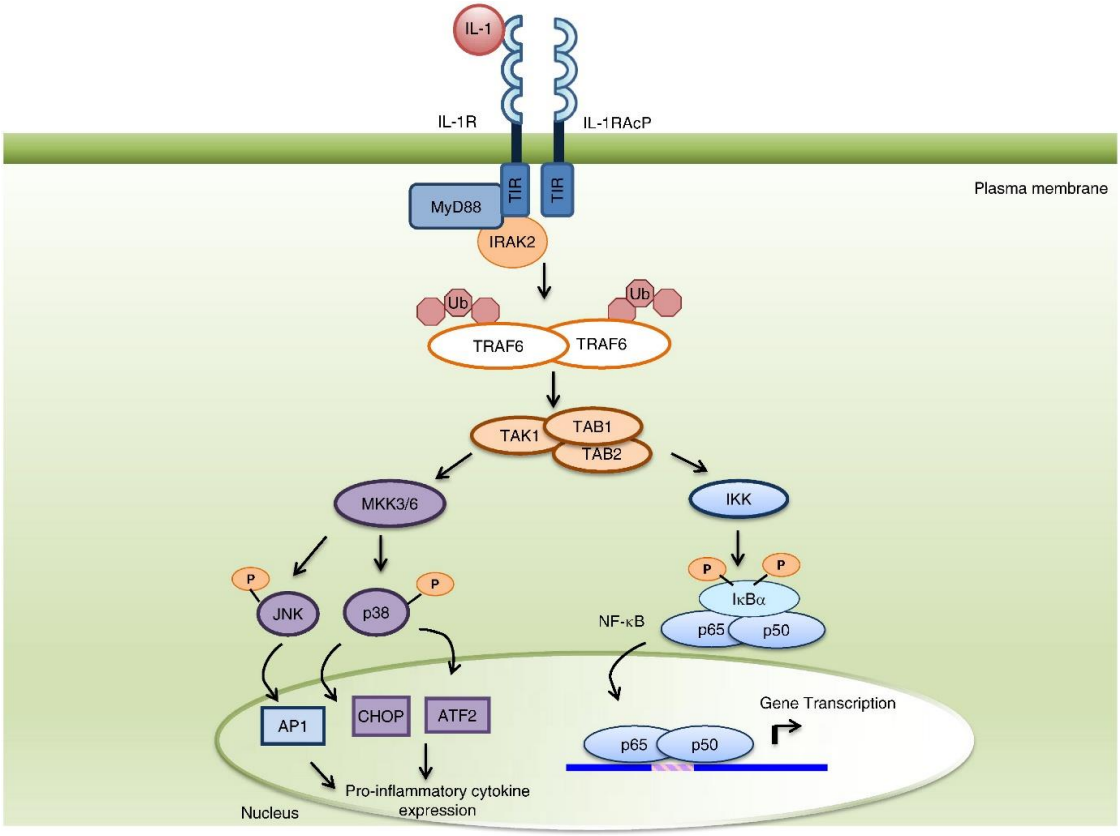


Figure 1-7: IL-1 signal transduction of NF-kB activation. IL-1 binds to IL-1R1 which then associates with the IL-1RAcP at the cell surface. MyD88 then interacts with the TIR domains of both IL-1R1 and IL-1RAcP. Subsequently, IL-1R associated kinases (IRAKs) are recruited to the MyD88/TIR complex. IRAKs then promote TNFR-associated factor 6 (TRAF6) polyubiquitination, which then interacts with TAK1 in complex with TAB1 and TAB2. This ultimately leads to the phosphorylation of IκBα, forcing its disassociation from NF-κb. Phosphorylated IκBα is subsequently ubiquitinated for degradation by the proteasome. The phosphorylated p65/p50 heterodimer then translocates to the nucleus where it binds to response elements in NF-κb controlled genes and leads to the induction of pro-inflammatory gene expression. Activation of the TAK1/TAB1/TAB2 complex also leads to the phosphorylation and subsequent activation of the mitogen-activated kinases (MAPKs), JNK and p38. These kinases then phosphorylate and activate transcription factors responsible for the expression of pro-inflammatory genes. Abbreviations: IKK, IκB kinase; IκBα, an inhibitor of κB; MyD88, myeloid differentiation factor 88; NF-κB, nuclear factor κB; TAB1, TAK1 binding protein 1; TAB2, TAK1 binding protein 2; TAK1, transforming growth factorβ-activated kinase 1. Image from Turner *et al.*, 2014 .

Tumour necrosis factor alpha (TNFα) is a potent inflammatory mediator which is central to the inflammatory action of the innate immune system including cytokine production, activation or expression of

adhesion molecules and growth stimulation (Rothe *et al.*, 1992; Tartaglia and Goeddel, 1992; Smith *et al.*, 1994). TNFα functions to stimulate proliferation in normal cells, but also exerts activity against tumour cells and causes inflammatory, antiviral and immunoregulatory effects (Gupta, 2002). It is mainly secreted from activated macrophages although it can be secreted from monocytes, T cells, mast cells and NK cells (Tracey *et al.*, 2008). TNFα is synthesised as a transmembrane precursor which is transported to the cell surface where it is cleaved into soluble TNFα by the TNFα converting metalloprotease (TACE) (Black *et al.*, 1997; Stow *et al.*, 2009).

Cleavage of the TNFα precursor produces an intracellular domain which translocates to the nucleus and induces pro-inflammatory cytokine signalling, particularly the expression of IL-12 (Friedmann *et al.*, 2006). Activation of TNF receptors by soluble TNFα leads to the activation of NF-κB and other transcription factors, causing the initiation of pro-inflammatory gene expression (Turner *et al.*, 2014).

Pro-inflammatory chemokines are produced by cells primarily to recruit leukocytes to the sites of infection or injury (Turner *et al.*, 2014). Chemokines function to induce integrin expression including the β2-integrin lymphocyte function-associated antigen (LFA-1) in leukocytes,

which act to arrest the rolling of these cells and increase infiltration through the endothelium (Constantin *et al.*, 2000). Chemokines can be divided into four families based on the positioning of the N-terminal cysteine residues. The C-X-C family is characterised by the separation of the first two cysteines by a variable amino acid, while in the C-C family, the cysteine residues are adjacent to each other (Turner *et al.*, 2014). The third family, C family, lacks the first and third cysteines and so only contains a single cysteine residue in the conserved position (Kelner *et al.*, 1994). The final family, CX3C, has the two N-terminal cysteine residues separated by three variable amino acids (Bazan *et al.*, 1997).

Interleukin-8 (IL-8) is also known as CXCL8 and belongs to the CXC chemokines (Hall *et al.*, 1999). The key role of IL-8 in inflammation is the recruitment of neutrophils (Hammond *et al.*, 1995). However, it is also responsible for the chemotactic migration and activation of monocytes, lymphocytes, basophils and eosinophils in areas of inflammation (Miller *et al.*, 1992). Although IL-8 can bind to both CXCR1 and CXCR2 receptors, chemotactic signalling is primarily via CXCR1 (Hall *et al.*, 1999). Following binding, a number of intracellular signalling cascades are activated within the target cells to induce chemotaxis and degranulation (Turner *et al.*, 2014).

Anti-inflammatory cytokines are immunoregulatory molecules which control the proinflammatory cytokine response; these anti-inflammatory cytokines act in concert with cytokine inhibitors and soluble cytokine receptors to regulate the immune response (Opal and DePalo, 2000). Cytokines which have anti-inflammatory activities include IL-1ra (receptor antagonist), IL-4, IL-6, IL-10, IL-11 and IL-13 and TGFβ (Opal and DePalo, 2000). In this review, the activities of IL-1ra, IL-10 and TGFβ will be detailed.

Two structural variants of IL-1ra have been described, a 17kDa which is mainly secreted from monocytes, macrophages and neutrophils which is termed sIL-1Ra. The 18-kDa form remains in the cytoplasm of epithelial cells, monocytes and fibroblasts referred to as icIL-1Ra ((Arend *et al.*, 1998).

Both variants of IL-1ra function by binding to IL-1. This prevents the binding of IL-1, blocking the proinflammatory signal which would be generated (Volarevic *et al.*, 2010).

IL-10 is considered the most important anti-inflammatory cytokine (Opal and DePalo, 2000). During infection, IL-10 inhibits the activity of Th1 cells, NK cells and macrophages, all of which are necessary for optimal pathogen clearance but also contribute to tissue damage

(Couper *et al.*, 2008). IL-10 has been noted to up-regulate expression of a small subset of genes in LPS activated macrophages including IL-1Ra and suppressor of cytokine signalling-3 (Lang *et al.*, 2002). IL-10 also inhibits cell surface expression of major histocompatibility complex class II molecules, and the lipopolysaccharide (LPS) recognition and signalling molecule CD14 (Opal *et al.*, 1998). IL-10 has also been noted to inhibit NF-κB DNA binding activity without affecting IκB degradation or translocation of NF-κB translocation to the nucleus (Clarke *et al.*, 1998). Other anti-inflammatory actions of IL-10 include increased degradation of pro-inflammatory cytokine messenger RNA (Opal *et al.*, 1998), and the attenuation of TNF expression in monocytes (Dickensheets *et al.*, 1997).

TGF-β is an essential regulator of cell proliferation, differentiation and formulation of the extracellular matrix (Letterio and Roberts, 1997). TGFβ has both pro and anti-inflammatory effects. It acts as a biological switch, able to modify the action of other cytokines or growth factors (Opal and DePalo, 2000). To this end, TGF-β can convert a site of active inflammation into one dominated by resolution and repair (Letterio and Roberts, 1997). TGF-β suppresses the proliferation and differentiation of T and B cells and limits IL-2, IFNγ and TNF production (Opal and

DePalo, 2000). Finally, TGF-β acts as a monocyte/ macrophage deactivator similarly to IL-10, albeit less potent (Letterio and Roberts, 1997).

In conclusion, a dynamic and ever-shifting balance exists between proinflammatory cytokines and anti-inflammatory elements of the immune system (Opal and DePalo, 2000). Perturbations of this regulatory network by genetic, environmental or microbial elements can have highly deleterious consequences (Docke *et al.*, 1997; Westendorp *et al.*, 1997; Lentsch *et al.*, 1999).

1.2.4 Pattern Recognition in the Innate Immune System

Receptors of the innate immune system known as pattern-recognition receptors (PRRs) detect conserved determinants of microbial and viral origin. Activation of these receptors initiates signalling events which bring about an effective immune response (Brubaker *et al.*, 2015). Most PRRs can be classified into one of five families based on protein domain homology. These five families consist of; Toll-like receptors (TLRs); C-type lectin receptors (CLRs); nucleotide binding domain receptors (NOD-like receptors or NLRs); RIG-I-like receptors (RLRs); and AIM2-like

receptors (ALRs) (Kumar *et al.*, 2011; Wang and Wang, 2013; Brubaker *et al.*, 2015).

A large component of pattern recognition receptor (PRR) induced innate immune response is transcriptional, leading to the production of proinflammatory cytokines and interferons (IFN). Production of these is critical for initiating innate and adaptive immune responses. Activation of PPRs also initiates many non-transcriptional responses such as phagocytosis, autophagy, cell death and cytokine processing (Palm and Medzhitov, 2009; Drummond and Brown, 2011; Deretic *et al.*, 2013; Lamkanfi and Dixit, 2014; Brubaker *et al.*, 2015).

Innate immune receptor signalling requires adaptor proteins which link receptors to an enzymatic signal. Each adaptor or set of adaptors contain domains which allow for protein-protein interactions with an upstream receptor as well as downstream signalling protein (Chen *et al.*, 2009; Geijtenbeek and Gringhuis, 2009). As an example of immune receptor signalling, TLRs will be used.

TLRs are type I transmembrane receptors expressed on many cell types including macrophages, dendritic cells, T lymphocytes and IECs (Frosali *et al.*, 2015). Genes corresponding to all ten TLR genes which have been identified in humans have also been fully cloned from pigs (Uenishi and

Shinkai, 2009). TLR molecules are divided into two groups. The first group includes TLR1, TLR2, TLR4, TLR5, TLR6 and TLR10. These are expressed on the cell surface and recognise products mainly derived from microbes. TLR 4 recognises Gram-negative bacteria by selecting for LPS or Lipid A which is the main component of LPS. TLR2 can sense Gram-positive microbes by selecting for peptidoglycans and lipoteichoic acid as well as lipoarabinomannan from mycobacteria, glycosylphosphatidylinositol from *Trypanosoma* and zymosan from yeasts and other fungi (Takeda and Akira, 2005). Unlike other TLRs which form homodimers to transmit signals downstream, TLR2 forms a heterodimer with TLR1 or TLR6 to sense triacylglyceride or diacylglyceride respectively (Gantner *et al.*, 2003; Uenishi and Shinkai, 2009). TLR5 recognises flagellin, a structural component of microbial flagella (Hayashi *et al.*, 2001). The specificity and biological function of TLR10 is yet to be fully elucidated however it has been demonstrated to be a modulatory receptor with mainly inhibitory effects (Oosting *et al.*, 2014).

The second group of TLRs consisting of TLR3, TLR7, TLR8 and TLR9 are expressed on the membrane of intracellular organelles such as endosomes (Heil *et al.*, 2003). These recognise nucleic acids and

derivatives. TLR3 recognises double-stranded RNA (Alexopoulou *et al.*, 2001) TLRs 7 and 8 recognise single-stranded RNA (Heil *et al.*, 2003). TLR9 is a receptor for unmethylated CpG DNA which is usually found in the bacterial genome as well as viruses such as herpes simplex virus-2 (Lund *et al.*, 2003).

There are two ways in which TLRs can signal to the nucleus; one is MyD88 (a TIR domain-containing molecule) whereas the other is independent of MyD88 (O'Neill and Bowie, 2007). MyD88 participates in the signalling of all TLRs except TLR3 and signals transcription of genes encoding inflammatory cytokines such as TNF-α via the complex of TNF receptor-associated factor 6 (TRAF6) and IκB kinase (IKK) (Uenishi and Shinkai, 2009). The interaction between TLR7 and TLR9 and MyD88 leads to induction of type I interferons via IRAK-1 and interferon regulatory factor-7 (IRF-7) (Uematsu *et al.*, 2005). TLR3 and TLR4 utilise another pathway, which is unrelated to MyD88 signalling, dependent upon TRIF (TIR domain-containing adaptor-inducing interferon-β). The TRIF dependent pathway induces transcription of type I IFNs via IRF-3 (Kawai *et al.*, 2001) (Figure 1-8).

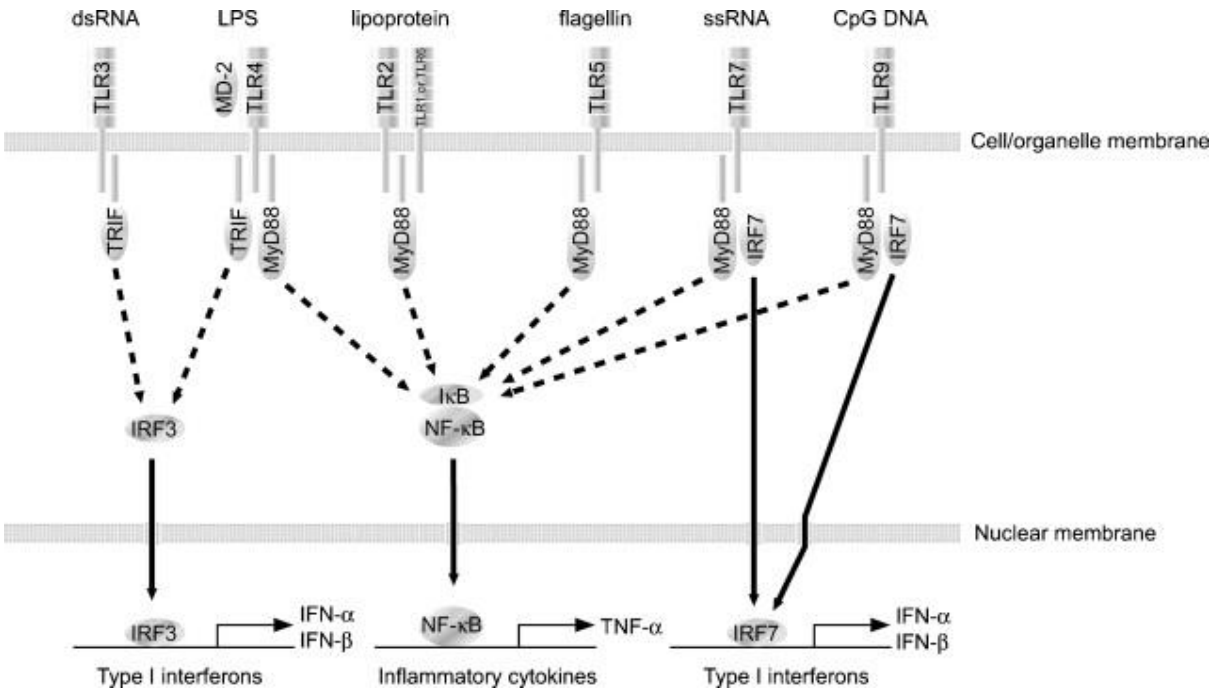


Figure 1-8: Schematic of signalling induced by TLR molecules. Only representative molecules in the signalling pathway are shown. Dotted arrows denote signal transduction. Solid lines show translocation of molecules

In Pigs, Increased expression of some TLRs have been noted in response to pathogen challenge, including the increased expression of TLR2 in the intestinal tissues of gnotobiotic pigs after treatment with *Escherichia coli*, *Lactobacillus fermentum* or the faeces of sows (Willing and Van Kessel, 2007). Additionally, increased expression of TLR5 and TLR9 has been observed in response to the feeding of *Salmonella enterica* serovar Typhimurium or serovar Choleraesuis (Burkey et al., 2007*)*.

Strong expression of TLR2 and TLR9 has been observed in the GALT of pre-suckling newborn swine, suggesting that these receptors can mediate the immune responses of the immature (Tohno *et al.*, 2006).

1.2.5 Immunoglobulins

Immunoglobulins are heterodimeric proteins comprised of two heavy (H) and two light (L) chains. The structure can be functionally separated into the variable (V) domains which bind antigens and the constant (C) domain which specify effector functions such as activation of complement or binding to Fc receptors (Schroeder and Cavacini, 2010). The V domains are created by a complex series of gene rearrangement events. Each V domain can be split into three regions of sequence variability, termed the complementarity determining regions or CDRs, and four regions of relatively constant sequence which is termed the framework regions (FRs). Three CDRs of the H chain are paired with three CDRs of the L chain to form the antigen binding site (Figure 1-9). There are five main classes of heavy chain C domains, IgM, IgG, IgA, IgD and IgE (Schroeder and Cavacini, 2010).

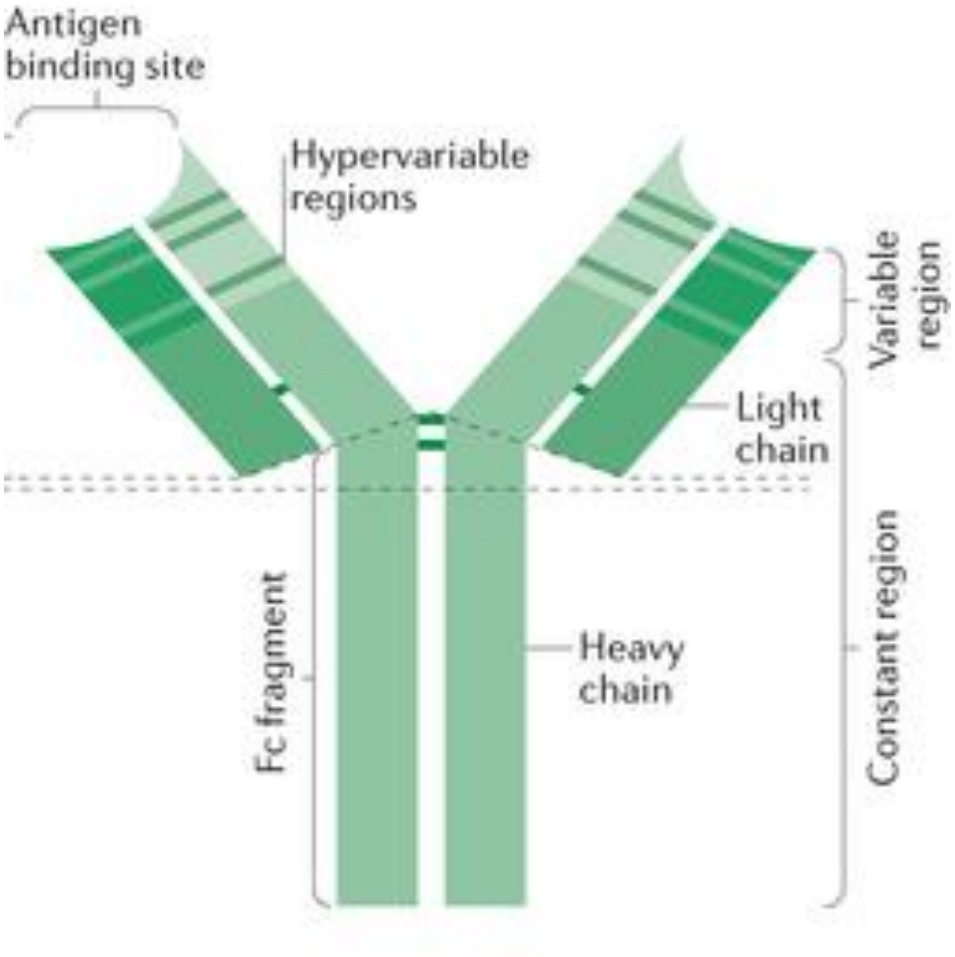


Figure 1-9: Two-dimensional schematic of immunoglobulins. All immunoglobulins have the same basic structure comprising two heavy chains (light green) and two light chains (dark green) which are held in a Y shape by disulphide bonds. The diagram also shows the variable regions which contribute to the specificity of antigen binding and the constant region which determines the ability of the immunoglobulin to bind to Fc receptors on phagocytic cells. Image adapted from (Crisp *et al.,* 2016).

IgM is multimeric (usually pentameric but rarely hexameric) (Schroeder and Cavacini, 2010). IgM antibodies (as well as IgG) constitute the major components of the natural pig antibodies (antibodies which are present in the serum of healthy individuals) (Roos *et al.*, 2001). IgM is the first class of antibodies produced during a primary antibody response (Ouchida *et al.*, 2012). Most pathogens elicit an immune

response which is characterised by an early increase in antigen-specific IgM followed by a rise in antigen-specific IgG, IgA and IgE antibodies (Boes, 2000).

IgD is found at very low levels in the serum, with a short half-life which may be attributed to the hinge region which is particularly sensitive to proteolysis (Schroeder and Cavacini, 2010). In mature B cells, membrane-bound antigen receptor normally consists of both IgM and IgD where it fine-tunes humoral responses (Geisberger *et al.*, 2006).

IgG is the predominant isotype found in the body and has the longest serum half-life of all immunoglobulin isotypes (Schroeder and Cavacini, 2010). Based on structural, antigenic and functional differences in the constant region of the heavy chain, four IgG subclasses have been identified. These classes include IgG1, IgG2, IgG3 and IgG4. IgG1 and IgG3 antibodies are induced in response to protein antigens whereas IgG2 and IgG4 are associated with polysaccharide antigens (Schroeder and Cavacini, 2010). IgG subclasses have multiple functions in that all but IgG4 interact with the complement system, which is an important means of clearance of opsonised pathogens but also contribute directly to the immune response by neutralisation of toxins and viruses (Scharf *et al.*, 2001; Cavacini *et al.*, 2003; Schroeder and Cavacini, 2010).

IgA is of interest as it is present in the highest levels of any immunoglobulin at mucosal surfaces and in secretions. It is also present in breast milk (Woof and Mestecky, 2005). In particular, IgA can contribute up to 50% of the protein in colostrum, the 'first milk' given to the neonate by the mother (Schroeder and Cavacini, 2010). In pigs, it is known that piglets deprived of their mother's colostrum exhibit strong apathy and develop watery diarrhoea, often resulting in death (Socha-Banasiak *et al.*, 2017).

IgA is critical for the protection of mucosal surfaces from toxins, virus and bacteria by direct neutralisation or by prevention of binding to the mucosal surface (Woof and Mestecky, 2005; Schroeder and Cavacini, 2010). The polymeric nature of secretory IgA may be important as polymeric IgA is more effective than monomeric IgA at preventing *Clostridium difficile* toxin A damage to epithelial cells (Stubbe *et al.*, 2000). Although IgA interaction with the complement system is not a major effector mechanism at the mucosal surface, IgA receptor is expressed on neutrophils. IgA may play a significant role in the immune response of intestinal tissues, by facilitating the uptake of antigens by dendritic cells (Stubbe *et al.*, 2000; Schroeder and Cavacini, 2010).

IgE has the lowest serum concentration of immunoglobulin isotypes, however it is a very potent immunoglobulin (Schroeder and Cavacini, 2010). It is associated with hypersensitivity and allergic reactions as well as the response to parasitic worm infections. These reactions are facilitated by extremely high affinity for its receptor on mast cells, basophils and eosinophils, indeed circulating IgE upregulates its receptor on these cells (Schroeder and Cavacini, 2010).

1.2.6 Colostrum and Milk Intake by Piglets

In pigs, colostrum is secreted from the udder immediately after farrowing and is high in proteins and immunoglobulins. A total of 2.5-5kg of colostrum is produced over 24 hours by a sow for a litter of 8-12 piglets (Farmer and Quesnel, 2009). The significant roles of colostrum are to provide the piglet with energy and passive immunity (Menchetti *et al.*, 2016). Before birth, the foetus is protected from antigens by the barrier of the placenta. However, after birth, the newborn piglet must be able to respond immunologically to the invasion of potentially harmful antigens from the surrounding environment (Sangild, 2003). In pigs, this is achieved by transfer of passive immunisation, via colostrum, from the sow until the piglet's active immune system is fully developed

(Kim, 1975; Sinkora *et al.*, 2000). The degree of passive immunisation after colostrum feeding depends upon the availability of colostrum and its immunoglobulin concentration; these factors can be affected by breed and parity of the sow (Klobasa and Butler, 1987; Jackson *et al.*, 1995).

The concentration of immunoglobulins in porcine colostrum at farrowing varies by type. IgG is found at a concentration of approximately 118.5 mg/ml whereas IgA and IgM are found at 23.7mg/ml and 12.1mg/ml respectively (Markowska-Daniel *et al.*, 2010).

Absorption of immunoglobulins by the piglet is at its peak between 8 and 12 hours after birth. However, the piglet's ability to absorb immunoglobulins falls rapidly to the point that 24 hours after birth the piglet is unable to absorb any immunoglobulin due to a decrease in gut wall permeability (Szeky *et al.*, 1979; Westrom *et al.*, 1985). Colostrum composition changes rapidly after farrowing into mature milk. This transition leads to lower total protein, whey protein and IgG but higher fat, lactose and IgA contents (King'ori, 2012). Colostrum contains growth factors for the normal development of the intestine. The gastrointestinal tract of the piglet grows and matures rapidly during the

two weeks after birth, this is stimulated by growth factors contained within colostrum including EGF-1, IGF-1 and TGF-β (Thapa, 2005; King'ori, 2012).

1.3 Pigs at Weaning

The first three months of life represent a considerable period of maturation and gastrointestinal development in the pig. During this time, intestinal epithelial, immune and nervous systems change dramatically as the neonate adapts to life in the extra-uterine environment (Leibbrandt *et al.*, 1975; Blecha *et al.*, 1983; Pohl *et al.*, 2017). Many of these developmental changes are as a result of genetic cues or biological clocks, but these changes are also influenced by environmental cues (Moeser *et al.*, 2017). The processes during this period exhibit a high degree of plasticity, therefore perturbations which occur during this critical period can shape long and short-term phenotype and GI function (Moeser *et al.*, 2017).

The epithelial barrier develops rapidly in early life and is characterised by a rapid decline in intestinal permeability (Figure 1-10) (Szeky *et al.*, 1979; Westrom *et al.*, 1985). This process is critical to initially allow absorption of immunoglobulins from colostrum while permeability is

high. As permeability reduces, environmental antigens from the unfamiliar environment and colonising microbiota which would otherwise trigger massive inflammation are excluded (Westrom *et al.*, 1985; Moeser *et al.*, 2017). Although the precise mechanisms of postnatal barrier development are not well understood, it is thought to be driven by several factors including genetic programming, microbial colonisation, colostrum and milk factors (Westrom *et al.*, 1985; Fawzy *et al.*, 2011; Rogier *et al.*, 2014).

Birth and weaning present a serious challenge to the underdeveloped immune system of the neonatal pig. Because of this, in addition to the rapid reduction in intestinal permeability, a number of exogenous and endogenous factors act to suppress immune activation which could otherwise be damaging (Moeser *et al.*, 2017). Exogenous factors include milk and colostrum derived immunoglobulins, maternal leukocytes and milk derived factors including anti-inflammatory cytokines which can act to modulate and neutralise intestinal microbes (Newburg and Walker, 2007). Endogenous factors to prevent overactivation of the immune system include a mechanism by which neonates are born with few lymphocytes and reduced expression of pro-inflammatory cytokines (Upham *et al.*, 2006; Nguyen *et al.*, 2010). Additionally, The

neonatal immune system is biased towards a T helper 2 (Th2) immune response via the suppression of proinflammatory cytokines associated with the T helper 1 (Th1) response such as IFNγ and IL-12, whereas anti-inflammatory cytokines such as IL-4, IL-10 and IL-13 are comparatively higher (Beverley, 1997). Several weeks after birth, neonates overcome the immunosuppressive stage when lymphocytes begin developing functionally (Butler *et al.*, 2000; Butler *et al.*, 2009). Suckling piglets achieve a stable number of lymphocytes at around six weeks of age, at the same time secondary lymphoid organs such as jejunal and ileal PPs rapidly mature (Pabst *et al.*, 1988; Barman *et al.*, 1997; Blikslager *et al.*, 1997). In summary, many mechanisms act to limit the immune response during early gut development, indicating the importance of an immunosuppressive environment during this period. Therefore inappropriate or excessive immune stimulation during this critical period has the potential to disrupt the development and function of the intestinal immune system (Moeser *et al.*, 2017).

In the commercial production environment, pigs are weaned at an early stage (17- 28 days of age), this contrasts to the natural weaning procedure in free-ranging domestic pigs which occurs at ~17 weeks (Jensen and Recén, 1989). In nature, weaning in pigs is gradual and

approaches completion at ~12-14 weeks of age which coincides with the near complete maturation of epithelial, immune and nervous systems (Figure 1-10) (Moeser *et al.*, 2017).

Weaning is a stressful event in the life of a commercial pig. Upon removal from the sow, the pig is subject to many stressors including a change in diet from milk to solid feed; mixing with pigs from other litters, resulting in conflict to re-establish the social hierarchy in weaned pigs; transportation and vaccination (Moeser *et al.*, 2017). These stressors manifest as reduced feed intake and performance (Boudry *et al.*, 2002; Boudry *et al.*, 2004). These performance factors are influenced by reduced intestinal health at weaning (Moeser *et al.*, 2007a; Moeser *et al.*, 2007b; Smith *et al.*, 2010), as well as increased susceptibility to pathogens (Merlot *et al.*, 2013). It is important to note that that early weaning occurs during a critical window of gastrointestinal barrier development, meaning weaning-associated stressors have the potential to disrupt the natural epithelial and immune developmental processes (Figure 1-10) (Moeser *et al.*, 2017).

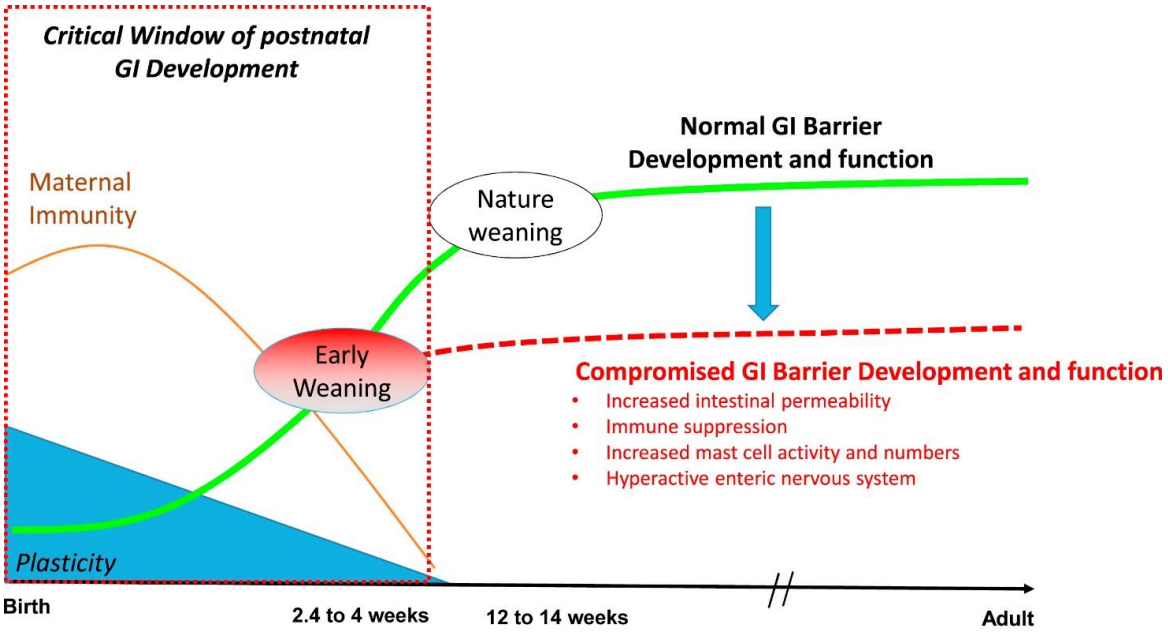


Figure 1-10: Impact of early weaning on the development of the GI Barrier. In nature, weaning is a gradual process occurring at ~12-14 weeks of age, at which time GI barrier is near fully developed. In commercial systems, weaning is abrupt and occurs at a critical period of GI barrier development between two and four weeks of age. Early weaned pigs exhibit altered intestinal barrier development which can result in permanent suboptimal barrier function and increased susceptibility to disease (red dotted line). Image from (Moeser *et al.*, 2017).

Many physiological changes have been reported as a result of weaning, the most widely studied is a deleterious effect on intestinal barrier function as a result of this stressful event. This breakdown in intestinal barrier function is characterised by a significant decline in intestinal transepithelial resistance, combined with increased permeability to paracellular probes in Ussing chamber experiments (Moeser *et al.*, 2007a; Moeser *et al.*, 2007b; Hu *et al.*, 2013). It has been demonstrated that when compared with age-matched suckling littermates, weaned pigs exhibited increased intestinal permeability which was most

pronounced at 24h post weaning but gradually declined over the two-week period post weaning (Moeser *et al.*, 2007a; Moeser *et al.*, 2007b; Peace *et al.*, 2011). In the same period, an upregulation of proinflammatory cytokines have been observed, suggesting activation of the gastrointestinal immune system following weaning (McCracken *et al.*, 1999; Hu *et al.*, 2013).

The primary method of monitoring the permeability of the intestinal barrier at weaning is via transepithelial flux. This is conducted by mounting intestinal tissue in an Ussing chamber and monitoring the mannitol or inulin flux across the epithelial tissue. In this case the higher the flux, the more permeable the tissue (Smith *et al.*, 2010; Hu *et al.*, 2013).

Weaning is a stressful event in pigs, as evidenced by the activation of the hypothalamic pituitary adrenal axis (HPA) and elevation of stress-related mediators including corticotropin-releasing factor (CRF) and cortisol in circulation (Moeser *et al.*, 2017). Activation of the HPA axis is a critical mechanism in responding to a stressor and subsequently returning to homeostasis (Moeser *et al.*, 2007b; Moeser *et al.*, 2017). This system will be described in full in section 1.4. Serum CRF levels have been shown to be elevated for the first-week postweaning, which

mirrored changes in transepithelial permeability in pigs weaned at 19 days of age (Moeser *et al.*, 2007b). In the same study, serum cortisol was also elevated in response to weaning; however unlike CRF levels, cortisol levels remained elevated throughout the weaning period. Because of this, serum cortisol did not mirror observed changes in intestinal barrier function (Moeser *et al.*, 2007b). In the intestine, the expression of CRF receptors in the jejunum, ileum and colon were upregulated in pigs weaned at 19 days of age, when compared to those weaned at 28 days of age (Moeser *et al.*, 2007b). At two weeks postweaning, pigs weaned at 15-20 days of age (early weaned) had higher jejunal CRF levels and decreased intestinal expression of CRF receptors. This suggests a downregulation of CRF receptors in response to elevated CRF (Smith *et al.*, 2010). In contrast, the expression of the receptor for cortisol (glucocorticoid receptor) was found to be increased in the jejunum of early weaned pigs compared to late weaned pigs (23-28 days) (Smith *et al.*, 2010).

Injection of CRF antagonist, alpha-helical CRF intraperitoneally to early weaned pigs at weaning, has been identified to abolish the stress-induced elevation in intestinal permeability, thus demonstrating a central role of the intestinal CRF receptor system in modulating

intestinal permeability in the weaning pig (Moeser *et al.*, 2007a; Moeser *et al.*, 2017). Other studies have demonstrated that the CRF system is upregulated in response to other stressors including *Salmonella* serovar Typhimurium challenge (Boyer *et al.*, 2015), and social stress as defined by housing a pig in a pen with three other pigs all from different litters (Li *et al.*, 2017). Taken together, these studies suggest that the intestinal CRF system is central to intestinal barrier disturbances in pigs (Moeser *et al.*, 2017).

The enteric nervous system also plays a role in bowel dysfunction (Moeser *et al.*, 2017). The complex interplay between endocrine and nervous mechanisms is apparent in stress-related bowel dysfunction. The barrier dysfunction effects of CRF administration in Ussing chamber experiments on ileal tissues harvested from six to eight-week-old pigs have been observed to be circumvented by administration of the nerve blocker tetrodotoxin. Tetrodotoxin acts by blocking nerve signal conduction by preventing the passage of sodium ions into nerve cells (Overman *et al.*, 2012). The implications and details of the effects of the enteric nervous system during weaning are discussed in section 1.5.

Studies have demonstrated an interaction between CRF receptor activation and mast cells, as CRF applied to porcine intestine in Ussing

chamber experiments has been shown to increase intestinal permeability via a mechanism involving the release of mast cell proteases and TNFα (Figure 1-11) (Smith *et al.*, 2010; Overman *et al.*, 2012; Moeser *et al.*, 2017). Mast cells are needed for host defence and wound healing. However, excessive activation of mast cells is a central mechanism in inflammatory diseases such as allergy, asthma and irritable bowel syndrome in humans (Galli and Tsai, 2012; Hamilton *et al.*, 2014; Boeckxstaens, 2015; Wouters *et al.*, 2016). Mast cells are detailed in section 1.4.4.

In the weaning pig, intestinal mast cells have been shown to be activated within 24h (Moeser *et al.*, 2007b), the weaning age is a critical factor in mast cell activity in pigs. When compared to late wean pigs (weaned at 28 days of age), early-weaned pigs (weaned at 19 days of age) exhibit greater intestinal mast cell activation at 24 h post weaning (Moeser *et al.*, 2007b). The importance of increased mast cell degranulation in early weaned pigs has further been demonstrated by the administration of the cromolyn, a mast cell stabiliser drug. This was found to prevent early weaning-induced increases in intestinal permeability (Moeser *et al.*, 2007b).

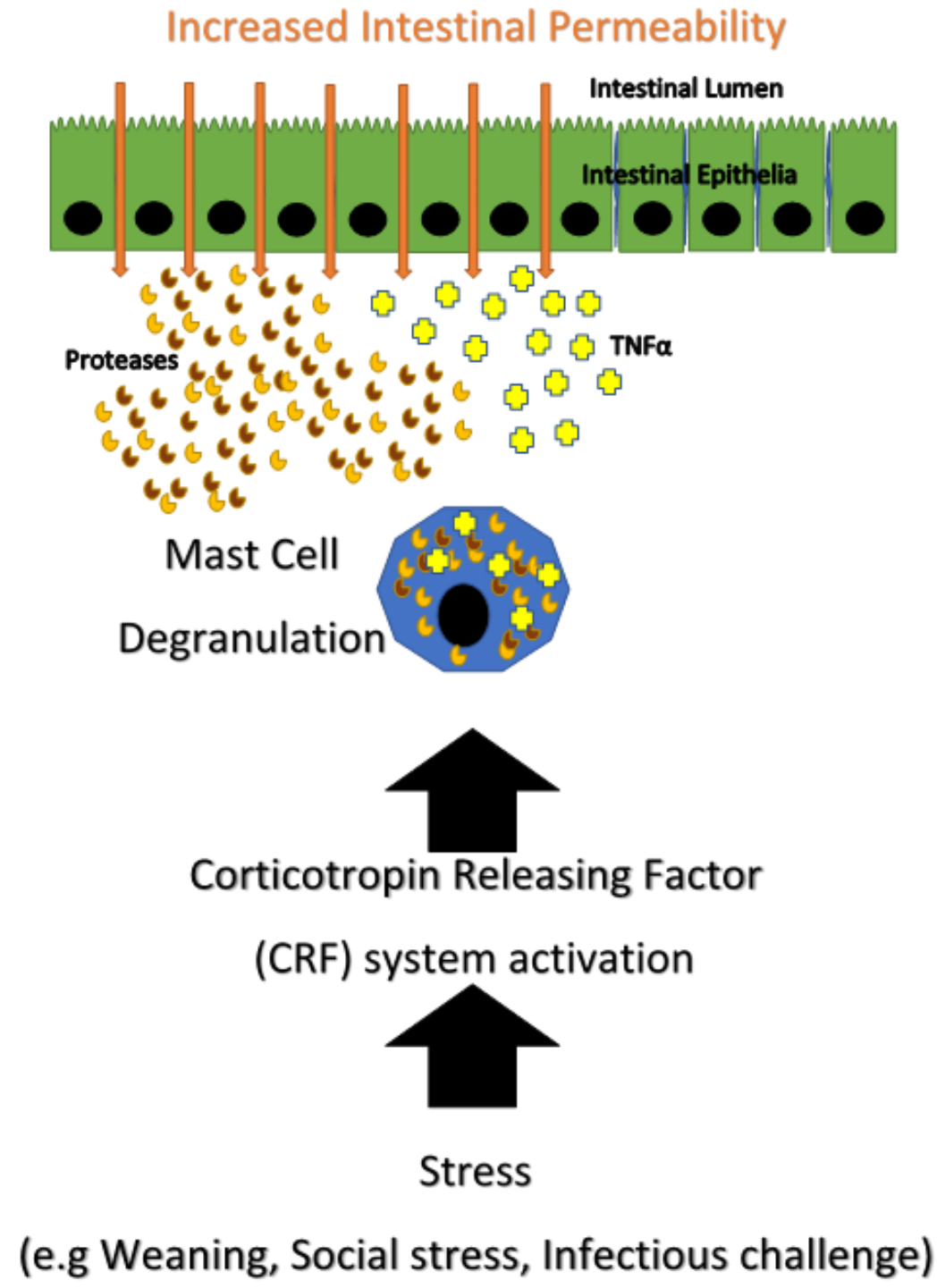


Figure 1-11: The CRF-mast cell axis. Stressors such as weaning, social stress and infectious disease trigger activation of intestinal CRF and its receptors. CRF receptor activation on mast cells causes degranulation, releasing mast cell mediators including proteases (including chymase and tryptase) and TNFα. These mast cell mediators bring about an increase in intestinal permeability.

Despite initial reductions in performance and feed intake, most weaned pigs will recover over the first week postweaning. However a subset of these pigs do not make a successful weaning transition (Moeser *et al.*, 2012), this subset is classified as having peri-weaning failure to thrive syndrome (PFTS).

Pathogens as the primary cause of PFTS has been disputed. It was found that in 51% of diarrhoeic pigs tested harboured no detectable pathogens, however, the incidence of diarrhoea increased in this study with the number of days post weaning (p <0.001) over the 3060 pigs tested (Huang *et al.*, 2012; Weber *et al.*, 2015).

PFTS is characterised by lack of eating after weaning, leading to decrease in body condition and in some cases death. Importantly, this is not a condition of the 'runts' of the litter at either birth or weaning. The condition has historically been observed at low prevalence (around 0.5% of weaned pigs) and occurs in the absence of discernible infectious, nutritional, management or environmental factors that can explain the clinical syndrome (Huang *et al.*, 2012). In this same study, a lack of convincing evidence was found after diagnostics for a number of pathogens, including viruses (e.g. rotavirus) as the causative factor of PFTS. To this extent, information available for PFTS will be considered in

conjunction with that for weaning alone as the causative factors may be intertwined, as in both cases no obvious pathogenic or animal management causes for loss of condition are apparent. This is especially important as weaning, and early life stressors may shape the long-term barrier function of the gut (Moeser *et al.*, 2012; Moeser *et al.*, 2017).

1.4 Stress and the Hypothalamic-Pituitary-Adrenal (HPA) Axis

During stress, the brain stem and the limbic system stimulates production and release of corticotropin-releasing factor (CRF) and arginine vasopressin (AVP) from the neurosecretory neurons of the paraventricular nucleus (PVN) of the hypothalamus (Smith and Vale, 2006; Ulrich-Lai and Herman, 2009).

These products travel via the hypophyseal portal system to the anterior pituitary gland where the interaction of CRF with CRF type I receptor (CRFR1) activates cyclic adenosine monophosphate (cAMP) pathway events which induce the release of adrenocorticotropic hormone (ACTH) (Smith and Vale, 2006). In the presence of CRF, AVP has a synergistic effect on ACTH release which is mediated through the vasopressin V_{1b} receptor (Webster and Sternberg, 2004). This acts by inducing the activation of phospholipase C which stimulates protein

kinase C, potentiating ACTH release (Birnbaumer, 2000). Circulating ACTH then acts upon melanocortin type 2 receptors (MC2-R) in the adrenal cortex (Smith and Vale, 2006). Via cAMP pathway events, ACTH stimulation of MC2-R promotes the conversion of cholesterol to 5-5 pregnenolone during the initial step of glucocorticoid synthesis. Leading to the production and secretion of glucocorticoids such as cortisol into systemic circulation (Tomas *et al.*, 2013).

Glucocorticoids form a negative feedback loop acting upon CRF in the PVN and ACTH in the anterior pituitary gland (Figure 1-12) (Dallman *et al.*, 1987; Watts, 2005).

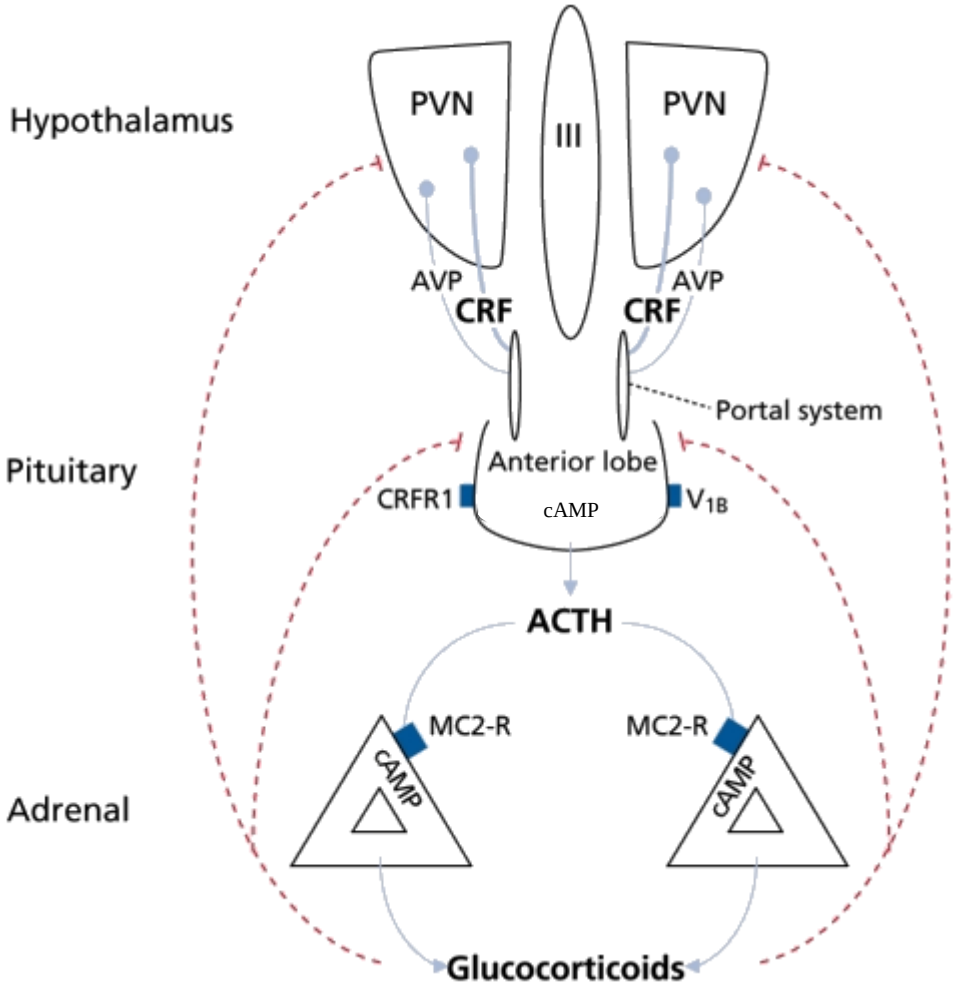


Figure 1-12: The hypothalamic-pituitary-adrenal axis. Neurons located in the paraventricular nucleus release corticotropin releasing factor (CRF) and arginine vasopressin (AVP) into the hypophyseal portal vessels in response to stress. Via these vessels, CRF and AVP interact with CRF type 1 receptor and vasopressin V1b receptors in the anterior pituitary gland. This interaction activates cAMP pathway events, inducing the release of adrenocorticotropic hormone (ACTH) into systemic circulation. Circulating ACTH binds to melanocortin type 2 receptor (MC2-R) in the adrenal cortex where it stimulates glucocorticoid synthesis and secretion into systemic circulation. Glucocorticoids, such as cortisol, regulate physiological events and inhibit further HPA axis activation (red dotted lines) through glucocorticoid receptor (GR) which is widely distributed throughout the brain and peripheral tissues. Image adapted from (Smith and Vale, 2006).

1.4.1 Cortisol and Immunity

Direct cross-talk exists between the HPA axis and the immune system. Immune cells can activate the HPA axis via cytokine release including TNF-α, IL-1 and IL-6 and type 1 interferon (Besedovsky *et al.*, 1986; van der Meer *et al.*, 1996; Turnbull and Rivier, 1999). Conversely, glucocorticoids such as cortisol can control the viability and function of many immune cell types including T-cells and granulocytes (Ashwell *et al.*, 2000; Caramori and Adcock, 2005), by suppressing the production and release of pro-inflammatory cytokines (Vandevyver *et al.*, 2013). This occurs due to the action of glucocorticoid receptor which when activated tethers and represses NF-κB, a principal regulator of the pro-inflammatory response (Dumbell *et al.*, 2016). This is why glucocorticoids are commonly used in the treatment of allergic and inflammatory disorders (Rhen and Cidlowski, 2005).

1.4.2 Cortisol and Circadian Rhythm

Molecular circadian rhythms exist in most cell types in mammals. This functions to synchronise physiological processes and behaviours to the appropriate time of day (Dumbell *et al.*, 2016). In humans, cortisol levels are subject to a robust 24-hour cycle with a peak usually between

0700 and 0800 (Kalsbeek *et al.*, 1996) and a steady rise during sleep in preparation for the stresses of waking and increased activity (Gamble *et al.*, 2014). In pigs of eight weeks of age, salivary cortisol follows a similar pattern with concentration peaking shortly after the start of 'daytime lighting' in the pig housing. Levels, however, remain high throughout the 'daytime lighting' period before dropping during the night cycle (Ekkel *et al.*, 1996). A separate study of pigs from birth to 30 days of age found that female pigs established a circadian rhythm in salivary cortisol from six days of age, whereas males displayed the same pattern from day ten (Gallagher *et al.*, 2002). Because of the circadian nature of cortisol, its use as a primary measurement of stress is disputed as concentrations can be affected by time of day, the day of the week and other circumstances (Lee do *et al.*, 2015; Martinez-Miro *et al.*, 2016).

1.4.3 CRF as an Effector of Stress

CRF is a 41-amino acid peptide which was first isolated from ovine hypothalamic tissue in 1981 (Vale *et al.*, 1981). Since its discovery, CRF has been shown to be the primary regulator of ACTH release from the anterior pituitary (Rivier and Vale, 1983). CRF is widely expressed throughout the central nervous system (CNS) and in a number of

peripheral tissues (Smith and Vale, 2006). In the brain, CRF expression is concentrated in the medial parvocellular subdivision of the PVN (Sawchenko *et al.*, 1993). In the periphery, CRF expression has been detected in the adrenal gland, testis, placenta, gastrointestinal tract, thymus and skin (Bruhn *et al.*, 1987; Audhya *et al.*, 1989; Bale and Vale, 2004).

Three other members of the CRF family have been identified; these include urocortin (Ucn) 1 (Vaughan *et al.*, 1995), Ucn2 (Reyes *et al.*, 2001) and Ucn3 (Lewis *et al.*, 2001). Ucn2 and Ucn3 are also known as stresscopin-related peptide and stresscopin respectively (Hsu and Hsueh, 2001). The widespread anatomical distribution of CRF and urocortin expression correlates with the diverse array of functions associated with this peptide family (Smith and Vale, 2006).

The physiological action of CRF is mediated through two distinct receptor subtypes belonging to the class B family of G-protein coupled receptors (Perrin and Vale, 1999). The CRF type 1 receptor (CRFR1) gene encodes one functional variant (α) along with several non-functional variants (Chang *et al.*, 1993; Chen *et al.*, 1993). CRF type 2 receptor (CRFR2) has three functional variants in humans (α, β and γ) (Perrin *et al.*, 1995) and two in rodents (α and β) (Stenzel *et al.*, 1995).

CRFR1 is highly expressed in the areas of the brain including the anterior pituitary, olfactory bulb, cerebral cortex, hippocampus and cerebellum. In peripheral tissues, low level CRFR1 expression is found in the adrenal gland, testis and ovary (Chang *et al.*, 1993; Chen *et al.*, 1993; Vita *et al.*, 1993). In contrast, CRFR2 is highly expressed in peripheral tissues and localised in only a small number of nuclei in the brain (Kishimoto *et al.*, 1995). The CRF type 2β variant expression is concentrated in the heart, skeletal muscle, skin and the gastrointestinal tract (Dautzenberg *et al.*, 2001; Dautzenberg and Hauger, 2002).

CRF binds to CRFR1 with higher affinity than to CRFR2 (Perrin and Vale, 1999; Dautzenberg and Hauger, 2002), Ucn1 has a high affinity for both CRFR1 and CRFR2, but is more potent than CRF at binding and activating CRFR2 (Vaughan *et al.*, 1995). Ucn2 and 3 are highly selective for CRFR2, with low affinity for CRFR1 (Figure 1-13) (Perrin and Vale, 1999).

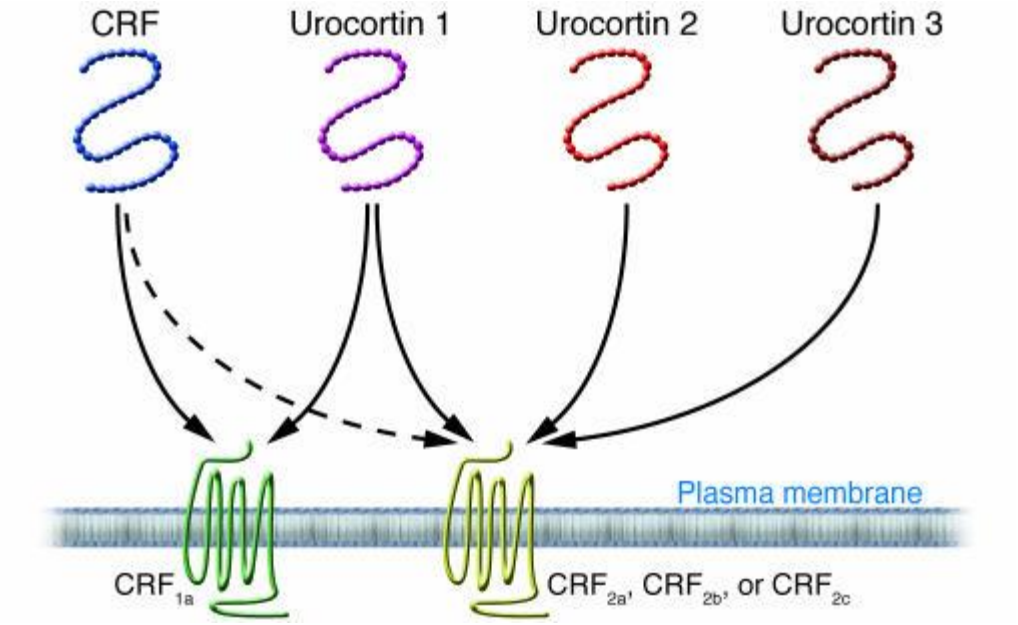


Figure 1-13: CRF receptor sensitivity. CRF binds to CRFR1 with high affinity and low affinity to CRFR2. Urocortin 1 has equal affinity for CRFR1 and CRFR2, however, is more potent then CRF at binding and activating CRFR2. Urocortins 2 and 3 are highly selective for CRFR2. Image adapted from (Tache and Bonaz, 2007).

The neuroendocrine activities of CRF are mediated through CRFR1 in the anterior pituitary gland. Binding of CRF to the CRFR1 receptor results in the stimulation of adenylate cyclase, leading to activation of the cAMP pathway which culminates in to release of ACTH from the pituitary (Bilezikjian and Vale, 1983; Perrin and Vale, 1999; Dautzenberg and Hauger, 2002). The role of CRFR2 in the regulation of the HPA axis and response to stress is less clear (Smith and Vale, 2006). Mice deficient for CRFR2 display an amplified HPA response to stress and display increased anxiety-like behaviours (Bale *et al.*, 2000; Coste *et al.*, 2000). However, administration of CRFR2 agonists and antagonists to

discrete brain regions reveal both anxiolytic and anxiogenic roles for CRFR2 (Kishimoto *et al.*, 2000).

CRF actions in the brain have subsequent effects in the gut. Activation of CRFR2 inhibits gastric function while activation of CRFR1 stimulates colonic function and enhances visceral sensitivity (Tache *et al.*, 2017). CRF pathways are also expressed within the gut wall, where CRFR1 activation in the colon stimulates the enteric nervous system, increases secretion of mucus (Chatzaki *et al.*, 2004) and alters mucosal permeability through mast cell activation (Tache and Perdue, 2004; Tache and Bonaz, 2007; Tache *et al.*, 2017). These actions are counteracted by the activation of CRFR2 in the colon of rodents (Tache *et al.*, 2017).

In the small intestine alterations in intestinal motor function have been noted in response to both physiological stress and cerebrospinal fluid injection of both CRF and Ucn1, where they exert an inhibitory effect on duodenal and small intestinal transit (Bueno and Fioramonti, 1986; Gue *et al.*, 1987; Lenz *et al.*, 1988b; Wittmann *et al.*, 1990; Kihara *et al.*, 2001). The inhibitory action is mediated directly by vagal nerves and is independent of HPA axis activation (Williams *et al.*, 1987; Lenz *et al.*, 1988a; Williams *et al.*, 1988).

In contrast to the inhibitory effects of stress (Miyata *et al.*, 1998), and cerebrospinal fluid injection of CRF and Ucn1 on small intestine and gastric function, these peptides stimulate colonic transit, defecation and diarrhea (Gue *et al.*, 1991; Monnikes *et al.*, 1996; Martinez *et al.*, 1997; Martinez *et al.*, 2004). The colonic motor activity induced by stress is mimicked by the cerebrospinal fluid injection of Ucn1 and the CRFR1 agonist ovine CRF (Perrin and Vale, 1999), whereas the selective CRFR2 agonists Ucn2 and Ucn3 injected in the same manner do not induce these effects (Martinez *et al.*, 2004). Additionally, central administration of nonspecific CRF receptor antagonists block the colonic motor stimulation induced by central injection of CRF and Ucn1, as well as by various stressors (Williams *et al.*, 1987; Gue *et al.*, 1991; Monnikes *et al.*, 1996; Martinez *et al.*, 1997; Miyata *et al.*, 1998). This is mimicked by the administration of selective CRFR1 antagonists, demonstrating that CRFR1 is central to increased colonic motility during stress (Martinez and Tache, 2006). Additionally, CRFR1 deficient mice have lower defecation scores than wild-type littermates (Bale *et al.*, 2002).

The CRF system is also implicated in increased intestinal permeability as a result of stress (Rodino-Janeiro *et al.*, 2015). Stress-induced enhancement of colonic permeability can be mimicked by

intraperitoneal administration of exogenous CRF in rats (Saunders *et al.*, 2002), and can be abolished by pre-treatment with the peripheral administration of the non-selective CRF antagonists astressin or α-helical CRF (Santos *et al.*, 1999; Soderholm *et al.*, 2002b; Barreau *et al.*, 2007).

In cultured human HT-29 cells, CRF has been observed to increase expression of TLR4, and pre-treatment of these cells with CRFR2 antagonist antalarmin abrogated this response (Yu *et al.*, 2013). Concomitant presence of CRF and lipopolysaccharide led to increased permeability to horseradish peroxidase and decreased transepithelial resistance. This effect was abolished by the application of CRFR2 antagonist astressin$_2$-B, mediated through the up-regulation of claudin 2 expression (Yu *et al.*, 2013).

A separate line of evidence in animal models highlights the relevant CRF interaction with mast cells in the regulation of intestinal permeability (Rodino-Janeiro *et al.*, 2015). CRF induced changes in intestinal permeability are significantly reduced in mast cell deficient rats (Santos *et al.*, 2000; Santos *et al.*, 2001; Soderholm *et al.*, 2002a; Santos *et al.*, 2008). Mast cells express both CRFR1 and CRFR2, activation of which

leads to the release of cytokines and other pro-inflammatory mediators (Smith *et al.*, 2010). The activity of mast cells is detailed in section 1.4.4.

CRF may also have local immune activity in the absence of psychological stress and activation of the HPA axis. When LPS, a known antigen common to gram-negative bacteria, is administered, a notable increase in CRF production is noted in the rat colon, suggesting a proinflammatory role of CRF in response to localised and systemic infection (Yuan *et al.*, 2010).

CRF may also play a role in appetite with central injection of CRF reducing food intake and weight gain, whereas administration of CRFR2 reversed this effect (Cullen *et al.*, 2001). As such, CRF production during stress in the weaning pig may contribute to the lack of feed intake during both the post-weaning growth check and PFTS.

CRF is a major factor in stress-related dysfunction in the colon by triggering the degranulation of mast cells and subsequent release of mediators causing increased permeability (Overman *et al.*, 2012). Mast cell activity in the gut breakdown is further discussed in section 1.4.4. CRF also effects the colon during times of stress via the interaction with the enteric nervous system which is detailed in section 1.5 (Figure 1-14).

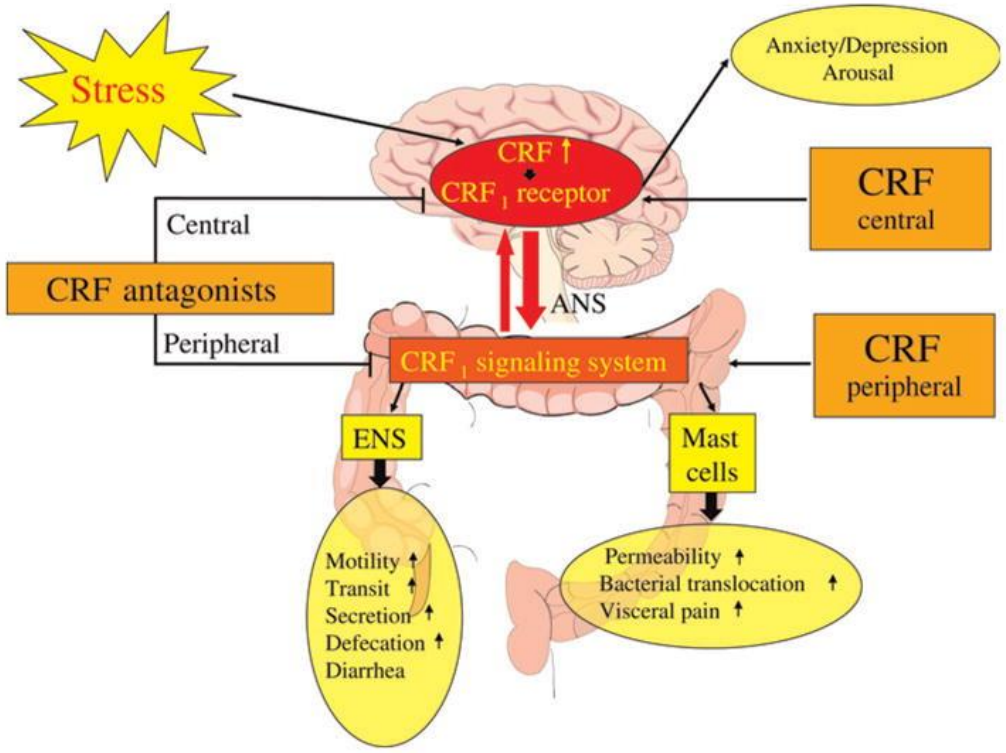


Figure 1-14: Central and peripheral actions of CRF: During stress, CRF production in the brain is increased activating the HPA axis producing systemic effects, as well as locally. Local production in the colon leads to activation and degranulation of Mast cells as well as neurons of the enteric nervous system. These processes can be reversed by CRF antagonist interaction with CRFR1. Image from (Stengel and Tache, 2010).

1.4.4 The Role of Mast Cell Granules

Mast cells are primitive cells which appear early in evolution and have evolved a multi-functional role in vertebrates (Crivellato and Ribatti, 2010). Mast cells have a key role in both innate and adaptive immunity where upon activation, mast cells release granules contained within.

Degranulation occurs within seconds of activation with the initial rapid phase complete in 5-10 minutes (Iwaki *et al.*, 2005). Mast cell granules

include proteases such as tryptases (Schwartz, 1994; McNeil *et al.*, 2007), chymases and carboxypeptidases. Histamine is the primary cause of acute reactions in mast cell activation (Jones and Kearns, 2011). The primary effects of mast cell histamine release include; increased vascular permeability and vasodilation. Also recruitment of additional mast cells and other immunocompetent cells to the site of release via activation of H4 receptors, a histamine receptor with chemotactic properties (Zampeli and Tiligada, 2009), by the histamine permeating from the site of mast cell activation (Gilfillan and Beaven, 2011). Proteases constitute 30-50% of total protein in mast cells (McNeil *et al.*, 2007). However, the proportions of tryptase, chymase and other proteases vary depending on the location of the mast cell. In mucosal surfaces such as the gut, mast cells primarily contain tryptase (Bradding, 2009). Within granules, proteases are complexed with proteoglycans which function to stabilise the proteases and regulate function (Stevens and Adachi, 2007). These proteases have been implicated in tissue remodelling and allergic inflammation upon mast cell activation (Stevens and Adachi, 2007; Gilfillan and Beaven, 2011).

1.4.5 Mast Cells in Tissue Remodelling, Repair and Fibrosis

Upon tissue injury, there are several stages of the repair process, namely: inflammation, fibroblast migration and proliferation, and remodelling. Fibrosis is the production of excessive amounts of connective tissue in the course of reactive and reparative processes (Wick *et al.*, 2013). Although the process of fibrosis is poorly understood, it is believed to be because of aberrant remodelling of the damaged tissue (Overed-Sayer *et al.*, 2013; Veerappan *et al.*, 2013). Although the absence of mast cells does not prevent wound closure, it does delay the process (Shiota *et al.*, 2010). Mast cells have been shown to accumulate at the site of injury within eight hours of mild damage to muscle (Gorospe *et al.*, 1996), and numbers may increase until ten days after injury (Trautmann *et al.*, 2000). Mast cells contribute to local inflammation via increased vascular permeability by histamine release, as well as recruitment of other cell types including fibroblasts, which are significant in wound repair (Levi-Schaffer and Kupietzky, 1990; Weller *et al.*, 2006).

Mast cells produce many mediators of tissue remodelling and wound repair, all of which have a role in normal wound repair, although the aberrant release of these can lead to fibrosis and tissue damage. These

include TGF -β which promotes fibroblast migration and proliferation (Postlethwaite *et al.*, 1987), as well as collagen formation by fibroblasts (Fine and Goldstein, 1987) and tryptases and chymases, both of which have effects on the extracellular matrix (Overed-Sayer *et al.*, 2013). Mast cell tryptase is also able to stimulate the production of type 1 collagen by fibroblasts (Cairns and Walls, 1997; Gruber *et al.*, 1997). However, both mast cell tryptase and mast cell chymase function to activate matrix metalloproteases (MMPs), leading to an increased extracellular matrix turnover in the presence of these enzymes (Tchougounova *et al.*, 2005; Iddamalgoda *et al.*, 2008). IL-13 is a cytokine which can also contribute to fibrosis through TGF-β dependent and independent mechanisms by stimulating proliferation and collagen deposition in fibroblasts (Oriente *et al.*, 2000; Saito *et al.*, 2003). CCL2 (chemokine) is another mast cell product implicated in fibrosis because it can increase fibroblast collagen deposition via upregulation of TGF-β expression (Holgate, 2008). CCL5 (also known as RANTES) acts as a mast cell chemoattractant which may contribute to the recruitment of mast cells to the site of injury in the days after the damage occurs (Mattoli *et al.*, 1995; da Silva *et al.*, 2014).

1.5 Stress & the Enteric Nervous System

The enteric nervous system (ENS) is also known as the 'brain-in-the-gut'. It can be divided into two sections: the submucosal plexus (SMP) which controls absorption and secretion in the mucosal epithelium, intermural blood flow and interactions with the immune system, and the myenteric plexus (MP) which functions to control motility (Li *et al.*, 2016b). The location of these sections within the intestine is noted in Figure 1-2. Normal function of these two systems is required for normal gut function.

A model of IBS in rats noted increased motility in the distal colon and rectum, visceral hypersensitivity and increased colonic secretion. The increased motility may contribute to the occurrence of diarrhoea and is considered a functional disorder as no pathological changes were detected in the epithelial tissues or brain (Li *et al.*, 2016b). In IBS patient biopsies, mast cells appear to locate closer to colonic nerve endings, and this may contribute to pain perception (Barbara *et al.*, 2004). It has also been demonstrated that the supernatant from IBS biopsies can activate the enteric nervous system dependent upon mast cell mediators including histamine, serotonin and proteases (Figure 1-15) (Buhner *et al.*, 2009; O'Malley, 2015).

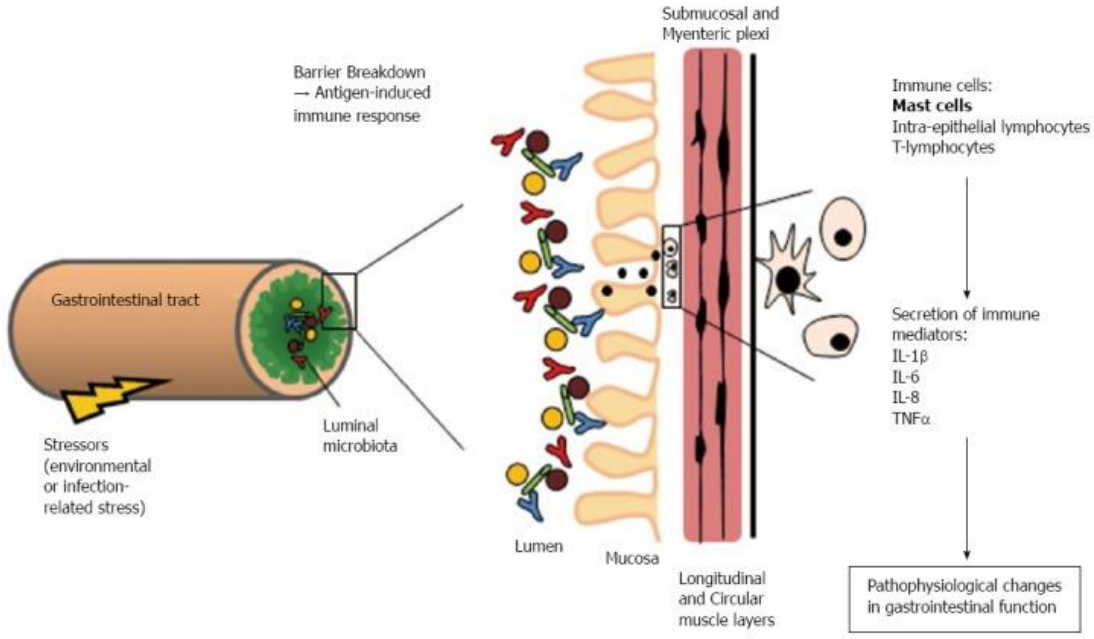


Figure 1-15: Enteric nervous system and gut breakdown: Following increased permeability brought about by the action of CRF in the intestine, a localised immune response is triggered recruiting immune cells such as mast cells and T-lymphocytes. Degranulation of mast cells in proximity to the submucosal and myenteric plexi lead to visceral sensitivity and episodes of IBS in humans. Image from (O'Malley, 2015)

Mast cell interaction with the nervous system is bidirectional (Figure 1-16). An estimated 70% of intestinal mucosal mast cells are in direct contact with nerves, and another 20% are within 2 µm (Stead *et al.*, 1989). Mast cell peptides such as histamine and tryptase bring about release of neuropeptides such as substance P from proximal nerve endings via the activation of protease-activated receptors 1 and 2 (van der Kleij *et al.*, 2003; Kleij and Bienenstock, 2005). Regulation of mast cell degranulation may also be under the control of neuroactive

peptides such as Substance P which will lead to further mast cell activation (Figure 1-16) (Matsuda *et al.*, 1989; Li and Zhao, 2015).

Crosstalk between the HPA axis and enteric nervous system is complex, CRF can be produced locally in the tissues of the intestine and not just in the paraventricular nucleus of the hypothalamus as detailed in section 1.4.3.

CRFR1 has been observed to be expressed in both the myenteric and submucosal plexuses in guinea pigs, however CRFR2 expression is absent (Liu *et al.*, 2005). In the same study, activation of these receptors evoked slowly activating depolarising responses associated with elevated excitability in both myenteric and submucosal neurons (Liu *et al.*, 2005).

In the colon CRF can act via CRFR1 located in the myenteric plexus, thereby stimulating colonic contractility (Buckley *et al.*, 2014). As such, CRF may be a stimulatory factor in bouts of IBS in humans and could contribute to diarrhoea and visceral sensitivity in animals during stress (Buhner and Schemann, 2012). To this extent, CRF plays a vital role in both the immune and nervous status of the gut during stressful life events such as weaning in pigs (Moeser *et al.*, 2017).

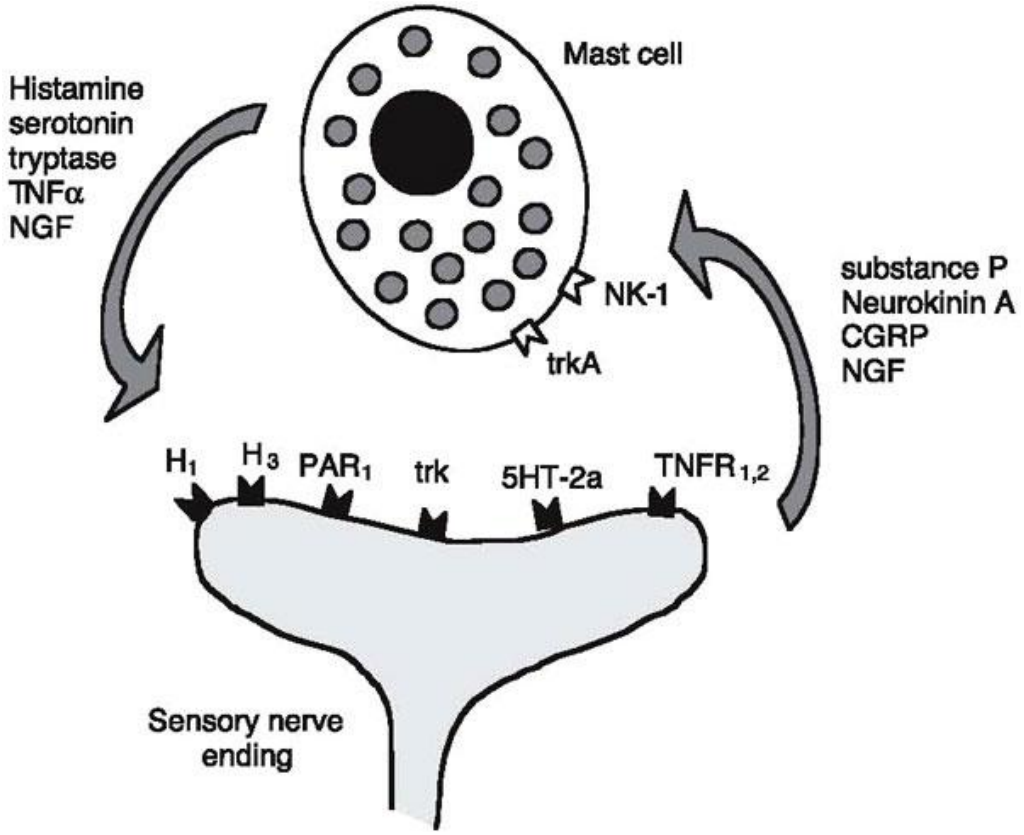


Figure 1-16: Interaction between mast cells and enteric nerve endings: Bi-directional signalling between mast cells and enteric nerve endings. Histamine, serotonin and tryptase can bring about the release of substance P and Neurokinin A from enteric nerve endings, which are in turn able to bring about mast cell degranulation. H = histamine; 5HT2A = serotonin 2a; NGF = nerve growth factor; NK-1 = neurokinin 1; PAR = protease-activated receptor; TNFR = tumour necrosis factor receptor; trk = neurotrophin tyrosine kinase receptor. Image from (Kleij and Bienenstock, 2005)

1.6 Probiotics Overview

In the previous sections, the physiology of the gut and causative factors of stress-related bowel dysfunction have been discussed. Although these processes are important for maintaining homeostasis during intermittent stressful episodes, the stress experienced by weaned animals in the commercial pig industry is exacerbated by the young age of the animals (McLamb *et al.*, 2013). The reduction in growth after

early weaning can increase the time taken for the animal to reach slaughter weight (Do, 2012), and as such incurs an economic cost. Weaning lends itself as a time for intervention to reduce stress. As communication along the brain-gut-axis is complex and may in some way be determined by the flora inhabiting the gut, a probiotic intervention may be an effective way to alleviate stress in the weaning pig (Moos *et al.*, 2016; Neufeld *et al.*, 2016). The use of probiotics as growth promoters as an alternative to antibiotic use which has dominated this function for around 50 years, is beneficial as the rise of antibiotic-resistant pathogens can be attributed to the increased use of these antimicrobials in both humans and animals (Thacker, 2013). This is particularly important when considered in the context of the 2006 European Union ban on the use of antibiotics as growth promoters and other restrictions on antibiotic use around the world (Maron *et al.*, 2013).

Probiotics are defined as live microorganisms which when administered in adequate amounts confer health benefits on the host (Indian Council of Medical Research Task *et al.*, 2011; Hungin *et al.*, 2013). These are distinct from prebiotics. Prebiotics are indigestible oligosaccharides which when administered to the host, select for the growth of

beneficial microorganisms. Symbiotic can be defined as a combination of a probiotic, and a prebiotic which selects for its growth (Hungin *et al.*, 2013).

Probiotic use has been applied to a variety of conditions with varying results. In the following sections, the activities of various probiotic species will be detailed with a view to the potential benefits to use in pigs during weaning.

1.7 Probiotics in Health

Newborn children and animals enter the world with a sterile gut, with the immediate exposure to the environment beginning the process of bacterial colonisation (Morelli, 2008). Initial colonisation is as a result of exposure to the vagina, rectum and skin of the mother as well as the surrounding environment (Sohn and Underwood, 2017). This bacterial colonisation is unstable and in flux for the first few weeks of life, however, after a year bacterial populations resemble adult patterns (Pamer, 2007). By seven to ten days of age, healthy breastfeeding neonates are colonised by microbiota including *Lactobacillus* sp, *Escherichia coli* sp and *Enterococcus* sp but with a clear-cut predominance for *Bifidobacterium* sp (Sanders *et al.*, 2010). However,

Lactobacillus and *Bifidobacterium* were only detected in 5% of premature infants one month after birth (Gewolb *et al.*, 1999).

The developing gut microflora has been implicated as a causal factor in the differentiation and maturation of the gut in zebrafish (Bates *et al.*, 2006). It is also believed to maintain a state of regulated inflammation, providing cross-talk between the microflora and the intestinal epithelium and GALT (Neu, 2007; Weng and Walker, 2013). This interaction aids in the development of the innate immune defences and promotes pathogen recognition while also enabling the establishment of commensal microflora (Kaplan *et al.*, 2011; Jakaitis and Denning, 2014). The early colonisation of the gut is likely to have a knock-on effect on the succession of the microbiome. According to the founder effect, the original colonising microbiota are instrumental in the successional direction of the microbiome (Groer *et al.*, 2014). As a result, early colonisation by certain bacteria may lead to long-term health issues such as obesity via changes in metabolite profiles (Mischke and Plosch, 2013).

It is important that neonates be exposed to non-pathogenic microorganisms at this early stage to establish a healthy intestinal microflora (Wilkins and Sequoia, 2017), particularly true with premature

births. To this extent, probiotic administration may be beneficial (Shi *et al.*, 2016). Indeed, many studies have observed the benefits of the administration of various probiotic species on preterm neonates (Bertelsen *et al.*, 2016; Sohn and Underwood, 2017; Uberos *et al.*, 2017).

The long-term application of *Lactobacillus acidophilus* NCIMB701748 and *Bifidobacterium bifidum* ATCC15696, on the bacterial colonisation of the gut of preterm infants increased proportions of these bacteria in stool samples from supplemented individuals during the period of supplementation (Abdulkadir *et al.*, 2016). However, levels of *Lactobacillus* dropped after cessation of probiotic administration, whereas *Bifidobacterium* levels remained higher than in the control group. This suggests that this species and strain of *Bifidobacterium* can effectively colonise the gut of pre-term infants where dysbiosis, the absence of normal colonisation (Bertelsen *et al.*, 2016), leaves an available niche. As such the colonisation with this 'beneficial' bacteria may improve the development of the gut microbiota in preterm infants where normal bacterial colonisation may be inhibited (Abdulkadir *et al.*, 2016).

The role of probiotic supplementation in healthy adults is less well documented because the diverse ecology of the gut microbiota is usually in balance, and therefore the intervention of a probiotic does not alter the microbial diversity (Kristensen *et al.*, 2016). Probiotics are most effective during episodes of dysbiosis when the probiotic fills the vacant ecological niche, defined as a multidimensional space of resources and environmental conditions that together define where an organism can survive and grow. If left vacant, such a niche may allow outgrowth of potentially pathogenic microorganisms usually held in check by normal intestinal flora (Dunne, 2001; Gareau *et al.*, 2010; Pereira and Berry, 2017).

Regular probiotic supplementation may be beneficial as prophylaxis against sudden instances of dysbiosis (Kopp-Hoolihan, 2001). However, some studies have reported improvements in day-to-day stress due to probiotic supplementation, including a reduction in examination related stress in medical students after *Lactobacillus casei* intake (Kato-Kataoka *et al.*, 2016). Administration of lactic acid bacteria such as *Lactobacillus acidophilus* has been observed to alleviate stomach cramps and other symptoms in individuals who experience lactose intolerance (Pakdaman *et al.*, 2016). In addition,

Lactobacillus helveticus MTCC 5463 has been observed to increase serum calcium uptake in geriatrics which may have a direct effect on bone density. Participants in this study also reported improved bowel movement and generalised wellbeing (Gohel *et al.*, 2016).

In pigs, it has been demonstrated that the commercially available probiotic preparations Bibalance (Shiseido Pharmaceutical Co. Ltd, Tokyo, Japan) which contains *Bifidobacterium longum* and *Bifidobacterium infantis*; Neoracton (Asahi Beer Pharmaceuticals Co. Ltd, Tokyo, Japan) which contains *Enterococcus faecalis* and *Bifidobacterium* sp.; Yakult Seichoyaku BL (Yakult Honsha Co. Ltd, Tokyo, Japan) which contains *Lactobacillus casei* and *Bifidobacterium breve* and Yakult Seichoyaku (Yakult Honsha Co. Ltd) containing *Lactobacillus casei* and *Enterococcus faecalis,* are all able to increase short chain fatty acid production in the caecal contents. This increases the short chain fatty acids available as an energy source for colonocytes. The increase in production is thought to be due to the breakdown of carbohydrates which are resistant to indigenous bacteria (Sakata *et al.*, 2003).

A number of different probiotic cultures have been identified to increase growth performance in pigs, including SynerZymeH10

(SynerBig, South Korea) which contains *Bacillus cogagulance*, *Bacillus linchenformis* and *Bacillus subtilis* (Balasubramanian *et al*., 2016); *Lactobacillus plantarum* ZJ315 (Suo *et al.*, 2012) and *Bacillus toyoi* (Kyriakis et al., 2003). The mode of action of these probiotic cultures is yet to be elucidated.

Although the modes of action in each instance differ, alterations in the metabolome, the total metabolite profile of the microbiome, brought about by introducing specific bacterial strains which possess metabolic pathways not present in the commensal bacteria changes the clinical outcome (Larsen and Dai, 2015; Ahmed *et al.*, 2016). This is particularly evident in the metabolism of lactose by lactic acid bacteria introduced into subjects with lactose intolerance, whereby lactic acid bacteria metabolise lactose into other sugars to which the subject is not intolerant. In other cases, the interaction may be more direct. In a study of the effects of *Lactobacillus casei* strain Shirota on the activity of the HPA axis during water avoidance stress in rats, where the rats were placed on a platform above a water-filled cage for one hour. A reduction in the number of CRF producing cells in the paraventricular nucleus of the hypothalamus coupled with a reduction in plasma corticosterone, cortisol in humans and pigs, was observed. The authors

suggest that *Lactobacillus casei* strain Shirota may prevent hypersecretion of cortisol via vagal afferent signalling from the gut to the brain (Takada *et al.*, 2016).

The brain-gut axis is an emerging field, with implications for many behavioural disorders (Evrensel and Ceylan, 2015). The bacteria within the gut produce antimicrobial compounds; short chain fatty acids, such as acetate, butyrate and propionate, which form the main energy source for colonic epithelial cells (Weir *et al.*, 2013; Larsen and Dai, 2015). They also produce most of the common neurotransmitters found in the brain (Dinan and Cryan, 2016). These interact with the enteric nervous system, although the exact interaction is not yet fully understood and may have strain-specific mechanisms depending on the resident microflora (Grenham *et al.*, 2011). Indeed, probiotic supplementation has been observed to bring about behavioural improvements in subjects with autism (Santocchi *et al.*, 2016), although this may be more closely related to improvements in dysbiosis experienced by autistic individuals brought about by probiotic supplementation. The composition of the intestinal microbiota may also play a role in anxiety and depressive disorders (Foster and McVey Neufeld, 2013).

The vagus nerve constitutes the primary route of information from the gut luminal environment to the central nervous system as anxiolytic activity observed after administration of *Bifidobacterium longum* NCC3001, which acts by reducing the sensitivity of enteric neurons, was absent after the experimental mice were vagotomised (Bercik *et al.*, 2011).

Therefore, the microbiota present in the colon of the pig at weaning may influence the perception of weaning stress and is certainly a key factor in the modulation of the HPA axis during stress.

1.8 Probiotics and Infectious Disease

Probiotics may play a dual role in the instance of infectious disease. Firstly the introduction of a probiotic may occupy a niche which may otherwise be inhabited by pathogenic bacteria (Dunne, 2001). Probiotics also serve to colonise the gut following antibiotic treatment for infection as antibiotic use will deplete both beneficial and pathogenic bacteria (Hickson, 2011). Secondly, probiotics have been observed to secrete proteins such as bacteriocins and metabolites which either inhibit the growth of pathogens or attack toxins (Dobson *et al.*, 2012; Hegarty *et al.*, 2016).

Probiotics have been widely studied as an intervention in hospital-acquired nosocomial infections, with a particular focus on *Clostridium difficile* infections (Hickson, 2011). In a co-culture experiment, it was observed that either *B. longum* IPLA20022 or *B. breve* IPLA20006 were able to inhibit *C. difficile* LMG21717 growth when fructooligosaccharides were provided as the carbon source (Valdes-Varela *et al.*, 2016). The same study also found that a combination of these probiotic strains and commercially available prebiotics could reduce the toxicity of *C. difficile* supernatant. It has been suggested that a protease secreted by *Bacillus clausii* may counteract the cytotoxic effects of *C. difficile* toxin (Ripert *et al.*, 2016).

Studies have been conducted in hospitals to observe the efficacy of various probiotics in the prevention of *C. difficile* infections following antibiotic use. In a retrospective study, *Lactobacillus plantarum* 299v was found to significantly reduce such infections in patients given antibiotics following transplantation or receiving immunosuppressive therapy for any other reason (Kujawa-Szewieczek *et al.*, 2015). The same results were observed when a combination of *Lactobacillus acidophilus* CL1285, *Lactobacillus casei* LBC80R, and *Lactobacillus rhamnosus* CLR2 were administered, reducing the number of infections

per 10,000 patient days from 18 to 2.3 (Maziade *et al.*, 2015). It is likely that in these instances, the ecological niche left after antibiotic therapy is occupied by the probiotic and therefore preventing pathogen colonisation (Dunne, 2001).

Probiotic cultures have been observed to have effects on other pathogens. A culture containing: *Lactobacillus murinus* DPC6002 and DPC6003, *Lactobacillus pentosus* DPC6004, *Lactobacillus salivarius* DPC6005, and *Pediococcus pentosaceus* DPC6006 has been observed to reduce diarrhoea in *Salmonella enterica* serovar Typhimurium challenged pigs (Casey *et al.*, 2007).

Faecal microbiota transplantation (FMT) is the process of transplanting the whole faecal microbiome of a healthy individual into an individual experiencing dysbiosis. This procedure has been observed to be very effective in the treatment of *C. difficile* infections with a 90% recovery rate and a low rate of recurrence (Borody *et al.*, 2015).

Clostridium difficile serves as an excellent example of a pathogen which is particularly well suited to probiotic intervention, as it is strongly associated with the dysbiosis brought about by antibiotic treatment (Lau and Chamberlain, 2016). However, probiotics have shown promise in the treatment of other infections including *Helicobacter pylori*

infection (Goli and Moniri, 2016), and *Cryptosporidium parvum* infection (Del Coco *et al.*, 2016).

In conclusion, a healthy adult human gut can harbour 300-500 different bacterial species, and many more strains (Quigley, 2013). The metagenome of this microbiome encodes around 5 million genes (D'Argenio and Salvatore, 2015). The net effect of this metagenome is to confer many metabolic, immune and protective functions on the host (Larsen and Dai, 2015; Ahmed *et al.*, 2016). As such, any member of this vast community may be selected for application as a probiotic (Sanders *et al.*, 2010; Papadimitriou *et al.*, 2015). However, when using the term 'probiotic' it is important to understand the diversity of both species, kingdoms including prokaryotes and fungi, and functional properties that this term encompasses. Each microorganism selected will have an individual mode of action and its own set of metabolic processes (Papadimitriou *et al.*, 2015), the net effects of which may be dependent upon the constituent members of the microbial ecosystem into which it is entered (McFarland, 2014).

Efforts have been made to improve the efficacy of probiotics via genetic engineering, to introduce desirable metabolic traits (Gosalbez and

Ramon, 2015). However, the application of genetically modified microorganisms as probiotics is beyond the scope of this review.

Although the majority of microorganisms utilised as probiotics are bacteria (Czerucka *et al.*, 2007), yeasts also form a small but important part of the intestinal ecosystem. Yeasts constitute less than 0.1% of healthy gastrointestinal microbiota with *Candida albicans* being the most prominent species (Czerucka *et al.*, 2007). *Saccharomyces cerevisiae boulardii,* which is not a natural member of the normal microbiota*,* is a yeast which has been utilised as a probiotic (West *et al.*, 2016), and its properties as a probiotic will be the subject of the next section and its effects are the subject of the present study.

1.9 Saccharomyces cerevisiae boulardii

Saccharomyces cerevisiae boulardii (SCB) is the only yeast currently approved as a probiotic for human consumption (Venugopalan *et al.*, 2010). As a probiotic it has been used to treat a variety of conditions including antibiotic-associated diarrhoea and recurrent *Clostridium difficile* infection (Khatri *et al.*, 2013).

In mice, concentrations of 10^7 colony forming units per gram of stool is achieved when 5 x 10^8 colony forming units of SCB is orally intubated daily. In this instance, the yeast still numbered 7.3 x 10^6 CFU g^{-1} of faeces three days after cessation of yeast administration with levels undetectable after one week (Barc *et al.*, 2008). In the present study, daily dosing of 3.3 x 10^9 CFU to pigs by oral syringe led to levels of ~10^5CFU g^{-1} in both faeces and colon digesta (Le Bon, 2012b).

One of the primary advantages of using a yeast as a probiotic is yeasts are not susceptible to antibiotic treatment which would kill bacterial probiotics, making it ideal for administration to human patients undergoing antibiotic therapy (Czerucka *et al.*, 2007). It is also advantageous that the transfer of antibiotic resistance genes is less frequent between yeast and bacteria than between different bacterial species (Alsmark *et al.*, 2013). SCB is a tropical yeast species which was first isolated from lychee and mangosteen fruit by the French scientist Henri Boulard in 1923 (Khatri *et al.*, 2013).

It is thought that SCB confers protection against diseases via specific proteins including a 54 kDa serine protease which has been observed to cleave *Clostridium difficile* toxins A and B, preventing interaction with colonic mucosa (Castagliuolo *et al.*, 1999). Another 120kDa protein may

reduce secretion caused by cholera toxin by reducing cyclic adenosine monophosphate (cAMP) levels (Czerucka *et al.*, 1994). A 63kDa phosphatase protein produced by SCB has also been observed to inhibit the *Escherichia coli* toxin in the rat small intestine (Buts *et al.*, 2006). However, upon further identification of these proteins after genome sequencing, it was found that these proteins are not exclusive to the boulardii strain of *Saccharomyces cerevisiae* (Khatri *et al.*, 2013).

In human colon cancer-derived cell line T-84, SCB administration decreased interleukin-8 secretion during enterohaemorrhagic *E.coli* (EHEC) and *Shigella flexneri* infection via inhibition of the NFκB signalling pathway (Dahan *et al.*, 2003; Mumy *et al.*, 2008). SCB also has effects upon adhesion, migration and processing of pathogenic microorganisms. These effects include reducing translocation of *Candida albicans* from the gastrointestinal tract to the mesenteric lymph nodes in mouse intestine (Berg *et al.*, 1993) and inhibition of adhesion of *Entamoeba histolytica* and *Clostridium difficile* in *in vitro* experiments (Rigothier *et al.*, 1994; Tasteyre *et al.*, 2002). The outer membrane of SCB is also rich in mannose when compared to other yeasts (Czerucka *et al.*, 2007; Tiago *et al.*, 2012). This outer membrane binds strongly with many enteric pathogens, therefore preventing

pathogens such as *Salmonella typhimurium* and *Escherichia coli* O157 from binding to the mucous membrane of the gastrointestinal tract (Gedek, 1999; Czerucka *et al.*, 2000; Tiago *et al.*, 2012).

SCB has been observed to have differential effects on the healthy and inflamed mucosa. Many studies on the effects of probiotic SCB note an immunomodulatory effect including increased production of IgA (Buts *et al.*, 1990; Rodrigues *et al.*, 2000). However, other studies have found no increase in immune modulation in the healthy intestinal tract, with no increase in B cells and no antibodies reactive to SCB detected in the mucosa even after multiple doses of the probiotic. This has been confirmed by minimal changes in transcription in mesenteric lymph nodes after SCB administration when assessed by RNA-seq, leading the authors to conclude that the minimal number of gene expression changes detected in this analysis suggest that administration of SCB in the context of the healthy mucosa does not induce an inflammatory immune response and has little effect in potentiating B and T cell responses (Hudson *et al.*, 2016).

Many benefits of probiotic SCB modulation during and after infection and inflammation have been observed. Indeed, in inflamed mucosa, SCB has been observed to exert a weak immune response which is not

specific to the yeast itself which may contribute to a protective mechanism provided by such low-grade inflammation (More and Swidsinski, 2015).

The constituent elements of the yeast cell wall may also act as a prebiotic. These elements such as mannose, glucans and chitins act as excellent fermentable substrates for microbial fermentation, especially in short-chain fatty acid producing bacteria (Czerucka *et al.*, 2007). This explains the increased butyrate production observed in the presence of SCB (Schneider *et al.*, 2005). Both live and autoclaved SCB administration has yielded increased butyrate production. However, this aspect of SCB requires additional study in a clinical setting (Oeztuerk *et al.*, 2005).

SCB may also provide functions to aid in the maintenance and repair of tight junctions and the extracellular matrix via different mechanisms. Firstly, by altering the expression of tight junction proteins including claudin and occludin genes (Czerucka *et al.*, 2000; Rajput *et al.*, 2013; Rao and Samak, 2013). SCB may also aid in the repair of the mucosal barrier via a physical barrier effect whereby SCB forms an interlaced structure at mucus membranes, therefore making it a stronger barrier

than mucus alone to prevent pathogenic microorganisms reaching the mucosa (Swidsinski *et al.*, 2009; Rao and Samak, 2013).

In healthy individuals the normal commensal bacteria compete for metabolites, hindering pathogen colonisation (Dunne, 2001). It is suggested that the presence of SCB in the gut may perform this sequestering function in situations of dysbiosis. However, the transient nature of SCB colonisation of the gut may mean SCB is not competitive enough to maintain colonisation once the commensal microbiota is restored (Samonis *et al.*, 2011). This 'makeshift' function allows the host to rebuild the mucus layer after insult while under the protection provided by the presence of SCB (More and Swidsinski, 2015).

Because of these many benefits of SCB administration, it lends itself as an ideal probiotic for intervention in weaning pigs where the animals may otherwise be susceptible to many of the pathogens and problems associated with both stress-related bowel breakdown and dysbiosis.

The genomes of a number of SCB strains have been sequenced. Strain ATCC MYA-796 was found to have a genome of 11.6 Mb, with 5, 305 putative open reading frames (Batista *et al.*, 2014). The genomes of *Sb-biocodex* and *Sb-unique28* comprise 12 and 12.1Mb respectively (Khatri *et al.*, 2017). SCB strains share ~3100 orthologous proteins with one or

more *Saccharomyces cerevisiae* strains suggesting a large conserved protein repertoire, however SCB cannot sporulate (Khatri *et al.*, 2017). Genomic analysis could not identify any probiotic features exclusive to SCB as all SCB proteins are homologous with proteins identified in *Saccharomyces cerevisiae* strains (Khatri *et al.*, 2017).

1.10 Next Generation Sequencing

Next-generation sequencing (NGS) has revolutionised the field of genetics. The term 'next-generation sequencing' refers to high output or highly parallel sequencing methods which produce data on the genome scale (Levy and Myers, 2016). Different methodologies exist, including Pacific Biosciences, Illumina, Ion Torrent and Roche 454 (Mardis, 2017).

These technologies can be categorised as either ensemble-based, i.e. sequencing many identical copies of a DNA molecule, or single molecule based i.e. sequencing a single DNA molecule. Ensemble-based technologies such as Illumina and Roche 454 benefit from low sequencing error rates (<1%) dominated by single mismatches (Kukurba and Montgomery, 2015). However, ensemble-based technologies produce relatively short reads of up to 350 bp. By comparison, Pacific

biosciences single-molecule real-time (SMRT) has a higher rate of errors (~5%) which results in misalignment and loss of sequencing reads due to the difficulty in aligning erroneous reads to a reference. However, this technology is capable of producing longer reads of 4200 to 8500 bp (Carneiro *et al.*, 2012). These long reads make the technology well suited to de novo transcriptome assembly (Kukurba and Montgomery, 2015).

As a reference exists for the *sus scrofa* genome and transcriptome, the long reads afforded by SMRT were not required for *de novo* transcriptome assembly. Therefore, the low error rate of Illumina sequencing made this technology the best suited to this porcine RNA-seq study.

Illumina technology depends upon bridge amplification of adaptor bound DNA sequences on the surface of a flow cell. The flow cell is covered with a lawn of sequences complementary to the adaptor sequence ligated to the DNA fragments of interest. Because of this setup and different adaptors annealed to each end of the target fragment, elongation will form a double-stranded bridge on the surface of the flow cell with the denaturation step freeing the two strands which are then both anchored to the surface of the flow cell (Goodwin

et al., 2016). This process is repeated until a 'colony' of identical sequences consisting of around 1000 sequences which measures approximately 1 μm across (Adessi *et al.*, 2000). Sequencing is then carried out with reversible terminator nucleotides which are fluorescently labelled, each with a distinct colour (Levy and Myers, 2016). In this sequencing process, the sequence complementary to one of the two adaptor sequences is used as a primer then one nucleotide is added at a time and imaged in steady state as each base added is a sequence terminator (Bentley, 2006). After the base added to each 'colony' is determined the fluorophore is cleaved off, and the terminating bases are activated allowing another round of base addition. Paired-end sequencing refers to sequencing in one direction by priming the sequencing using a sequence complementary to one adaptor, and then in the other direction using a sequence complementary to the other adaptor sequence. Both ends of the DNA fragments are available for sequencing from the bridge polymerised chain reaction (PCR) process (Figure 1-17).

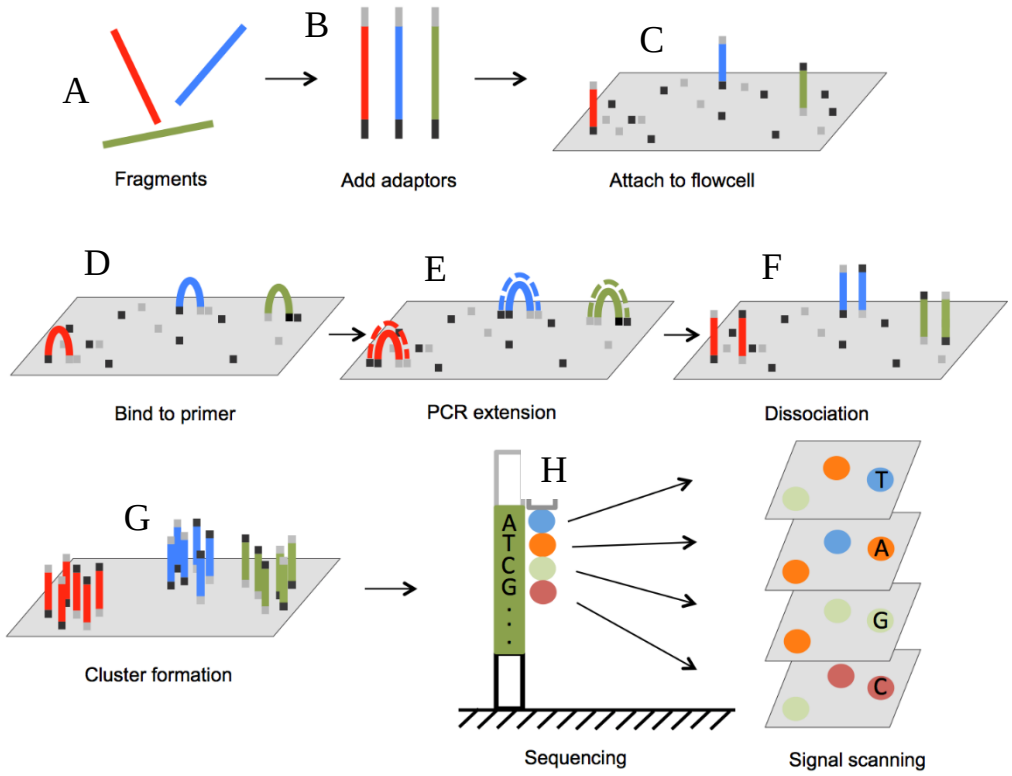


Figure 1-17: Illumina sequencing: A diagram to show the process of sequencing DNA fragments using Illumina sequencing. A. DNA sample of interest is fragmented and size selected to the required length. B. sequencing adaptors are ligated to the size selected DNA and made single-stranded C. DNA fragments are washed across a flow cell where the adaptor sequences bind with the primers mounted on the flow cell. D. adaptor sequences on the unattached end of the DNA sequences hybridise with corresponding primers on the flow cell surface forming a 'bridge'. E. PCR amplification provides the complementary strand to the bound sequence. F. disassociation of these sequences allows steps D and E to be repeated until a cluster of identical sequences in both orientations is formed (G). H. a PCR primer which hybridises with the adaptor ligated to one end of the DNA fragments is added. DNA polymerase binds to this primer and adds the first fluorescently-labelled terminator to the sequence. Lasers are used to activate the fluorescent label to allow imaging and identification. The terminator group is then removed from the first base, allowing the next base to be added. Each of the terminator bases (A, T, G and C) fluoresces at a different wavelength to allow identification. This process is repeated a predetermined number of times to provide a given length read and is conducted simultaneously on every cluster on the flow cell. Image adapted from (Yuan Lu, 2016).

1.10.1 Transcriptome Profiling

Techniques for profiling of the transcriptome has advanced in line with advances in sequencing technology. Early attempts in the 1990s to characterise the transcriptome utilised expressed sequence tag (EST)

sequencing. This technique involved cloning of cDNA sequences before sequencing, providing information on presence and abundance of these sequence tags which represented specific transcripts (White *et al.*, 1993). However, the high cost and semi-quantitative nature of this technique led to limited use.

Serial analysis of gene expression (SAGE) also emerged during this period. This drove down the cost of sequencing by utilising smaller tag length, 15 bp for the short SAGE method, 21bp for the long SAGE method (Velculescu *et al.*, 1995; Powell, 1998). However, with the emergence of DNA microarray technology in the mid-1990s, earlier techniques for quantifying transcript abundance across the whole transcriptome became obsolete. This technique involves the hybridisation of fluorescently labelled sequences representing a given transcript to complementary sequences which are attached to a solid surface. The main limitation of this technique is that prior knowledge of a transcript is required to design a probe to detect its presence and abundance, although problems were also encountered with cross hybridisation and high background noise (Hrdlickova *et al.*, 2016).

The advent of highly parallel sequencing (Next-generation sequencing) in the 2000s brought about a paradigm change in this area of research,

its ever-decreasing costs and increasing applications, contributing to large uptake of this technology (Levy and Myers, 2016). Advantages of utilising next-generation sequencing technology to characterise transcriptomes include no need to have prior knowledge of transcripts leading to transcript discovery, as well as identification of single nucleotide polymorphisms and alternative splicing events (Wang *et al.*, 2009; Burgess, 2016). Many applications of this technique require a full genome of the target species to 'map' the transcriptomic data onto, however, where this is not available a *de novo* transcriptome can be constructed directly from the data to serve as a reference for differential expression calculations (Lowe *et al.*, 2017).

RNA sequencing utilises next-generation sequencing to sequence fragments of messenger RNA to quantify the gene expression of every gene in a given tissue (Wang *et al.*, 2009; Lowe *et al.*, 2017). Sequencing library generation requires the extraction of total RNA from a given tissue or cell type followed by a step to deplete the ribosomal RNA from the sample (Abernathy and Overturf, 2016). This step is necessary as ribosomal RNA typically constitutes over 90% of the total RNA in the cell, and removal of this selects for the 1-2% comprising messenger RNA (Conesa *et al.*, 2016). The sample is then subjected to reverse

transcription into double-stranded cDNA. Adapters are then ligated to cDNA fragments as with genomic sequencing, and the library is sequenced as in Figure 1-17 (Marguerat and Bahler, 2010). Data are then mapped to a reference, e.g. genome of the origin species, providing a number of sequencing reads which map to each annotated feature in the reference. Normalisation techniques then allow direct comparison between samples and calculation of differential gene expression to identify transcriptional changes between treatments (Finotello and Di Camillo, 2015).

RNA sequencing techniques have been applied to a wide range of porcine studies. These studies include the identification of gene expression alterations in piglet livers after dietary treatment with *Fusarium* mycotoxins (Reddy *et al.*, 2017), identification of gene expression in porcine skeletal muscle in response to nutrient uptake compared to fasting pigs (Cardoso *et al.*, 2017b) and whole blood transcriptome differences between the pig breeds Dapulian and Landrace (Hu *et al.*, 2016). However, the studies concerning the porcine intestine are of the greatest interest in the context of the current study. Such studies include the application of RNA sequencing to identify a transcriptional profile of different sections of the porcine intestine.

These sections included the duodenum, jejunum, ileum and ileal PPs. This study found that samples clustered by tissue type rather than individual (n = 4). 1349 genes were identified as differentially expressed between duodenum and ileum samples, amongst which, nucleic acid metabolism and vitamin and mineral metabolism gene ontology terms were highly enriched. 3455 genes were differentially expressed between the duodenum and ileum, again highlighting nucleic acid metabolism and vitamin and mineral metabolism. The gene expression profile of the ileal PPs was identified to be considerably different from all other tissues with 7027, 6122 and 6991 genes identified as differentially expressed in comparisons with the tissues of the duodenum, jejunum and ileum respectively. These highlighted significant differences in immune-related gene expression in PPs compared to all other intestinal tissues with nine immune-related gene ontologies highly enriched in all three comparisons. However, these comparisons showed that gene expression in PPs was different from the other tissues in a very wide range of molecular and cellular functions (Mach *et al.*, 2014).

Other studies detailing the transcriptome of pig intestine utilise DNA microarray technology. One such study found that weaning affects the

transcriptome profile and PP development in piglet ileum (Inoue *et al.*, 2015). This study encompassed weaned and suckling pigs of 14, 21, 28 and 35 days of age. The transcriptome profiles of these pigs identified pigs of 14 days of age to be most dissimilar to the other age group, a finding which the authors attribute to a drastic period of development in the ileum in the period between 14 and 21 days of age. Weaning at 21 days of age was observed to increase expression of genes related to the *apoptosis and survival caspase cascade* (five of 33 genes), *cell adhesion/ tight junction* (five of 35 genes), and *regulation of metabolism/bile acids regulation of glucose and lipid metabolism via FXR* (five of 37 genes) gene ontology terms when tissue was collected from the animals at 28 days of age. Conversely weaning downregulated genes associated with the immune response/BCR pathway (ten of 54 genes), immune response/PIP3 signalling in B lymphocytes (nine of 42 genes) and chemotaxis/leukocyte chemotaxis (eleven of 75 genes) gene ontology terms. The authors attribute the enrichment of immunity and chemotaxis related terms amongst genes downregulated by weaning to the maldevelopment of PPs.

1.11 General Hypothesis and Aims

In the pork production industry, pigs are subject to weaning which manifests as early life stress. This has been widely reported to result in scouring as a result of perturbations in the structure and function of the intestinal mucosal barrier (Moeser *et al.*, 2012). In previous work on the present trial by M. Le Bon (2012), stress was monitored via ELISA plasma cortisol, a stress marker, which confirmed that weaned animals had higher cortisol levels than suckling pigs (p <0.001).

To this extent, there are two primary aims:

- To investigate weaning stress related transcriptional changes in the colon resulting from weaning
- To investigate the transcriptional effects of probiotic *Saccharomyces cerevisiae boulardii* on the colon of weaned and suckling pigs

The primary hypothesis of this study is that weaning stress brings about transcriptional changes in the porcine gut, reducing the efficiency of the mucosal barrier and that probiotic *Saccharomyces cerevisiae boulardii* confers protective functions during the weaning period which acts to dampen the transcriptional response to weaning.

2 Chapter 2: Materials and Methods

2.1 Sample Set

The trial was designed and implemented by Dr K Mellits, Dr S. Tötemeyer and Melanie Le Bon; samples were collected by Melanie Le Bon (Le Bon, 2012a).

All animals were treated in accordance with the University of Nottingham ethical guidelines and codes of practice applying to care and management of animals (no home office licence required).

Litters from eight Landrace X Large White Sows (JSR Genetics, Driffield, UK) of parity seven, each sow had previously given birth to seven litters, were used in this study. Nine Sows were transported to the Sutton Bonington campus of the University of Nottingham after 94 days of gestation and group-housed until 113 days' gestation when they were separated into individual farrowing pens, eight of these were used in the trial. All sows received a wheat-based feed containing 16% protein, 4.5% oil, 5.5% crude fibre, 5.5% ash, 0.75% lysine, 1000 iu kg^{-1} vitamin A, 2000 iu kg^{-1} vitamin D3, 100 iu kg^{-1} vitamin E, 0.40 mg kg^{-1} selenium and 25 mg kg^{-1} copper three times per day (BOCM Pauls ltd, Wherstead, UK, Appendix 1). Sows which had not farrowed by 115 days of gestation

were induced by injection of 2 ml Planate (Intervet, Milton Keynes, UK) and 1 ml Oxytocin-S (Intervet, Milton Keynes, UK). Each of the litters was assigned randomly using coded balls, to control or probiotic treatment by random control block design (Addelman, 1969; O'Connor *et al.*, 2010) (Figure 2-2).

Pigs were weaned at 21 days of age (Figure 2-3). Probiotic supplementation of piglets began at 14 days before weaning (seven days of age) and ended at 35 days of age. Probiotic litters were administered 4.43 Log_{10} CFU of *Saccharomyces cerevisiae boulardii* (SCB) CNCM I-1079 (SCB; Levucell SB, Lallemand, France) suspended in a flavoured paste (soya oil, Sipernat 50S, icing sugar, Tween 80, Flavour), given orally by syringe daily. This dosage was optimised during previous experimentation, with concentration in colon contents ranging between 5.5 ± 0.23 Log_{10} CFU g^{-1} at one day post weaning and 4.2 ± 0.41 Log_{10} CFU g^{-1} at fourteen days post weaning (Le Bon, 2012b). Control litters were administered the same paste without SCB load. Three piglets per litter, randomly selected, were weaned at 21 d of age (Figure 2-3). These were allocated to one of three weaning pens and mixed with non-littermates from the same treatment group to give a total of four pigs in each weaning pen (heating, ventilation and air conditioning

(HVAC)-controlled flat deck pens, 1.25 m x 2.0 m). Weaned piglets received *ad libitum* access to feed and water from 21 days of age onwards. Suckling piglets also had *ad libitum* access to a small amount of weaner diet as creep feed to supplement milk intake from 25 days of age. At 22 days of age (one day post weaning, Figure 2-4), 25 days of age (four days post weaning, Figure 2-5) and 35 days of age (14 days post weaning, Figure 2-6) a total of 16 pigs were euthanised by intraperitoneal injection of Dolethal (1 ml kg^{-1} body weight; 20% w/v Pentobarbitone Sodium, Vétoquinol, Buckingham, UK). Of the 16 pigs euthanised on each slaughter day; four were weaned with probiotic supplementation; four weaned control; four were selected as one from each of the suckling litters which had been administered SCB and the final four were selected as one from each of the four suckling control litters. Sex and slaughter weight information for these animals can be found in Appendix 4.

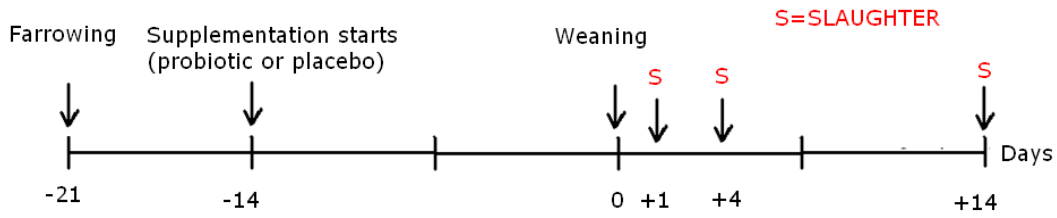


Figure 2-1: Trial timeline. Timeline to demonstrate that probiotic supplementation begins at 14 days pre-weaning with slaughter days at +1, +4 and +14 days' post weaning (Le Bon, 2012a).

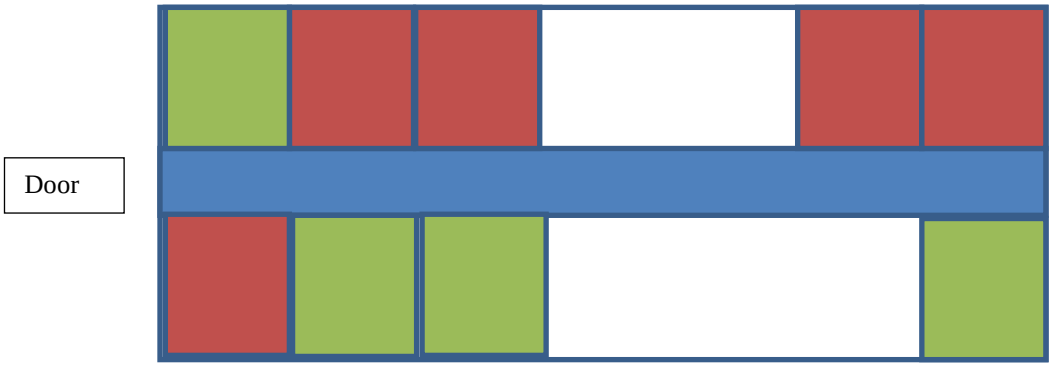


Figure 2-2: Random allocation of experimental and control sows to pens in wean trial. Red boxes show pens in which litters were administered *Saccharomyces cerevisiae boulardii;* green boxes show pens in which the placebo was administered. The blue box shows the central walkway, and the white areas show unused pens and feed storage areas

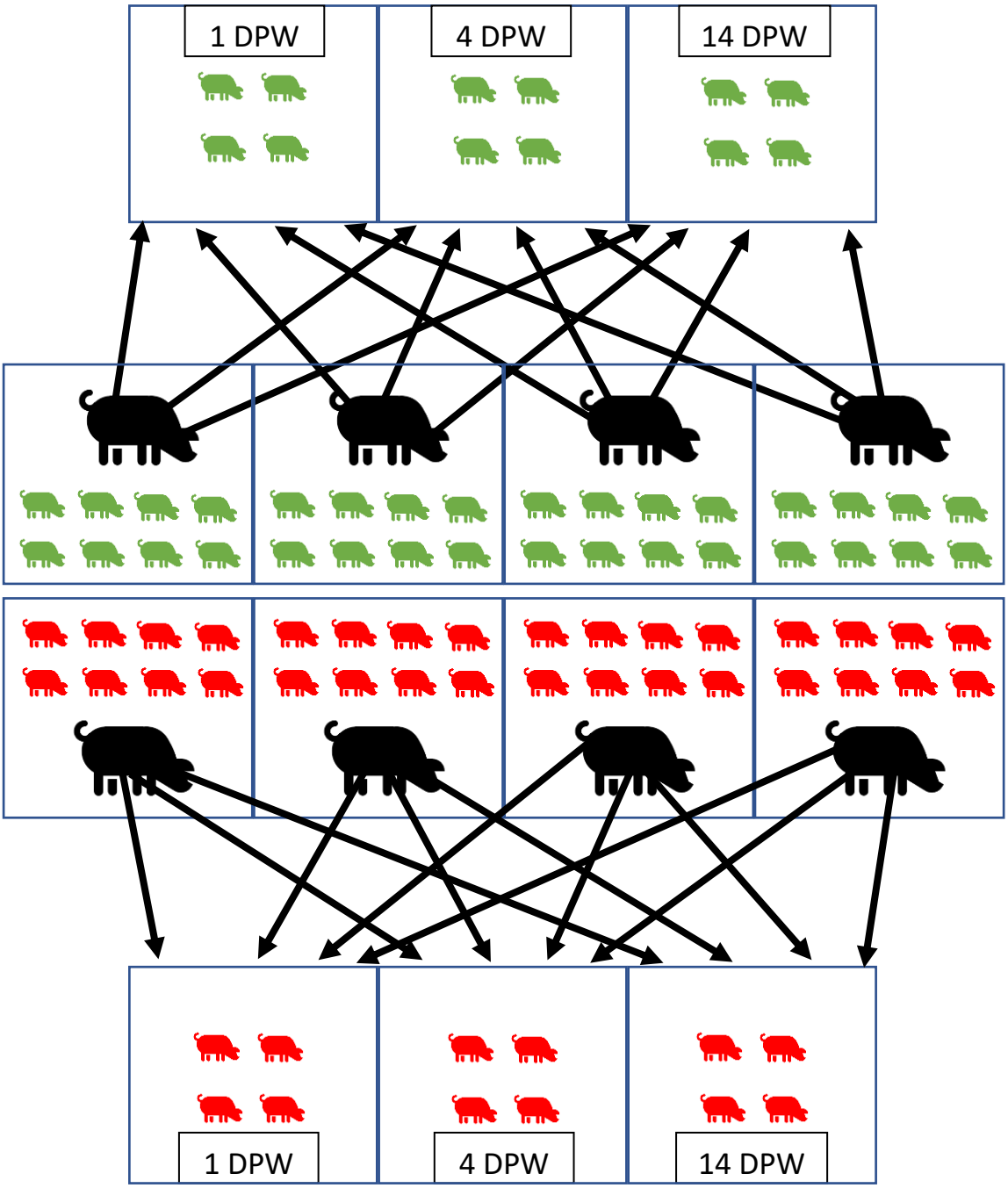


Figure 2-3: The weaning process. At 21 days of age, a weight matched pig from each litter was weaned into a pen with non-littermates from three other litters. This process was repeated three times to provide a weaning pen containing four pigs for each of the three slaughter points at one, four and 14 days post weaning (DPW). This entire process was conducted for both litters administered *Saccharomyces cerevisiae boulardii* and control litters. The result of this weaning strategy was that four treatments were defined: weaned+ SCB, weaned control, suckling + SCB and suckling control. Each arrow represents a single pig. SCB administered pigs are shown in green, control pigs shown in red.

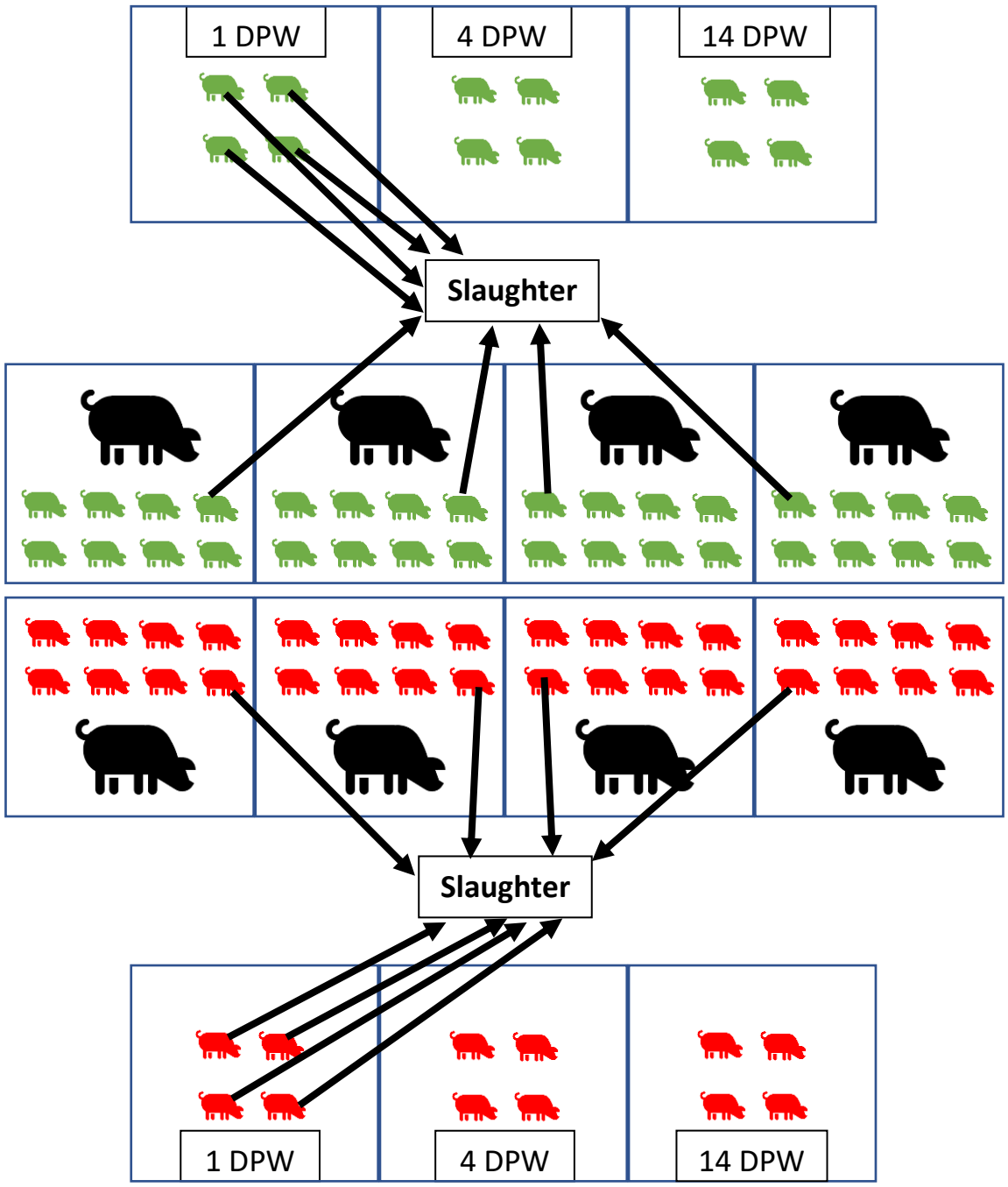


Figure 2-4: The one day post weaning slaughter point. At one-day post weaning (22 days of age) a total of 16 pigs were euthanized: Four pigs from the weaning pen containing SCB supplemented pigs; four from the corresponding control weaning pen; one from each of the four SCB supplemented n-weaned litters and one from each of the control suckling litters. Each arrow indicates a single pig. SCB supplemented pigs are shown in green, control pigs in red. DPW, days post weaning.

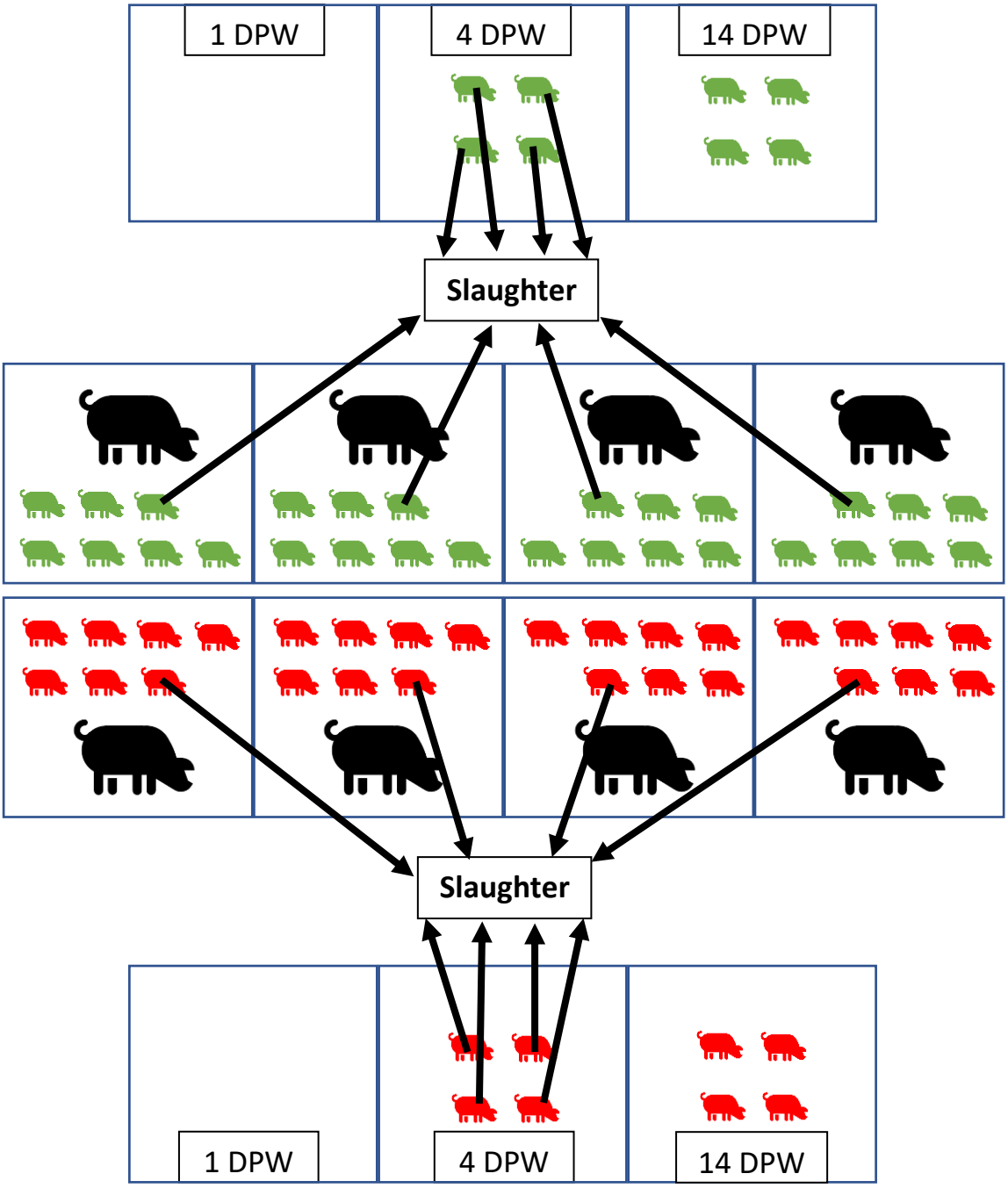


Figure 2-5: The four days post weaning slaughter point. At four days post weaning (25 days of age). A total of 16 pigs were euthanized: Four pigs from the weaning pen containing SCB supplemented pigs; four from the corresponding control weaning pen; one from each of the four SCB supplemented n-weaned litters and one from each of the control suckling litters. Each arrow indicates a single pig. SCB supplemented pigs are shown in green, control pigs in red. DPW, days post weaning.

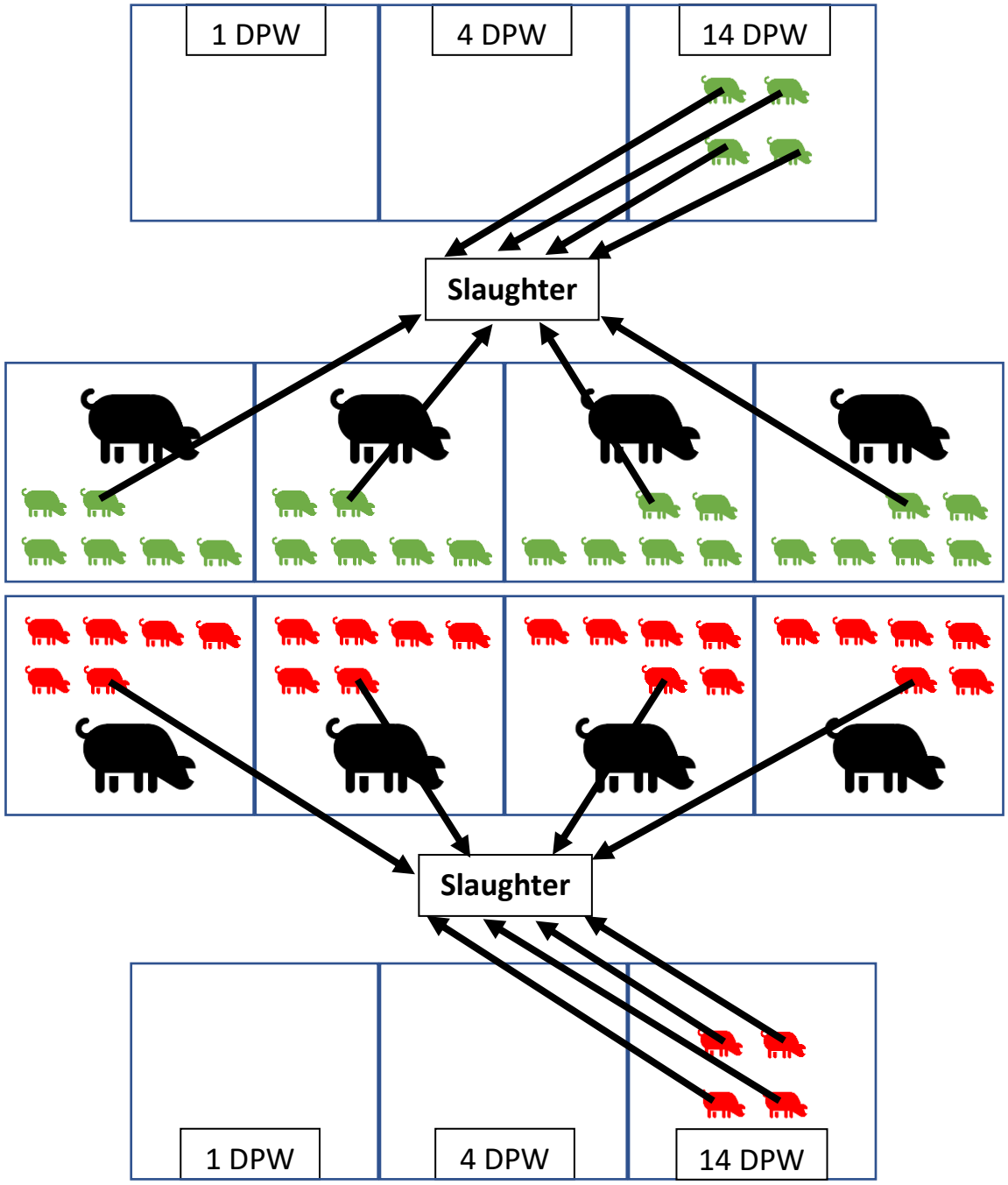


Figure 2-6: The 14 days post weaning slaughter point. At fourteen days post weaning (335 days of age), A total of 16 pigs were euthanized: Four pigs from the weaning pen containing SCB supplemented pigs; four from the corresponding control weaning pen; one from each of the four SCB supplemented n-weaned litters and one from each of the control suckling litters. Each arrow indicates a single pig. SCB supplemented pigs are shown in green, control pigs in red. DPW, days post weaning.

2.2 Colon Sample Collection and RNA Extraction

At slaughter, tissue pieces from ascending (mid)colon were collected and preserved in RNA later (Invitrogen, Paisley, UK) at 4°C for 24-48 h to allow tissue penetration, then stored in a freezer at -80 °C. This location in the porcine colon was selected to match existing studies on the effects of weaning in the porcine gastrointestinal tract (Moeser *et al.*, 2007a; Moeser *et al.*, 2007b; Li *et al.*, 2017). 10-30 mg of colon tissue was homogenised in a 2 ml round bottomed tube (Fisher Scientific, Loughborough, UK) containing 350 µl of guanidine thiocyanate buffer (RA1 buffer, Macherey-Nagel, Düren, Germany) and 3.5 µl of 0.1 mM β-mercaptoethanol using a 5 mm stainless steel bead (Retsch, Hope Valley, UK) for two periods of 2 min at 3,000 rpm using a Retsch MM200 homogeniser (Figure 2-7).

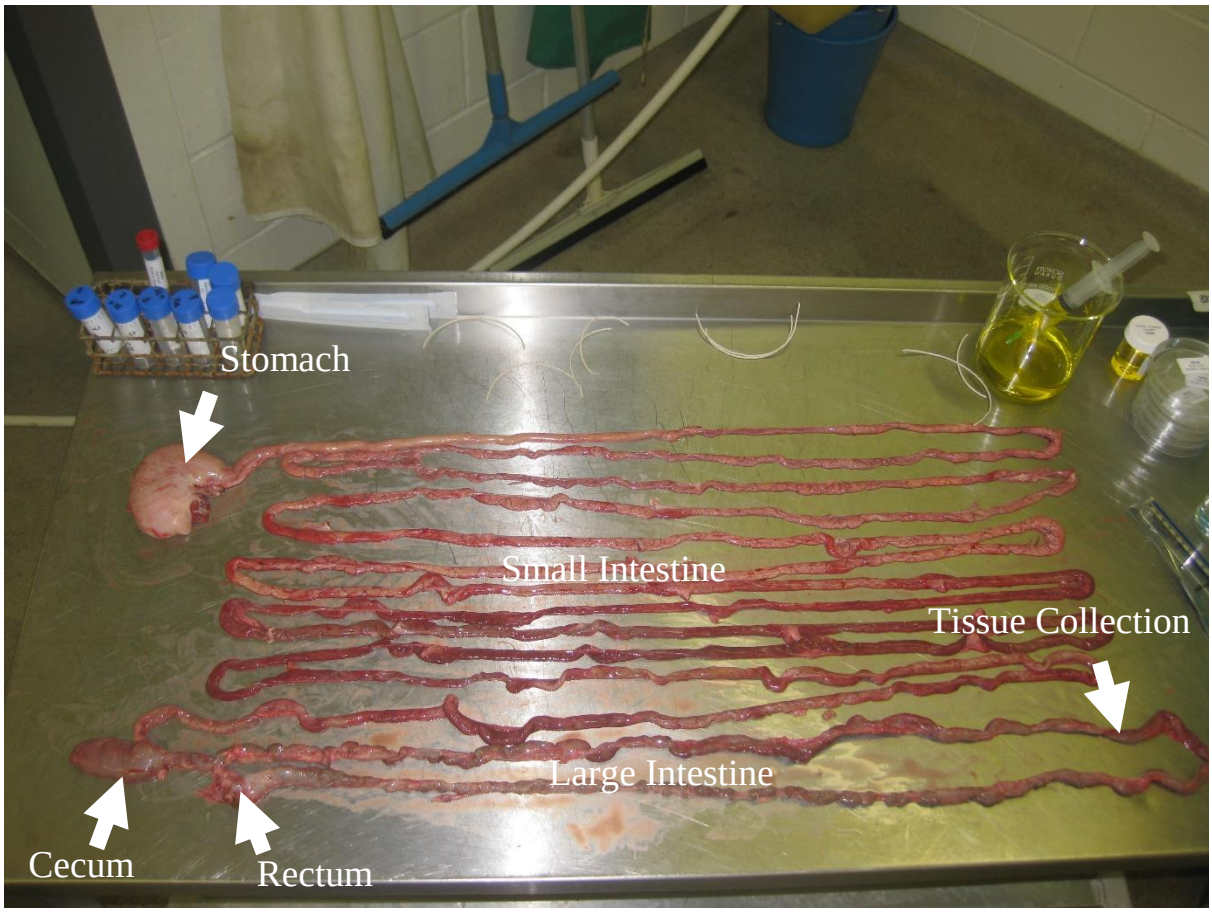


Figure 2-7: Tissue collection at slaughter. Image shows how the porcine gastrointestinal tract was laid out after slaughter. Colon samples were taken from a location equidistant between the cecum and rectum.

2.2.1 RNA Extraction

RNA extraction was conducted using a NucleoSpin RNA extraction kit (Macherey-Nagel). Crude lysate from bead beating disruption of tissue was transferred into a NucleoSpin filter column (Macherey-Nagel) (300 µl). This filter column was placed in a collection tube (Macherey-Nagel). The column was then centrifuged at 11,000g for 1 minute. The filter column was then discarded and 300 µl of freshly prepared 70% v/v

ethanol (EtOH) was added to the collection tube containing the run through from the filter column. The total volume (600 µl) was pipetted up and down six times to ensure thorough mixing.

The solution (600 µl) was then transferred to a NucleoSpin binding column (Macherey-Nagel) which was placed in a new collection tube (Macherey-Nagel). The column was then centrifuged at 11,000 g for 1 minute. This allowed binding of RNA to the column. The column run through was then discarded, and the column placed back onto the collection tube. 350 µl of MBD (desalting buffer) was added to each column, and the columns were centrifuged at 11,000 g for 1 minute.

DNAse solution (95 µl) prepared to manufacturers instructions (Macherey-Nagel) was added to each column. The columns were then incubated at room temperature for 15 minutes to allow degradation of DNA contaminants.

Next, 200 µl of buffer RA2 (Macherey-Nagel) was then added to each column, and the columns were centrifuged at 11,000 g for 1 minute. This buffer deactivates DNAse activity. 600 µl of RA3 wash buffer (Macherey-Nagel) was then added to each column, and the columns were centrifuged at 11,000 g for 1 minute. Column throughflow was then discarded. A second wash step was then conducted by adding 250

µl of RA3 wash buffer (Macherey-Nagel) to each column and centrifuging the columns at 11,000 g for 4 minutes.

Finally, RNA was eluted from the column by placing the column in new RNAse free microcentrifuge tube (Fisher Scientific) before adding 60 µl of RNAse free water (Macherey-Nagel) to each column. The columns were then centrifuged at 11,000 g for 1 minute to elute the RNA from the columns. Two microliters of this RNA solution was transferred into an RNAse free PCR tube for analysis with an Agilent Bioanalyzer 2100 (Agilent Technologies, Manchester, UK). The remaining RNA solution was stored at -80 ^{o}C for later sequencing applications.

2.2.2 RNA Quality Control

RNA quality control was conducted using an Agilent 2100 Bioanalyzer (Agilent Technologies). Firstly, the Bioanalyzer dye (Agilent Technologies) was removed from 4^{o}C storage and allowed to equilibrate at room temperature for 30 minutes. The dye was then briefly vortexed to ensure thorough mixing. One microliter of dye was then added to 65 µl of pre-filtered gel matrix (Agilent Technologies). An Agilent RNA 6000 Nanochip (Agilent Technologies) was then placed on the Agilent ChipDock (Agilent Technologies). Nine microliters of gel-dye solution

was then added to the well marked with a 'G' enclosed in a circle. After ensuring that the attached syringe is at the 1 ml position, the dock was closed and the syringe compressed. The dock was then left for 30 seconds to allow full penetration of the dye-gel solution.

After 30 seconds had elapsed, the dock clip was released and 9 µl of gel-dye solution was added to all wells marked with a 'G'. At this stage, RNA samples were denatured in a constant temperature water bath at 70°C for 2 minutes. Five microliters of RNA 6000 marker (25 bp, 5 ng μl^{-1}, Agilent Technologies) was then added to each sample well and the ladder well on the Agilent RNA 6000 Nanochip (Agilent Technologies). 1 µl of RNA ladder (150 ng μl^{-1}, Agilent Technologies) was then added to the ladder well on the chip. One microliter of RNA sample was added to each sample well. Finally, the chip was vortexed for 1 minute at 2400 rpm on an IKA Vortex 4 (IKA, Staufen, Germany) using the Agilent adaptor.

The chip was then loaded into the Agilent Bioanalyzer 2100, and the RNA nano II program was executed. The RNA integrity number (RIN) provided by this system indicates the level of RNA degradation in the sample. In this scale of 1-10, 10 represents the highest quality RNA. Figure 2-8 shows an example output trace from an Agilent Bioanalyzer

2100 when a sample with a RIN of 6 was tested. Information on individual sample RNA quality can be found in Appendix 2. This stage of RNA preparation was conducted in conjunction with M. Le Bon (Le Bon, 2012a).

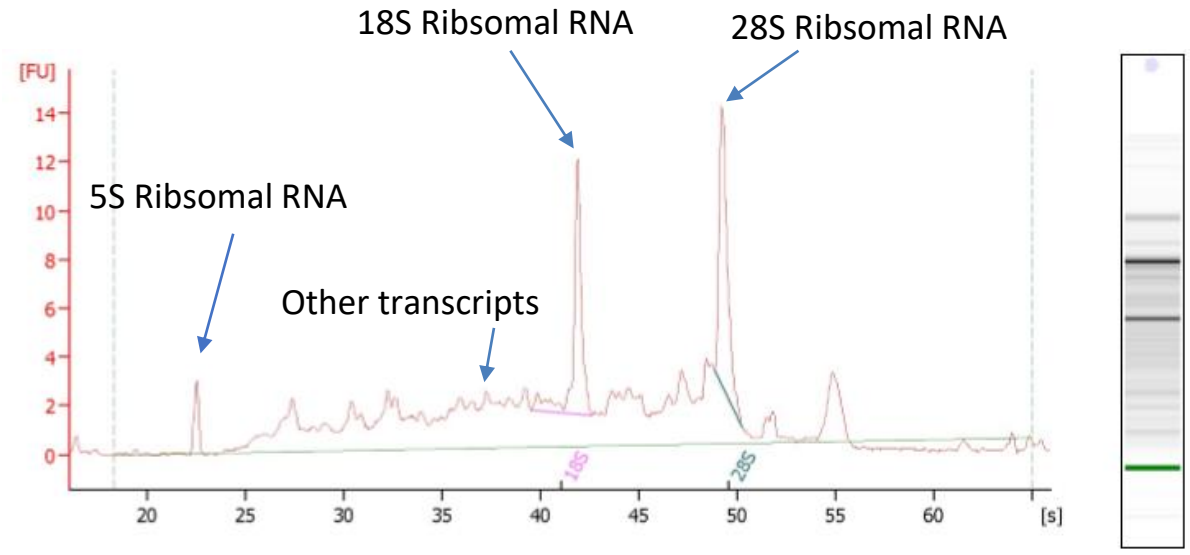


Figure 2-8: Example of Agilent 2100 Bioanalyzer output at RNA integrity number (RIN) of 6.

2.3 Transcriptomics

2.3.1 Library Preparation for Next Generation Sequencing Technology

RNA was sequenced in 2011 by Ark Genomics (Edinburgh, UK). Library preparation was conducted using the Illumina TruSeq RNA sample preparation guide version two protocol for low throughput (revision B, February 2012). This protocol utilised one microgram of total RNA per

sample. Positive and negative controls were prepared alongside sample preparation. Human brain RNA product AM7962 (Ambion, Paisley, UK) was used for the positive control, whereas the negative control replaced RNA with ultra-pure RNAse free water. These controls were discarded after the library validation step.

2.3.2 Sample Purification and mRNA Selection

The first stage of library preparation was purification and fragmentation of mRNA. Total RNA was diluted with nuclease-free ultra-pure water to a final volume of 50 µl and pipetted into a 96 well 0.3 ml PCR plate. Diluted total RNA was then mixed with 50 µl oligo-dT RNA purification beads (Illumina, Cambridge, UK). The 96 well PCR plate was then sealed and placed on a thermal cycler (Dyad, MJ Research, Watford, UK) at 65 ^{o}C for five minutes with a 4 ^{o}C hold. After the thermal cycler reached 4^{o}C, the plate was removed and incubated at room temperature for five minutes. The initial heating of the solution to 65 ^{o}C functioned to denature the RNA, with the following five-minute incubation at room temperature allowing the binding of polyA RNA to the oligo-Td magnetic beads.

The seal was then removed from the 96-well PCR plate, and the plate placed on a magnetic stand (DynaMag-96 side skirted magnet, Invitrogen) at room temperature for five minutes to separate the polyA RNA bound beads from the solution. The supernatant was then removed and discarded. The 96-well PCR plate was then removed from the magnetic stand, and the beads were washed by adding 200 µl bead washing buffer (Illumina) and pipetting the entire volume up and down six times to mix thoroughly. The 96-well PCR plate was then replaced on the magnetic stand at room temperature for five minutes to separate the magnetic beads from the solution again.

All supernatant was then removed and discarded. This removed most of the remaining ribosomal and other non-messenger RNA, leaving only poly-adenylated RNA annealed to the magnetic beads. The 96-well plate was then removed from the magnetic stand, and 50 µl of elution buffer (Illumina) was added to each of the wells. The total volume of each well was gently pipetted up and down six times to mix the solution thoroughly.

The 96-well plate was then sealed and placed on a thermal cycler (Dyad, MJ Research). It was then subjected to 80^{o}C for 2 minutes (25^{o}C hold) to elute the mRNA and any contaminant rRNA from the beads. The plate

was removed from the thermal cycler when the temperature reached 25°C and the seal removed.

50 µl of bread binding buffer (Illumina) was then added to each well of the 96-well plate; this allows mRNA to specifically rebind the beads while reducing ribosomal RNA which non-specifically binds. The entire volume of this solution was then gently pipetted up and down six times to mix thoroughly. The plate was then incubated at room temperature for five minutes. The 96 well plate was again placed on a magnetic stand at room temperature for five minutes to separate the beads from the solution, after which all supernatant was discarded.

The plate was then removed from the magnetic stand, and the beads were washed by adding 200 µl of bead washing buffer (Illumina) to each of the wells. The entire solution was gently pipetted up and down six times to mix thoroughly. The plate was then again placed on a magnetic stand for five minutes at room temperature to separate the magnetic beads from the solution. All supernatant was then discarded. This contained residual ribosomal RNA and other contaminants which were released during the first elution but did not re-bind the beads.

The 96-well plate was removed from the magnetic stand, and 19.5 µl of eluting, prime, fragment mix (Illumina) was added to each well. The

solution was then gently pipetted up and down six times to mix thoroughly. The elute, prime, fragment mix contains random hexamers for reverse transcription priming and serves as the first strand cDNA synthesis reaction buffer.

The 96-well plate was then sealed and placed on a thermal cycler (Dyad, MJ Research) and subjected to 94 ^{o}C for 8 minutes (4 ^{o}C hold) to elute, fragment and prime the RNA. The 96-well PCR plate was removed from the thermal cycler when it reached 4 ^{o}C and centrifuged for 20 seconds in an Eppendorf 1415 microfuge (Eppendorf, Stevenage, UK).

2.3.3 First-Strand Synthesis

First-strand synthesis was conducted by placing the 96-well plate on a magnetic stand (DynaMag-96 side skirted magnet, Invitrogen) at room temperature for five minutes. The plate seal was then removed while the plate was still on the magnetic stand. 17 µl of the supernatant which contained fragmented and primed mRNA from each well was transferred into a new 0.3 ml 96-well PCR plate.

The first strand master mix was prepared by adding 50 µl of SuperScriptII reverse transcriptase (Thermo Fisher Scientific,

Loughborough, UK) to the first strand master mix tube (Illumina). This provides a ratio of 1 µl SuperScriptII for each 9 µl of first strand master mix. This solution was then mixed gently but thoroughly and then briefly centrifuged (1415 microfuge, Eppendorf). 8µl of this mixture was added to each of the wells on the 96-well plate which contained supernatant. The plate was then sealed.

The 96-well plate was then placed in a thermal cycler (Dyad, MJ Research) with the pre-heated lid option set to 100 ^{o}C, followed by 25 ^{o}C for ten minutes; 42 ^{o}C for 50 minutes; 70 ^{o}C for 15 minutes and a final hold at 4 ^{o}C. This reverse transcribed the mRNA fragments in the solution which were primed with random hexamers, contained within the first strand master mix (FSM, Illumina), into first strand cDNA.

2.3.4 Second Strand Synthesis

The next step in the library preparation was the synthesis of second strand cDNA. This process removed the RNA template and synthesised a replacement strand to generate double-stranded cDNA. The adhesive seal was removed from the 96-well plate and 25 µl of second strand master mix was added to each used well of the plate. This solution was

then gently pipetted up and down six times to mix thoroughly. The plate was then re-sealed.

The 96-well plate was then placed on a thermal cycler (Dyad, MJ Research) and incubated at 16 ^{o}C for one hour. It was then removed from the thermal cycler, the adhesive seal removed and allowed to stand until it reached room temperature.

Next, 90 µl of well-mixed Agencourt AMPure XP beads (Beckman Coulter, Indianapolis, USA) were added to each used well of the 96-well plate. The total volume was then gently pipetted up and down ten times to ensure thorough mixing. The plate was then incubated at room temperature for 15 minutes, before placing it on a magnetic stand (DynaMag-96 side skirted magnet, Invitrogen) at room temperature for five minutes to make sure that all the beads are bound to the side of the wells. These beads bind the double-stranded cDNA in the solution.

While still placed upon the magnetic stand, 135 µl of supernatant from each well was discarded. Still while on the magnetic stand, 200 µl of freshly prepared 80% v/v EtOH was added to each well without disturbing the beads. The plate was then incubated at room temperature for 30 seconds before all supernatant was removed and discarded. Another 200 µl 80% v/v EtOH wash was then conducted, a

total of two washes. After the washes, the plate was allowed to stand at room temperature for 15 minutes to dry. The plate was then removed from the magnetic stand.

Next, 52.5 µl of resuspension buffer was then added to each well, gently pipetting the solution up and down ten times to mix thoroughly. The plate was then incubated at room temperature for two minutes before being transferred to a magnetic stand for an additional five minutes. Finally, 50 µl of the supernatant from each well containing double-stranded cDNA was then transferred to a new 0.3 ml 96-well PCR plate.

2.3.5 End Repair

The next stage of the library preparation process was performing end repair. This process converts the overhangs resulting from fragmentation into blunt ends using an end repair mix.

First, 40 µl of end repair mix (Illumina) and 10 µl resuspension buffer (Illumina) were added to each well. This was then mixed thoroughly by gently pipetting the solution up and down ten times. The plate was then sealed and placed on a thermal cycler (Dyad, MJ Research) at 30 ^{o}C for

30 minutes. The plate was then removed from the thermal cycler and the adhesive seal removed.

Next, 160 µl of well-mixed Agencourt AMPure XP beads (Beckman Coulter) was then added to each well containing 100 µl of end repair mix. This was then gently pipetted up and down ten times to ensure thorough mixing. The plate was then incubated at room temperature for 15 minutes, before being placed on a magnetic stand (DynaMag-96 side skirted magnet, Invitrogen) until the liquid was clear.

Next, 127.5 µl of the supernatant was removed and discarded from each of the used wells. This procedure was repeated a second time so that a total of 255 µl of supernatant was removed from each well. The beads were then washed by adding 200 µl of freshly prepared 80% EtOH to each well without disturbing the beads. This wash was incubated at room temperature for 30 seconds before all supernatant was removed from each well and discarded. This wash step was repeated one additional time for a total of two washes.

The plate was then allowed to dry at room temperature for 15 minutes on the magnetic stand. 17.5 µl of resuspension buffer (Illumina) was then added to each used well, and the entire volume was gently pipetted up and down ten times to mix thoroughly. The plate was then

incubated at room temperature for two minutes before being transferred to a magnetic stand for five minutes to separate the beads from the supernatant. 15 µl of the supernatant from each well was then transferred to a new 0.3 ml 96-well PCR plate.

2.3.6 Adenylate 3' Ends

A single 'A' nucleotide was added to the 3' ends of the blunt fragments to prevent them ligating to one another during the adapter ligation reaction. A corresponding single 'T' nucleotide on the 3' end of the adapter provides a complementary overhang for ligating the adapter to the fragment. This strategy ensures a low rate of chimera (concatenated template) formation.

To achieve this, 12.5 µl of A-tailing Mix (Illumina) and 2.5 µl of resuspension buffer (Illumina) were added to each plate well, and the entire volume was gently pipetted up and down ten times to mix thoroughly. The plate was then sealed and placed on a thermal cycler (Dyad, MJ Research) with the pre-heated lid option set to 100 °C; followed by 30 °C for 30 minutes; 70 °C for five minutes and a final hold at 4 °C.

2.3.7 Adapter Ligation

This part of the library preparation process ligates multiple indexing adapters to the ends of the double-stranded cDNA, preparing them for hybridization onto a flow cell. The seal was removed from the 96-well PCR plate, and 2.5 µl of resuspension buffer (Illumina) was added to each of the used wells. 2.5 µl of RNA adapter index (Illumina), which is individual to each sample, was also added to each well before gently pipetting the total volume up and down ten times to mix thoroughly. The plate was then sealed and placed on a thermal cycler (Dyad, MJ Research) for incubation at 30°C for ten minutes.

The plate was removed from the thermal cycler, and five microliters of stop ligation buffer (Illumina) was added to each well to inactivate the ligation. The total volume of each well was gently pipetted up and down ten times to mix thoroughly. 42 µl of well-mixed AMPure XP beads (Beckman Coulter) were then added to each well, and the solution was pipetted up and down ten times to ensure thorough mixing.

The plate was then incubated at room temperature for 15 minutes before being placed on a magnetic stand (DynaMag-96 side skirted magnet, Invitrogen) for five minutes to clear the beads from the liquid. While still on the magnetic stand, 79.5 µl of supernatant was then

removed from each well and discarded, being careful not to disturb the magnetic beads.

With the plate still located on the magnetic stand, 200 µl of freshly prepared 80% v/v EtOH was added to each well. After 30 seconds of incubation at room temperature, all supernatant was removed and discarded. This wash step was repeated to a total of two washes, after which the plate was air dried at room temperature for 15 minutes.

The 96-well plate was then removed from the magnetic stand, and 52.5 µl of resuspension buffer (Illumina) was added to each well. The solution was then gently pipetted up and down ten times to fully resuspend the beads in the solution. The plate was then incubated at room temperature for two minutes before being placed on a magnetic stand for five minutes to clear the beads from the solution.

Fifty microliters of the supernatant from each well was then transferred to a new 0.3 ml 96-well PCR plate without disturbing the magnetic beads in the wells of the original plate. Fifty microliters of well-mixed AMPure XP magnetic beads (Beckman Coulter) were added to each well of the new plate. The resulting 100 µl volume was gently pipetted up and down ten times to ensure thorough resuspension of the magnetic beads. The plate was then incubated at room temperature for 15

minutes, before being placed on a magnetic stand for five minutes to clear the magnetic beads from the solution.

Ninety-five microliters of supernatant was then removed and discarded from each well, taking care not to disturb the magnetic beads. The beads were then washed while the plate was still located on the magnetic stand by adding 200 µl of freshly prepared 80% EtOH to each well. The plate was then incubated at room temperature for 30 seconds before carefully removing the supernatant without disturbing the beads. This wash process was repeated to a total of two wash cycles. The plate was then air dried at room temperature for 15 minutes.

Finally, 22.5 µl of resuspension buffer (Illumina) was then added to each well, and the total volume of each well was gently pipetted up and down ten times to resuspend the magnetic beads. The plate was then incubated at room temperature for two minutes before being transferred to a magnetic stand for five minutes to precipitate the magnetic beads from the solution. Twenty microliters of supernatant was then transferred to a new 0.3 ml 96-well plate, with care being taken not to disturb the magnetic beads during this transfer.

2.3.8 DNA Fragment Enrichment

Enrichment of DNA fragments selectively enriches those DNA fragments which have the adapter molecules on both ends and amplifies the amount of DNA in the library. The PCR was performed with a PCR primer cocktail which anneals to the ends of the adapters. This is important as only DNA fragments with adapters ligated to both ends can hybridise to surface-bound primers in the flow cell and subsequently form clusters.

To begin the process, 5 µl of primer cocktail (Illumina) and 25 µl of PCR master mix (Illumina) was added to each well of the 96-well plate that resulted from the completion of the adapter ligation step. The total volume of each well was gently pipetted up and down ten times to ensure thorough mixing before the plate was sealed with an adhesive seal.

The plate was then placed on a thermal cycler (Dyad, MJ Research) with the pre-heated lid option set to 100^{o}C. It was then subjected to 98^{o}C for 30 seconds followed by 15 cycles of 98^{o}C for 10 seconds; 60^{o}C for 30 seconds and 72^{o}C for 30 seconds followed by a final elongation step of 72^{o}C for 5 minutes. The final hold temperature was set to 10^{o}C.

After amplification of the DNA fragments is complete, the reaction must be cleaned for downstream sequencing. To achieve this, first, the adhesive seal was removed from the 96-well plate. Fifty microliters of well-mixed AMPure XP magnetic beads (Beckman Coulter) was added to each well containing 50 µl of PCR amplified library. The total volume of 100 µl was then pipetted up and down ten times to suspend the magnetic beads in the solution. The 96-well plate was then incubated at room temperature for 15 minutes before being transferred to a magnetic stand (DynaMag-96 side skirted magnet, Invitrogen) at room temperature for 5 minutes to clear the liquid of the beads. 95 µl of supernatant was then removed from each well and discarded.

While still on the magnetic stand, 200 µl of freshly prepared 80% EtOH was added to each well. After a 30 second incubation period, all supernatant was removed and discarded. This wash process was repeated a second time to a total of two washes. The plate was then air dried for 15 minutes at room temperature.

The 96-well PCR plate was then removed from the magnetic stand, and the pellet in each well was resuspended in 32.5 µl of resuspension buffer (Illumina) by gently pipetting the total volume up and down ten times. The plate was then incubated at room temperature for two

minutes before being transferred back to a magnetic stand for five minutes to precipitate the magnetic beads from the solution. Finally, 30 µl of the supernatant was transferred to the corresponding well in a new 0.3 ml 96-well PCR plate.

2.3.9 Library Validation

Library validation was conducted by loading one microliter of library construct onto an Agilent DNA 1000 chip (Agilent Technologies) and subsequent analysis using a 2100 Bioanalyzer (Agilent technologies). Individual sample validation information can be found in Appendix 2.

2.3.10 Normalization and Library Pooling

This final stage of library preparation was conducted to normalise the concentration of the library for each sample and to pool these libraries for sequencing.

Ten microliters of sample library obtained from the DNA fragment amplification step was transferred to the corresponding well on a new 0.3 ml 96-well plate. Concentration information obtained during library validation was then used to normalise the concentration of each sample

library to 10 nM using Tris-HCl 10 mM, pH 8.5 with 0.1% Tween 20 as a diluent. The entire normalised sample library volume was then pipetted up and down ten times to mix thoroughly.

As there are eight lanes on a Hi-seq 2000 flow cell, and two cells were used in this study, 16 lanes were available. As this study produced 48 sample libraries, each pool contained three samples. As only 27 unique indexes are provided, added at the adaptor ligation stage, some of these had to be used more than once. Because of this, pooled samples had to be carefully selected to ensure that a given index only represented a single sample within the pool.

To complete pooling of samples, 10 µl of normalised library from each of the samples to be pooled together was transferred to an 8-tube nuclease free PCR strip (Thermo Fisher Scientific) to a total of 30µl for each pool (3 samples). This completed library preparation, ready for cluster generation on the flow cells. Two 8-tube nuclease free PCR strips were used to contain all libraries.

2.3.11 Cluster Generation

Cluster generation was conducted by ARK genomics (Edinburgh, UK) on a cBot system (Illumina) using the TruSeq paired-end cluster kit v3 (Illumina). This process is described in Figure 1-17.

2.3.12 Sequencing

The sequencing reaction was conducted by ARK genomics (Edinburgh, UK) on a HiSeq-2000 sequencer (Illumina) using TruSeq v3 chemistry (Illumina). The options were selected for paired-end reads and single indexes.

The number of cycles was then selected. For 50 bp paired-end reads this was 107 cycles. This consists of 50 read cycles per end and seven cycles to sequence the index to identify which sample the read belongs to. For later 100 bp paired-end sequencing the number of cycles was set to 207, two sets of 100 read cycles and seven index cycles.

2.3.13 Preparation of Sequencing Data for Bioinformatic Analysis

Primary output files from the HiSeq 2000 sequencer were demultiplexed into paired fastq files corresponding experimental

samples. This was conducted by ARK genomics (Edinburgh, UK) using bclfastq software version 1.8.4 (Illumina). This demultiplexed data was received on a 1TB portable hard drive.

2.3.14 Quality Filtering and Adaptor Removal

An adaptor removal step was incorporated to remove any remaining adaptor sequences which may remain within the data after automated removal during the Illumina sequencing pipeline. Adaptor removal was conducted using Cutadapt (Version 1.12) (Martin, 2011). Cutadapt was also used to remove reads smaller than 20 bp (Williams *et al.*, 2016) and those with an average Phred score of less than 10 (Mach *et al.*, 2014; Macmanes, 2014).

2.3.15 Quality Metrics

In order to monitor the overall quality of the data, FastQC (Version 0.11.5) (Andrews, 2010) was applied to datasets before and after filtering steps were conducted. This tool allows identification of average quality by base, average quality per read, the presence of adaptor

sequences as well as several other metrics which may indicate problems within a dataset.

2.3.16 Mapping of Illumina Sequence Data

The *Sus scrofa10.2* genome data was downloaded from Illumina iGenomes (https://support.illumina.com/sequencing/sequencing_software/igenome.html) on 01/02/17. This contained gene annotation files from Ensembl release 81. Data which passed the filtering steps were mapped to this genome using HISAT2 version 2.0.5 (Kim *et al.*, 2015). The resulting sequence alignment map (SAM) files were converted to binary alignment map (BAM) files using samtools version 1.3.1 (Li *et al.*, 2009).

Genes and transcripts were then assembled and quantified using stringtie version 1.3.2b (Pertea *et al.*, 2015). Transcripts from all samples were merged, which allowed transcript abundances for each sample to be estimated and table counts for downstream analysis to be constructed.

The second method of alignment was applied to further interrogate the RNA-seq datasets. Kallisto (version 0.43.0) (Bray *et al.*, 2016) utilises a

pseudo alignment technique whereby k-mers present in the reference are matched to those present in the sequencing reads to identify the most probable location for a given read. As Kallisto requires a transcriptome rather than a genome as a reference, the *Sus scrofa* 10.2 cDNA library (build 79) obtained from Ensembl was used for this purpose *(*ftp://ftp.ensembl.org/pub/release-79/fasta/sus_scrofa/cdna/Sus_scrofa.Sscrofa10.2.cdna.all.fa.gz). A bootstrap value of 100 was set for these alignments.

2.3.17 Differential Gene Expression

Differential expression analysis was conducted using Ballgown 2.6.0 (Frazee *et al.*, 2015). This package was used with R version 3.3.2.

Differential expression analysis of Kallisto alignments was conducted using Sleuth (version 0.29.0) (Pimentel *et al.*, 2017). This package was designed by the same group as Kallisto, making it completely compatible with Kallisto alignments. Cut-offs of $q < 0.1$ and Log_2 FC ≥ 1 or ≤ -1 were applied to differential transcript expression data.

2.3.18 Gene Ontology and Gene Pathway Enrichment

Enriched gene ontologies and KEGG pathways were determined using NIPA (Version 0.6.3) (Richard Emes, personal correspondence). NIPA is available from GitHub (https://github.com/ADAC-UoN/NIPA). NIPA code determines enriched gene ontology and pathways using hypergeometric tests. This was used to identify gene ontologies associated with biological processes (BP), Cellular components (CC) and molecular functions (MF).

CC refers to the place in the cell where a gene product is active. These terms reflect our understanding of eukaryotic cell structure (Ashburner *et al.*, 2000). CC includes such terms as 'nuclear membrane' or 'Golgi apparatus'.

MF is defined as the biochemical activity, including specific binding to ligands or structures, of a gene product. These terms describe only what is done, without specifying when or where this interaction occurs. Examples of MF terms include 'adenylate cyclase' or 'Toll receptor ligand' (Ashburner *et al.*, 2000).

BP refers to a biological objective to which the gene or gene product contributes. A biological process is accomplished via an assembly of one or more molecular functions. These processes often involve a chemical

or physical transformation. Examples of BP terms include 'cell growth and maintenance' and 'signal transduction' (Ashburner *et al.*, 2000)

Differentially expressed transcripts with $q < 0.1$ (False detection rate corrected p-value) and Log2 FC ≥ 1 or ≤ -1 were used as input. Up and downregulated genes were screened for enrichment separately as this is more powerful than analysing all the differentially expressed genes together (Hong *et al.*, 2014). Gene ontologies were considered enriched if they contained 2 or more differentially expressed genes and if the term met the significance cutoff of $q < 0.05$ (Li *et al.*, 2016c).

2.4 Graphics and Statistical Analysis

Graphical representation of data was performed using R (version 3.3.2) and Bioconductor (version 3.6). Principal component analysis (PCA) and hierarchical clustering were carried out using FactoMineR (version 1.14) (Lê *et al.*, 2008). Venn diagrams were constructed using Venny (Version 2.1) (Oliveros, 2007-2015).

Heatmaps and additional PCA plots were constructed using ClustVis (https://biit.cs.ut.ee/clustvis/)(Metsalu and Vilo, 2015).

False detection rate correction was conducted using the Benjamini-Hochberg method (Benjamini and Hochberg, 1995). False detection rate corrected *p*-value will henceforth be referred to as *q*-value.

3 Chapter 3: The Transcriptional Effect of Weaning on the Porcine Colon Observed after HiSat2 Mapping

3.1 Introduction

Pigs experience biological stress such as physiological, environmental and social challenges when weaned from the sow (Campbell *et al.*, 2013; Gresse *et al.*, 2017). This stressful event can contribute to detrimental effects on piglet gut health leading to weight loss immediately after weaning (He *et al.*, 2017; Rhouma *et al.*, 2017; Stokes, 2017). It has been suggested that these detrimental effects may be brought about due to the interruption of mucosal barrier development, which is ongoing during this period (Moeser *et al.*, 2017; Stokes, 2017).

In the colon, some limited transcriptional changes have been observed in response to weaning, including an early increase in *IL-1β* up to two days post-weaning and a later increase in *IL-8* and decrease in *IL-12* expression between two and eight days post-weaning (Pie *et al.*, 2004). However, many studies which concern gene expression in the porcine

colon post-weaning compare the weaning pig with and without a dietary supplement. These include; seaweed extract (Walsh *et al.*, 2012); additional protein (Zhang *et al.*, 2017); dietary calcium (Metzler-Zebeli *et al.*, 2015); pea fibre (Che *et al.*, 2014) and soybean meal (Kroger *et al.*, 2013) amongst others. As such, there is limited information available on the transcriptional changes in the colon of the weaning pig which can be solely attributed to weaning alone.

To gain an insight into the transcriptional effects of weaning in the colon, this chapter details the differential gene expression observed by RNA-seq between weaned (n= 4) and suckling pigs (n =4) for three time points of 22, 25 and 35 days of age. The weaned specimens were weaned at 21 days of age providing a view to the transcriptional effects of weaning one, four and 14 days after this stressful life event.

The initial stage of dataset manipulation in a transcriptomic workflow consists of an analysis of data quality. In the workflow presented in this study, FastQC (Andrews, 2010) was used to visualise metrics such as per base sequence quality; per sequence quality; sequence length distribution and per base composition. These metrics can be used to identify problems within a dataset. Following initial visualisation of these metrics, Cutadapt (a trimming and filtering package, (Martin,

2011)) was used to remove Illumina adaptor contamination, reads shorter than 20bp and reads with an average Phred score of less than ten. This stage removed reads which are unsuitable for downstream mapping. Examples of quality control before and after trimming and filtering of datasets containing only 50 bp and a combination of 50 and 100 bp reads can be found in Appendix 3.

After the completion of trimming and filtering, the next stage of the workflow was the mapping stage. Datasets were aligned to the S*us scrofa* 10.2 genome using HiSat2 (Kim *et al.*, 2015). Read counts were extracted from these alignments using Stringtie (Pertea *et al.*, 2015) and differential gene expression analysis was conducted using Ballgown (Pertea *et al.*, 2016). The results section of this chapter will first address alignment and expression values obtained from all samples before focusing on differential expression identified between colon samples obtained from weaned and suckling pigs.

3.2 Results

3.2.1 Raw Transcriptomic Reads

Datasets for 48 samples of colon RNA-seq (Weaned & Suckling ± Probiotic) for one, four and 14 days' post-weaning arrived as 50 bp paired-end reads. Additional reads were provided for 20 of the samples later as 100 bp paired-end reads (Appendix 2), by resequencing the same library preparation constructed for the sequencing of the 50 bp paired-end reads.The 50 bp paired-end datasets without the addition of the 100 bp reads contained a mean of 47,052,031± 8,706,623 paired-end reads (4,755.79 ± 901.12 Mbp). The 20 additional datasets contained a mean of 12,103,425 ± 5,120,224 100 bp paired-end reads (2,444.89 ± 1,034.12 Mbp). Where 100 and 50 bp reads were provided for a single sample, these were combined into a single dataset for downstream analysis. After this concatenation, final datasets contained a mean of 52,353,342 ± 4,511,140 paired-end reads (5,826.67 ± 845.92 Mbp). Information on individual samples can be found in Appendix 2.

3.2.2 Overview of Read Usage

The 48 raw datasets for colon RNA-seq contained a mean of 52,353,342 ± 4,511,140 reads. Filtering these datasets using Cutadapt (Martin, 2011) to remove Illumina adaptors, reads with an average quality score

and length of less than 20bp removed a mean of 341,022 ± 79,346 (0.65% ± 0.14%) from the datasets. Filtered data sets were then mapped to the *Sus scrofa* 10.2 genome using HiSat2 (Kim *et al.*, 2015). A mean of 8,410,623 ± 769,489 reads either could not be mapped to the *Sus scrofa* genome or could not be mapped uniquely to a single position. This constituting 16.08% ± 0.78% of the raw datasets. The remaining reads 43,601,697 ± 3,838,314 reads, 83.27% ±0.82% of the raw datasets, were mapped exclusively to the genome. Graphical representation of this information can be found in Figure 3-1 and Figure 3-2. A table to denote treatments from sample number can be found in Appendix 4, and individual sample information can be found in Appendix 5.

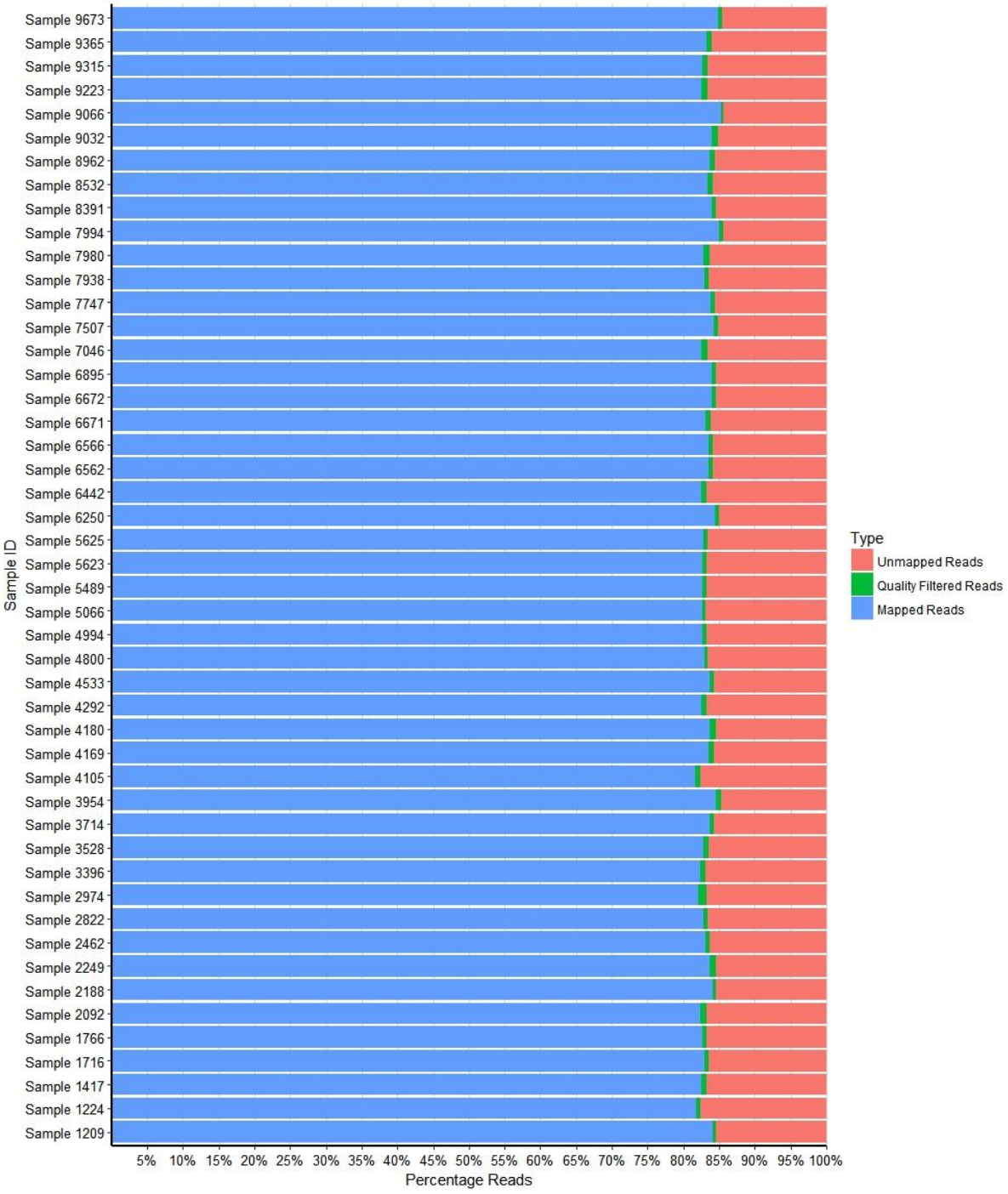


Figure 3-1: Percentages of RNAseq datasets mapped uniquely, unmapped and removed by quality filtering.

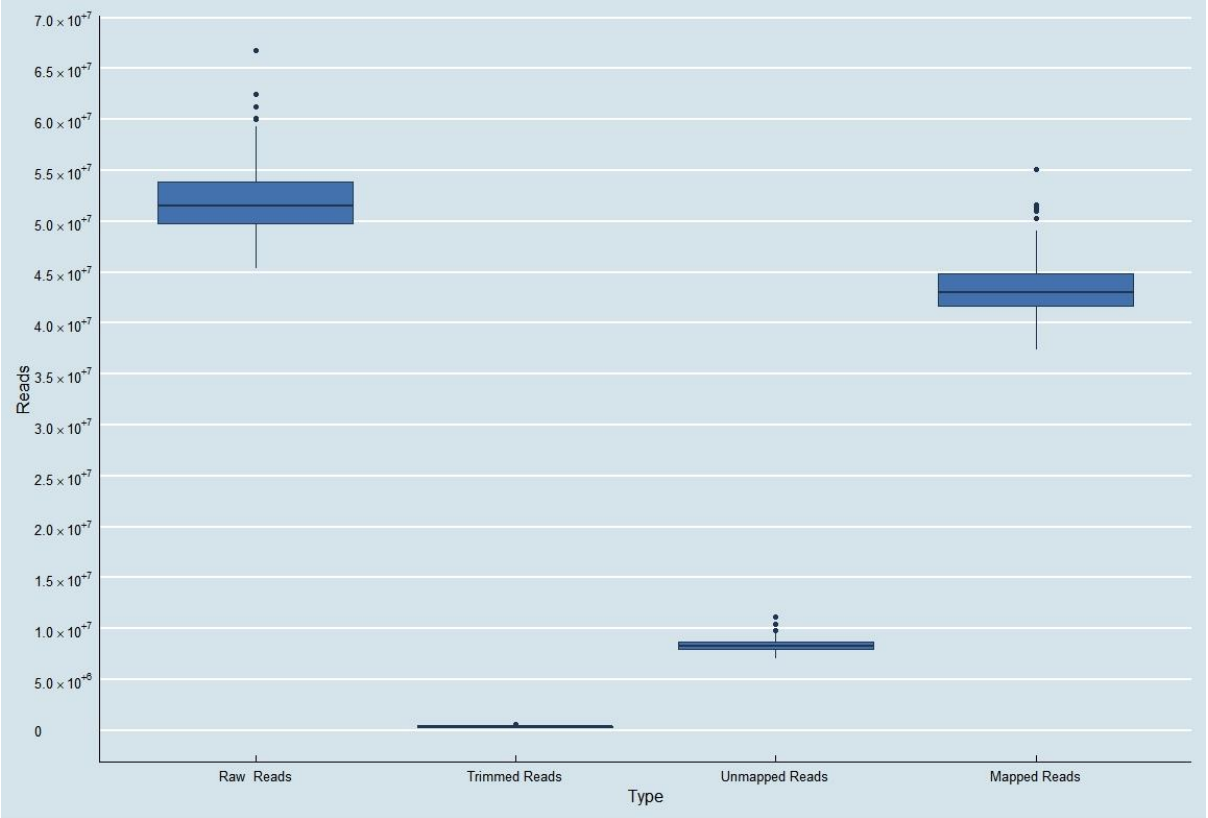


Figure 3-2: Box plots to show the number of raw RNAseq reads, reads removed by trimming, reads which were unmapped and reads which mapped successfully. Blue box represents the interquartile range with the central line showing the median value. The upper whisker shows quartile one plus 1.5 times the interquartile range, lower whisker shows quartile three minus 1.5 times the interquartile range. Outliers are data points which lie outside these ranges.

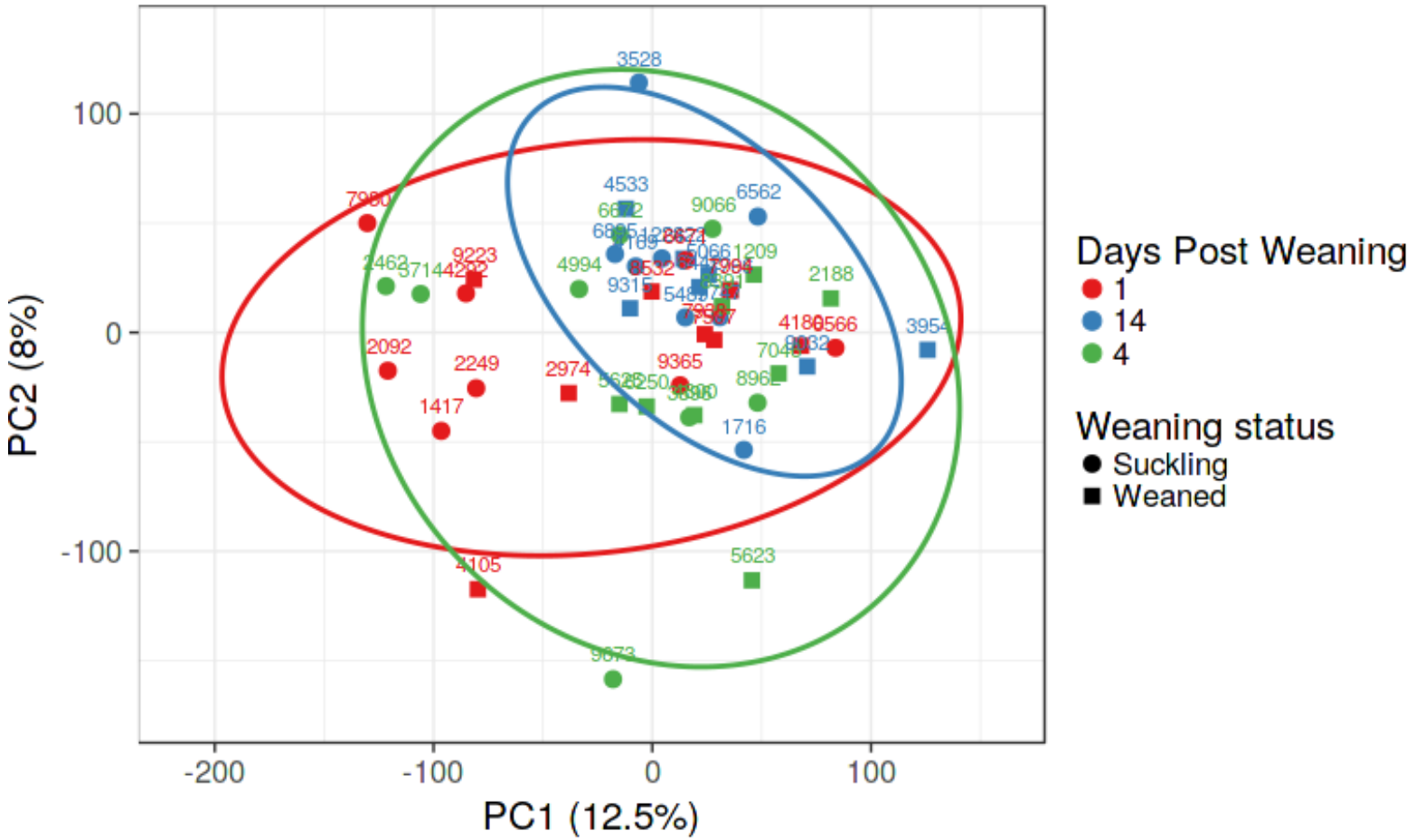
3.2.3 Principal Component Analysis of FPKM Profiles

Principal component analysis was conducted on all FPKM profiles.

Principal component analysis is a statistical procedure which converts a set of observations into principal components which are a measure of the spread of the data. The first principal component accounts for as much of the variability in the dataset as possible. The second principal

component accounts for as much of the remaining variability as possible. In this manner, the variability of large datasets can be summarised on a two-dimensional graph.

Figure 3-3 shows the PCA plot for sample FPKM profiles coloured by the number of days after weaning that the source animal was slaughtered. This shows no obvious grouping of samples by slaughter point. 95% Confidence ellipses for each slaughter point overlap, confirming that samples from individual slaughter points cannot be separated according to the two largest sources of variability. The PCA plots shown in Figure 3-4 indicate the same FPKM profiles coloured by weaning status and split into individual time points. Again, a graphical representation of principal component 1 and 2 are unable to separate samples from weaned and suckling animals at any of the three time points (one, four and 14 days post weaning). Finally, Figure 3-5 shows these same plots but this time coloured by whether the source animal was given probiotic *Saccharomyces cerevisiae boulardii.* As with the previous groupings, no differences between these treatments was observed at any timepoint, with samples from the two treatments overlapping. A hierarchical clustering plot representing the FPKM profiles plotted can be found in Appendix 6.



***Fi*gure 3-3: PCA of FPKM profiles coloured by slaughter point**. Principal component analysis to show variation between samples. Samples are coloured by slaughter point. Red denotes one day post weaning, green denotes four days post weaning and blue denotes 14 days post weaning. Weaning status is also indicated as circles show suckling animals whereas squares show weaned animals. The corresponding coloured ellipses show 95% confidence.

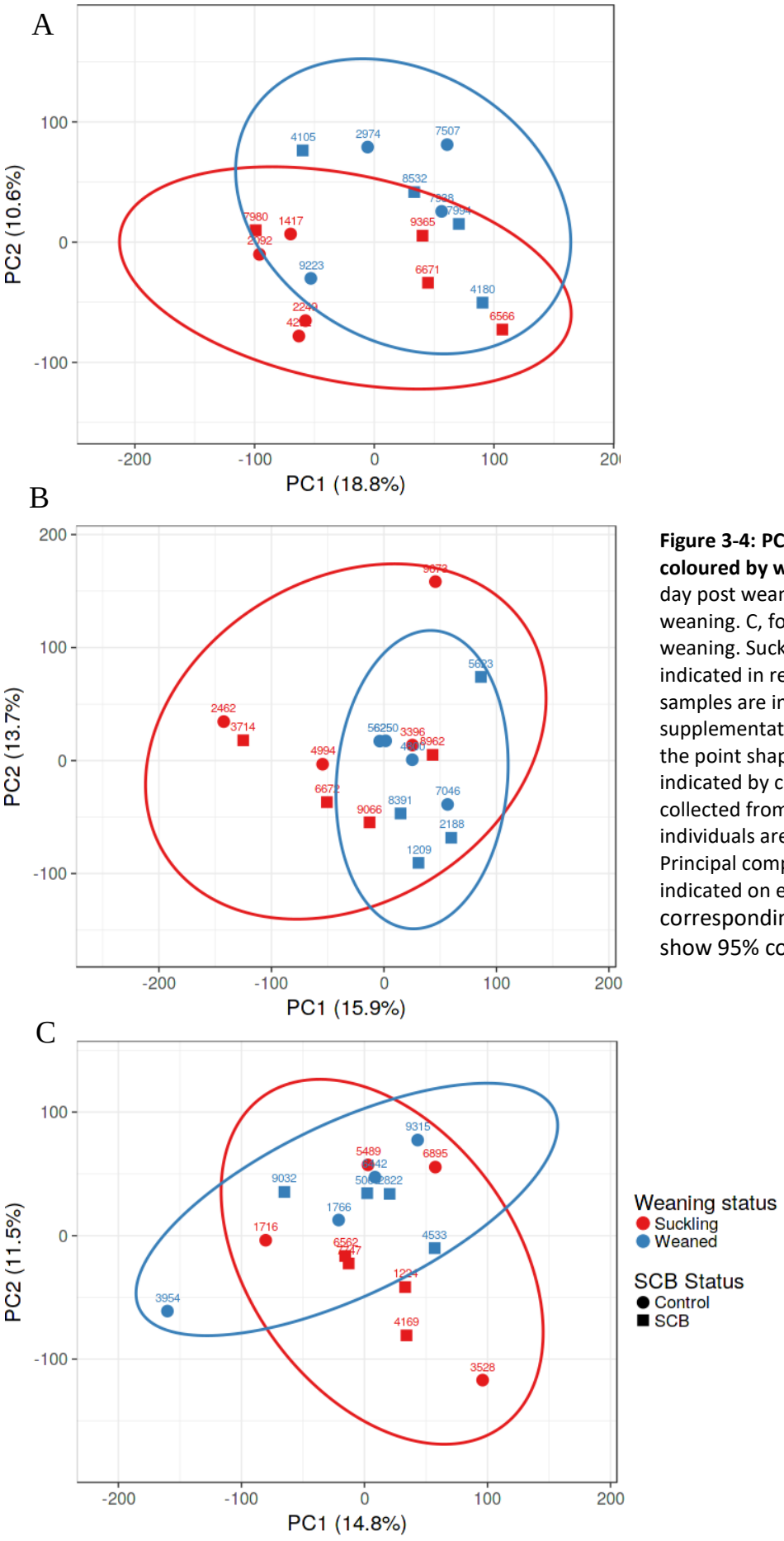


Figure 3-4: PCA of FPKM profiles coloured by weaning status. A, one day post weaning. B, four days post weaning. C, fourteen days post weaning. Suckling samples are indicated in red whereas weaned samples are indicated in blue. SCB supplementation is also indicated by the point shape with control samples indicated by circles whereas samples collected from SCB supplemented individuals are indicated by squares. Principal component one and two are indicated on each graph. The corresponding coloured ellipses show 95% confidence.

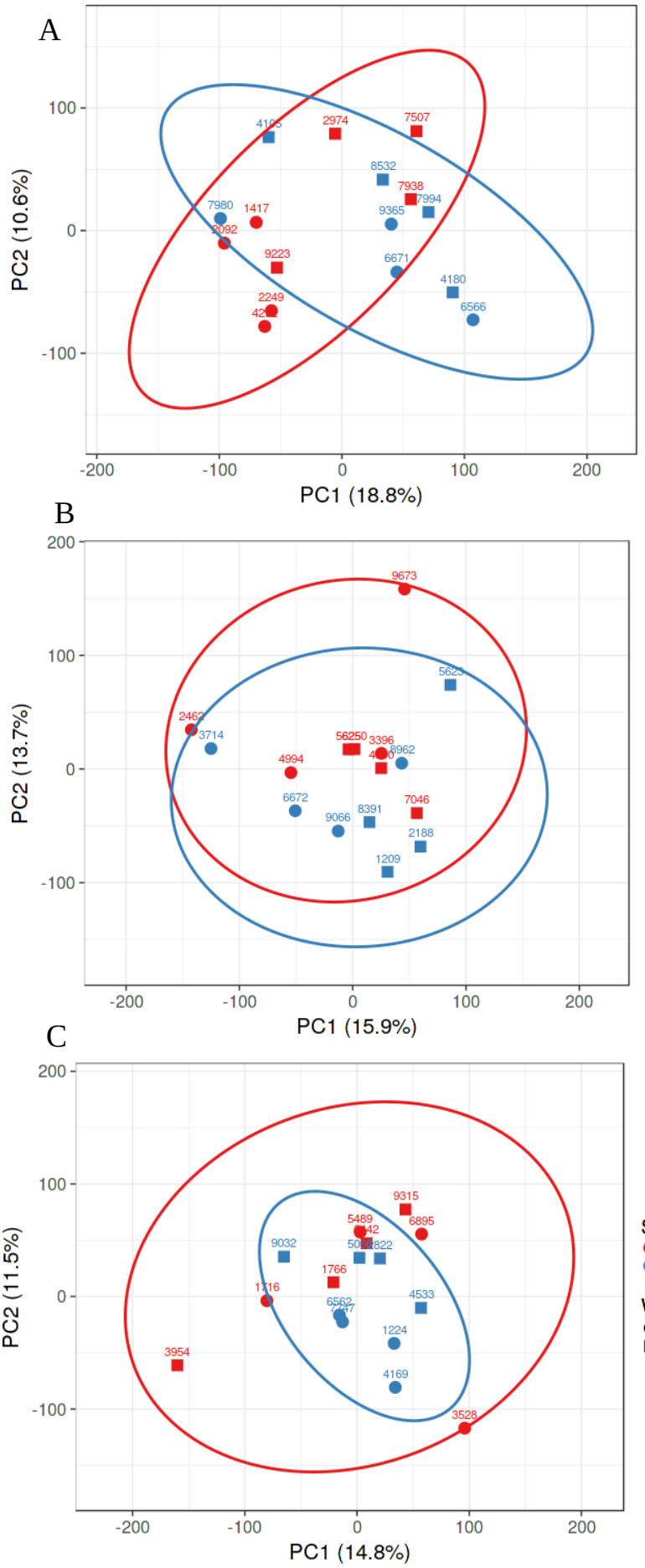


Figure 3-5: PCA of FPKM profiles coloured by probiotic status. A, one day post weaning. B, four days post weaning. C, fourteen days post weaning. Control samples are indicated in red whereas samples collected from SCB supplemented animals are indicated in blue. Weaning status is also indicated by the point shape with suckling samples indicated by circles whereas samples from weaned animals are indicated by squares. Principal component one and two are indicated on each graph. The corresponding coloured ellipses show 95% confidence.

3.2.4 Overview of Weaning Related Differential Gene Expression

To visualise differential gene expression between the weaned and suckling cohorts, a volcano plot for each time point was constructed. These plot the fold change against the probability value for each transcript monitored. Figure 3-6 shows all three of these plots, as a false detection rate corrected probability value (*q* value) of less than 0.1 was considered significant, all transcripts which met this threshold have been coloured in red. Considering the findings of the previous chapter, whereby PCA analysis suggested that only subtle changes in gene expression may be observed, no fold change cut-off has been applied.

The volcano plot Figure 3-6A shows the differential gene expression observed at one-day post-weaning (21 days of age). When comparing the four pigs from the suckling control cohort to the corresponding four of the weaned control cohort, seven transcripts were identified as significantly differentially expressed ($q < 0.1$). At four days post-weaning (25 days of age), the comparison found only two transcripts were significantly differentially expressed (Figure 3-6B). Finally, at 14 days post-weaning (35 days of age,) no transcripts were significantly differentially expressed (Figure 3-6C).

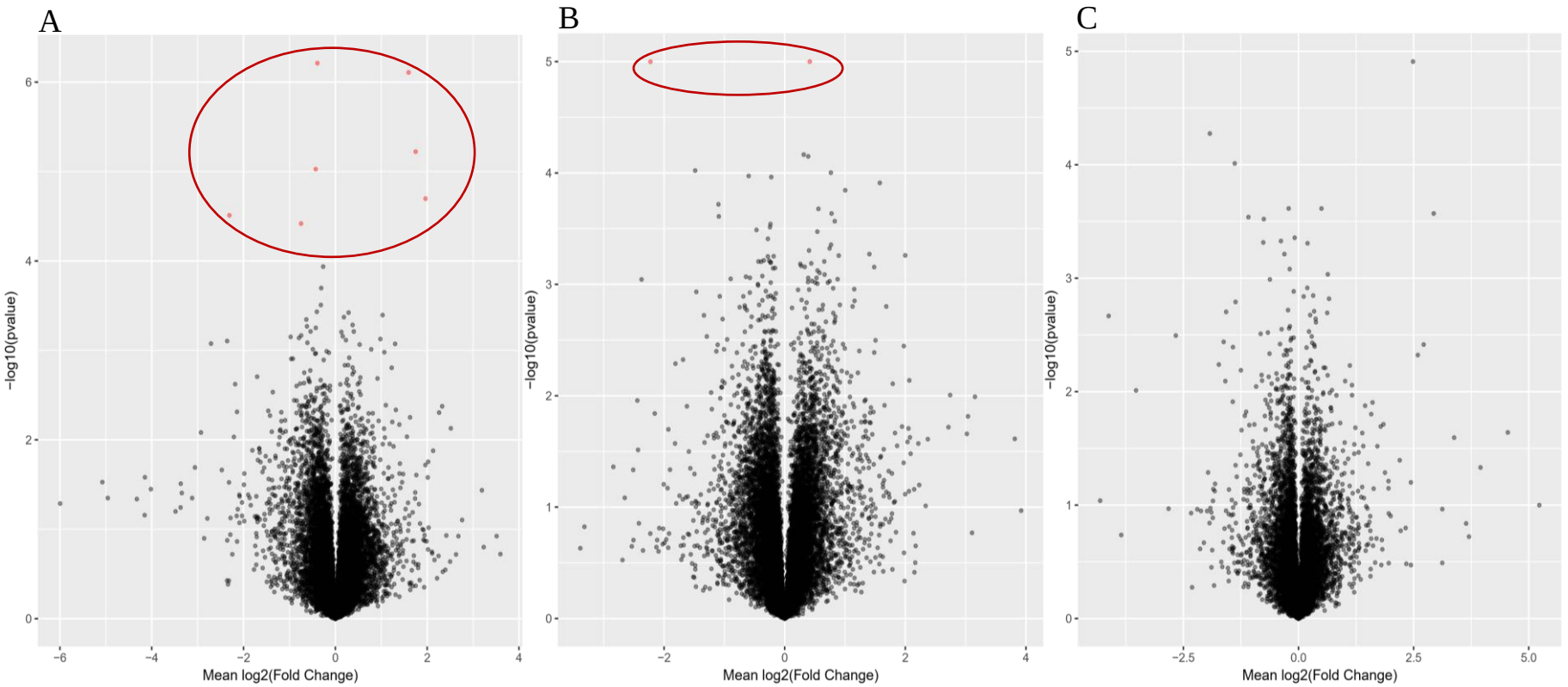


Figure 3-6: Volcano Plots to show differential gene expression when comparing weaned and suckling control pigs at one, four and 14 days post-weaning. -log10 of the probability value is plotted against Log2 fold change for each transcript. Differential gene expression calculated by Ballgown from HiSat2 mappings. A, one-day post-weaning (22 days of age). B, four Days post-weaning (25 days of age). C, 14 days post-weaning (35 days of age). Transcripts $q <$ 0.1 indicated by red points and contained within red ellipses.

3.2.5 Comparison of Differential Gene Expression between One, Four and 14 days Post-Weaning

The lists of transcripts identified as differentially expressed at one, four and 14 days post-weaning were compared to identify any transcripts which are similarly differentially expressed across the time series. As only a total of nine transcripts were identified as significantly differentially expressed (q<0.1), the comparison was also made with all transcripts differentially expressed with a probability value <0.01.

Figure 3-7A shows the shared differentially expressed transcripts (p <0.01). With this probability value cut-off, only a single transcript was differentially expressed at all three time points. Nine were shared between one and four days post-weaning, seven shared between four and 14 days post-weaning and five shared between one and 14 days post-weaning. However, as this probability value cut-off is not sufficient for downstream analysis, this information is only provided as context. When transcripts which met the q-value cut-off of <0.1 are compared, none are shared between time points. With the seven significantly differentially expressed transcripts at one day post-weaning exclusive to this time point, and the same can be said for the two significantly differentially expressed transcripts at four days post-weaning. No

differentially expressed transcripts at 14 days post-weaning met this *q* value cut-off, so this timepoint is not represented in Figure 3-7B.

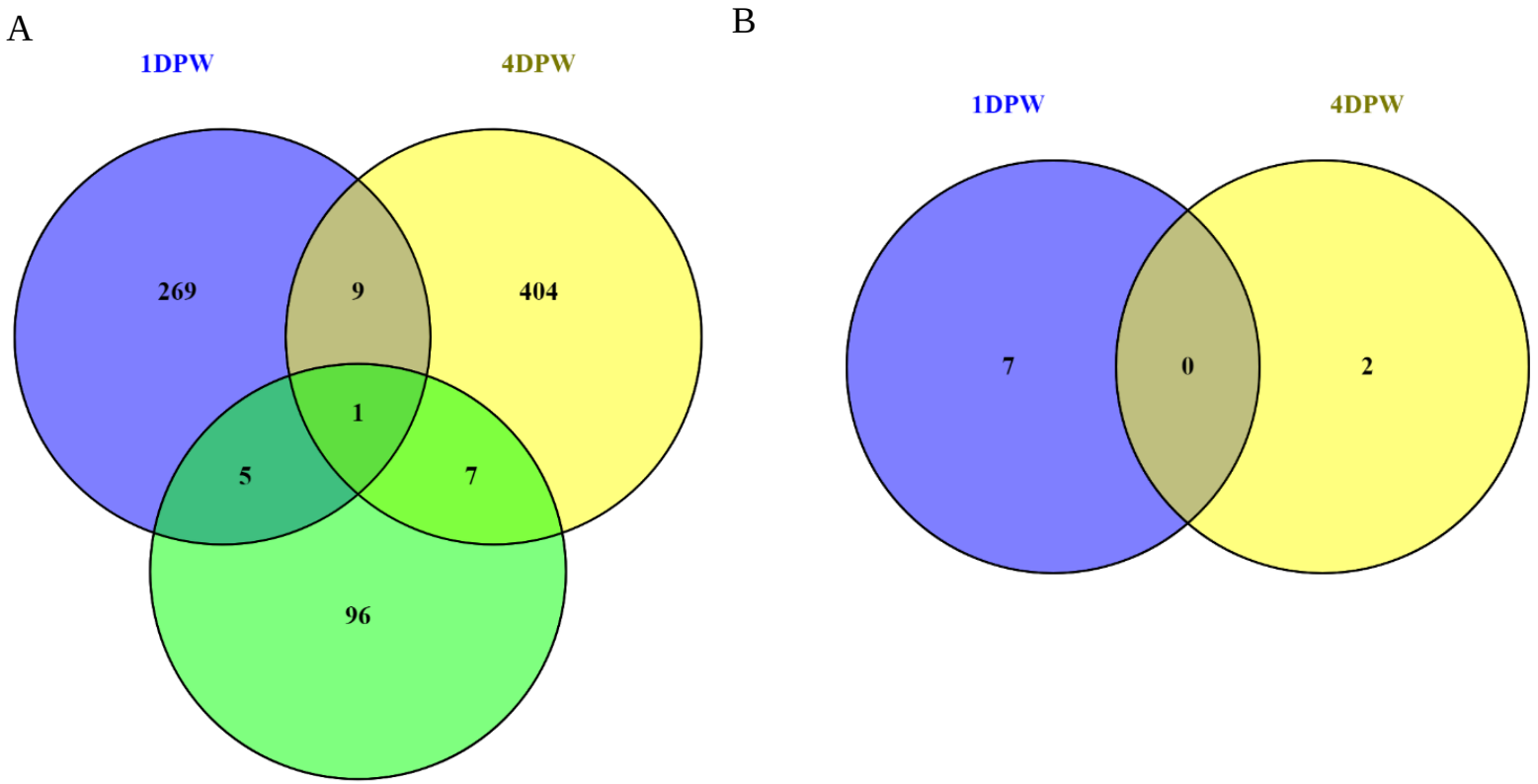


Figure 3-7: Venn diagrams to show differentially expressed transcripts shared between timepoints. 1DPW; one day post weaning shown in blue. 4DPW; four days post weaning, shown in yellow. 14DPW; 14 days post weaning, shown in green. A, differentially expressed transcripts p <0.01. B, differentially expressed transcripts q <0.1.

3.2.6 Differentially Expressed Transcripts

Table 3-1 contains all transcripts identified as significantly differentially expressed ($q < 0.1$) in comparisons between weaned control and suckling control colon samples. 14 days post-weaning is not represented as no transcripts met the significance threshold in this comparison.

At one-day post-weaning, seven transcripts were identified as significantly differentially expressed, however only three of these transcripts exhibited a greater than one Log_2 fold change. Transcripts encoding multiple epidermal growth factor-like domains 9 (*MEGF9*), growth arrest-specific two like 3 (*GAS2L3*), and thioredoxin-related transmembrane protein 3 (*TMX3*) all exhibited an approximately 3-fold change increase in the weaned samples (Log_2 FC 1.59-1.96).

The other four significantly differentially expressed transcripts at this time point were sepiapterin reductase (*SPR*); C2 calcium-dependent domain containing 2 (*C2CD2*); ectonucleotide pyrophosphatase/phosphodiesterase family member 7 (*ENPP7*) and tetraspanin (*TSPAN11*). All of which were downregulated by weaning with a fold change of between 0.76 and 0.2 (Log_2 FC –0.39 to -2.3).

At four days post-weaning, there was a 1.3-fold change (Log_2 FC = 0.42) in the expression of dual specificity phosphatase 23 (*DUSP23*) in the weaned samples as well as a 0.2-fold change (Log_2 FC = -2.23) in the expression of mitochondrial ribosomal protein S16 (*MRPS16*). As so few transcripts were identified as differentially expressed, no gene network or gene ontology enrichment analyses were conducted.

Table 3-1: Differentially expressed transcripts (q <0.1) identified using Ballgown

One Day Post Weaning								
Fold Change	**Log_2 FC**	**p value**	**q value**	**Transcript ID**	**Gene ID**	**Gene Symbol**	**Gene Name**	**Change with Weaning**
0.76165944	-0.39278	6.14E-07	0.006184762	ENSSSCT00000009100	ENSSSCG00000008309	SPR	Sepiapterin reductase	Down
3.020903298	1.59498	7.81E-07	0.006184762	ENSSSCT00000006055	ENSSSCG00000005506	MEGF9	Multiple epidermal growth factor-like domains 9	Up
3.360128776	1.748517	5.99E-06	0.031659963	ENSSSCT00000030549	ENSSSCG00000000874	GAS2L3	Growth arrest specific 2 like 3	Up
0.743035091	-0.4285	9.41E-06	0.037281922	ENSSSCT00000030786	ENSSSCG00000025821	C2CD2	C2 calcium-dependent domain containing 2	Down
3.898561039	1.962942	2.01E-05	0.063659439	ENSSSCT00000005390	ENSSSCG00000004884	TMX3	Thioredoxin related transmembrane protein 3	Up
0.201814074	-2.3089	3.09E-05	0.081636692	ENSSSCT00000001916	ENSSSCG00000022542	ENPP7	Ectonucleotide pyrophosphatase/phosphodiesterase family member 7	Down
0.595548973	-0.74771	3.82E-05	0.086521168	ENSSSCT00000000797	ENSSSCG00000000734	TSPAN11	Tetraspanin	Down
Four Days Post Weaning								
Fold Change	**Log_2 FC**	**p value**	**q value**	**Transcript ID**	**Gene ID**	**Gene Symbol**	**Gene Name**	**Change with Weaning**
1.335081477	0.416928	1.00E-05	0.077360076	ENSSSCT00000027662	ENSSSCG00000028090	DUSP23	Dual Specificity Phosphatase 23	Up
0.213831378	-2.22545	1.00E-05	0.077360076	ENSSSCT00000024853	ENSSSCG00000028634	MRPS16	Mitochondrial ribosomal protein S16	Down

3.3 Discussion

The quality of the sequences within the RNA-seq datasets was observed to be generally very high, with the majority of per sequence and per-base quality scores found to be a Phred score of 30 or greater (Appendix 3). Quality filtering removed only the reads with an average Phred score of ten or less. However, as the input sequences were of high quality, this filter did not bring about a substantial change in the spread of per-base quality scores (Appendix 3). The function of this filter was to remove any reads of insufficient quality for accurate alignment (Li and Homer, 2010). To this end, no reads with an average Phred score of less than ten remained after filtering. Any remaining poor bases at the 3' or 5' end of reads can be dealt with during mapping by the ability of HiSat2 to 'soft-clip' (Kim *et al.,* 2015). Soft clipping allows low-quality bases at the ends of reads to be ignored during alignment.

FastQC (Andrews, 2010) is unable to detect the presence of Illumina adaptors within the data either before or after filtering (Appendix 3). However, the variation in read length after trimming can only be attributed to the removal of these sequences by Cutadapt (Martin,

2011), as none of the other selected parameters could do this. This may be attributed to FastQC only checking the first 20,000 reads. However, these sequences exist in small quantities throughout the rest of the dataset and are removed by the adaptor trimming step, resulting in shorter reads.

Before adaptor trimming, all sequences were a uniform length of 51bp, or a combination of 51 and 101 bp as detailed in Appendix 3. The additional base is an artefact of sequencing. After trimming, all reads less than 20bp in length were removed (Appendix 3). This filter was applied as short sequences resulting from trimming can contribute to bias in RNA-seq results. Applying a length filter minimises the introduction of unpredictable changes in expression estimates (Williams et al., 2016).

Per-base sequence composition diagrams (Appendix 3) show variation in base composition in the first 13 bases. The remainder of the reads show a composition of 25% A, T, G and C nucleotide contributions. The bias in base composition observed in the first 13 bases is reproducible between experiments and even species. It can be attributed to the use of random hexamers in the priming of reverse transcription of RNA into cDNA, the initial stage of library preparation (Hansen et al., 2010). The

composition of 25 % A, T, G and C nucleotide contributions in subsequent bases is consistent with that observed in other porcine RNA-seq studies (Esteve-Codina *et al.*, 2011; Ayuso *et al.*, 2015).

In summary, sequencing reads from the 48 RNA-seq datasets were of high quality. However, reads of very low quality, adaptor sequences and reads shorter than 20bp were removed. This ensured that the remaining raw data were suitable for downstream mapping and expression calling.

Read usage statistics were found to be uniform across samples with approximately 83% of the approximately 53 million raw reads per sample, approximately 43 million paired-end reads, were successfully mapped to the *Sus scrofa* genome (Figure 3-1,Figure 3-2). Other porcine RNA-seq studies vary widely in the number of input reads, from 10 million reads per sample (Li *et al.*, 2016d) to 133 million (Cardoso et al., 2017a). However, the majority of studies are at the lower end of this range such as 23 million (Jung et al., 2012), 30 million (Gunawan et al., 2013) and 40 million (Chen et al., 2011). In these studies, the percentage of reads mapping to the genome also varies from 54% of 23 million reads per sample (Jung et al., 2012), to 72.8% of 133 million reads per sample (Cardoso et al., 2017a). However, some studies do not

publish mapping statistics (Bauer *et al.*, 2010; Li *et al.*, 2016d; Wang *et al.*, 2016), or even the number of input reads (Ramayo-Caldas *et al.*, 2012; Sodhi *et al.*, 2014; Hu *et al.*, 2016), making it impossible to draw a comparison. In the context of these pig RNA-seq studies, 43 million mapped reads per sample suitable for expression calling constitutes greater transcriptome coverage than many existing studies.

Few transcripts were identified as significantly differentially expressed ($q < 0.1$) when comparing colon samples from weaned and suckling pigs at one, four and 14 days post-weaning. Of the seven significantly differentially expressed transcripts identified at one-day post-weaning, and two at four days post-weaning, only four transcripts at one-day post-weaning and one transcript at four days post-weaning exhibited greater than one Log_2 fold change in expression.

Although the biological relevance of fold change depends on the nature of the gene product, a fold change cut-off is often applied to RNA-seq studies. Examples of this in pig studies include Log_2 FC cut-offs of ≥ 1.2 and ≤ -1.2 (Puig-Oliveras et al., 2014); ≥ 1 and ≤ -1 (Esteve-Codina *et al.*, 2011; Li *et al.*, 2016d). If the lower of these cut-offs were to be applied to the current findings, then only five differentially expressed transcripts would meet both criteria of $q < 0.1$ and Log_2 FC ≥ 1 and ≤ -1.

Three of these transcripts, at one-day post-weaning show an approximately 3-fold increase in the weaned cohort (Table 3-1). Multiple epidermal growth factor-like domains 9 (*MEGF9,*) is one of these upregulated transcripts. The *MEGF9* gene has been shown to be induced by cortisol in human foetal cells (Salaria *et al.,* 2006) and in weaned pigs after adrenocorticotropin hormone injection (Sautron *et al.,* 2015). This is consistent with the current study where the weaned pigs at one day after weaning had greater circulating cortisol than the corresponding suckling animals (Le Bon, 2012b). The function of MEGF9 is poorly understood. However, it has been observed to be expressed in the central and peripheral nervous systems, as well as non-neuronal tissues. It has been suggested that it may have a role as a guidance or signalling molecule and that it may play a role in myelination of nerve cells (Brandt-Bohne *et al.,* 2007).

The remaining two upregulated transcripts showing an approximately 3-fold change in favour of the weaned cohort at one-day post-weaning were growth arrest-specific two like 3 (*GAS2L3*) and thioredoxin-related transmembrane protein 3 (*TMX3*). *GAS2L3* is widely conserved throughout evolution and is ubiquitously expressed in human tissues (Stroud *et al.,* 2011). GAS2L3 binds both microtubules and the actin

cytoskeleton, as such, it is essential in development and cellular proliferation (Stroud *et al.*, 2011; Zhang *et al.*, 2016). As such, the observed upregulation may be because of increased development of the porcine intestine to accommodate the solid diet after weaning. Although no weaning studies identified differential expression of this gene, TMX3 is an enzyme with thiol oxidase activity associated with the endoplasmic reticulum (Haugstetter *et al.,* 2005). Function and expression of *TMX3* in the gastrointestinal tract has not been characterised.

A single significantly downregulated transcript met the criteria of ≤1 Log_2 FC at one-day post-weaning. This transcript encoded *ENPP7*. This gene encodes alkaline sphingomyelinase, an enzyme which digests sphingomyelin. Sphingomyelin is present in milk, where it has been demonstrated to promote the development of the intestinal mucosa in newborn rats (Motouri *et al.*, 2003; Zhang *et al.*, 2011). Downregulation of this enzyme in the colon of weaned pigs may result from the absence of milk in the diet of weaned animals.

The only differentially expressed transcript which meets the selection criteria at four days post-weaning was downregulated and encoded

Mitochondrial ribosomal protein S16. As this gene is not widely studied, the effects of downregulation are not well understood.

The number of differentially expressed transcripts detected could have been increased by relaxing the identification criteria of q <0.1 and Log_2 FC ≥ 1 or ≤ -1. The distribution of points in volcano plots for each of the time points shown in Figure 3-6 suggest that relaxing the *q* value cut off would have this effect. However, relaxing this criterion would increase the number of false positives detected (Li *et al.*, 2012). The *q* value cut off 0.1 used in this study suggests that 10 % of identified transcripts are false positives. Increasing this cut-off to 0.2 would increase the rate of false positives to 20 %. Because of this effect, the *q* value cut-off is a trade-off between the number of differentially expressed transcripts detected, and the number of those transcripts which are incorrectly identified as differentially expressed (Reiner *et al.*, 2003).

Published studies of porcine RNA-seq vary in the *q* value cut off set from $q < 0.01$ (Hu *et al.*, 2016) and $q < 0.05$ (Mach *et al.*, 2014; Cardoso *et al.*, 2017a) to $q < 0.1$ (do Nascimento *et al.*, 2018). Therefore, the q value cut off used in this study is relaxed when compared to relevant literature and further relaxation of this criteria would introduce an unacceptable level of false positives.

As so few differentially expressed transcripts were found, identification of canonical pathway and gene ontology enrichment was not appropriate. As such it is difficult to assign biological function to so few differentially expressed genes with any certainty. The only global observation which can be made is that there is a reduction in the number of significantly differentially expressed transcripts along the time series, with the largest number (seven) occurring at one-day post-weaning. This is reduced to two at four days post-weaning, and none are observed at 14 days after weaning. This may represent a minor change in gene expression immediately after weaning due to the abrupt stresses associated with this incident. This is followed by gradual settling of these responses which is complete by 14 days after weaning when the weaned and suckling cohorts exhibit similar gene expression.

However, the few observed changes in gene expression may be a product of the methodology employed. Many different tools for calculating differential gene expression from RNA-seq data exist, (Anders and Huber, 2010; Hardcastle and Kelly, 2010; Robinson *et al.*, 2010; Wang *et al.*, 2010; Trapnell *et al.*, 2012; Leng *et al.*, 2013; Li and Tibshirani, 2013; Law *et al.*, 2014; Love *et al.*, 2014; Schurch *et al.*, 2016; Pimentel *et al.*, 2017). Each tool makes assumptions about the

statistical properties inherent to RNA-seq data, and they use a range of different normalisation and statistical analyses to compute the magnitude of a differential gene expression result and estimate its significance (Schurch *et al.*, 2016). It may be the case that due to the subtle nature of the differences between samples, a more sensitive method may be more successful at identifying differential gene expression in the present study. As such the implementation of a second method may aid in the deduction of biologically relevant changes in gene expression.

3.4 Conclusion

Very few significant changes in transcript expression were observed between weaned and suckling pigs using the HiSat2, StringTie, Ballgown method. This made any explanation of these few changes extremely difficult in the context of the complex biological system of the porcine colon. To better characterise the changes in gene expression, with a view to inferring biological function, a second method of RNA-seq analysis will be employed.

4 Chapter 4: The Transcriptional Effect of Weaning on the Porcine Colon Observed by a Pseudoalignment Technique

4.1 Introduction

To further investigate differential gene expression in the porcine colon at weaning, a second method of RNA-seq analysis was applied. This second methodology utilised Kallisto for RNA-seq quantification (Bray *et al.*, 2016). Kallisto pseudoaligns reads to a reference without the need to align individual bases to the reference. This is achieved by the identification of k-mers, short sequences, within the input transcriptome by constructing a transcriptome De Bruijn graph (T-DBG) (Compeau *et al.*, 2011). These are then compared to motifs present within the sequencing reads. Alignment of k-mers in each read to those present in the reference provides a Kallisto compatibility value, which identifies the most probable location for the read. This method differs from the HiSat2 alignment method, where an attempt is made to align every base within a read to the reference to identify the correct location (Kim *et al.*, 2015; Pertea *et al.*, 2016).

Because of the contrasting methods of alignment, different approaches are taken to the handling of miscalled bases. HiSat2 utilises soft clipping of poor bases from the 5' end of reads (Kim *et al.*, 2015). However, Kallisto handles errors quite differently. An error in a sequencing read k-mer will result in that k-mer not matching to the reference. In such an instance, the k-mer is ignored (Bray *et al.*, 2016). The issue of errors is also handled by the removal of redundant k-mers from computation based on the information in the T-DBG. As fewer k-mers are inspected, there is less opportunity for erroneous k-mers to produce misleading results (Bray *et al.*, 2016).

Due to the pseudo-alignment mapping method, and its inherent differences from conventional mapping approaches, differential gene and transcript expression analysis was conducted using Sleuth as Sleuth was explicitly designed for the analysis of Kallisto pseudo-alignments (Pimentel *et al.*, 2017). The authors report that this workflow is more sensitive when detecting differentially expressed transcripts than workflows combining HiSat2 mapping and a wide range of differential expression programs, a finding which the authors attribute to the statistical model applied in Sleuth (Pimentel *et al.*, 2017). This increased sensitivity allowed the observation of a greater number of differentially

expressed transcripts when comparing porcine colon RNA-seq datasets. This allowed a more complete view of differential transcript expression during the weaning period.

To mirror the findings of the previous chapter, datasets were subjected to the same quality filters as those applied before mapping with HiSat2 i.e. removal of adaptor contamination; removal of reads shorter in length than 20 bp and removal of reads with an average Phred score of less than ten.

The first section of this chapter will detail Kallisto mapping statistics for the trial, and the expression pattern observed after this mapping in colon samples obtained from weaned and suckling animals without *Saccharomyces cerevisiae boulardii* supplementation. The remainder of the chapter will address the differential expression between these cohorts, suckling control (n=4) and weaned control (n =4). Colon samples were compared for each of the three slaughter points, one, four and 14 days post-weaning, to observe a longitudinal timeline of differential transcript expression after weaning. Differential expression analysis in this chapter will concern only samples which were obtained from animals who did not receive *Saccharomyces cerevisiae boulardii*

supplementation to describe the transcriptional effect of weaning without treatment.

4.2 Results

4.2.1 Overview of RNA-seq Mapping using Kallisto

Mapping of RNA-seq datasets with Kallisto yielded a mean of 31,763,663 ± 2,654,475 aligned reads across the 48 samples encompassed by this study. This represented 60.7 ± 1.72% of total raw reads. As the methodology for filtering for inadequate quality and contaminant reads was identical to that represented in chapter 3, these will not be further discussed. Alignment with Kallisto yielded fewer usable mapped reads than HiSat2, where an average of 43,601,697 ± 3,838,314 reads, 83.27% ± 0.82% of the raw datasets were exclusively mapped to the genome. An individual breakdown of Kallisto alignment percentages by sample is shown in Figure 4-1. This figure shows the uniformity of alignment percentages between samples. All Kallisto mapping statistics can be found in Appendix 5.

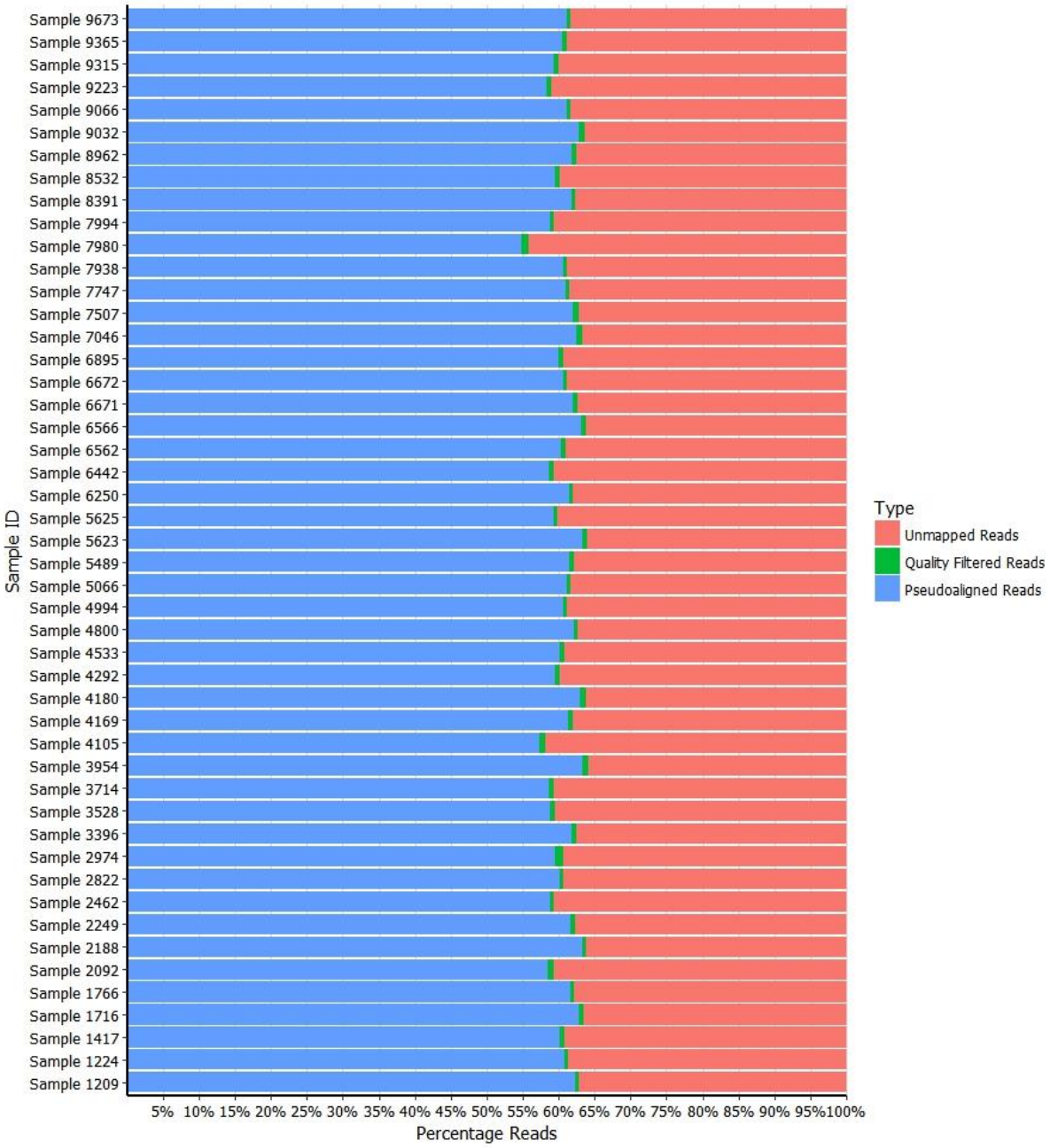


Figure 4-1: Percentages of RNA-seq datasets pseudo-aligned, unmapped and quality filtered when using the Kallisto methodology. The percentage of pseudo-aligned reads is shown in blue, unmapped reads in red and quality filtered reads (reads removed for insufficient quality, Phred < 10 and length < 20) in green.

4.2.2 Comparison of Global Expression between Weaned and Suckling Pigs at 22, 25 and 35 Days of Age (Weaning at 21 days of age)

To visualise the difference in global expression patterns between weaned and suckling samples, principal component analysis was conducted on the transcripts per million profiles obtained from Kallisto mapping.

Figure 4-2 shows principal component analysis plots for weaned and suckling samples at 22, 25 and 35 days of age, one, four and 14 days post-weaning respectively. At 22 days of age (Figure 4-2A) weaned samples show greater variation between samples than their suckling counterparts. However, samples cannot be separated according to weaning status as sample 9223 groups amongst the cluster of suckling samples containing sample 1417, 2249 and 4292. Indeed, according to the 95% confidence ellipses, any additional weaned samples could be expected to fall within the 95% confidence ellipse computed for suckling samples due to the high variability between weaned samples.

At 25 days of age, four days post-weaning, (Figure 4-2B) this pattern switches, with a tight grouping of weaned samples also containing the suckling sample 3396. In comparison, suckling samples show high

variability. Due to this variability, the 95% confidence ellipse for the suckling samples is large and encompasses much of the ellipse computed for weaned samples. Because of this intersection, any additional weaned or suckling samples would likely fall within the confidence ellipse calculated for suckling samples.

At 35 days of age, 14 days post-weaning, (Figure 4-2C), neither weaned nor suckling samples show any grouping as individuals from both cohorts are interspersed. As with the previous timepoints, confidence ellipses for the cohorts intersect almost completely.

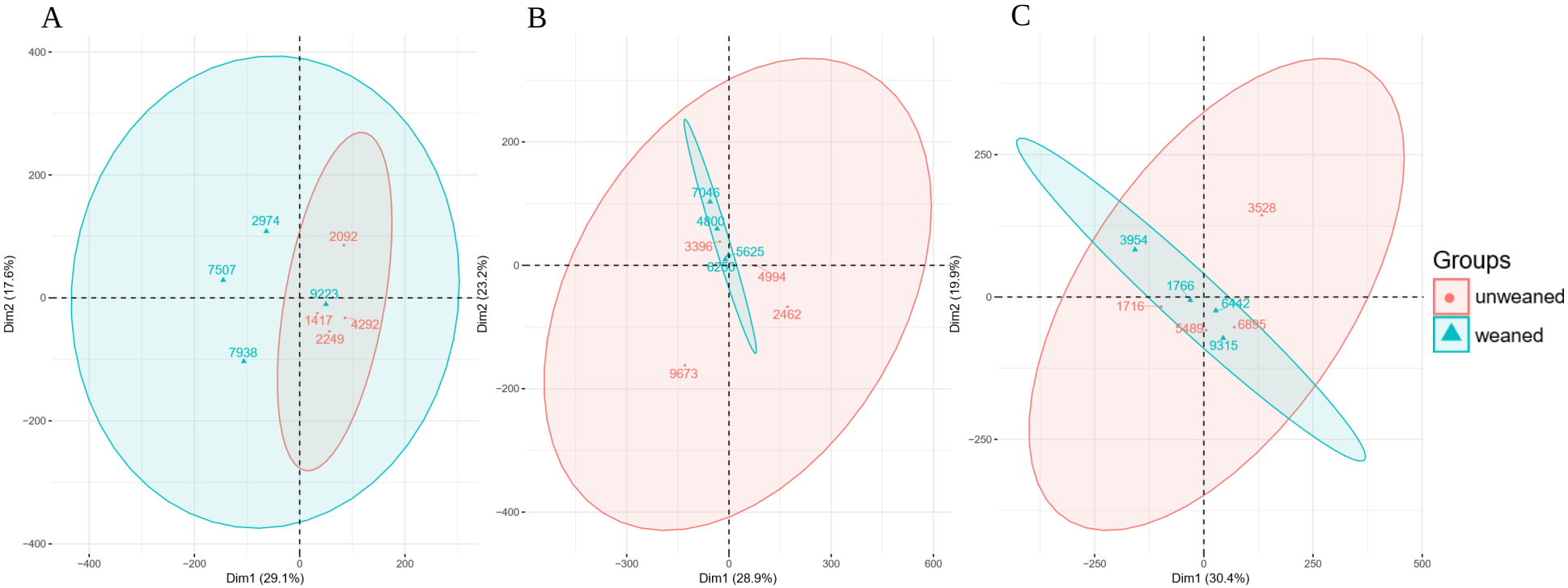


Figure 4-2: PCA plots to show similarity in global expression pattern between weaned and suckling control colon samples at 22, 25 and 35 days of age. Plot A indicates 22 days of age (one day post-weaning), plot B indicates 25 days of age (four days post-weaning) and plot C indicates 35 days of age (14 days post-weaning). Samples from suckling pigs are indicated in red, the corresponding samples from weaned pigs are indicated in blue. Principal component analysis was applied to transcripts per million (TPM) information obtained from Kallisto mapping. X and Y axis show principal component 1 and principal component 2 respectively (percentage of variance indicated on each plot). Prediction ellipses are such that with probability 0.95, a new observation from the same group will fall inside the ellipse.

4.2.3 Overview of Differential Gene Expression in the Porcine Colon at Weaning Observed using a Pseudo-alignment Method

Application of Kallisto pseudo-alignment and Sleuth differential gene expression methodology, to identify differentially expressed transcripts in the colon of pigs at weaning with no fold change cut-off applied, identified 1350 transcripts differentially expressed ($q < 0.1$) between the four weaned and four suckling samples collected at one-day post-weaning. 195 and four transcripts were identified at four and 14 days post-weaning respectively. Of these differentially expressed transcripts, 353 met a two-fold change cut-off at one-day post-weaning compared to 78 and four at four and 14 days post-weaning respectively (Figure 4-4). Further information concerning differentially expressed transcripts identified at these three-time points can be found in additional files one, two & three.

Of the 353 differentially expressed transcripts identified at one-day post-weaning, 22 days of age, 138 were upregulated by weaning whereas 215 were downregulated. At four days post-weaning, 25 days of age, 51 transcripts were upregulated by weaning and 27 downregulated. Finally, at 14 days post-weaning, 35 days of age, two of

the three differentially expressed transcripts were upregulated by weaning, with the remaining transcript downregulated.

This timewise decrease in the number of observed differentially expressed transcripts with the greatest number identified at one-day post-weaning and the fewest at 14 days post-weaning is indicated in the volcano plots for the corresponding time points (Figure 4-3).

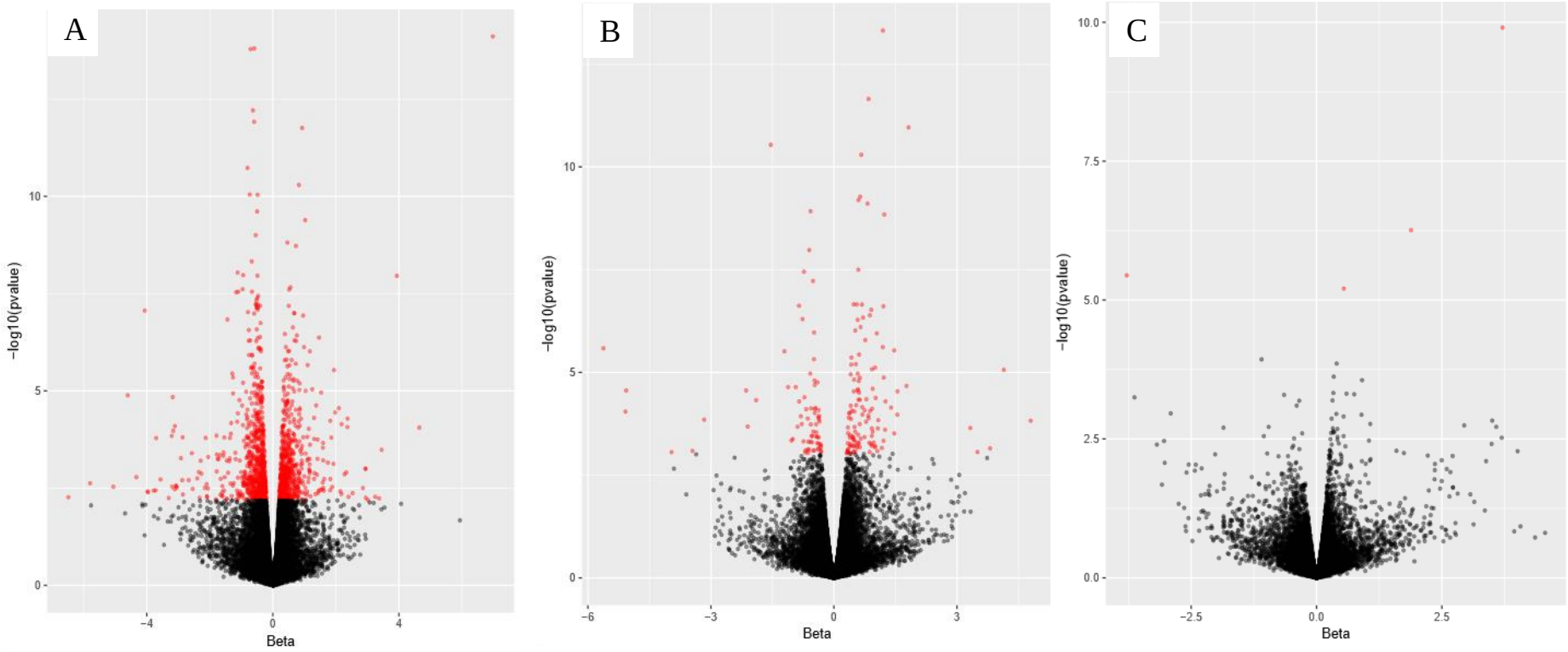


Figure 4-3: Volcano plots to show differential expression of transcripts in the porcine colon at one, four and 14 days post-weaning. -log10 *p* value plotted against beta value. Beta value is an estimator of fold change used in the model applied by Sleuth. Transcripts with a Benjamini-Hochberg false detection rate corrected *p*- value <0.1 are indicated in red. A, differentially expressed transcripts at one day post-weaning. B, differentially expressed transcripts at four days post-weaning. C, differentially expressed transcripts at 14 days post-weaning.

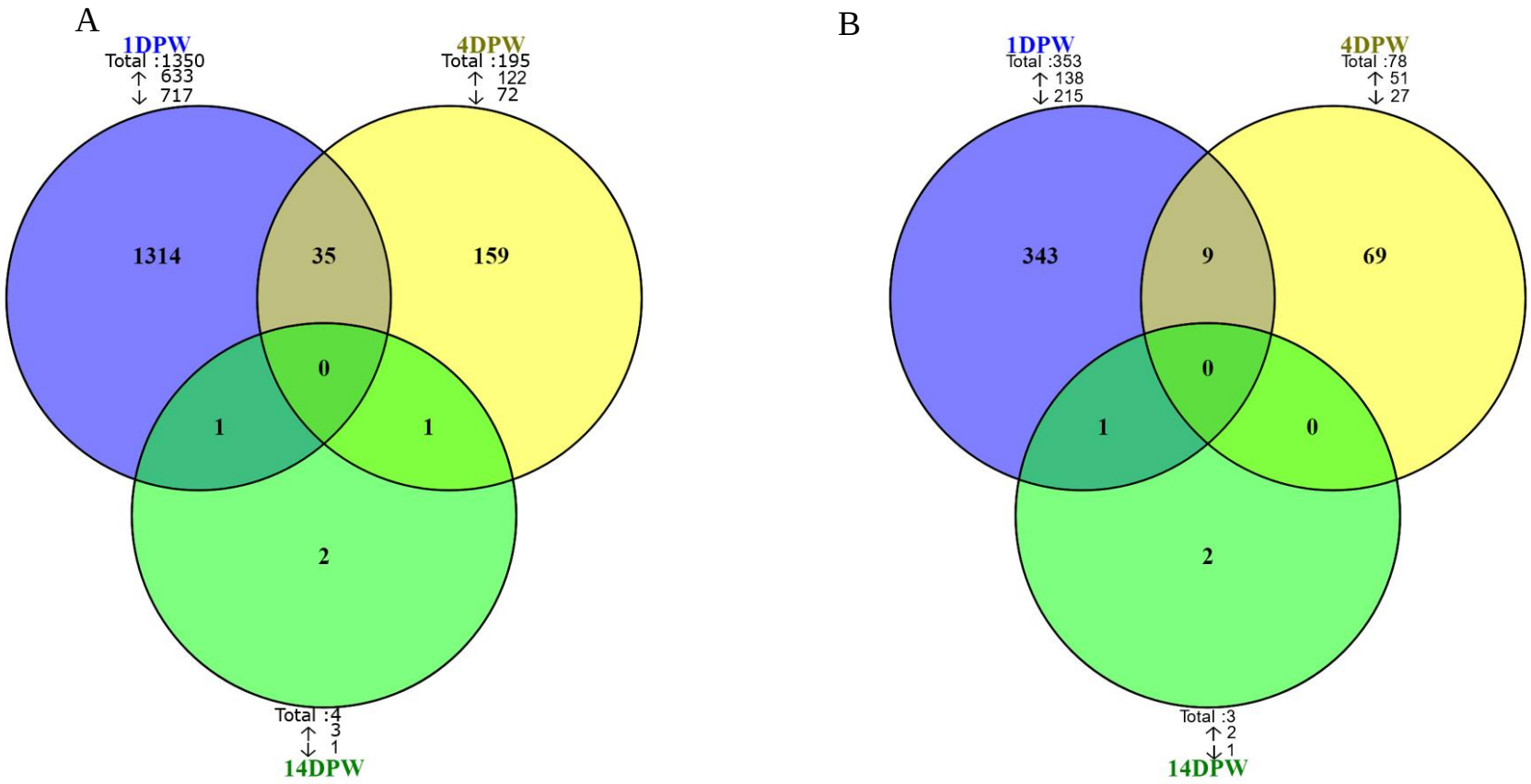


Figure 4-4: Venn diagram to display differentially expressed transcripts observed at one, four and 14 days post-weaning. A, all differentially expressed transcripts $q < 0.1$. B, differentially expressed transcripts $q < 0.1$ and fold change > 2. DPW, days post-weaning. Upregulated transcripts are indicated with an up arrow (↑). Downregulated transcripts are indicated with a down arrow (↓).

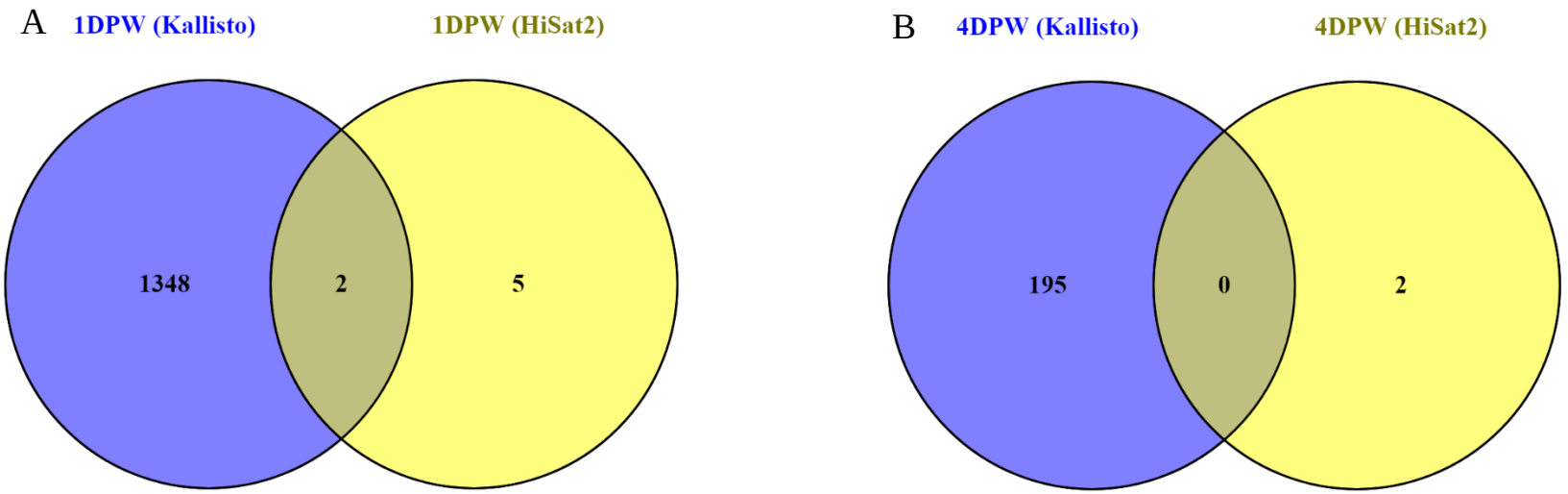
4.2.4 Comparison between Differential Expression Observed Using Conventional and Pseudo-alignment Methods

The primary difference in results obtained from the two methodologies is the number of transcripts identified as significantly differentially expressed, q <0.1. At one-day post-weaning, the HiSat2/Ballgown method identified seven differentially expressed transcripts, compared to 1350 identified when the Kallisto/Sleuth method is applied. This difference continues in the subsequent time point comparisons with two transcripts identified as significantly differentially expressed by HiSat/Ballgown at four days post-weaning compared to the 195 identified by the Kallisto/Sleuth pseudo-alignment method (Figure 4-4). At 14 days post-weaning, no significantly differentially expressed transcripts were identified by the HiSat2/Ballgown method compared to the four found by Kallisto/Sleuth.

When a fold change cut-off of two was applied, the number of significantly differentially expressed transcripts is further reduced to only three at one-day post-weaning when using the HiSat2/Ballgown method with none identified at the other two time points. This is a notable reduction compared to the 353, 78 and three identified by the

Kallisto/Sleuth method at one, four and 14 days post-weaning, respectively.

When the significantly differentially expressed transcripts identified by the two methods were compared, only two transcripts were shared at one-day post-weaning (Figure 4-5). Tetraspanin was identified by both methods as downregulated at one-day post-weaning, as was C2 calcium-dependent domain containing two. However, only the former reached the one Log_2 fold change cutoff after Sleuth differential expression analysis (Figure 4-5).



Transcript ID	Gene ID	Gene Symbol	Gene Name	HiSat2/Ballgown Change with Weaning	Hisat2/Ballgown Log2FC	Kallisto/Sleuth Change with Weaning	Kallisto/Sleuth Log2FC
ENSSSCT00000000797	ENSSSCG00000000734	TSPAN11	Tetraspanin	Down	-0.7477	Down	-1.0058
ENSSSCT00000030786	ENSSSCG00000025821	C2CD2	C2 calcium-dependent domain containing 2	Down	-0.4285	Down	-0.5223

Figure 4-5: Venn diagrams to show significantly differentially expressed transcripts shared between the HiSat2/Ballgown and Kallisto/Sleuth methodologies. A, significantly differentially expressed transcripts (q <0.1) at one-day post-weaning, B, significantly differentially expressed transcripts (q<0.1) at four days post-weaning. DPW, days post-weaning. 14 days post-weaning not shown as no significantly differentially expressed transcripts were identified by HiSat2/Ballgown. The table contains information on the two transcripts which are shared between the two methodologies at one-day post-weaning.

4.2.5 Inter-Sample Expression Variation in Differentially Expressed Transcripts

To visualise the sample to sample variation in the expression of transcripts identified as differentially expressed, heatmaps were constructed for each of the three time points. These heatmaps are based on the TPM values for the transcripts, which met the thresholds set for identification of differential expression ($q < 0.1$, Log_2 FC ≥ 1 and ≤ -1).

In all three heatmaps, clustering separates samples according to weaning status and clusters up and downregulated genes separately. Sample clustering is to be expected as only differentially expressed features are included in the heatmap. Separate clusters for up and downregulated transcripts are apparent due to the omission of all transcripts which did not meet the q value and fold change cut-offs.

The heatmap demonstrated in Figure 4-6 shows differentially expressed transcripts at one-day post-weaning. The 353 differentially expressed transcripts observed at this early stage after weaning are displayed. The expression profile is quite different between samples of the same treatment, indicating animal to animal variation. The separation of samples based on up and downregulated genes is generally clear by the

switch from red to blue areas representing high and low expression. The only exception to this is sample 9223, the expression profile of which is lower amongst transcripts which are otherwise highly expressed amongst weaned samples.

The heatmap showing the TPM profile of differentially expressed transcripts at four days post-weaning (Figure 4-7) includes the 78 differentially expressed transcripts identified. Again, the individual sample profiles vary within the weaned and suckling cohorts. Sample 3396 stands out amongst the suckling cohort as the TPM profile it displays for transcripts otherwise highly expressed in this cohort, is relatively low.

The heatmap displaying differentially expressed transcripts at 14 days post-weaning (Figure 4-8) contains only three transcripts. The TPM profile again varies within cohorts as before, although as so few differentially expressed transcripts were identified, this effect is not as obvious.



Figure 4-6: Heatmap to show variation in sample TPM values for transcripts identified as differentially expressed at one-day post-weaning. The input to construct this heatmap was TPM values for differentially expressed genes (q <0.1, Log_2 FC ≥ 1 or ≤ -1). Unit variance scaling was applied to transcript TPM values. Both transcripts and samples are clustered using correlation distance and average linkage. 353 transcripts are represented.

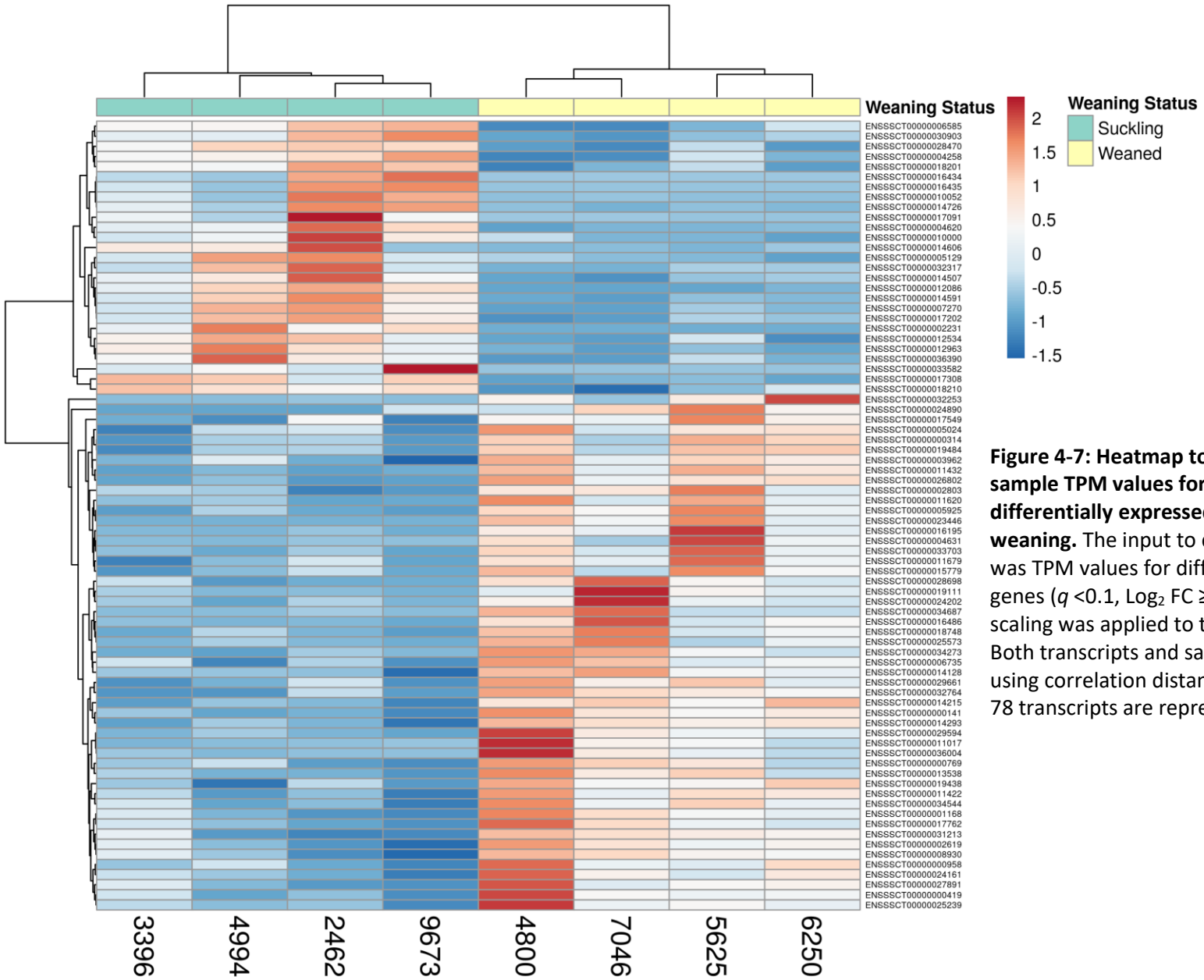


Figure 4-7: Heatmap to show variation in sample TPM values for transcripts identified as differentially expressed at four days post-weaning. The input to construct this heatmap was TPM values for differentially expressed genes (q <0.1, Log_2 FC ≥ 1 or ≤ -1). Unit variance scaling was applied to transcript TPM values. Both transcripts and samples are clustered using correlation distance and average linkage. 78 transcripts are represented.

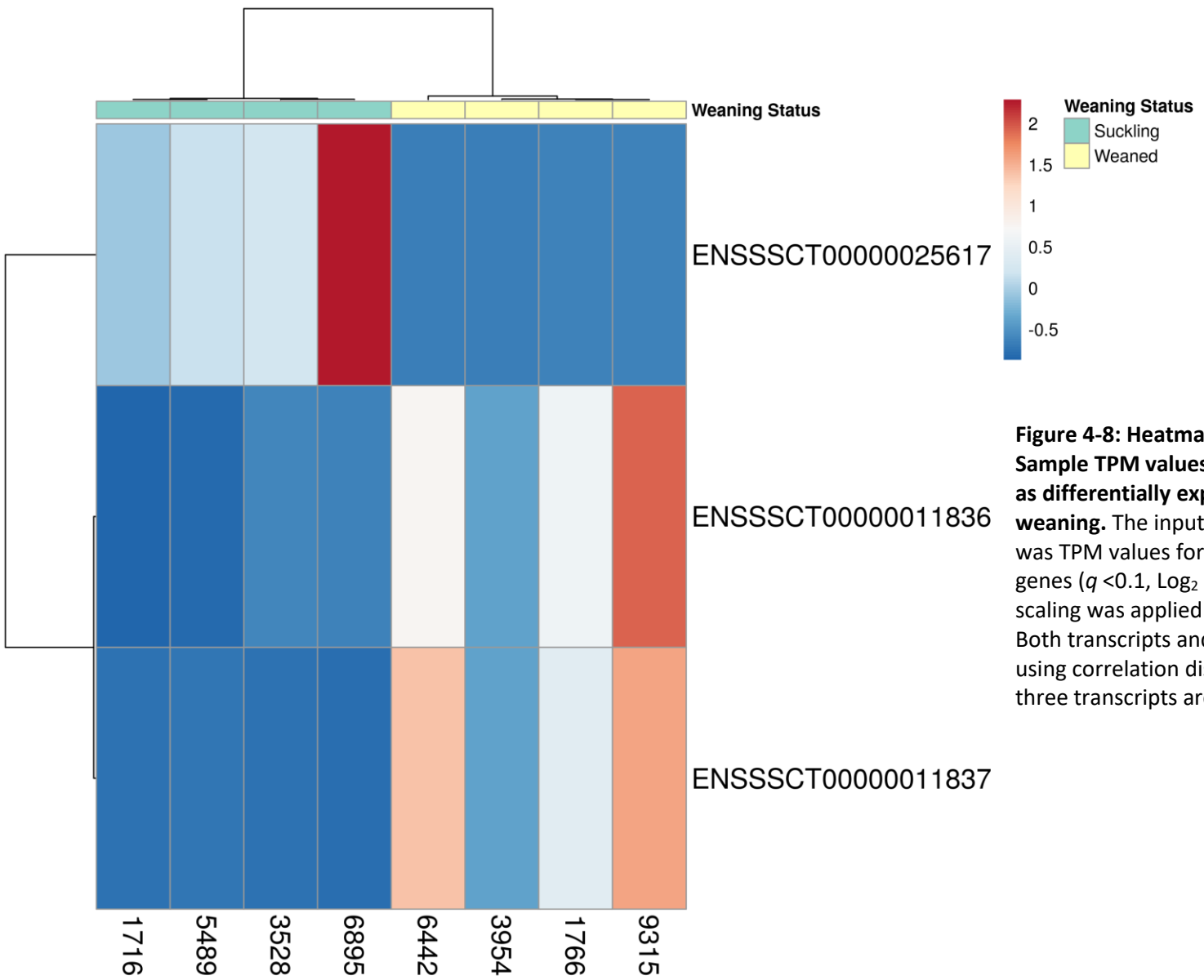


Figure 4-8: Heatmap to show variation in Sample TPM values for transcripts identified as differentially expressed at 14 days post-weaning. The input to construct this heatmap was TPM values for differentially expressed genes (q <0.1, Log_2 FC ≥ 1 or ≤ -1). Unit variance scaling was applied to transcript TPM values. Both transcripts and samples are clustered using correlation distance and average linkage. three transcripts are represented.

4.2.6 Gene Ontology Analysis of Differentially Expressed Genes to Characterise the Transcriptomic Differences between Colon Samples Obtained from Weaned and Suckling Pigs

Gene ontology (GO) analysis was conducted separately on transcripts identified as differentially expressed ($q < 0.1$, Log_2 FC ≥ 1 or ≤ -1) at 22 and 25 days of age, one and four days post-weaning. As only three transcripts were identified as differentially expressed between weaned and suckling samples at 35 days of age, 14 days post weaning, this analysis was not suitable due to insufficient differential expression information. Therefore, these three transcripts will be discussed individually. GO analysis was conducted on the gene rather than transcript level as multiple differentially expressed transcripts from the same gene may skew gene ontology enrichment. Genes identified as differentially expressed at 22 and 25 days of age were analysed using the separate-DE approach, whereby up and downregulated genes were analysed for gene ontology enrichment separately. This is a more powerful method of analysis than analysing all differentially expressed genes together (Hong *et al.*, 2014). In each case enrichment for the three ontologies, or superfamilies, for up and downregulated genes will be shown side by side.

4.2.6.1 Gene Ontology Analysis of Differentially Expressed Genes to Characterise the Transcriptomic Differences Between Colon Samples of Weaned and Suckling Pigs at 22 Days of Age (one-day post weaning)

At 22 days of age or one-day post weaning, a total of 353 transcripts met the criteria for identification of differential expression ($q < 0.1$, Log_2 FC ≥ 1 or ≤ -1). 138 of these transcripts were identified as upregulated by weaning. These 138 transcripts originate from 130 unique genes. Multiple upregulated transcripts from five different genes were identified. These include four C-type domain family two member D transcripts (*CLEC2D*), three NADPH oxidase 1 (NOX1) transcripts and two transcripts from each of dual oxidase two (*DUOX2*), 5' AMP-activated protein kinase subunit beta-2 (*PRKAB2*) and serine dehydratase (*SDS*).

215 transcripts from 211 genes were identified as downregulated by weaning. Two transcripts from each of basal cell adhesion molecule (*BCAM*), calpain13 (*CAPN13*), solute carrier family 7 member 8 (*SCL7A8*) and nestin (*NES*) are included in the number of differentially expressed transcripts.

4.2.6.1.1 Enrichment of Biological Process GO Terms

Biological process enrichment analysis revealed twelve GO terms significantly enriched amongst genes upregulated by weaning, however, eight of these terms contained only two differentially expressed genes. The ten most significantly enriched terms are shown in Figure 4-9A.

Positive regulation of glucose transport was statistically the most enriched term with two of the three genes contained within this term upregulated in pigs one-day post weaning, *NR4A3*, nuclear receptor subfamily 4 group A member 3 and *C3*, complement C3.

Terms which were enriched by greater than two genes included: *cellular oxidant detoxification*; *positive regulation of vascular endothelial growth factor production*; *immune response* and *negative regulation of endopeptidase activity*.

Cellular oxidant detoxification was enriched with five of the 44 genes upregulated by weaning. These genes included thioredoxin reductase 1 (*TXNRD1*); dual oxidase 1 & 2 (*DUOX1* & *DUOX2*); fatty acid binding protein 1 (*FABP1*) and peroxiredoxin 6 (*PXDN6*). *DUOX1* & *DUOX2* also constitute the only enrichment of the *hydrogen peroxide biosynthetic process* term.

Positive regulation of vascular endothelial growth factor production was enriched by the up-regulation of interleukin 1 alpha (*IL1A*); *NOX1* and complement 3 (*C3*). *IL1A* upregulation also contributes to the enrichment of *fever generation* and *immune response*.

The *immune response* term was enriched with eight of the 192 genes this term encompasses upregulated by weaning. These eight genes include: interleukin 1 beta 2 (*IL1B2*); *IL1*A; complement 7 & 9 (*C7* & C9) and tumor necrosis factor superfamily members 8 & 10 (*TNFSF8* & *TNFSF10*).

Negative regulation of endopeptidase activity was also enriched amongst genes upregulated by weaning. The genes in this term which are affected include four serine peptidase inhibitors (*SERPINA11*, *SERPINA10*, *SERPINB2* and *SERPINB5*) as well as *C3*.

Biological process GO term enrichment analysis of downregulated genes identified ten terms which were significantly enriched. The most significantly enriched of which was *embryonic limb morphogenesis*. Six of the genes encompassed by this term were downregulated by weaning, these included: homeobox D10 and 13 (*HOXD10* & *HOXD13*); Fraser syndrome 1 (*FRAS1*); fibroblast growth factor receptor 1 (*FGFR1*);

growth differentiation factor 5 (*GDF5*) and aldehyde dehydrogenase 1 family member A2 (*ALDH1A2*).

HOXD13 along with secreted frizzled-related protein 1 precursor (*SFRP1*) are the only genes enriching the terms *prostate epithelial cord arborization involved in prostate glandular acinus morphogenesis* and *regulation of branching involved in prostate gland morphogenesis*.

The downregulation of mesenchyme homeobox one and two (*MEOX1* & *MEOX2*) contributes to the enrichment of the terms *somite specification* and along with frizzled-related protein B (*FRXB*) *somite development*.

Eighteen downregulated genes contribute to the enrichment of the high-level GO term *transport*, however, due to the non-specific nature of this term, enrichment of molecular function terms is more illuminating as to the function. All GO enrichment information including gene identifiers and *q*-values for biological process enrichment of genes differentially regulated by weaning in colon samples at one-day post-weaning can be found in Appendix 8.

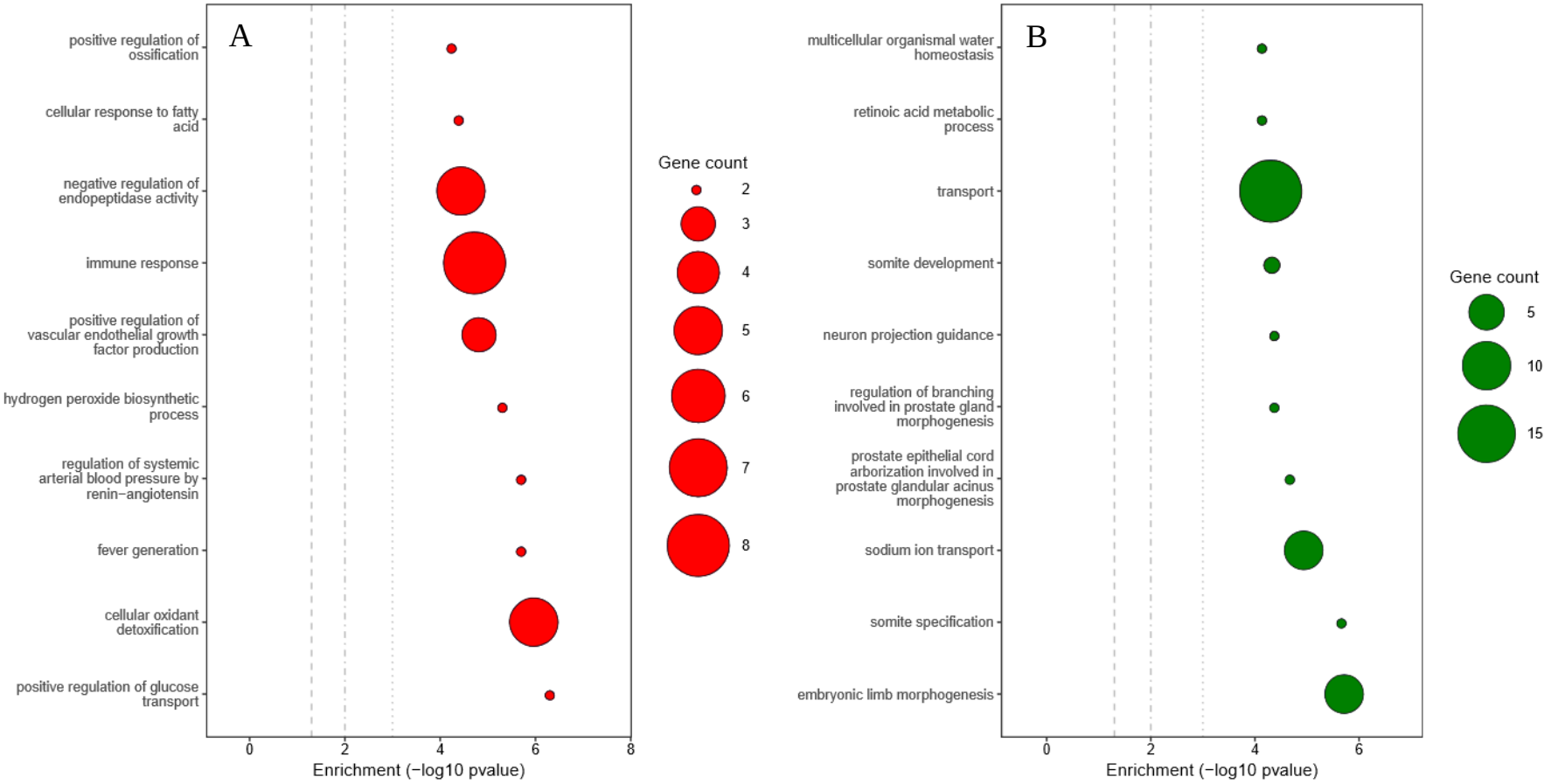


Figure 4-9: Enrichment of biological process terms in genes identified as up and downregulated in colon tissue at one-day post-weaning. A, biological process enrichment of genes upregulated by weaning. B, biological process enrichment of genes downregulated by weaning. Top 10 most significantly enriched terms displayed. All terms shown contain equal to or greater than two differentially expressed genes and are significantly enriched ($q \leq 0.05$). Information on all significantly enriched terms including gene names and identifiers can be found in Appendix 8.

4.2.6.1.2 Enrichment of Cellular Compartment GO Terms

Cellular compartment GO enrichment analysis of genes differentially expressed at one-day post weaning identified enrichment of terms associated with the extracellular space and extracellular matrix in analyses of both up and downregulated genes.

Enrichment analysis of genes upregulated by weaning identified enrichment of three terms (Figure 4-10A). Two of these terms: *invadopodium membrane* and *membrane attack complex* were enriched by the upregulation of two genes each. The former term was enriched by the upregulation of *NOX1* and *FAP* (fibroblast activation protein). The later was enriched by the increased transcription of *C7* &*C9*. These two-low level, specific terms, encompass a total of five and six genes respectively. The third term significantly enriched amongst genes upregulated by weaning was the high-level term *extracellular space*. Due to the general nature of this term, a total of 966 genes fall under this umbrella term. 18 constituents of this term were upregulated by weaning at one-day post-weaning. These genes include the serine peptidase inhibitors (SERPINA*11*, *SERPINA10*, *SERPINB2* and *SERPINB5*) identified in the biological process gene ontology analysis as negative regulators of protease activity. Other enriched constituents include

IL1B2, *C3* & *C9*, polymeric immunoglobulin receptor (*PIGR*), olfactomedin 4 (*OLFM4*) and TNF superfamily member 10 (*TNFSF10*). The full list of enriched genes can be found in Appendix 9.

Cellular component enrichment analysis of downregulated genes identified significant enrichment of four terms (Figure 4-10B). Three of these terms concern the extracellular matrix and extracellular region. *Proteinaceous extracellular matrix*, *extracellular region* and *extracellular matrix* are all high-level terms, encompassing 167, 670 and 251 genes and were enriched by 11, 21 and ten genes respectively. Due to the related nature of these terms, some upregulated genes contribute to the enrichment of all three. An example of this is matrix metalloprotease 20 (*MMP20*) which falls under all three terms. The terms *proteinaceous extracellular matrix* and *extracellular matrix* both include; periostin (*POSTN*); *BCAM*; *SFRP1* and biglycan (*BGN*). All enrichment of these terms can be found in Appendix 9

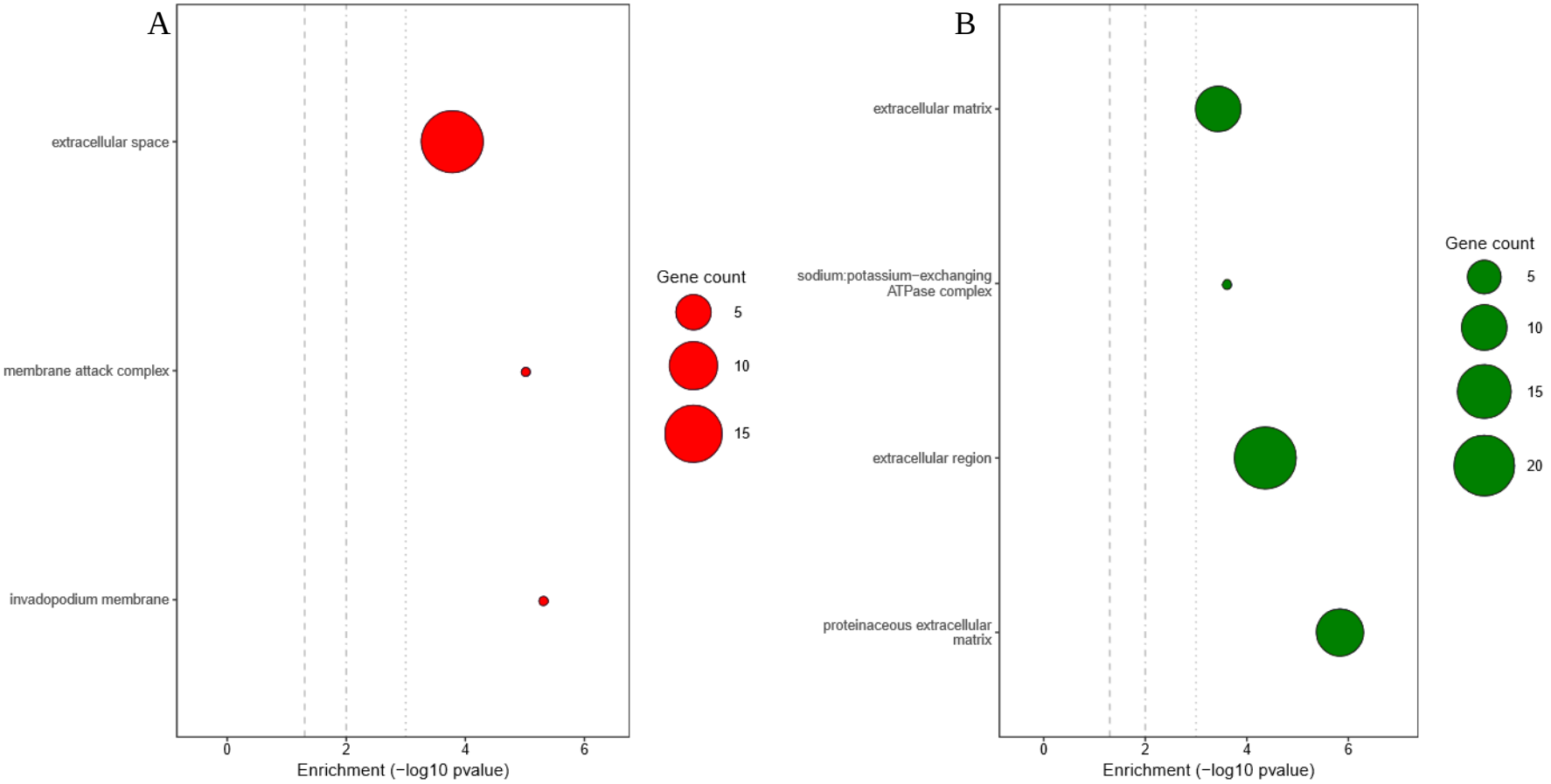


Figure 4-10: Enrichment of cellular compartment terms in genes identified as up and downregulated in colon tissue at one-day post-weaning. A, cellular component enrichment of genes upregulated by weaning. B, cellular component enrichment of genes downregulated by weaning. All significantly enriched terms displayed. All terms shown contain equal to or greater than two differentially expressed genes and are significantly enriched ($q \leq 0.05$). Information on all significantly enriched terms including gene names and identifiers can be found in Appendix 9.

4.2.6.1.3 Enrichment of Molecular Function GO Terms

Molecular function ontology enrichment was conducted on up and downregulated genes to provide some insight into the biochemical activities which may be affected by weaning. Seven terms were significantly enriched by upregulated genes (

Figure 4-11A). Enrichment of these terms was however dominated by a small number of genes. The upregulation of *DUOX1* & *DUOX2* resulted in the enrichment of the *NADPH oxidase activity* term and, in combination with *PRDX6*, the *peroxidase activity* term. In turn, the upregulation of *PRDX6* in addition to *FABP1* led to enrichment of the *antioxidant activity* term.

Upregulation of activin A receptor type 1C (*ACVR1C*) and bone morphogenic protein receptor type 2 pecursor (*BMPR2*) is solely responsible for the enrichment of *transmembrane receptor protein serine/threonine kinase activity* and *signal transducer, downstream of receptor, with serine/threonine kinase activity*.

Interleukin-1 receptor binding was enriched by the upregulation of *IL1B2* & *IL1A*. The final molecular function gene ontology term significantly enriched amongst upregulated genes was *serine-type*

endopeptidase activity. This was implicated due to the upregulation of the four serine peptidase inhibitors previously mentioned (SERPINA*11*, *SERPINA10*, *SERPINB2* and *SERPINB5*).

Molecular function GO enrichment analysis of downregulated genes provided a more instructive breakdown of the function of some of the downregulated genes responsible for the enrichment of the biological process *transport* term. A total of six genes enriched four molecular function GO terms (

Figure 4-11B). *ligand-gated sodium channel activity* and *sodium channel activity* contained the downregulated sodium voltage-gated channel alpha subunit 4 (*SCN4A*) and acid-sensing ion channel subunit 3 (*ASIC3*), with the later also influenced by the downregulation of sodium channel epithelial 1 beta subunit (*SCNN1B*).

The *extracellular ligand-gated ion channel activity* and *acetylcholine receptor activity* were also enriched collectively by the downregulation of three genes. The former by cholinergic receptor nicotinic beta 4 subunit (*CHRNB4*), cholinergic receptor nicotinic alpha 2 subunit (*CHRNA2*) and gamma-aminobutyric acid type a receptor alpha 5 subunit (*GABRA5*). The latter by *CHRNB4* and *CHRNA2*.

The full table containing all molecular function GO enrichment information can be found in Appendix 1

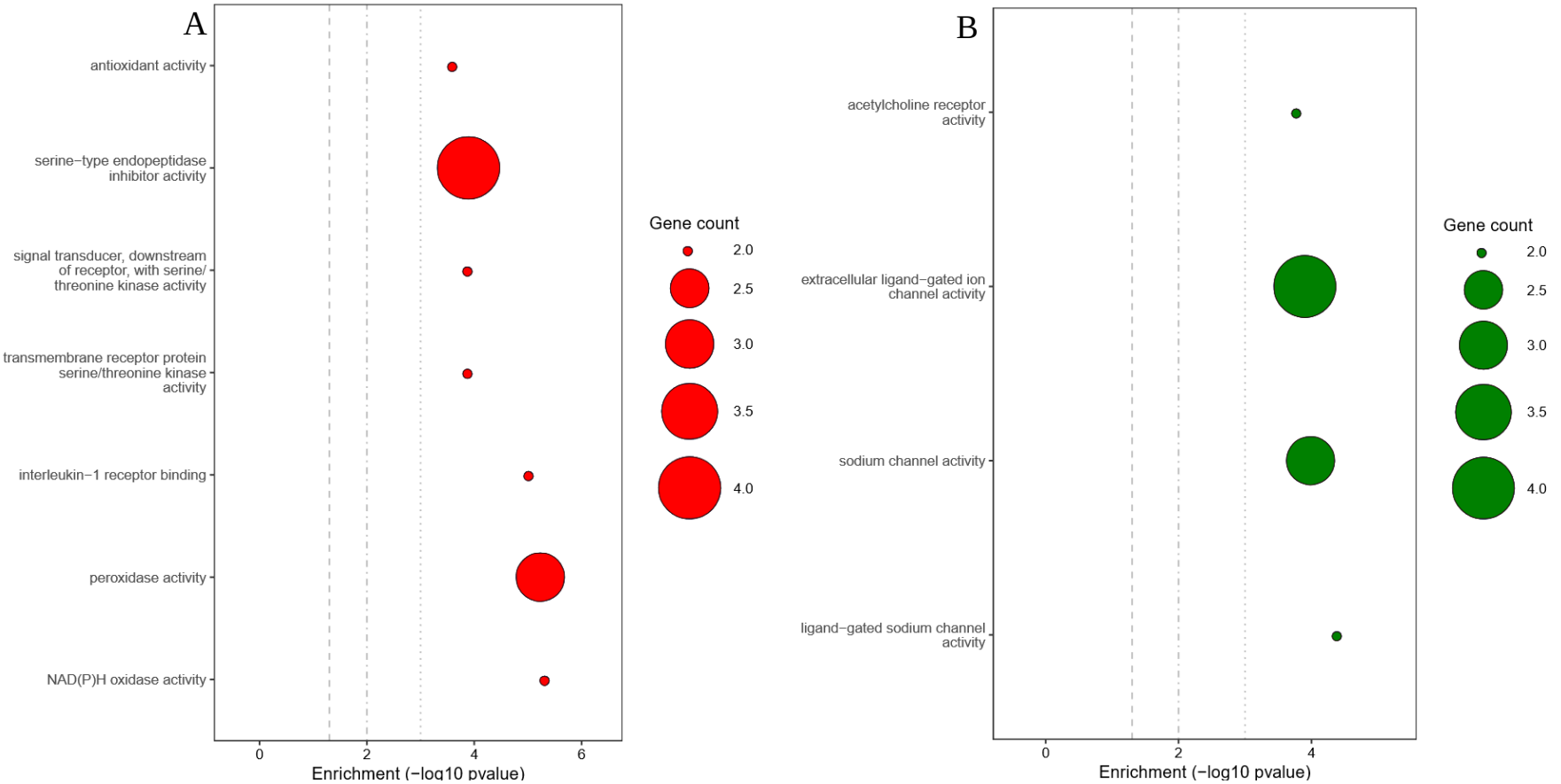


Figure 4-11: Enrichment of molecular function terms in genes identified as up and downregulated in colon tissue at one-day post weaning. A, molecular function enrichment of genes upregulated by weaning. B, molecular enrichment of genes downregulated by weaning. All significantly enriched terms displayed. All terms shown contain equal to or greater than two differentially expressed genes and are significantly enriched (q ≤0.05). Information on all significantly enriched terms including gene names and identifiers can be found in Appendix 10.

4.2.6.2 GO Analysis of Differentially Expressed Genes to Characterise the Transcriptomic Differences Between Colon Samples of Weaned and Suckling Pigs at 25 Days of Age (four days post-weaning)

In the comparison of weaned and suckling colon samples obtained at four days post weaning, 78 transcripts were identified as significantly differentially expressed (q <0.1, FC >2). 51 of these were upregulated by weaning; the remaining 21 were downregulated.

The 51 upregulated transcripts originated from 46 exclusive genes. Four transcripts originating from the gamma-glutamyltransferase 1 (*GTT1*) and three encoding bifunctional 3' phosphoadenosine 5'-phosphosulphate synthetase 2 (*PAPSS2*) account for the difference between genes and transcripts. Amongst the 27 downregulated transcripts, multiple up transcripts from a gene only appear once. In this instance, two transcripts of fibroblast activation protein alpha (*FAP*) were downregulated by weaning. As the gene ontology analyses were conducted on the gene level, multiple transcripts are not considered.

4.2.6.2.1 Enrichment of biological process gene ontology terms

Two biological process GO terms were significantly enriched by the genes upregulated by weaning at four days post weaning (Figure 4-12A). These were *regulation of angiogenesis* and *intracellular receptor signalling pathway.* In both instances, two genes contributed to the enrichment. *Regulation of angiogenesis* was enriched by the upregulation of integrin α5 (*ITGA5*) and tumour necrosis factor superfamily member 12 (*TNFSF12A*). The unrelated *intracellular receptor signalling pathway* was enriched by the upregulation of nuclear receptor subfamily 1 group H member 4 (*NR1H4*) and nuclear receptor superfamily 4 group A member 3 (*NR4A3*).

The same analysis of the 26 downregulated genes identified four significantly enriched terms (Figure 4-12B). However, all four of these terms relating to lipid processing were enriched by the downregulation of the same two genes, namely microsomal triglyceride transfer protein (*MTTP*) and apolipoprotein C3 (*APOC3*). All information on these GO analyses is contained in Appendix 11.

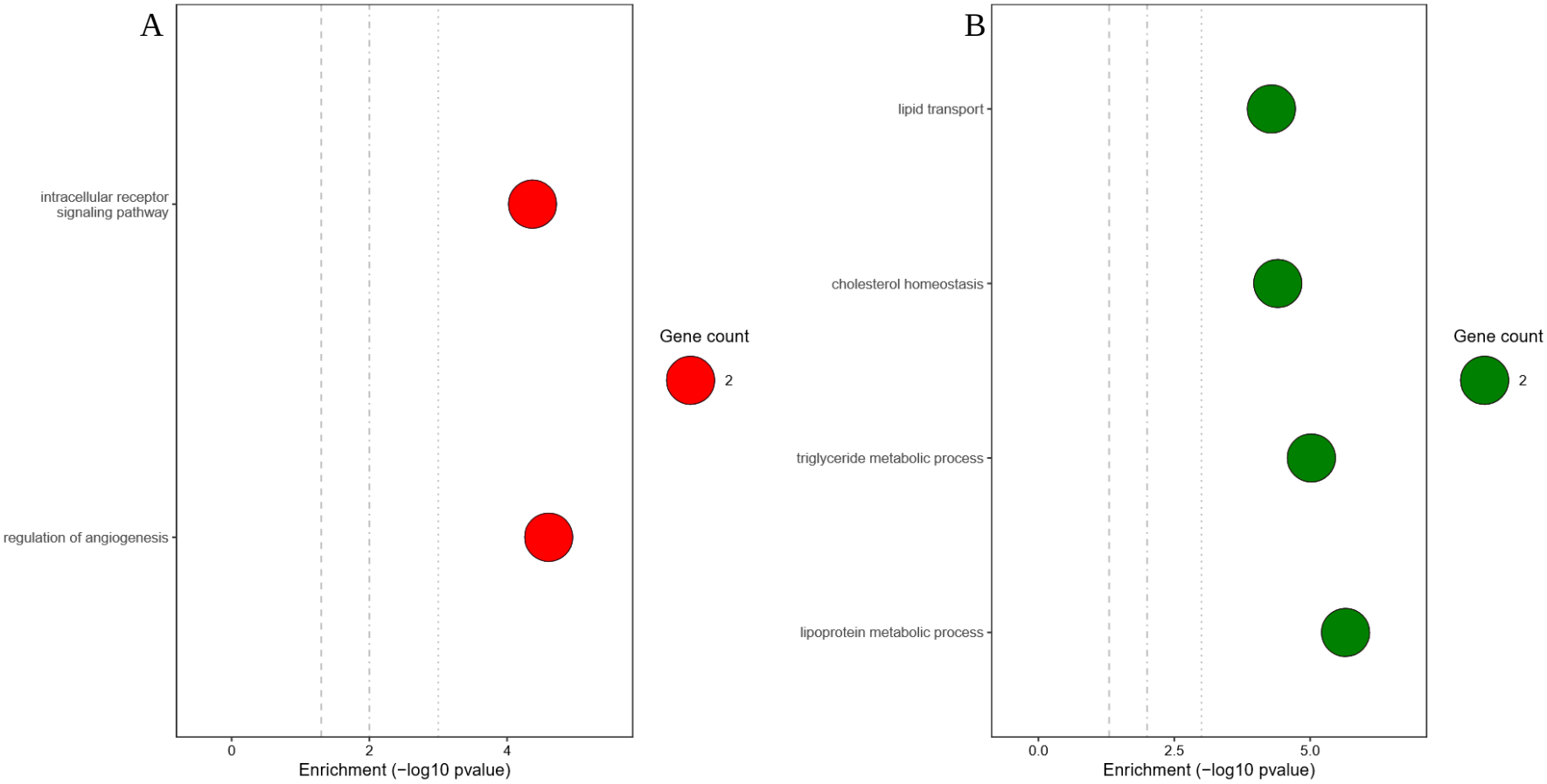


Figure 4-12: Enrichment of biological process terms in genes identified as up and downregulated in colon tissue at four days post-weaning. A, biological process enrichment of genes upregulated by weaning. B, biological process enrichment of genes downregulated by weaning. Top 10 most significantly enriched terms displayed. All terms shown contain equal to or greater than two differentially expressed genes and are significantly enriched ($q \leq 0.05$). Information on all significantly enriched terms including gene names and identifiers can be found in Appendix 11.

4.2.6.2.2 Enrichment of Cellular Compartment GO Terms

No cellular compartment GO terms were significantly enriched amongst upregulated genes at four days post-weaning. However, a single significantly enriched term was observed amongst those downregulated (Figure 4-13). Two of the 66 genes encompassed by the term *apical part of cell* were downregulated by weaning. These two genes encode glutamyl aminopeptidase (*ENPEP*) and *FAP*. Additional information can be found in Appendix 12.

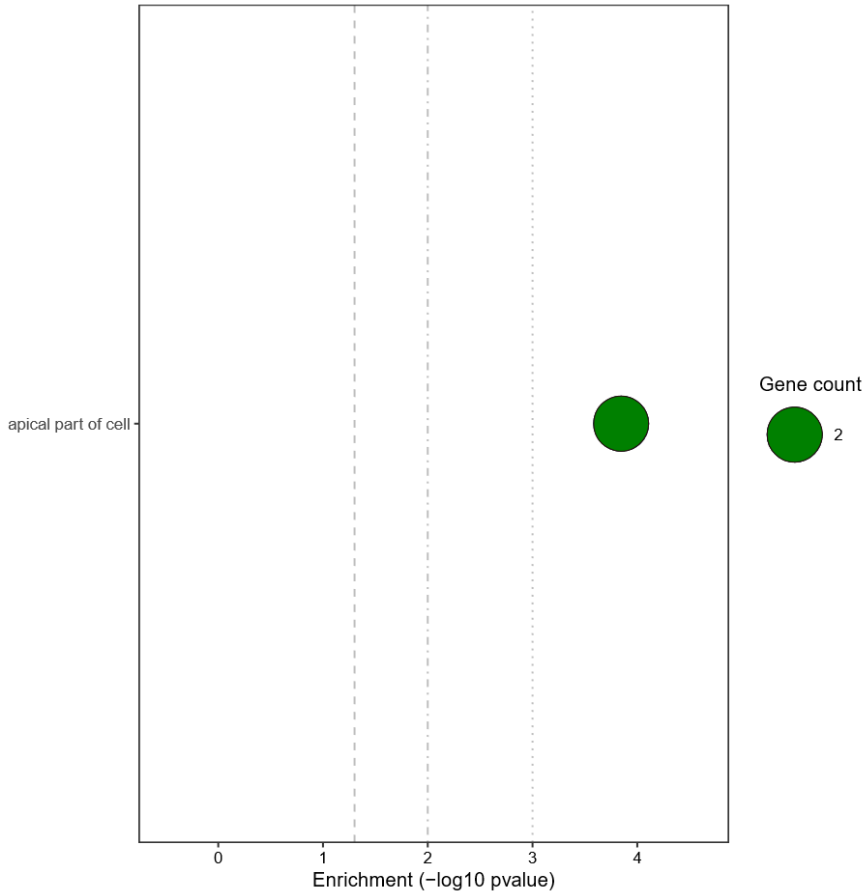


Figure 4-13: Enrichment of cellular compartment terms in genes identified as up and downregulated in colon tissue at four days post-weaning. Only cellular compartment terms enriched by downregulated genes shown as no terms were significantly enriched by upregulated genes. All significantly enriched terms displayed. All terms shown contain equal to or greater than two differentially expressed genes and are significantly enriched (q ≤0.05). Information on all significantly enriched terms including gene names and identifiers can be found in Appendix 12.

4.2.6.2.3 Enrichment of Molecular Function GO Terms

Two molecular function terms were significantly enriched by upregulated genes (Figure 4-14A). *Nuclear receptor activity* and *steroid hormone receptor activity* were both enriched by the upregulation of genes encoding nuclear receptor subfamily 1 group H member 4 (*NR1H4*) and nuclear receptor subfamily 4 group A member 3 (*NR4A3*).

Two terms were also significantly enriched amongst downregulated genes (Figure 4-13B). *Pyridoxal phosphate binding* and *catalytic activity* share the downregulation of genes encoding histidine decarboxylase (*HDC*) and the 1-aminocyclopropane-1-carboxylate synthetase homolog (*ACCSL*). *Catalytic activity* was further enriched by the downregulation of genes encoding ectonucleotide pyrophosphatase/phosphodiesterase 2 (*ENPP2*) and phosphoglycerate mutase 1 (*PGAM1*). Additional information on these gene ontology analyses can be found in Appendix 13.

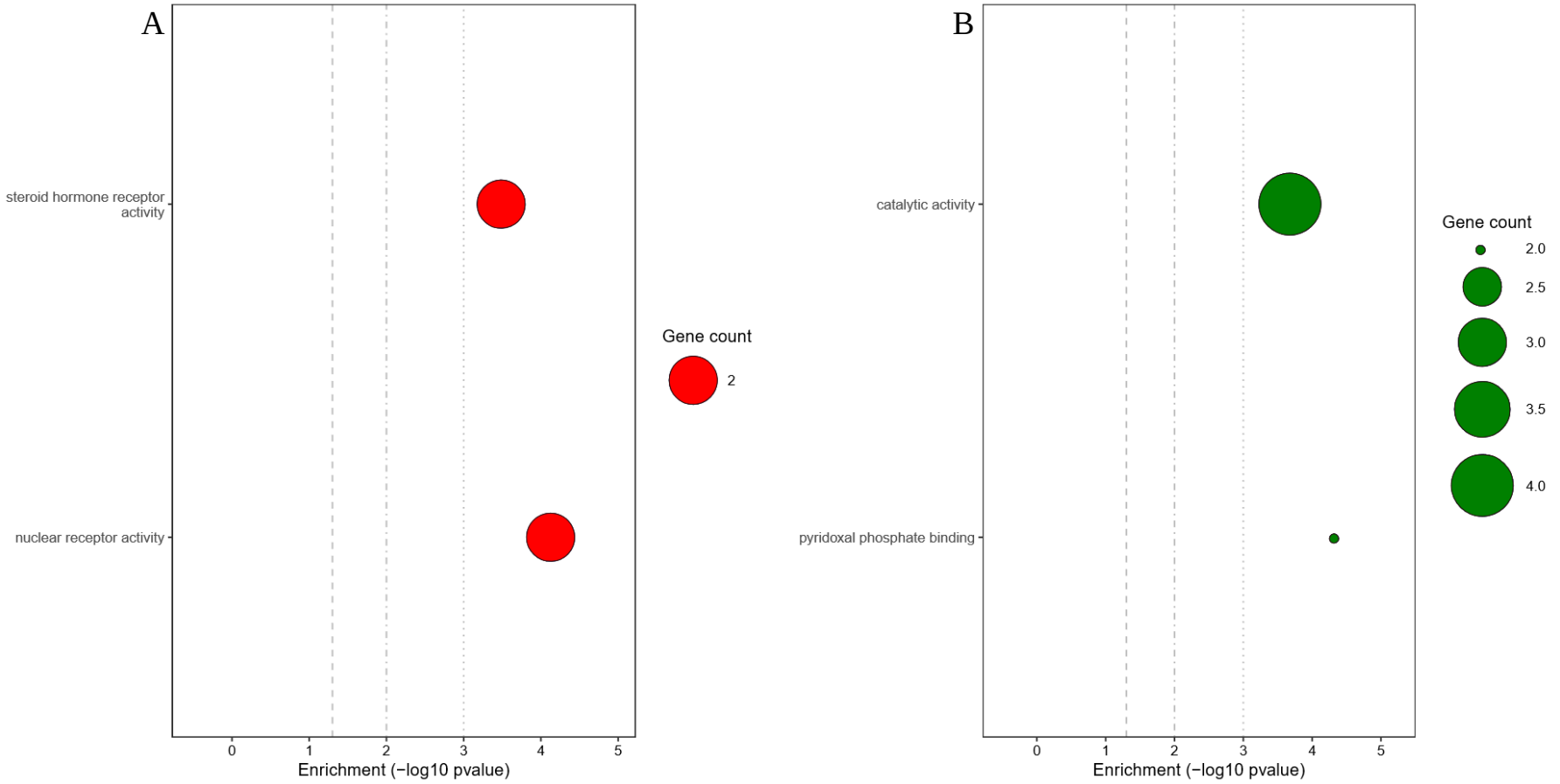


Figure 4-14: Enrichment of molecular function terms in genes identified as up and downregulated in colon tissue at four days post-weaning. A, molecular function enrichment of genes upregulated by weaning. B, molecular function enrichment of genes downregulated by weaning. All significantly enriched terms displayed. All terms shown contain equal to or greater than two differentially expressed genes and are significantly enriched ($q \leq 0.05$). Information on all significantly enriched terms including gene names and identifiers can be found in Appendix 13.

4.2.6.3 Differential Expression Between Colon Samples from Weaned and Suckling Pigs at 14 Days Post-Weaning

At 14 days post-weaning, 35 days of age, only three transcripts were identified as significantly differentially expressed (q <0.1, Log_2 FC ≥ 1 or ≤ -1) between colon samples obtained from suckling and weaned pigs. Two of the three transcripts were upregulated by weaning. These two transcripts included: a transcript which originated from a gene encoding zinc transporter 10 (*ALC30A10*) and a transcript from an uncharacterized gene (ENSSSCG00000010820). The single downregulated transcript encoded desmoglein 3 (*DSG3*).

4.3 Discussion

Pseudo alignment is a recent advance in transcriptomic analysis. This methodology uses a *k*-mer alignment strategy to ascertain the transcript from which a read originates (Bray *et al.*, 2016). This strategy differs from the conventional alignment approach used in the previous chapter in that the focus is shifted from pinpointing precisely how full read sequences align to the reference to an approach where small sections (*k* -mers) of reads are matched to corresponding sections in the reference (Bray *et al.*, 2016).

A major advantage of this methodology over conventional mapping approaches such as HiSat2 (Kim *et al.*, 2015; Pertea *et al.*, 2016) is the reduced computational requirements, and therefore faster processing speed. Kallisto can process 30 million reads in less than 10 minutes on a 1.3-GHz laptop, requiring only 3.2 Gb of RAM per sample. This performance is only rivalled by HiSat2 only when using significantly more computational resources (three cores of a 3.7-GHz processor and 64 Gb of RAM) (Kim *et al.*, 2015; Bray *et al.*, 2016).

There are advantages and disadvantages of the two methodologies. Conventional alignment approaches such as the HiSat2 methodology allows for detection of insertions, deletions and single nucleotide

polymorphisms (Kim *et al.*, 2015). A function which cannot be achieved with Kallisto as only small sections of reads are aligned. Kallisto, however, has advantages in the detection of transcript level differential expression as the k-compatibility class generated during pseudoalignment increases the accuracy of assigning reads to the transcript from which they originate (Pimentel *et al.*, 2017).

When processing the sequencing reads in the current study, HiSat2 successfully aligned a mean of 43,601,697 reads, whereas Kallisto achieved a mean of 31,763,663. This reduction in the number of mapped reads can be attributed to several factors. The reference used for HiSat2 alignment was the full *Sus scrofa* genome (10.2), whereas the transcriptome from the same version was used as the reference for Kallisto alignment. The primary reason for this discrepancy in the number of reads mapped is likely to be an alignment of reads to intergenic regions and unannotated features in the genome by HiSat2. As these regions do not exist within the transcriptome reference, these reads are not mapped by Kallisto (Zhao, 2014; Conesa *et al.*, 2016).

Another probable reason for this difference may be due to error handling by the two methods. Due to the alignment of full-length reads, HiSat2 is capable of handling errors and indels as single base differences

will not prevent alignment of a long read (Kim *et al.*, 2015). The *k*-mer approach adopted by Kallisto handles errors differently, an error in a read *k*-mer will result in that *k*-mer not appearing in the transcriptome. In this case, other *k*-mers within the read must allow the exclusive assignment of a read to a transcript or this read will be discarded as unmapped (Bray *et al.*, 2016). This approach may increase the number of unmapped reads.

Despite the reduction, the approximately 30 million mapped reads per sample is still equivalent to the number of reads mapped in published pig RNA-seq studies (Chen *et al.*, 2011; Jung *et al.*, 2012; Gunawan *et al.*, 2013). The percentage of aligned reads was uniform across all samples (Figure 4-1) showing no alignment problems with individual samples.

The substantial difference between the number of significantly differentially expressed transcripts identified by Sleuth and Ballgown can be attributed to the higher sensitivity of Sleuth to detect transcript level differential expression (Pimentel *et al.*, 2017). This difference can be attributed specifically to the differential gene expression package used as PCA plots explaining normalised expression values after mapping with Sleuth and HiSat2 show similar distribution (Appendix 7).

The authors of Sleuth attribute increased sensitivity to the statistical model used in this package (Pimentel *et al.*, 2017). However, fundamentally the Stringtie/Ballgown methodology is better suited to the identification and interrogation of gene isoforms (Frazee *et al.*, 2015; Pertea *et al.*, 2016). Conversely, Sleuth is designed specifically for the identification of differential expression and is not able to detect any gene isoforms not contained within the reference. This combined with the superior accuracy of Sleuth compared to other differential gene expression packages at an FDR range of 0-10% (Pimentel *et al.*, 2017), makes the combination of Kallisto pseudoalignment and Sleuth differential expression analysis ideally suited to the aims and *q* value criteria of this study.

4.3.1 The Transcriptomic Effect of Weaning in the Porcine Colon

Comparison of the global expression patterns of weaned and suckling individuals by was conducted by comparing TPM values for all transcriptionally active transcripts via the use of principal component analysis (Figure 4-2). This showed some grouping of weaned and suckling samples collected at one and four days post-weaning, however in neither instance were the two cohorts distinct (95% confidence

ellipses overlapped). Which suggests that although there were some similarities in expression within the cohorts, additional samples from either cohort could reasonably be expected to display the same expression pattern as any existing sample. At the 14 days post-weaning time point, all samples were entirely interspersed when observed in the same manner. Taken together, this suggested that some differential expression may be detected at one and four days post-weaning. However, at 14 days post-weaning, the spatial distribution of samples suggested that the expression pattern in all samples was similar, making it unlikely that any large-scale differential expression would be detected.

These observations were supported by differential expression analysis conducted using Sleuth (Pimentel *et al.*, 2017).The Venn diagram in Figure 4-3 indicates that the greatest number of significantly differentially expressed transcripts are found when comparing suckling and weaned samples at one-day post-weaning. This number is reduced at four days post-weaning, and the number is negligible at 14 days after weaning. This is consistent with a change in gene expression immediately after weaning, which is reduced three days later, and by 14

days after weaning, gene expression in the colon of weaned pigs is like that of their suckling counterparts.

Heatmaps were constructed to observe the expression values of transcripts identified as differentially expressed (Figure 4-6-Figure 4-8). This approach was taken to view the range of expression within the weaned and suckling cohorts. Clustering by weaning status and the clear differentiation between up and downregulated genes in these plots is a truism, as only transcripts which have previously been identified as differentially expressed are included. A good deal of animal-to-animal variation is apparent in all three plots, which vary in size according to the number of differentially expressed transcripts identified at each time point.

In the heatmap plotted to display the expression values of differentially expressed transcripts at one-day post-weaning (Figure 4-6), the expression pattern of sample 9223 (a weaned sample) is lower amongst transcripts otherwise highly expressed in the weaned cohort. The expression pattern of this sample is also higher when compared with lower expression values in other weaned samples. This must have contributed to the similarity observed in the overall expression pattern

of this sample when compared to the suckling cohort observed by principal component analysis (Figure 4-2A).

A similar effect is evident in the plot displaying the expression values of differentially expressed transcripts at four days post-weaning. In this instance, the expression of transcripts otherwise highly expressed in the suckling cohort is notably lower in sample 3396 than others (Figure 4-7). This again must have contributed to the similarity between this sample and the weaned cohort when the overall expression profile is compared by principal component analysis (Figure 4-2B).

Literature concerning sample-to-sample variation in RNA-seq is sparse, with existing studies finding greater differences between tissues than between biological replicates in mice and rats (Sollner *et al.*, 2017). No clear standard exists to assess reproducibility among biological replicates, as this depends on the heterogeneity of the experimental system (Conesa *et al.*, 2016).

In the current study, several factors may contribute to variability within samples of a cohort. The first is the nature of the sample from which RNA was extracted. Colon tissue consists of five major cell types: epithelia, glandular/endocrine epithelia, immune cells, neuronal cells and mesenchymal cells (muscle and connective tissue) (Freeman *et al.*,

2012). Differing proportions of these cell types in a sample may contribute some variation between samples (Liu *et al.*, 2016b). Other factors which may contribute to variation is variations in the gut microbiota composition (Richards *et al.*, 2017), and the time elapsed between the animals' last meal and slaughter as this may affect colon gene expression (Holt and DuBois, 1991; Van Erk *et al.*, 2004). This effect is pertinent as weaned pigs had unmonitored *ad libitum* access to creep feed from 21 days of age, whereas suckling pigs had access to this feed from 25 days of age. Consumption of creep feed is a variable which may shape the microbiota of these animals (Frese *et al.*, 2015).

As variation in a complex tissue is to be expected, biological replicates are used to find a consensus of expression. A recent investigation into the number of biological replicates required for RNA-seq experiments identified a minimum of six (Schurch *et al.*, 2016). In this study, when just three of the 42 biological replicates per treatment were compared, only 20-40% of the differentially expressed genes observed when all replicates were included were retained. The authors suggest that when fewer than six biological replicates are available, a fold change cut-off of greater than two is advisable. This approach has been adopted in the current study. To obtain a full picture of all differential expression at

weaning, FC >0.5, a minimum of 12 samples would be required. Therefore, the picture of the transcriptional effect of weaning described in this study lacks the subtler changes which would be available with a greater number of biological replicates.

Transcription viewed using RNA-seq may not directly correlate with protein expression due to post-transcriptional modulation (Liu *et al.*, 2016b). However, as the technique applied in this study solely concerns messenger RNA, no comment can be made concerning protein-mRNA relationships. Instead, gene ontology analysis was conducted to elucidate the possible biological implications of observed differential gene expression on the colon of the weaning pig (Ashburner *et al.*, 2000).

4.3.2 The Transcriptional Effect of Weaning in the Colon of 22 Day Old Pigs (One Day Post-Weaning)

At one-day after weaning, several biological processes are significantly enriched by genes upregulated by weaning (Figure 4-9). Amongst these, evidence can be found for increased activity of the immune system. Some of the genes upregulated by weaning which contribute towards this are cytokines. Interleukin 1β2, Interleukin 1α, tumour

necrosis factor superfamily member 10 and tumour necrosis factor superfamily member 8 are all upregulated by weaning.

Interleukin 1 (IL-1) is a cytokine which has been shown to have a major role in inflammatory and immunological immune responses, expression of *IL-1* is increased in the colon during inflammatory bowel disease (Ligumsky *et al.*, 1990). The activity and signalling of IL-1 is described in section 1.2.3. Tumour necrosis factor superfamily members 8 and 10, known as CD30L and TRAIL, respectively, also have pro-inflammatory effects. CD30L interacts with CD30+ B cells to promote proliferation and antibody production in a cytokine-dependent manner (Kennedy *et al.*, 2006). TRAIL is an apoptosis-inducing ligand, overexpression of which has been noted to disrupt intestinal epithelium integrity during inflammatory bowel disease by induction of epithelial cell apoptosis (Begue *et al.*, 2006; Aggarwal *et al.*, 2012; Slebioda and Kmiec, 2014). Taken together, the greater than two-fold increase in expression of these four proinflammatory cytokines suggests immune activation one day after weaning.

These findings contrast with the expression of proinflammatory cytokines observed in the colon following seven days of mixing/crowding stress. In this instance, a significant reduction in TNFα

and IL-1β mRNA was seen in stressed pigs compared to control animals (Li *et al.*, 2017). Another study noted increased expression of IL-1β mRNA in the early response to weaning in pigs, zero to two days post-weaning, but no significant increase in TNFα mRNA (Pie *et al.*, 2004).

Other immune-related genes upregulated by weaning included members of the complement membrane attack complex, C3, C7 & C9. The complement system plays a key role as an effector of innate immunity (Sugihara *et al.*, 2010; Sarma and Ward, 2011). The complement system is activated in response to invading pathogens whereby the membrane attack complex can lyse bacteria (Bolger *et al.*, 2007). Expression of these complement factors is not widely researched, however, increased expression of C3 has been observed in the inflamed mucosa of human IBD patients (Sugihara *et al.*, 2010).

Another group of genes upregulated by weaning encode the serine peptidase inhibitors A10, A11, B2 and B5. Members of the serine peptidase inhibitor family are known to regulate proteinases involved in many cellular processes including inflammation, cell death and development (Gatto *et al.*, 2013). Although the activity of these inhibitors in the gut is poorly understood, it has been suggested that

they may have a role in preventing the necrosis of gastrointestinal cells during necrotising enterocolitis in mice (Jung *et al.*, 2015).

Another process enriched amongst genes upregulated by weaning was the positive regulation of glucose transport. However, only C3 and the transcription factor NR4A3 enriched this process. However, In addition to activity in glucose transport activity (Liu *et al.*, 2013), NR4A3 expression in $CD103^{+}$ dendritic cells is essential for the migration of these cells to lymph nodes (Park *et al.*, 2016). Increased expression of this transcription factor may indicate increased migration of dendritic cells to the mesenteric lymph nodes in weaned individuals. This may result from the sudden shift in the antigenic composition of the intestinal contents due to the change in diet of weaned individuals (Bailey *et al.*, 2005).

Processes and functions enriched amongst genes downregulated by weaning included a number associated with development including somite development and specification as well as embryonic limb development. Central to the enrichment of these terms are mesenchyme homeobox one & two. These regulatory elements are important in the normal development of skeletal muscle (Otto *et al.*, 2010). Also downregulated by weaning are the homeobox genes D10

and D13, unlike the mesenchyme homeobox genes, these have a documented role in the development of the intestine concerning differentiation of both the muscular layer and the epithelium. *HOXD* deficient mice do not thrive as well as wild-type littermates, which is attributed to reduced digestion efficacy due to a shorter gut (Zacchetti *et al.*, 2007). The downregulation of these regulatory elements may have a detrimental effect on colon development during this early post-weaning period.

Downregulation of 18 genes contained in the 'transport' biological process GO term is also observed because of weaning. When molecular function enrichment is conducted (Figure 4-11), these genes indicate a downregulation of sodium channel, acetylcholine and ligand-gated ion channel activity. This downregulation may result from elevated pro-inflammatory cytokine production in the colon (Amasheh *et al.*, 2004).

4.3.3 The Transcriptional Effect of Weaning in 25 Day Old Pigs (4 Days Post-Weaning)

Although only 78 transcripts were differentially expressed at four days post-weaning, GO enrichment was applied to elucidate the biological processes and functions which might be affected by both up and

downregulated transcripts. The small number of differentially expressed transcripts is reflected in the number of genes enriching each GO term, with the majority only enriched by two genes (Figure 4-12-Figure 4-14).

Two biological process terms were significantly enriched by the upregulated genes at this time point. 'regulation of angiogenesis' refers to the formation of new blood vessels (Nishida *et al.*, 2006). This process was enriched by the upregulation by weaning of integrin α5 (*ITGA5*) and tumour necrosis factor superfamily 12A (*TNFSF12A*) transcripts. Integrins are transmembrane molecules that mediate cell-cell and cell-substratum adhesion (Stallmach *et al.*, 1992). Degradation and turnover of integrin α5 is required for the proper migration of fibroblasts (Lobert *et al.*, 2010) and can regulate cellular proliferation via interaction with fibronectin (Varner *et al.*, 1995). Tumour necrosis factor superfamily 12A (also known as TWEAK, tumour necrosis factor-like weak inducer of apoptosis) interacts with its receptor fibroblast growth factor-inducible 14 (Fn14) to regulate multiple cellular responses including stimulation of proliferation, migration, apoptosis and angiogenesis (Shui *et al.*, 2008). The upregulation of these two genes by weaning suggests increased activity of fibroblasts in the colon of weaned animals.

The second biological process term enriched amongst genes upregulated by weaning is *intracellular receptor signalling pathway*. This term is enriched by two genes: *NR1H4* and *NR4A3,* the upregulation of which also enriches the molecular function terms *nuclear receptor activity* and *steroid hormone receptor activity*.

The product of *NR1H4* is farsenoid X receptor (FXR) which regulates the expression of genes involved in bile acid synthesis as well as lipid and glucose metabolism (Ding *et al.*, 2015; Selmin *et al.*, 2016). Expression of *NR1H4* is localised primarily to fully differentiated cells lining the intestinal epithelium of the ileum and colon (Modica *et al.*, 2010). FXR participates in immune modulation and barrier function in the intestine, where it alleviates inflammation and preserves the integrity of the intestinal barrier by regulating the extent of the inflammatory response (Gadaleta *et al.*, 2010; Ding *et al.*, 2015). FXR activation inhibits proinflammatory cytokine production *in vivo* in the mouse colonic mucosa and *ex vivo* in different immune cell populations (Gadaleta *et al.*, 2010), and mRNA expression is reduced in IBD (Nijmeijer *et al.*, 2011; Jahnel *et al.*, 2014). Therefore, the greater than two-fold increase in *NR1H4* transcription in the colon of weaned pigs at four days post-

weaning may constitute a delayed response to dampen the activation of proinflammatory cytokine genes observed at one-day post weaning.

The second upregulated gene contributing to the enrichment of these terms is *NR4A3.* A transcript of this gene was also upregulated by weaning at one-day post-weaning. The gene product, NOR-1, is essential for dendritic cell migration to lymph nodes (Park *et al.*, 2016). Expression of *NR4A3* in dendritic cells is increased in the presence of lipopolysaccharide and plays a central role in Toll-like receptor-mediated activation and gene expression in this cell population (Nagaoka *et al.*, 2017). The increased expression observed in the colon of weaned animals may be representative of the recruitment and subsequent larger population of $CD103^{+}$ dendritic cells resulting weaning related immune activation. This recruitment has been noted in a mouse model (Lantier *et al.*, 2013).

GO enrichment of genes downregulated by weaning at 25 days of age, four days post-weaning, indicated biological processes associated with lipid and triglyceride processing were downregulated. However, the enrichment of all four terms (Figure 4-12) was a result of just two downregulated genes: *MTTP* and *APOC3*.

Microsomal transfer protein (MTTP) is required for lipid uptake as virtually no dietary fat uptake was observed in a knockout model in mice (Xie *et al.*, 2013). Studies concerning the transcriptional activity of *MTTP* found that expression is increased in both IPEC-1 cell culture and the newborn swine small intestine in response to lipid absorption (Lu *et al.*, 2002; Yao *et al.*, 2011). It was also observed that expression in the jejunum of newborn swine paralleled the intake of a high-fat breast milk diet but declined after weaning (Lu *et al.*, 2002).

The product of the second gene, apolipoprotein C3 (*APOC3*), acts to increase plasma triglyceride levels by inhibiting hydrolysis of triglyceride-rich lipoproteins by lipoprotein lipase (Ginsberg *et al.*, 1986; Jorgensen *et al.*, 2014). As with *MTTP,* the dietary content of the animals may lead to this reduction in expression as this effect was observed in the jejunum of pre-weaning calves when access to milk was restricted (Hammon et al., 2018). Taken together, the decreased expression of these genes in the colon of weaned pigs compared to their suckling counterparts may reflect the high milk, and therefore lipid, content of the diet of suckling animals (creep feed composition available in Appendix 1).

Gene ontology analysis also highlighted the downregulation of genes associated with *pyridoxal phosphate binding* and *catalytic activity,* although the activity of these genes in the colon is unclear.

Transcriptional activity in the colon of 35 day old weaned and suckling pigs was found to be very similar, with only three transcripts identified as exhibiting a greater than two-fold change. As so few differentially expressed transcripts were identified, GO analysis was inappropriate. One of these transcripts, ENSSSCG00000010820, was the product of a predicted gene with no available information. The two remaining transcripts encoded *SCL30A10*, a manganese transporter (Chen *et al.*, 2015) which was upregulated in the weaned cohort, and desmoglein 3 (*DSG3*) which was downregulated. With so little information, a functional effect of these changes cannot be identified.

4.4 Conclusion

Kallisto pseudo-alignment combined with Sleuth differential expression calling is a more sensitive method of identifying transcript level differential expression in the pig colon.

Of the three post-weaning timepoints compared, the greatest number of transcriptional changes were observed at one-day after weaning, this was reduced by four days post-weaning and at 14 days after weaning. Extremely few transcriptional differences between the colon of weaned and suckling animals could be identified.

One-day after weaning there is evidence of increased transcriptional activity of proinflammatory cytokines in the colon of weaned pigs compared to suckling animals, particularly *IL1A* and *IL1B2* and members of the tumour necrosis factor superfamily. There is also evidence of downregulation of homeobox regulatory elements associated with development in weaned animals at this early stage after weaning.

By four days after weaning, the early evidence of an immune response had been dampened. However, some transcriptional evidence of the dietary differences between weaned and suckling pigs was identified.

By fourteen days after weaning, transcription in the colon of weaned and suckling individuals was so similar that extremely few transcriptional differences could be detected. This suggests that by two weeks after weaning the weaning effect on the colon is complete, leaving the transcriptome of weaned and suckling samples practically indistinguishable.

5 Chapter 5: The Transcriptional Effect of Dietary Intake of *Saccharomyces cerevisiae boulardii* in the Colon of Weaning Pigs

5.1 Introduction

Weaning is a stressful period in swine production, which impairs performance and induces a perturbation of the intestinal microbiota (Castillo *et al.*, 2007).

As a result of the EU-wide ban on antibiotic growth promoters (EC Regulation No. 1831/2003) (Millet and Maertens, 2011), the application of probiotic microorganisms to weaning pigs has been investigated as an alternative to control pathogen-associated suppression of growth and production (Collier *et al.*, 2011; Kenny *et al.*, 2011; Hayakawa *et al.*, 2016; Lan *et al.*, 2016).

One such microorganism which is authorised for use as a probiotic is the yeast *Saccharomyces cerevisiae boulardii* (SCB) (Venugopalan *et al*., 2010). Reported effects of SCB supplementation in pigs include a reduction of porcine neonatal diarrhoea after a single dose (Hancox *et al.*, 2015), reduction of enterotoxigenic *E. coli* F4 attachment in the

ileum after challenge (Daudelin *et al.*, 2011) and increased colonic microbiota diversity at two weeks post-weaning after administration of 9 Log_{10} cfu per day from one day of age (Brousseau *et al.*, 2015). However, no porcine studies detailing the transcriptional effect of SCB in the colon exist.

To expand this knowledgebase, this chapter will first aim to identify transcriptional changes in the porcine colon of suckling pigs of 22, 25 and 35 days of age in response to SCB supplementation from 7 days of age, 4.43 Log_{10} cfu/day. A second analysis will detail the effect of SCB supplementation in weaned pigs of the same ages after weaning at 21 days of age.

5.2 Results

5.2.1 The Effect of Oral *Saccharomyces cerevisiae boulardii* Supplementation on the Colon of Suckling Pigs

To identify transcriptional changes brought about by SCB supplementation in suckling pigs, the global expression pattern of colon tissue collected from suckling pigs with and without SCB supplementation was compared. After mapping with Kallisto and differential expression analysis with Sleuth (Bray *et al.*, 2016; Pimentel *et al.*, 2017), differentially expressed transcripts were identified as those with greater than 2-fold change(Log2 FC ≥ 1 or ≤ -1) with a *q* value of less than 0.1 (Schurch *et al.*, 2016).

5.2.1.1 Comparison of Global Expression Patterns of Colon Tissue Extracted from Suckling Pigs with and without SCB Supplementation using Principal Component Analysis

Principal component analysis was conducted on all TPM values obtained from mapping datasets to the *Sus scrofa* transcriptome (Figure 5-1). This analysis demonstrated some grouping of control and SCB supplemented samples at 22 days of age (Figure 5-1A), suggesting that

some differential gene expression may be identified, although the 95% confidence interval ellipses intersected. At 25 and 35 days of age, no separation of expression profiles was observed between the cohorts (Figure 5-1B & C). This suggests that the greatest number of differentially expressed transcripts would be identified between 22-day old pigs.

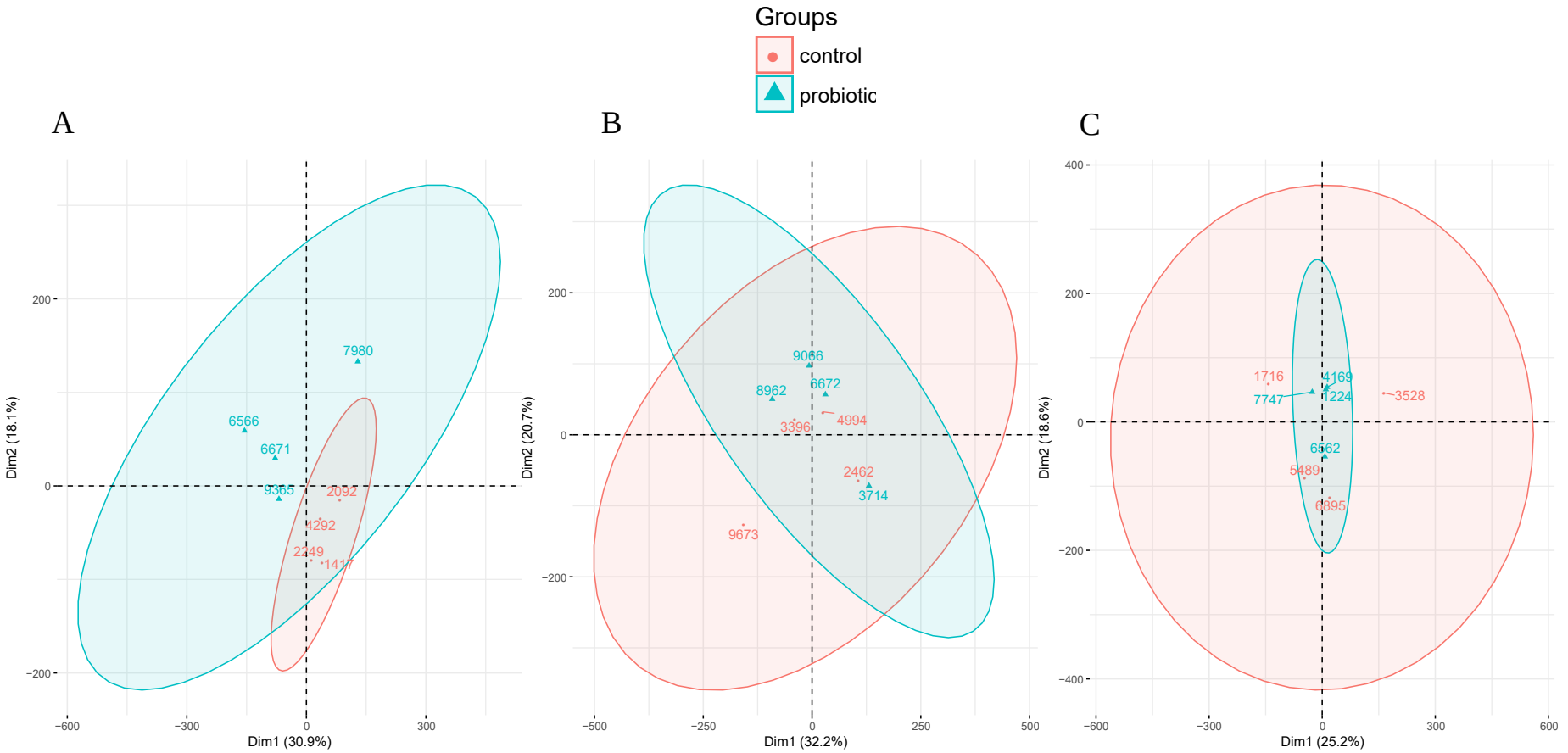


Figure 5-1: Principal component analysis to compare the global expression pattern of suckling pig colon samples with and without SCB supplementation at 22, 25 and 35 days of age. Plot A indicates 22 days of age; plot B indicates 25 days of age and plot C indicates 35 days of age. Samples from control pigs are indicated in red, the corresponding samples from SCB supplemented pigs are indicated in blue. Principal component analysis was applied to transcripts per million (TPM) information obtained from Kallisto mapping. X and Y axis show principal component 1 and principal component 2 respectively (percentage of variance indicated on each plot). Prediction ellipses are such that with probability 0.95, a new observation from the same group will fall inside the ellipse

5.2.1.2 Overview of Differential Transcript Expression between Colon Tissue Extracted from Suckling Pigs with and without SCB Supplementation

Volcano plots describing differential expression by plotting beta, an estimator of Log_2 fold change, against $-Log_{10}$ p-value, at each of the three time points (Figure 5-2) identified 197 differentially expressed transcripts (Log_2 FC ≥ 1 or ≤ -1, q >0.1) which can be attributed to SCB supplementation in suckling pigs at 22 days of age (Additional file 4). Six and two were identified at 25 and 35 days of age respectively (additional files 5 & 6). Of the 197 differentially expressed transcripts at 22 days of age, 62 were upregulated by SCB and 135 were downregulated. At 25 days of age, four transcripts were upregulated and two downregulated by SCB supplementation. Both significantly differentially expressed transcripts at 35 days of age were upregulated by SCB (Figure 5-3).

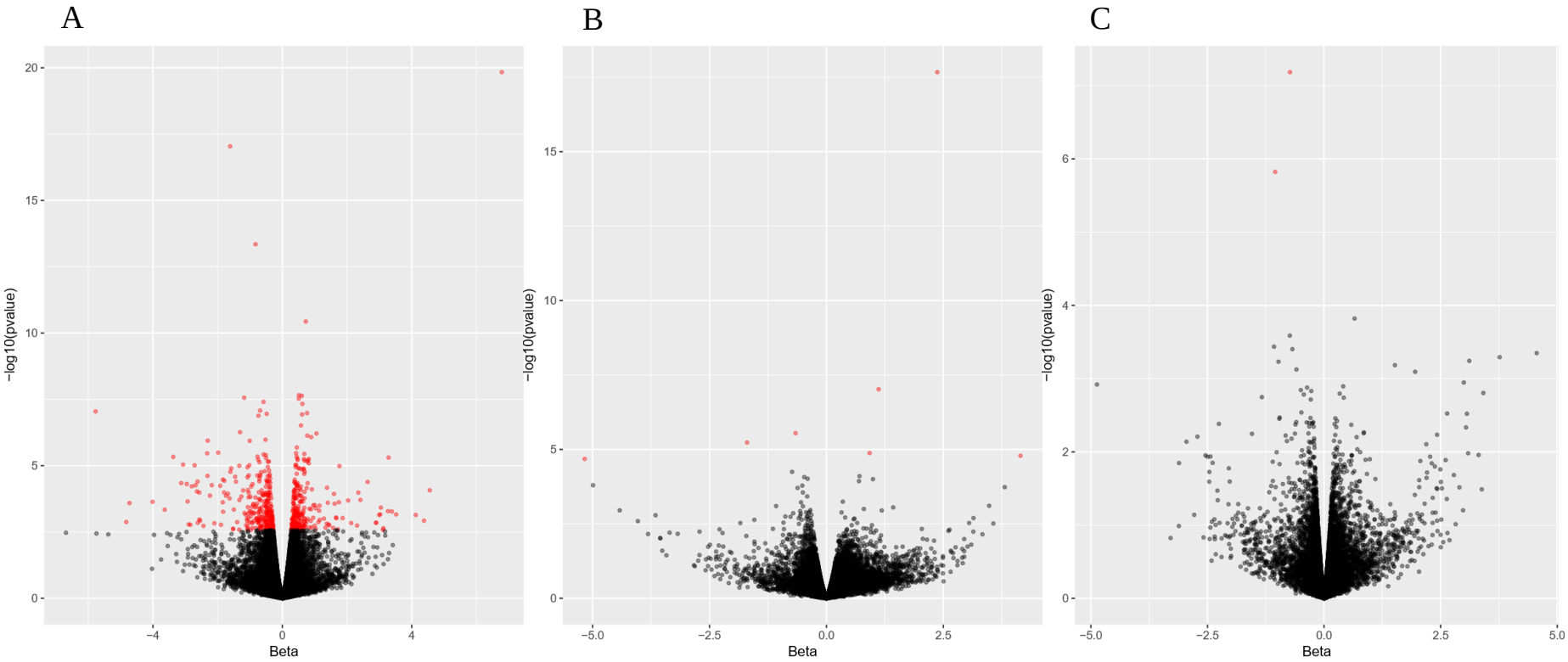


Figure 5-2: Volcano plots to show differential expression of transcripts in the colon of suckling pigs in response to SCB supplementation. -$\log_{10}$ *p*-value plotted against beta value. Beta value is an estimator of fold change used in the model applied by Sleuth. Transcripts with a Benjamini-Hochberg false detection rate corrected *p*-value <0.1 are indicated in red. A, differentially expressed transcripts at 22 days of age. B, differentially expressed transcripts at 25 days of age. C, differentially expressed transcripts at 35 days of age.

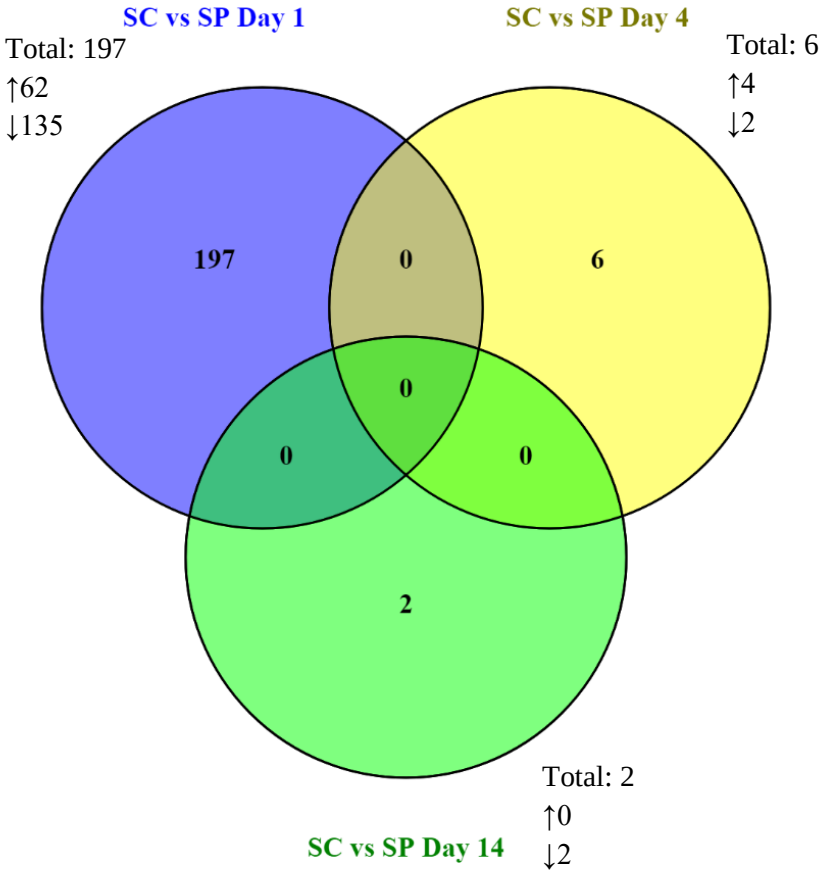


Figure 5-3: Venn diagram to demonstrate differential expression observed between suckling pigs with and without SCB supplementation at 22, 25 and 35 days of age. SC vs SP, suckling control vs Suckling + Probiotic (SCB). Day one, 22 days of age. Day four, 25 days of age, Day 14, 35 days of age. Total transcripts, up (↑) and down (↓) regulated transcripts are indicated. All transcripts Log_2 FC ≥ 1 or ≤ -1, q < 0.1.

5.2.1.3 Sample-to-Sample Variation in Expression Values for Differentially Expressed Transcripts

To assess the sample to sample variation in expression values, TPM values for differentially expressed transcripts were visualised as a heatmap. This was only conducted for differentially expressed transcripts at 22 days of age, as few differentially expressed transcripts were identified in animals of 25 and 35 days of age. In the resulting heatmap, samples cluster by treatment and transcripts group by up and downregulation. This is a truism as only features which distinguish the treatments are plotted. The resulting heatmap showed that each sample showed a unique expression pattern across these transcripts with sample 2092 of the control cohort most unlike the rest of the control cohort. The same can be said of sample 7980 in the SCB cohort (Figure 5-4). These findings reflect those observed when conducting principal component analysis on the global expression pattern of these samples (Figure 5-1A).

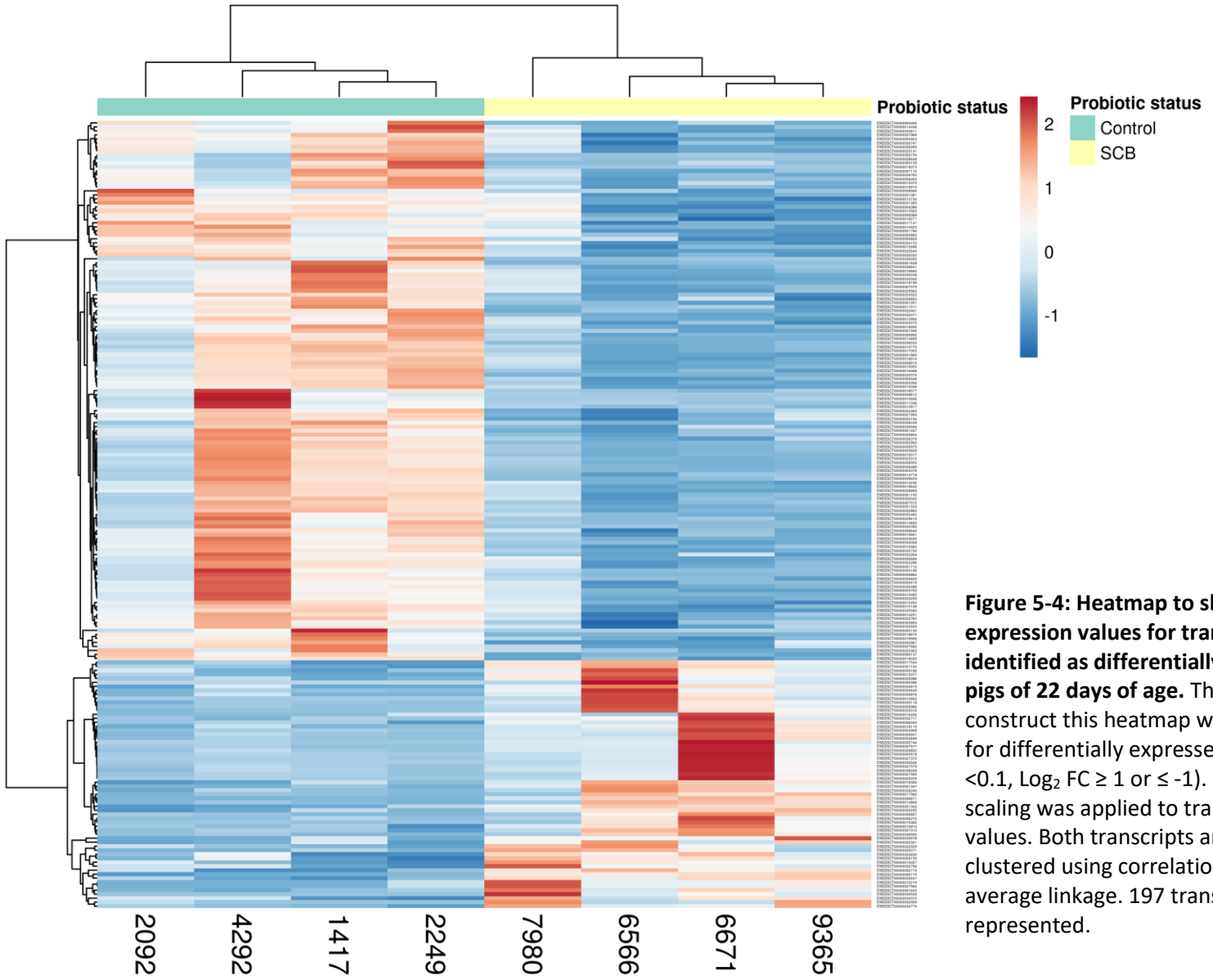


Figure 5-4: Heatmap to show TPM expression values for transcripts identified as differentially expressed in pigs of 22 days of age. The input to construct this heatmap was TPM values for differentially expressed transcripts (*q* <0.1, Log_2 FC ≥ 1 or ≤ -1). Unit variance scaling was applied to transcript TPM values. Both transcripts and samples are clustered using correlation distance and average linkage. 197 transcripts are represented.

5.2.1.4 GO Analysis of Transcripts Differentially Expressed in the Colon of Pigs at 22 Days of Age in Response to SCB Supplementation

GO analysis was conducted on Ensembl gene IDs associated with differentially expressed transcripts. This analysis was conducted separately for up and downregulated transcripts. Ontologies were considered significantly enriched by two or greater genes and $q \leq 0.05$ (Li *et al.*, 2016c).

5.2.1.5 Biological Process Enrichment

Biological process enrichment of upregulated genes identified: *innate immune response; double-strand break repair; positive regulation of neutrophil chemotaxis* and *cellular response to lipopolysaccharide* as significantly enriched amongst transcripts upregulated in suckling animals supplemented with SCB (Figure 5-5A).

Three of the 162 genes encompassed by the *innate immune response* term were upregulated by SCB supplementation. These were: tripartite motif containing 10 (*TRIM10*); complement 9 (*C9*) and lipopolysaccharide binding protein (*LBP*). Two of the 52 genes associated with *double-strand break repair* were upregulated, these were: nibrin (*NBN*) and E3 ubiquitin-protein ligase (*DTX3L*). *Positive*

regulation of neutrophil chemotaxis and *cellular response to lipopolysaccharide* were enriched by two and four genes respectively. The former by interleukin 8 (*CXCL8*) and *LBP*. The latter by these two genes in addition to tumour necrosis factor α interacting protein 3 (*TNFAIP3*) and aconitate decarboxylase 1 (*ACOD1*).

Biological process enrichment of downregulated genes identified ten significantly enriched terms. These included *positive regulation of myoblast differentiation; lymph node development; cellular response to calcium ion; response to zinc ion; establishment of protein localization to membrane; negative regulation of cytokine secretion; negative regulation of intrinsic apoptotic signaling pathway in response to DNA damage by p53 class mediator; striated muscle myosin thick filament assembly; leukocyte chemotaxis* and *B cell receptor signaling pathway* (Figure 5-5B).

Positive regulation of myoblast differentiation was enriched by the downregulation of RHO family interacting cell polarisation regulator 2 (*RIPOR2*) and myocyte enhancer factor 2C (*MEF2C*). Lymph node development was enriched by the downregulation of lymphotoxin beta (*LTB*) and C-X-C chemokine receptor type 5 (*CXCR5*). Establishment of protein localisation to the membrane was enriched by the

downregulation of FERM and PDZ domain-containing protein 1 (*FRMPD1*) and acetylcholinesterase collagenic tail peptide (*COLQ*). *Leukocyte chemotaxis* was enriched by the downregulation of C-X-C chemokine receptor type 5 (*CXCR5*) and cannabinoid receptor 2 (*CNR2*). *B cell receptor signaling pathway* was enriched by the downregulation of B-lymphocyte antigen C19 (*CD19*), myocyte enhancer factor 2C (*MEF2C*), cluster of differentiation 79B (*CD79B*) and tyrosine-protein kinase Blk (*BLK*). An exhaustive list of ontologies enriched by both up and downregulated genes, including associated Ensembl IDs can be found in Appendix 14.

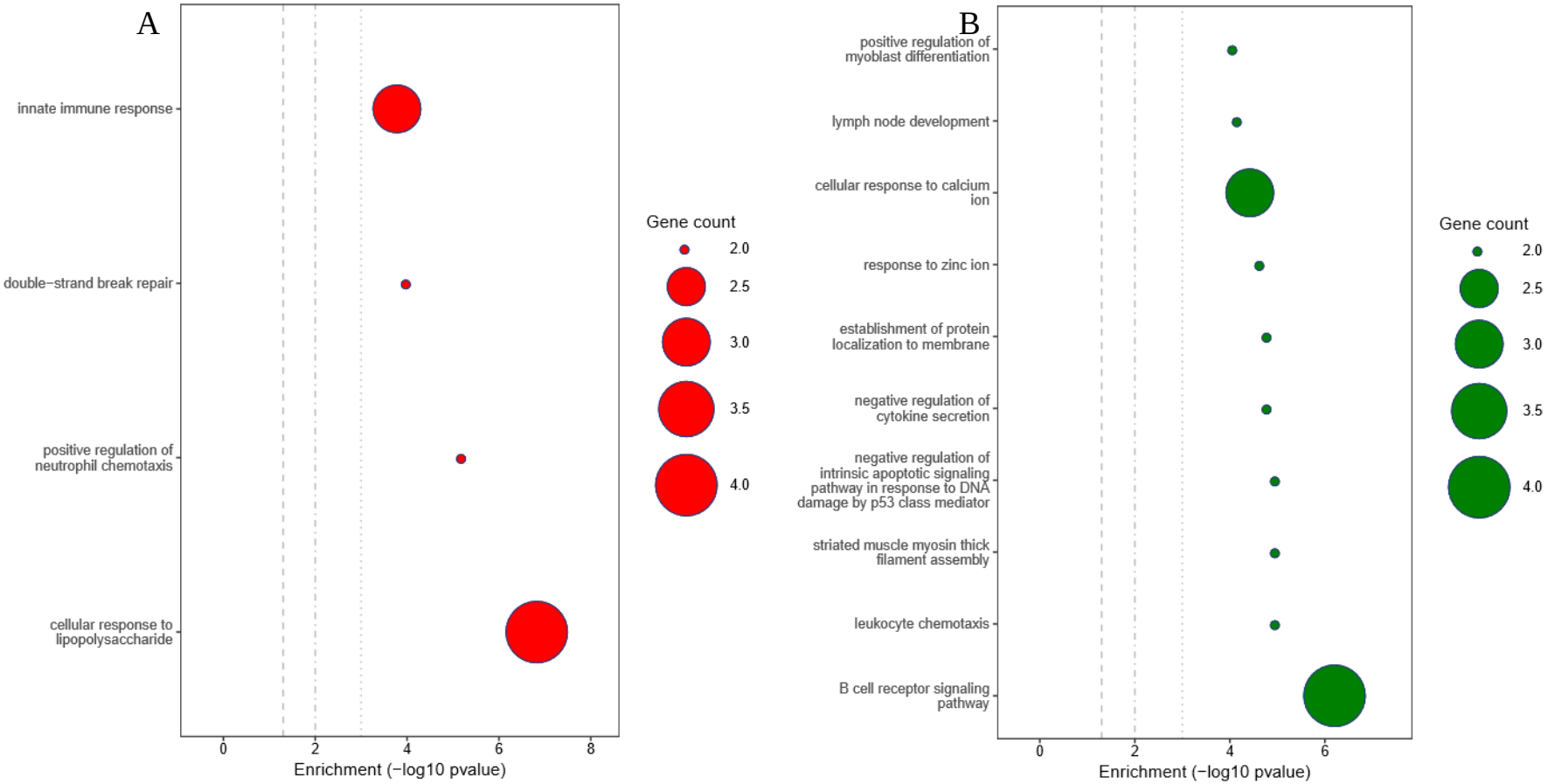


Figure 5-5: Enrichment of biological process terms in genes identified as up and downregulated by SCB in the colon tissue of suckling pigs at 22 days of age. A, biological process enrichment of genes upregulated by SCB supplementation. B, biological process enrichment of genes downregulated by SCB supplementation. Top 10 most significantly enriched terms displayed where available. Terms shown contain equal to or greater than two differentially expressed genes and are significantly enriched (q ≤0.05). Information on all significantly enriched terms including gene names and identifiers can be found in Appendix 14.

5.2.1.5.1 Cellular Compartment Enrichment

Cellular compartment GO enrichment identified two terms significantly enriched by transcripts identified as upregulated. These were *extracellular space* and *blood microparticle* (Figure 5-6A).

Six of the 966 genes associated with extracellular space were upregulated by SCB supplementation. These six genes were: serine peptidase inhibitor B2 (*SERPINB2*); interleukin 8 (*CXCL8*); complement factor I (*CFI)*; complement component 4 binding protein alpha (*C4BPA*); complement 9 (*C9*) and lipopolysaccharide binding protein (*LBP*). Two of the 73 genes associated with blood microparticle were upregulated: complement component 4 binding protein alpha (*C4BPA*) and complement 9 (*C9*).

Cellular compartment GO enrichment of downregulated genes identified five terms as significantly enriched. These were: *M band*; *external side of plasma membrane*; *membrane*; *muscle myosin complex* and *integral component of membrane* (Figure 5-6B).

M band and muscle myosin complex were enriched by the downregulation of the same two genes: myosin binding protein C, cardiac (*MYBPC3*) and novel gene ENSSSCG00000015747 which is orthologous to myomesin 2 (*MYOM2*) in other species. The *external*

side of plasma membrane term was enriched by the downregulation of six of the 155 associated genes. These were: Milk fat globule-EGF factor 8 protein (*MFGE8*); B-lymphocyte antigen C19 (*CD19*); C-X-C chemokine receptor type 5 (*CXCR5*); cluster of differentiation 79B (*CD79B*); B-lymphocyte antigen CD20 (*MS4A1*) and beta subunit of epithelial sodium channel ENaC (*SCNN1B*).

The high-level terms *membrane* and *integral component of membrane* were enriched by 47 of 4910 and 44 of 3806 genes respectively. Many of the downregulated genes are shared between the two GO terms. These genes include but are not limited to: Toll-like receptor 10 (*TLR10*); B-lymphocyte antigen C19 (*CD19*); C-X-C chemokine receptor type 5 (*CXCR5*); cluster of differentiation 79B (*CD79B*) and B-lymphocyte antigen CD20 (*MS4A1*). A full list of downregulated genes associated with these terms, and all cellular component gene enrichment, can be found in Appendix 15.

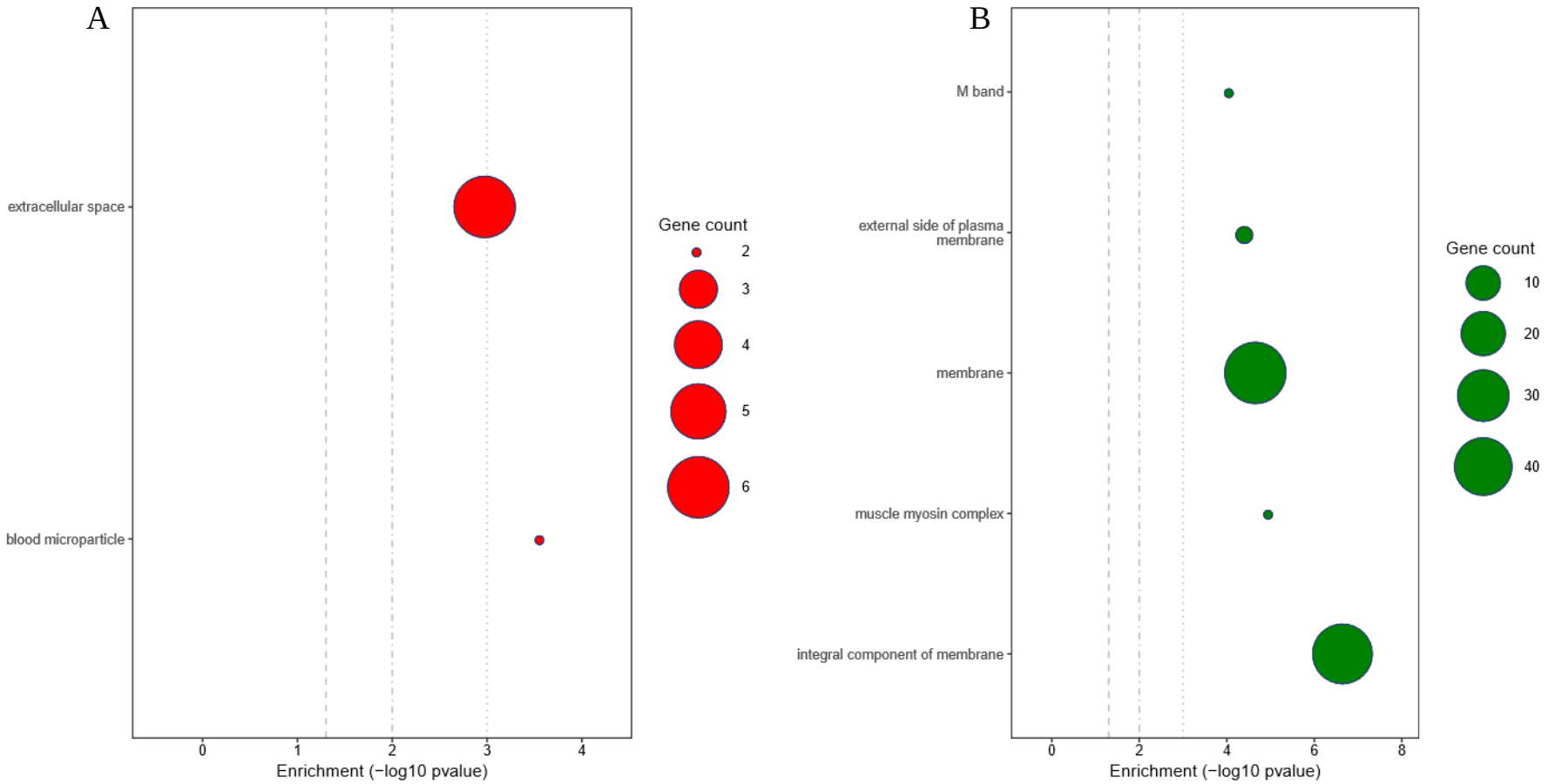


Figure 5-6:Enrichment of cellular component terms in genes identified as up and downregulated by SCB in the colon tissue of suckling pigs at 22 days of age. A, cellular component enrichment of genes upregulated by SCB supplementation. B, cellular component enrichment of genes downregulated by SCB supplementation. Top 10 most significantly enriched terms displayed where available. All terms shown contain equal to or greater than two differentially expressed genes and are significantly enriched (q ≤0.05). Information on all significantly enriched terms including gene names and identifiers can be found in Appendix 1

5.2.1.5.2 Molecular Function GO Enrichment

Molecular function GO enrichment of upregulated genes identified a single term as significantly enriched (Figure 5-7A). *GTPase* activity was enriched by the upregulation of three of its 195 associated genes. These three genes were guanylate binding protein 2 (*GBP2*) and novel genes ENSSSCG00000030801 and ENSSSCG00000006919 orthologous to guanylate binding protein 6 (*GBP6*) and guanylate binding protein 7 (*GBP7*) respectively in other species.

Molecular function GO enrichment of downregulated genes identified seven significantly enriched terms. These were, in order of significance from highest to lowest: *structural constituent of muscle*; *HMG box domain binding*; *MHC class II protein complex binding*; *muscle alpha-actinin binding*; *structural molecule activity conferring elasticity*; *sodium channel activity* and *ligand-gated sodium channel activity* (Figure **5-7**).

Structural constituent of muscle (2/20 genes), *muscle alpha-actinin binding* (2/11 genes) and *structural molecule activity conferring elasticity* (2/9 genes) were all enriched by the same two genes: myosin binding protein C, cardiac (*MYBPC3*) and novel gene ENSSSCG00000015747 which is orthologous to myomesin 2 (*MYOM2*) in other species. *HMG box domain binding* (2/12 genes) was enriched by

the downregulation of myocyte enhancer factor 2C (*MEF2C*) and mesenchyme homeobox 1 (*MEOX1*). MHC class II protein complex binding (2/12 genes) was enriched by the downregulation of HLA class II histocompatibility antigen DO beta chain (*HLA-DOB*) and B-lymphocyte antigen CD20 (*MS4A1*).

Sodium channel activity (3/20 genes) and *ligand-gated sodium channel activity* (2/6 genes) were both enriched by the downregulation of acid-sensing ion channel subunit 3 (*ASIC3*) and beta subunit of epithelial sodium channel ENaC (*SCNN1B*). The former was further enriched the downregulation of sodium channel protein type 4 subunit alpha (*SCN4A*). Additional information on this molecular function gene ontology enrichment can be found in Appendix 16.

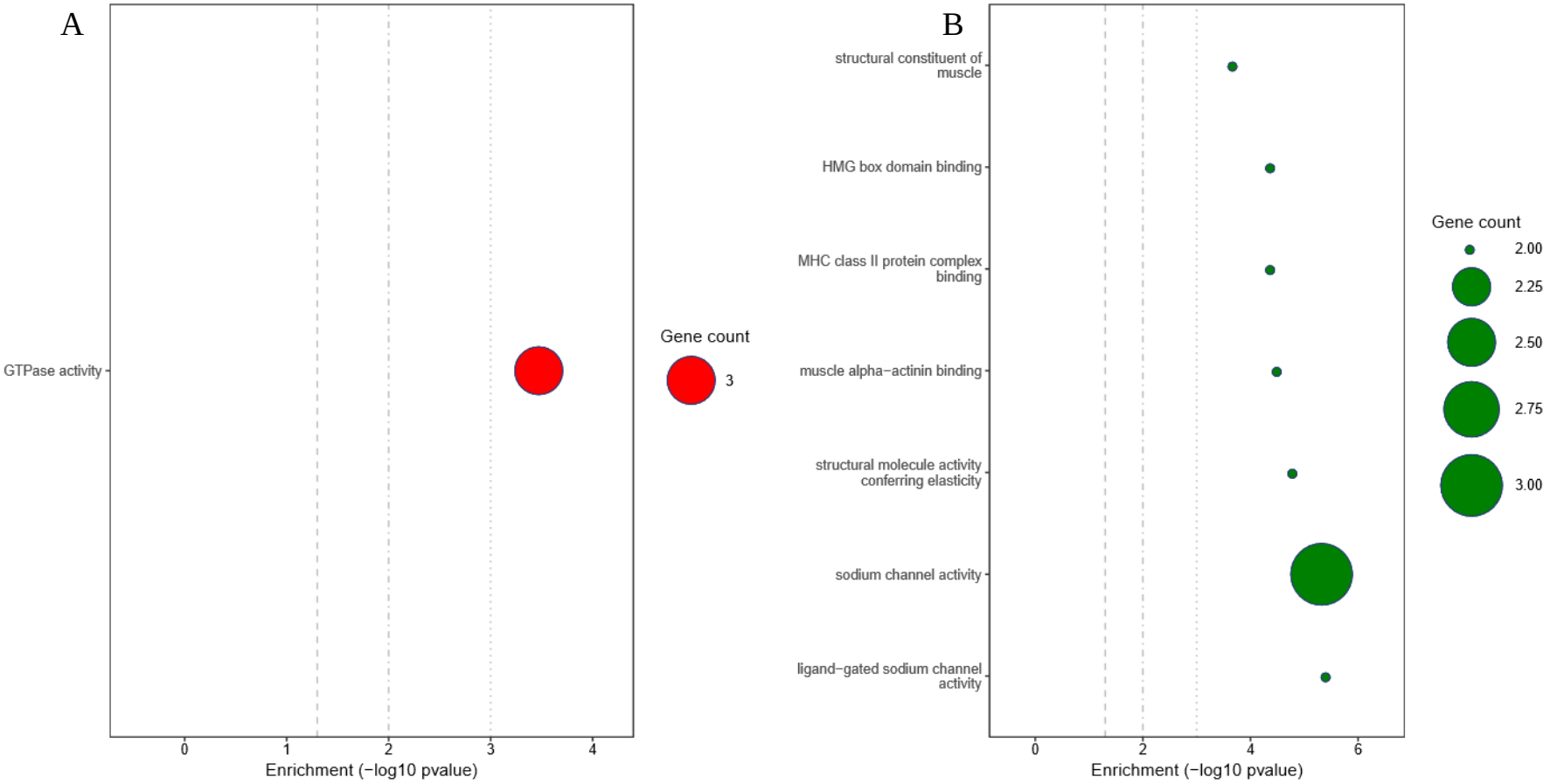


Figure 5-7: Enrichment of molecular function terms in genes identified as up and downregulated by SCB in the colon tissue of suckling pigs at 22 days of age. A, molecular function enrichment of genes upregulated by SCB supplementation. B, molecular function enrichment of genes downregulated by SCB supplementation. Top 10 most significantly enriched terms displayed where available. All terms shown contain equal to or greater than two differentially expressed genes and are significantly enriched ($q \leq 0.05$). Information on all significantly enriched terms including gene names and identifiers can be found in Appendix 16.

5.2.1.5.3 Differential Gene Expression Resulting from SCB Supplementation of Suckling Pigs at 25 and 35 Days of Age

At 25 days of age, six transcripts were significantly differentially expressed (Log2 FC ≥ 1 or ≤ -1, $q < 0.1$). One of the downregulated transcripts, ENSSSCT00000023884, is uncharacterised and has been retired in the most recent (Sus *scrofa* 11) gene set. Additionally, a novel transcript of an uncharacterised gene was upregulated, ENSSSCT00000023496, and a second upregulated transcript of C-type lectin domain containing 7A (*CLEC7A*) has been retired ENSSSCT00000033700. Of the three remaining transcripts, ubiquitin specific peptidase 3 (*USP3*) was downregulated by SCB supplementation, whereas fucosyltransferase 2 (*FUT2*) and dual specificity phosphatase 27 (*DUSP27*) were upregulated.

At 35 days of age, only two transcripts were differentially regulated between SCB and control cohorts, both of which were downregulated by SCB supplementation. These originated from porcine genes orthologous to nuclear receptor subfamily 1 group D member 2 (ENSSSCG00000027017) and calcitonin-related polypeptide alpha (ENSSSCG00000026512) in other speci

5.2.2 The Effect of Oral *Saccharomyces cerevisiae boulardii* Supplementation in the Colon of Weaned Pigs

To identify the transcriptional effect of *Saccharomyces cerevisiae boulardii* supplementation in the colon of weaned pigs, the expression pattern in the colon of weaned pigs with and without probiotic SCB supplementation was compared at one, four and 14 days post-weaning (22, 25 and 35 days of age).

5.2.2.1 Comparison of Global Expression Patterns of Colon Tissue Extracted from Weaned Pigs With and Without SCB Supplementation using Principal Component Analysis

Principal component analysis was performed on the TPM profiles of weaned pigs with and without SCB supplementation at each time point (Figure 5-8). This analysis showed that the colon TPM expression profiles for weaned pigs with and without SCB supplementation were similar at 22 days of age and 35 days of age (one and 14 days post weaning), with no distinct grouping of samples by treatment at these time points. However, at four days post weaning, some grouping of the two treatments is apparent (Figure 5-8B). Although 95% confidence

ellipses intersect, separate treatment groups are depicted with only sample 7046 of the control cohort located outside a tight group of the other three control samples. These findings suggest that there may be more profound transcriptional differences between treatments in animals of 25 days of age than the other time points.

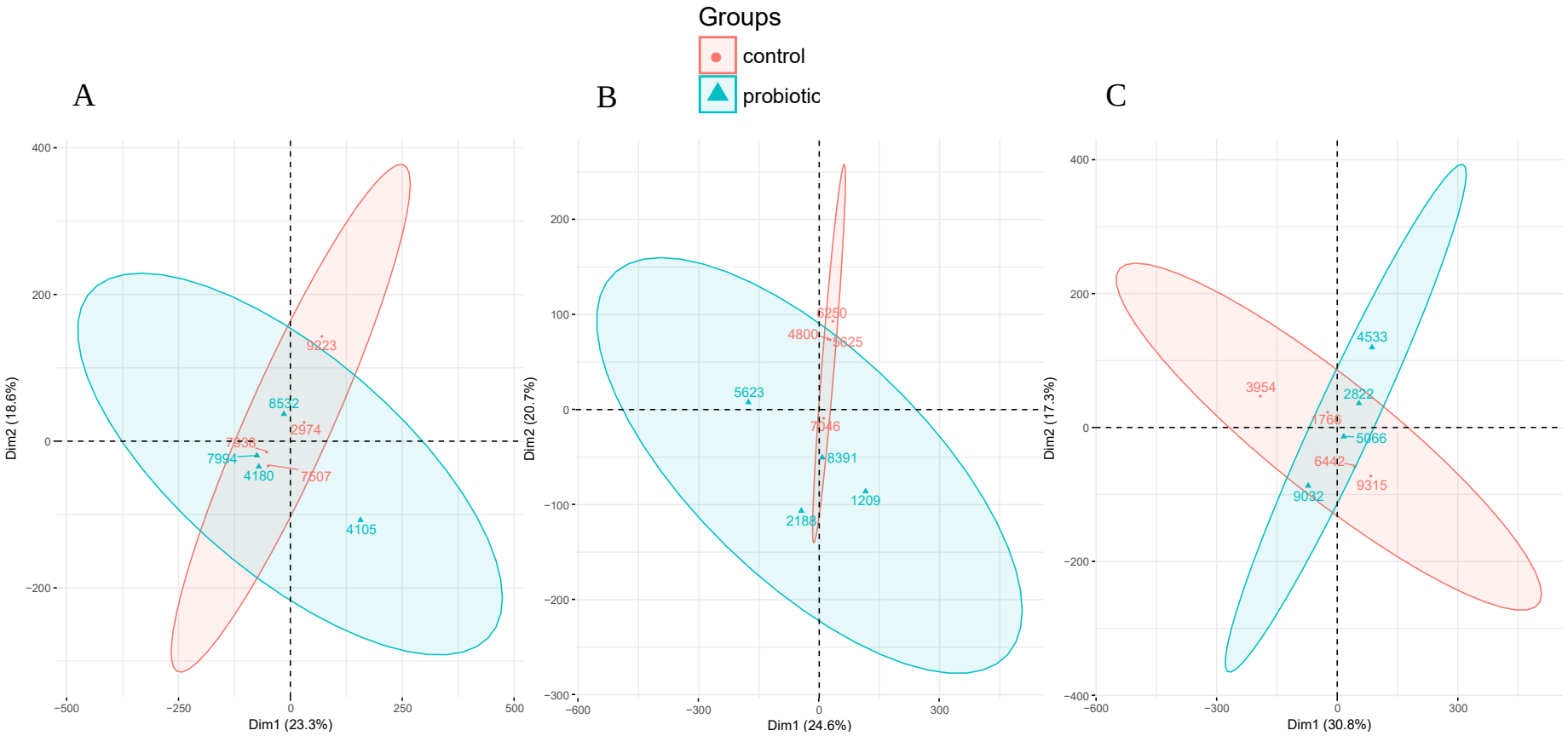


Figure 5-8: PCA to compare the global expression pattern of weaned pig colon samples with and without SCB supplementation at 22, 25 and 35 days of age. Plot A indicates 22 days of age, plot B indicates 25 days of age and plot C indicates 35 days of age. Samples from control pigs are indicated in red, the corresponding samples from SCB supplemented pigs are indicated in blue. Principal component analysis was applied to TPM information obtained from Kallisto mapping. X and Y axis show principal component 1 and principal component 2 respectively (percentage of variance indicated on each plot). Prediction ellipses are such that with probability 0.95, a new observation from the same group will fall inside the ellipse

5.2.2.2 Overview of Differential Transcript Expression Between Colon Tissue Extracted from Weaned Pigs With and Without SCB Supplementation

Volcano plots describing the relationship between beta, an estimator of $\log_2$ fold change, and $-\log_{10}$ *p*-value (Figure 5-9) reflect the relationships between expression patterns observed using principal component analysis (Figure 5-8). Only a single transcript was significantly differentially expressed between SCB supplemented and control cohorts at 22 and 35 days of age (additional files 7 & 9). However, in samples collected from animals of 25 days of age, 77 transcripts were significantly differentially expressed with a greater than two-fold change (additional file 8). Of these 77 transcripts, 38 were upregulated and 39 downregulated (Figure 5-10). No differentially expressed transcripts were shared between any two of the three ages.

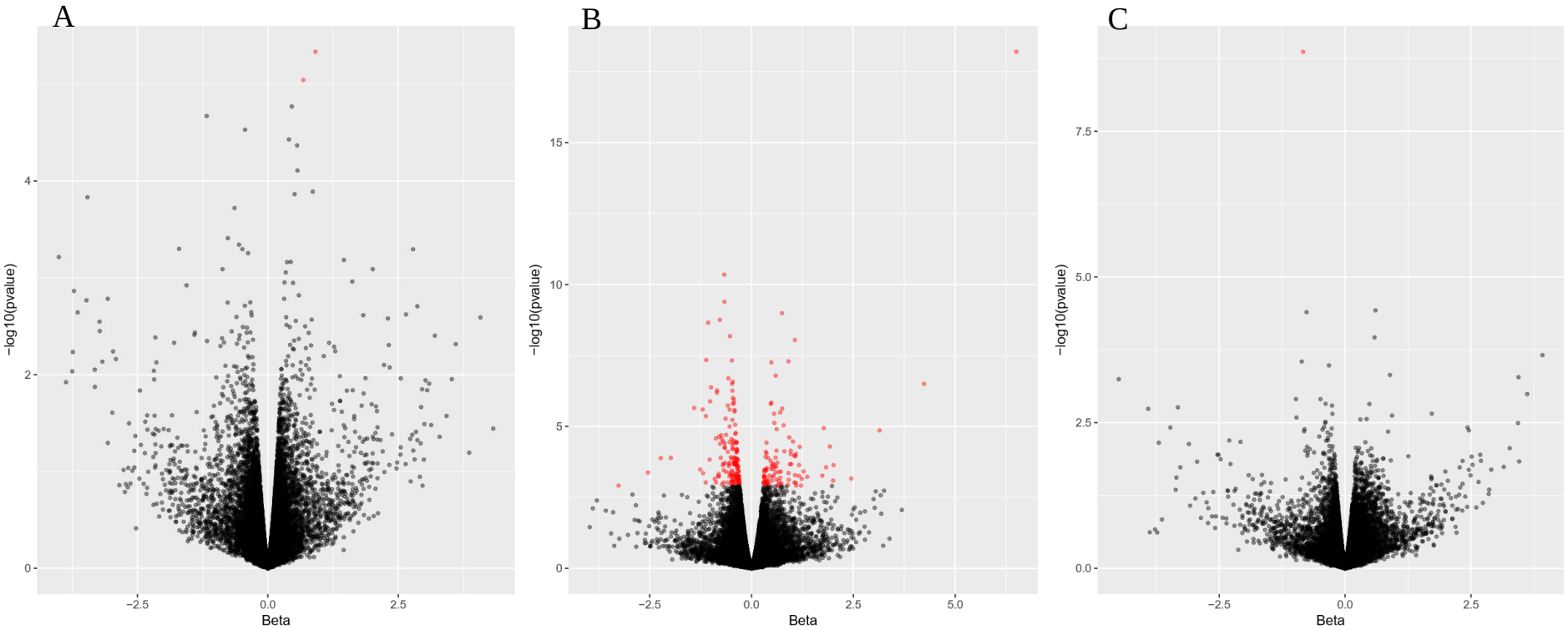


Figure 5-9: Volcano plots to show differential expression of transcripts in the colon of weaned pigs in response to SCB supplementation. -log10 *p*-value plotted against beta value. Beta value is an estimator of fold change used in the model applied by Sleuth. Transcripts with a Benjamini-Hochberg false detection rate corrected *p*-value <0.1 are indicated in red. A, differentially expressed transcripts at 22 days of age. B, differentially expressed transcripts at 25 days of age. C. differentially expressed transcripts at 35 days of age.

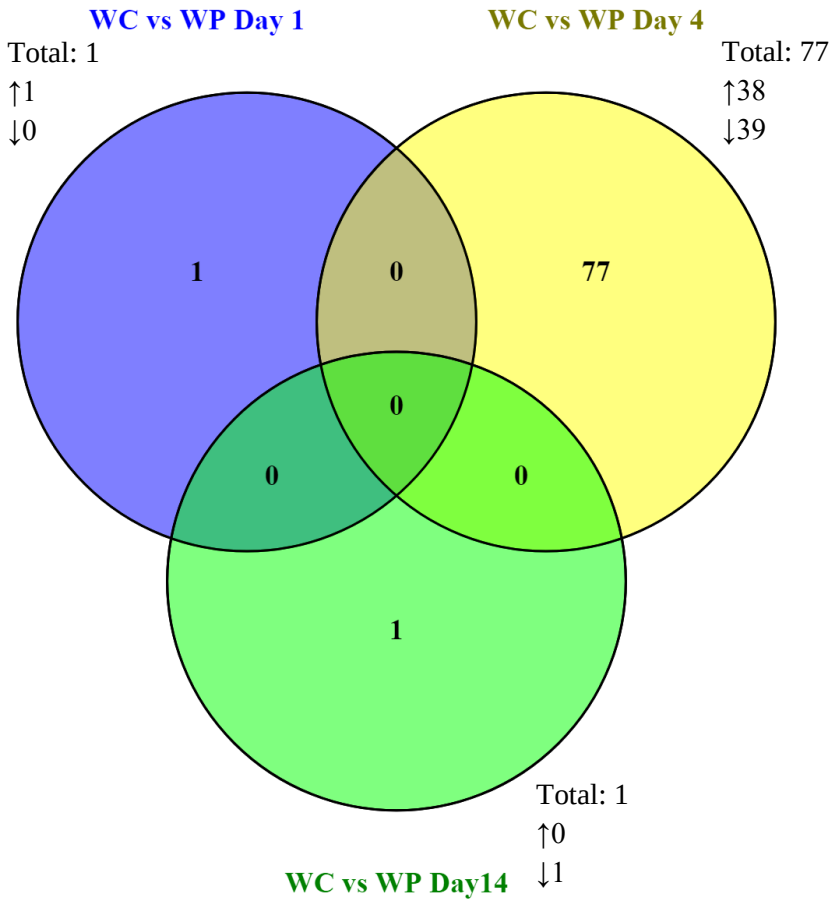


Figure 5-10:Venn diagram to demonstrate differential expression observed between suckling pigs with and without SCB supplementation at 22, 25 and 35 days of age. WC vs WP, Weaned control vs Weaned + Probiotic (SCB). Day one, 22 days of age (one-day post-weaning). Day four, 25 days of age (four days post-weaning). Day 14, 35 days of age (14 days post-weaning). Total transcripts, up (↑) and down (↓) regulated transcripts are indicated. All transcripts Log2 FC ≥ 1 or ≤ -1, $q < 0.1$.

5.2.2.3 Sample-to-Sample Variation in Expression Values for Differentially Expressed Transcripts

To visualise the sample to sample variation in TPM expression values for differentially expressed transcripts, a heatmap was constructed to show these values. This was only applied to differentially expressed transcripts identified in animals of 25 days of age, as only a single differentially expressed transcript was identified in animals of 22 and 35 days of age. The resulting heatmap clustered samples by treatment and transcripts by up and down regulation as only transcripts which distinguished the treatments were plotted (Figure 5-11). The scaled expression values reflected the differences seen when comparing the global TPM profile using principal component analysis in that sample 7046 was the most unlike the other three control samples, particularly amongst transcripts otherwise highly expressed in this cohort. The same observation can be made with sample 5623 of the SCB supplemented cohort.

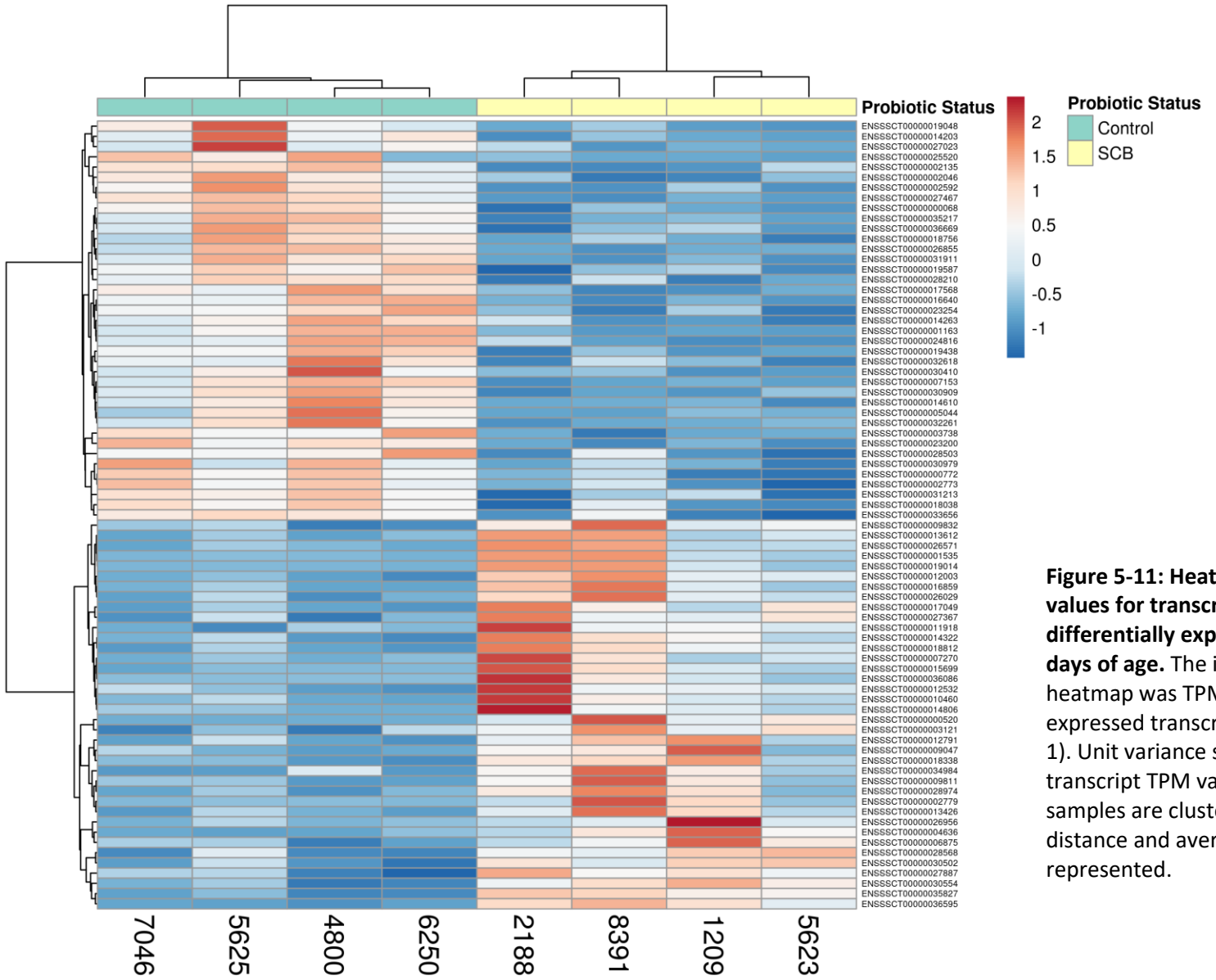


Figure 5-11: Heatmap to show TPM expression values for transcripts identified as differentially expressed in weaned pigs of 25 days of age. The input to construct this heatmap was TPM values for differentially expressed transcripts (q <0.1, Log2 FC ≥ 1 or ≤ -1). Unit variance scaling was applied to transcript TPM values. Both transcripts and samples are clustered using correlation distance and average linkage. 77 transcripts are represented.

5.2.2.4 GO Analysis of Transcripts Differentially Expressed in the Colon of Weaned Pigs at 25 Days of Age in Response to SCB Supplementation

GO analysis was conducted separately on up and downregulated transcripts using the Ensembl gene IDs associated with the transcript. Ontologies were considered significantly enriched by two or greater genes and $q < 0.05$.

5.2.2.4.1 Biological Process Enrichment

Biological process enrichment of genes upregulated by SCB in weaned pigs of 25 days of age identified 24 significantly enriched biological process terms (Figure 5-12A). However, seven of these terms were enriched by the same two genes. *Cellular response to tumour necrosis factor* (2/66 genes); *cellular response to interleukin-1* (2/38 genes); *neutrophil chemotaxis* (2/32 genes)*; cellular response to interferon-gamma* (2/27 genes); *monocyte chemotaxis* (2/20 genes); *lymphocyte chemotaxis* (2/15 genes) and *myeloid dendritic cell chemotaxis* (2/3 genes) were all enriched by the upregulation of C-C motif chemokine 22 (*CCL22*) and C-C motif ligand 19 (*CCL19*). Additionally, *positive*

regulation of ERK1 and ERK2 cascade (3/125 genes) is enriched by these two genes as well as chitinase-3-like protein 1 (*CHI3L1*).

Upregulation of interleukin 10 (*IL10*) contributed to the enrichment of eight biological process terms including *negative regulation of inflammatory response* (2/61 genes) was enriched by *IL10.* In addition to TNF alpha-induced protein 8 like 2 (*TNFAIP8L2*); *negative regulation of endothelial cell apoptotic process* (2/22 genes) was enriched by IL10 in addition to serine peptidase inhibitor E1 (*SERPINE1*) and *cellular response to lipopolysaccharide* (3/73 genes) was enriched by *IL10, SERPINE1* and cluster of differentiation 14 (*CD14*).

Upregulation of *CCL19*, *CCL22* and *IL10* was central to the most significantly enriched terms: *inflammatory response (7/147 genes)* and *immune response* (7/192 genes). *Inflammatory response* was enriched by these three genes as well as: alveolar macrophage-derived chemotactic factor-II (*AMCF-II*); cluster of differentiation 14 (*CD14*); chitinase-3-like protein 1 (*CHI3L1*) and C-C chemokine receptor type 7 (*CCR7*). The immune response was enriched by a similar subset of genes. However, *CD14* and *CHI3L1* were exchanged for lymphotoxin beta (*LBT*) and tumour necrosis factor ligand superfamily member 13B (*TNFSF13B*).

Upregulation of *SERPINE1* in addition to tissue inhibitor of metalloproteinases 1 (*TIMP1*) contributed to the enrichment of the terms *negative regulation of endopeptidase activity* (3/80) and re*gulation of receptor activity* (6/256 genes). An exhaustive list of biological process GO terms enriched amongst genes upregulated by SCB supplementation in the weaned pigs can be found in Appendix 17.

Only two biological process GO terms were significantly enriched amongst genes downregulated by SCB supplementation in the weaned pig of 25 days of age (Figure 5-12B). o*ne-carbon metabolic process* (2/22 genes) was enriched as carbonic anhydrase 12 (*CA12*), and adenosylhomocysteinase like 2 (*AHCYL2*) were downregulated. The second term, *cytoskeleton organization* (3/84 genes) was enriched by cyclase-associated actin cytoskeleton regulatory protein 2 (*CAP2*); spectrin repeat containing nuclear envelope family member 3 (*SYNE3*) and tubulin alpha like 3 (*TUBAL3*). Further information concerning gene ontologies enriched by genes downregulated by SCB supplementation in weaned pigs of 25 days of age can be found in Appendix 17.

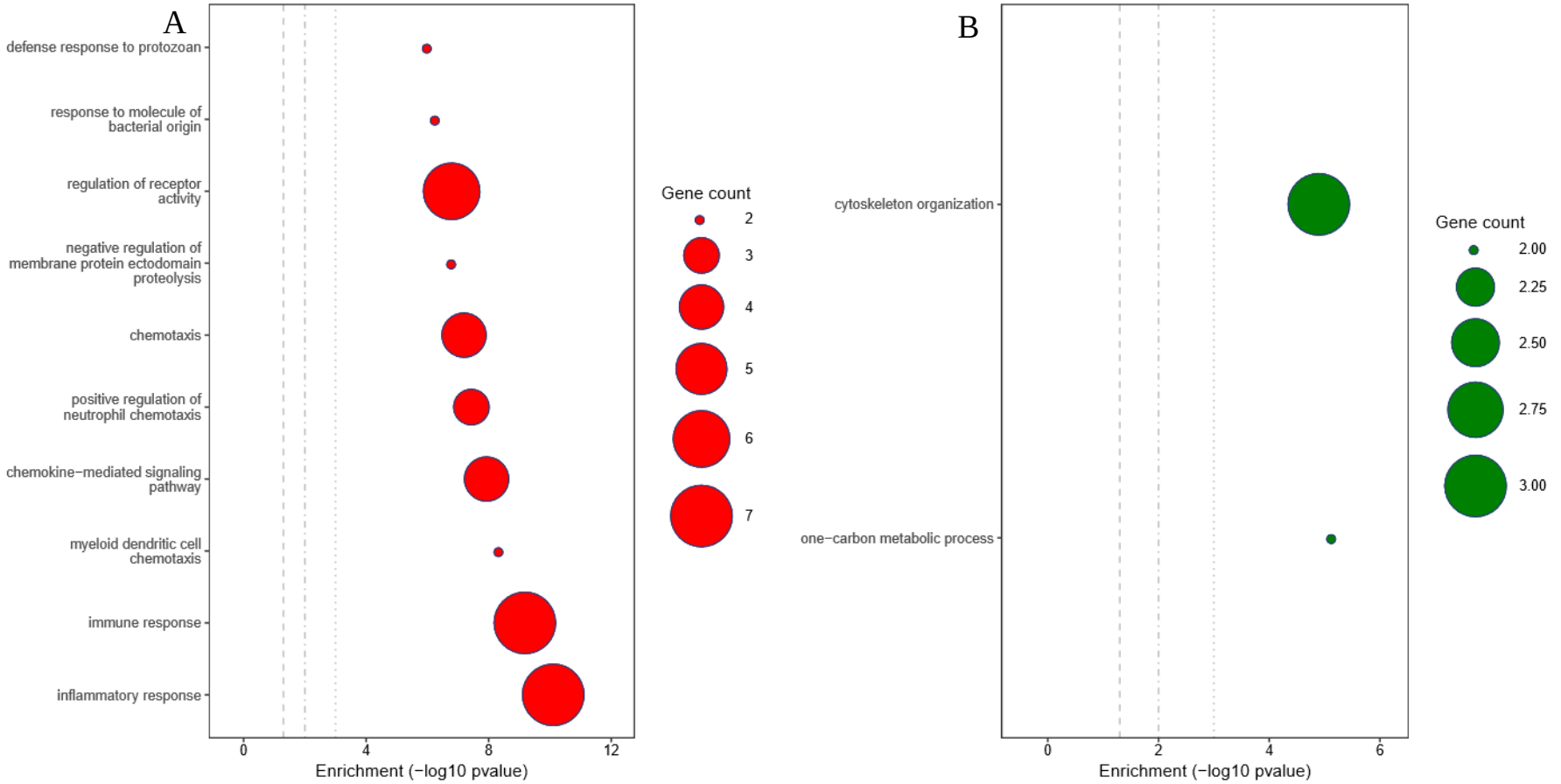


Figure 5-12: Enrichment of biological process terms in genes identified as up and downregulated by SCB in the colon tissue of weaned pigs at 25 days of age. A, biological process enrichment of genes upregulated by SCB supplementation. B, biological process enrichment of genes downregulated by SCB supplementation. Top 10 most significantly enriched terms displayed where available. All terms shown contain equal to or greater than two differentially expressed genes and are significantly enriched ($q \leq 0.05$). Information on all significantly enriched terms including gene names and identifiers can be found in Appendix 17.

5.2.2.4.2 Cellular Component Enrichment

Cellular component GO enrichment identified four cellular component terms which were significantly enriched amongst genes upregulated by SCB supplementation of weaned animals of 35 days of age (Figure 5-13). These were: *extracellular space* (10/966 genes); *extracellular region* (8/670 genes); *cell periphery* (2/54 genes) and *external side of plasma membrane* (3/155 genes).

Extracellular space was enriched by the upregulation of lymphotoxin beta (*LBT*); C-C motif chemokine 22 (*CCL22*); arginase 1 (*ARG1*); alveolar macrophage-derived chemotactic factor-II (*AMCF-II*); C-C motif ligand 19 (*CCL19*); tissue inhibitor of metalloproteinases 1 (*TIMP1*); cluster of differentiation 14 (*CD14*); chitinase-3-like protein 1 (*CHI3L1*); interleukin 10 (*IL10*) and serine peptidase inhibitor E1 (*SERPINE1*).

Extracellular region was enriched by interleukin 22 (*IL22*); C-C motif chemokine 22 (*CCL22*); alveolar macrophage-derived chemotactic factor-II (AMCF-II); C-C motif ligand 19 (*CCL19*); procollagen C-endopeptidase enhancer 2 (*PCOLCE2*); tissue inhibitor of metalloproteinases 1 (*TIMP1*); interleukin 10 (*IL10*) and serine peptidase inhibitor E1 (*SERPINE1*).

Cell periphery was enriched by adhesion G protein-coupled receptor E1 (*ADGRE1*) and solute carrier family 1 member 3 (*SLC1A3*). Finally, *external side of plasma membrane* was enriched by: adhesion G protein-coupled receptor E1 (*ADGRE1*); cluster of differentiation 14 (*CD14*) and C-C chemokine receptor type 7 (*CCR7*). No cellular component GO terms were significantly enriched amongst genes downregulated by SCB supplementation. A full list of significantly enriched gene ontologies, including gene identifiers, can be found in Appendix 18.

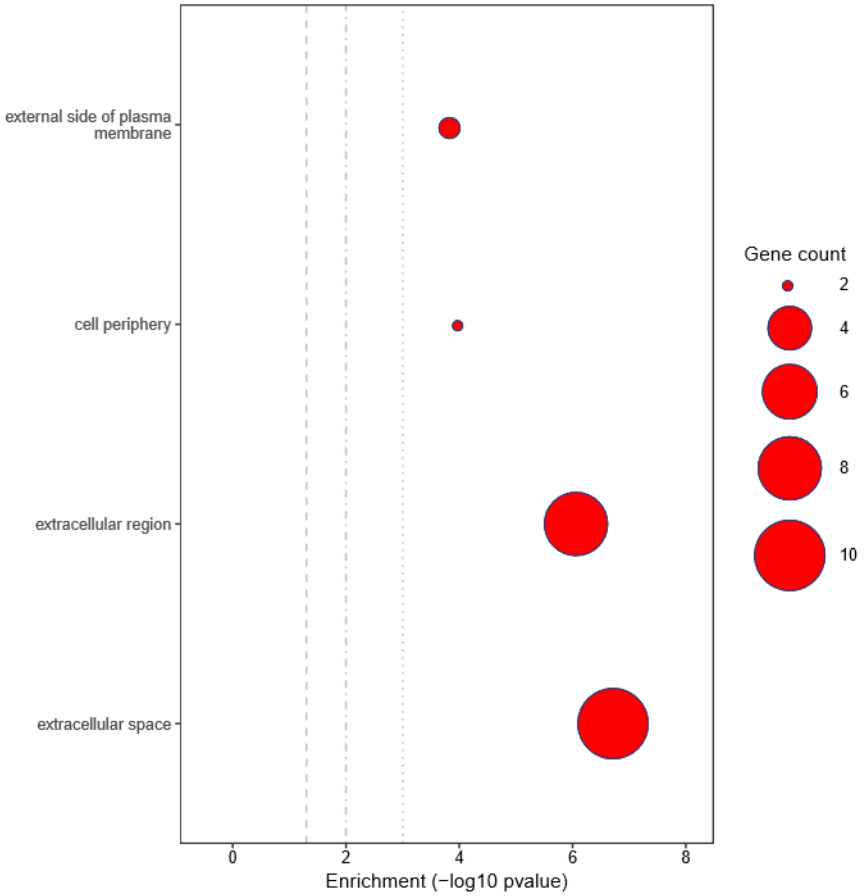


Figure 5-13: Enrichment of cellular component terms in genes identified as up and downregulated by SCB in the colon tissue of weaned pigs at 25 days of age. Cellular component enrichment of genes upregulated by SCB supplementation. No terms were significantly enriched amongst downregulated genes. All four significantly enriched terms displayed. All terms shown contain equal to or greater than two differentially expressed genes and are significantly enriched (q ≤0.05). Information on all significantly enriched terms including gene names and identifiers can be found in Appendix 18.

5.2.2.4.3 Molecular Function Enrichment

Five molecular function GO were significantly enriched amongst upregulated genes: *cytokine activity* (6/ 141 genes); *chemokine activity* (3/31 genes); *CRR chemokine receptor binding* (2/12 genes); *tumour necrosis factor receptor binding* (2/23 genes) and *serine-type endopeptidase inhibitor activity* (2/63 genes) (Figure 5-14A).

Cytokine activity was enriched by lymphotoxin beta (*LBT*); C-C motif chemokine 22 (*CCL22*); alveolar macrophage-derived chemotactic factor-II (*AMCF-II*); C-C motif ligand 19 (*CCL19*); tissue inhibitor of metalloproteinases 1 (*TIMP1*) and interleukin 10 (*IL10*). *Chemokine activity* and *CCR chemokine receptor binding* were both enriched by C-C motif chemokine 22 (*CCL22*) and C-C motif ligand 19 (*CCL19*), with the former also enriched by *AMCF-II*. Tumour necrosis factor receptor binding was enriched by *LBT* and tumour necrosis factor ligand superfamily member 13B (*TNFSF13B*). Finally*, serine-type endopeptidase inhibitor activity* was enriched by inter-alpha-trypsin inhibitor heavy chain 3 (*ITIH3*) and serine peptidase inhibitor E1 (*SERPINE1*). A table containing additional information can be found in Appendix 19.

Two molecular function GO terms were significantly enriched amongst gene downregulated by SCB supplementation of 25-day old weaned pigs (Figure 5-14B). These were: *cation channel activity* (2/20) and *ion channel binding* (2/71).

Cation channel activity was enriched by the downregulation of transient receptor potential cation channel, subfamily V, member 3 (*TRPV3*) and glutamate ionotropic receptor NMDA type subunit 2C (*GRIN2C*). *Ion channel binding* was enriched by ring finger protein 207 (*RNF207*) and a novel gene orthologous to ankyrin 3 (*ANK3*) in other species (ENSSSCG0000001021

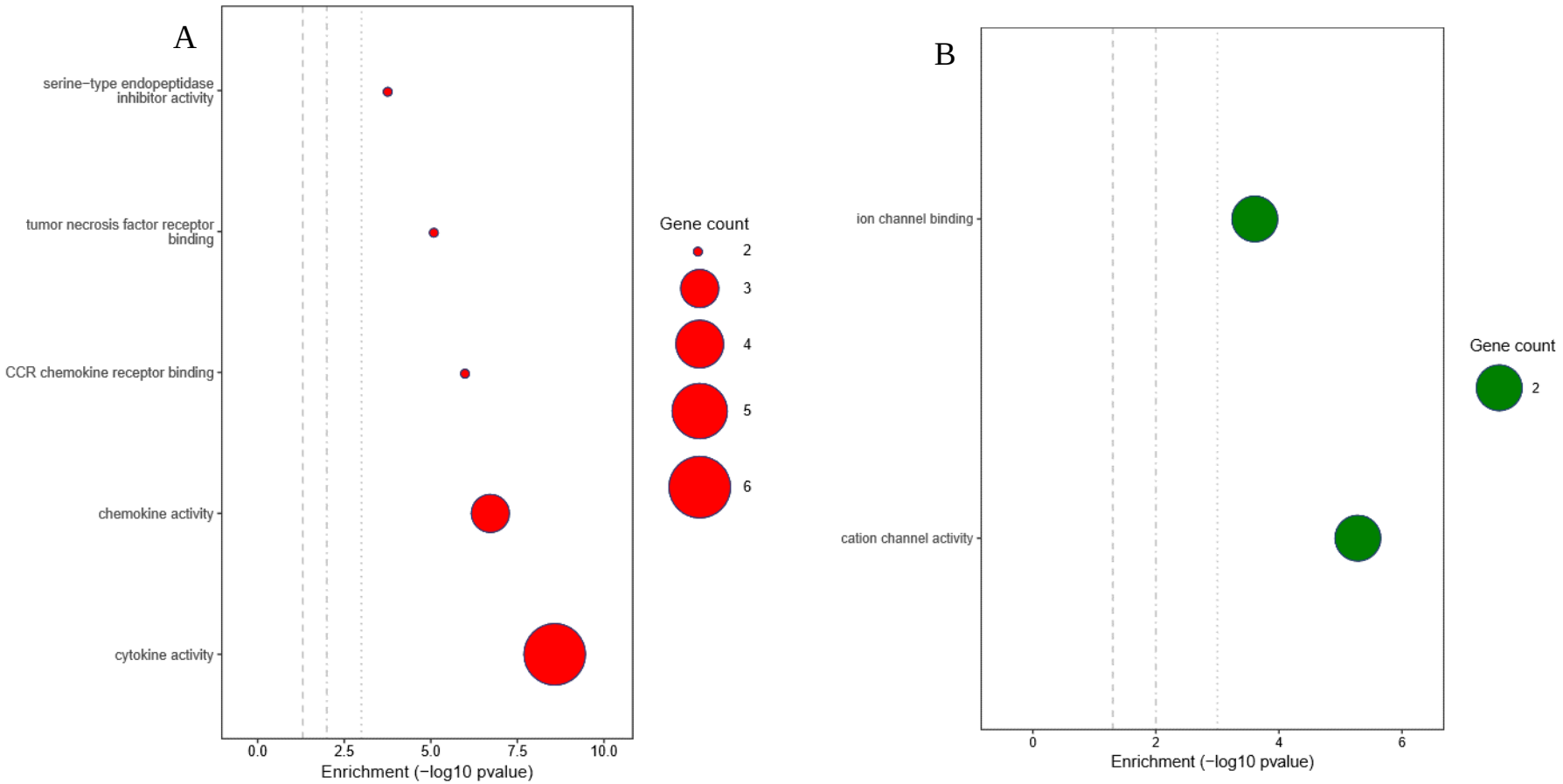


Figure 5-14: Enrichment of molecular function terms in genes identified as up and downregulated by SCB in the colon tissue of weaned pigs at 25 days of age. A, molecular function enrichment of genes upregulated by SCB supplementation. B, molecular function enrichment of genes downregulated by SCB supplementation. Top 10 most significantly enriched terms displayed where available. All terms shown contain equal to or greater than two differentially expressed genes and are significantly enriched ($q \leq 0.05$). Information on all significantly enriched terms including gene names and identifiers can be found in Appendix 19.

5.2.2.5 Differential Gene Expression Resulting from SCB Supplementation of Weaned Pigs at 22 and 35 Days of Age

A single transcript was identified as significantly (with a greater than two-fold change) differentially expressed between weaned pigs with and without SCB supplementation of both 22 and 35 days of age. At 22 days of age, the single upregulated transcript was ENSSSCT00000027647, a retired transcript of secreted frizzled-related protein 1 (*SFRP1*). In 35-day old pigs, the single downregulated transcript encoded complement factor properdin (*CFP*)

5.3 Discussion

The transcriptional effect of *Saccharomyces cerevisiae boulardii* (SCB) in the porcine colon was observed to have a different pattern in weaned and suckling animals. In suckling animals, most differential gene expression was observed in animals 22 days old, whereas few differences were identified in animals of 25 and 35 days of age. In weaned animals, SCB supplementation had the biggest transcriptional effect in 25-day old animals. The later effect of SCB in weaned animals may be representative of a varied immediate transcriptional response in the colon one day after weaning, confounding statistical identification of SCB related transcriptional changes. In both weaned and suckling animals, extremely few significantly differentially expressed transcripts were identified in animals of 35 days of age, suggesting that the effect of SCB is concluded by this point. This could be due to the natural maturation of the intestine by this age (Moeser *et al.*, 2017).

5.3.1 The Effect of *Saccharomyces cerevisiae boulardii* in Suckling Pigs

In 22-day old suckling pigs, 197 transcripts were identified as significantly differentially expressed by SCB supplementation. GO

analysis identified several immune-related biological processes which were affected by SCB supplementation. Enrichment of those which were positively affected by SCB was dominated by interleukin 8 (*CXCL8*) and lipopolysaccharide binding protein (*LBP*).

The increased expression of *CXCL8* by SCB contrasts with published studies where live SCB reduced enterotoxigenic *E. coli* induced mRNA expression in IP1-2I cell culture to baseline levels (Zanello *et al.*, 2011; Badia *et al.*, 2012). However, *CXCL8* mRNA levels were upregulated in the presence of killed yeast, an effect the authors attribute to a reaction to yeast wall structures such as β-glucans (Sonck *et al.*, 2010; Zanello *et al.*, 2011). Interleukin 8 is produced by macrophages, endothelial cells and a variety of other cell types, and is a potent inflammatory agent and chemoattractant for neutrophils (Singer and Sansonetti, 2004; Nanduri *et al.*, 2013). LBP plays a key role in the innate immune response to bacterial challenge, however, does not interact with β-glucan or yeast (Koizumi *et al.*, 1997; Ding and Jin, 2014). Bacterial interaction is further suggested by increased expression of complement 9 (*C9*), a member of the complement membrane attack complex (Khoa and Wimmers, 2015).

Although some of the expression information suggests bacterial interaction, the presence of β- glucans and other yeast cell wall components have been demonstrated to stimulate non-specific immune responses (Sonck *et al.*, 2010). It is important to note that the immune system of pigs during this period is under development (Sinkora *et al.*, 2002). This may lead to immune activation associated with the establishment of immune tolerance to environmental bacteria and antigens (Stokes, 2017). A response which may be exacerbated by the adjuvant effect of SCB cell wall components (Adachi *et al.*, 1994; Mucksova *et al.*, 2001; Sonck *et al.*, 2010).

GO enrichment of genes downregulated by SCB in 22-day old suckling pigs identified downregulation of genes associated with B cell receptor signalling and leukocyte chemotaxis. *CD19,* one of the downregulated genes contributing to this enrichment, is a B cell biomarker which plays roles in the antigen-independent development as well as immunoglobulin-induced activation of B cells (Wang *et al.*, 2012). CD19 plays a critical role in maintaining the balance between antigen-induced response and tolerance induction (Wang *et al.*, 2012). Downregulation was also observed in C-X-C chemokine receptor type 5 (*CXCR5*), expression of this chemokine receptor is needed for B cell migration

into lymphoid follicles (Pevzner *et al.*, 1999). *CD44,* another downregulated gene is a ubiquitously expressed cell surface protein primarily involved in aggregation, migration and activation of cells (Senbanjo and Chellaiah, 2017). Taken together, the downregulation of these genes suggests that SCB supplementation of suckling pigs alters B-cell trafficking and recruitment.

Cellular compartment (localisation) GO enrichment of differentially expressed genes identified a significant enrichment of terms associated with the cell membrane amongst those downregulated by SCB supplementation, suggesting that SCB supplementation in suckling pigs influences the cell membrane in colon tissue.

Molecular function gene ontology enrichment highlighted genes associated with sodium channel activity as negatively affected by SCB supplementation. The same effect is observed in the weaning comparison described in Chapter 5. Indeed, the same genes are identified as downregulated (*ASIC3, SCNN1B* & *SCN4A*). This suggests that expression of these genes was high in the 22-day old suckling control cohort compared to both weaned control and SCB supplemented suckling animals, although the cause of this increased expression is unclear.

As so few differentially expressed transcripts were detected between suckling pigs with and without SCB supplementation at 25 and 35 days of age, no biologically relevant conclusions can be drawn from these comparisons.

5.3.2 The Effect of *Saccharomyces cerevisiae boulardii* in Weaned Pigs

In contrast to the effect of SCB in suckling pigs, the greatest number of transcriptional differences were identified in 25-day old weaned pigs. Biological process GO analysis of genes upregulated by SCB was dominated by a small number of genes which enriched a range of immune and cytokine-related terms. These genes included: Interleukin 10 (*IL10*); C-C motif ligand 19 (*CCL19*); C-C motif ligand 22 (*CCL22*); Tissue inhibitor of metalloprotease 1 (*TIMP1*) and Serine peptidase inhibitor E1 (*SERPINE1*). As such, this part of the discussion will focus on this subset of genes.

Interleukin 10 is a regulatory cytokine which inhibits both antigen presentation and subsequent pro-inflammatory cytokine release (Li and He, 2004). Because of this activity, localised and systemic administration of IL-10 has been studied as a treatment for inflammatory diseases (Bickston and Cominelli, 2000), although large

systemic doses of IL-10 may be detrimental rather than helpful (Herfarth and Scholmerich, 2002). SCB has previously been noted to induce *IL-10* mRNA expression in mouse model of DSS induced IBD which inhibits intestinal injury (Yanaba *et al.*, 2011; Jawhara *et al.*, 2012). This suggests that the increased expression of *IL10* in weaned animals supplemented with SCB may provide some protection against weaning related bowel dysfunction.

C-C motif ligand 19 (CCL19) is an essential molecule for facilitating the trafficking of mature dendritic cells (Yan *et al.*, 2016). CCL19 is commonly referred to as a homeostatic chemokine as it is constitutively expressed in secondary lymphoid tissue and regulates the homing of lymphocytes and dendritic cells through its receptor CCR7 which is also upregulated (Forster *et al.*, 2008). However, studies suggest that CCL19 may also promote inflammatory responses (Noor and Wilson, 2012; Astrup *et al.*, 2014). C-C motif ligand 22 (CCL22) is a macrophage-derived chemokine which is constitutively produced by human colonic epithelial cell lines. However, expression is upregulated in response to proinflammatory cytokines or infection with enteroinvasive bacteria (Berin *et al.*, 2001). The increased expression of these chemokines in the colon of 25 day old weaned pigs supplemented with SCB

demonstrates that the effect of SCB is not purely anti-inflammatory. However, reduced *CCL22* expression has been noted in autoimmunity, leading to a reduction in the infiltration of regulatory T cells which keep auto-reactive T-cells in check (Bischoff *et al.*, 2015; Elhussein Mohamed *et al.*, 2016). Therefore, Increased expression of *CCL22* in the SCB cohort may dampen weaning related immune activation by recruitment of regulatory T cells (Bailey *et al.*, 2005).

Increased expression of protease inhibitors *TIMP1* and *SERPINE1* (also known as PAI-1) suggests an inhibition of protease activity in the colon of SCB treated weaned animals. *SERPINE1* inhibits the activation of metalloproteinases via inhibition of plasmin production from plasminogen. Metalloproteinases degrade extracellular matrix proteins, which modulate cellular adhesion and migration (Barbareschi *et al.*, 1995; Bajou *et al.*, 2002; Mutoh *et al.*, 2008). TIMP1 can inhibit all matrix metalloproteinases (McKaig *et al.*, 2003). Increased expression has been noted in the inflamed colon mucosa of human IBD patients where it has been associated with the presence of fibrotic structures (von Lampe *et al.*, 2000; McKaig *et al.*, 2003; Kapsoritakis *et al.*, 2008). Increased expression of these protease inhibitors in the context of weaning may lead to the reduced breakdown of extracellular matrix

proteins in the colon of SCB supplemented individuals. This may reduce weaning related increases in intestinal permeability and weaning related histological changes caused by increased extracellular matrix breakdown (McCracken *et al.*, 1999).

Cellular compartment GO analysis points to SCB upregulation of genes associated with the extracellular space and cell membrane, which follows as the products of the genes mentioned have actions on the extracellular space. Molecular function analysis reinforced the finding of upregulated cytokine and chemokine activity.

GO enrichment of genes downregulated by SCB supplementation highlighted *one-carbon metabolic process* and *cytoskeleton organisation* as the only significantly enriched biological processes. However, the biological implication of upregulation in these genes is unclear.

5.4 Conclusion

The effect of probiotic *Saccharomyces cerevisiae boulardii* supplementation from 7 days of age in suckling animals, in the time series of 22, 25 and 35 old animals presented here, is most pronounced

in 22-day old animals. This contrasts with weaned animals where transcriptional differences are most pronounced in 25-day old animals. This may represent the chaotic nature of gene expression one day after weaning, obscuring differential expression which could be attributed to SCB supplementation.

Differential gene expression in suckling animals pointed to alterations in B-cell trafficking and chemotaxis resulting from SCB supplementation. In weaned pigs differentially expressed genes suggested an anti-inflammatory effect of SCB, with increased expression of *IL-10* as well as increased expression of chemokines associated with the recruitment of regulatory T cells (CCL22) and dendritic cells (CCL19).

These findings indicate that the transcriptional effect of SCB in weaned and suckling pigs is distinct.

6 Chapter 7: The Effect of Dietary *Saccharomyces cerevisiae boulardii* on Weaning Induced Transcription in the Porcine Colon

6.1 Introduction

This final results chapter will aim to identify any modulation of the transcriptional effect of weaning in the colon. To achieve this, transcripts differentially expressed between control suckling and SCB supplemented weaned animals will be identified. The results of this comparison will then be compared to the profile of differentially expressed transcripts identified when comparing suckling control and weaned control animals. This will provide a comparative model of the differences in colon transcription during weaning with and without SCB supplementation of the weaned animals.

Finally, the differential expression which can be attributed to oral SCB supplementation will be compared to differential expression identified in the previous chapter to identify any universal transcriptional effect of SCB supplementation. As with previous chapters, comparisons will be

conducted on samples collected from 22, 25 and 35-day old animals (one, four and 14 days post weaning).

6.2 Results

6.2.1 Comparison of Global Gene Expression in Suckling Control and SCB Supplemented Weaned Colon Samples

Comparison of the TPM profiles of suckling control samples and SCB supplemented weaned samples by principal component analysis identified a separation based on the treatment of 22-day old animals (one-day post weaning). At this time point, only a small intersection of 95% confidence ellipses was observed, demonstrating that the transcriptional profile of the colon of suckling control and SCB supplemented weaned animals are distinct at one-day post weaning (Figure 6-1A). In samples collected from 25-day old animals, four days post-weaning, although some grouping is apparent the confidence ellipses for the two cohorts overlap almost completely (Figure 6-1B). The comparison at 35 days of age, 14 days post weaning, showed no grouping of samples by treatment, with samples from the two treatments interspersed and confidence ellipses overlapping entirely (Figure 6-1C).

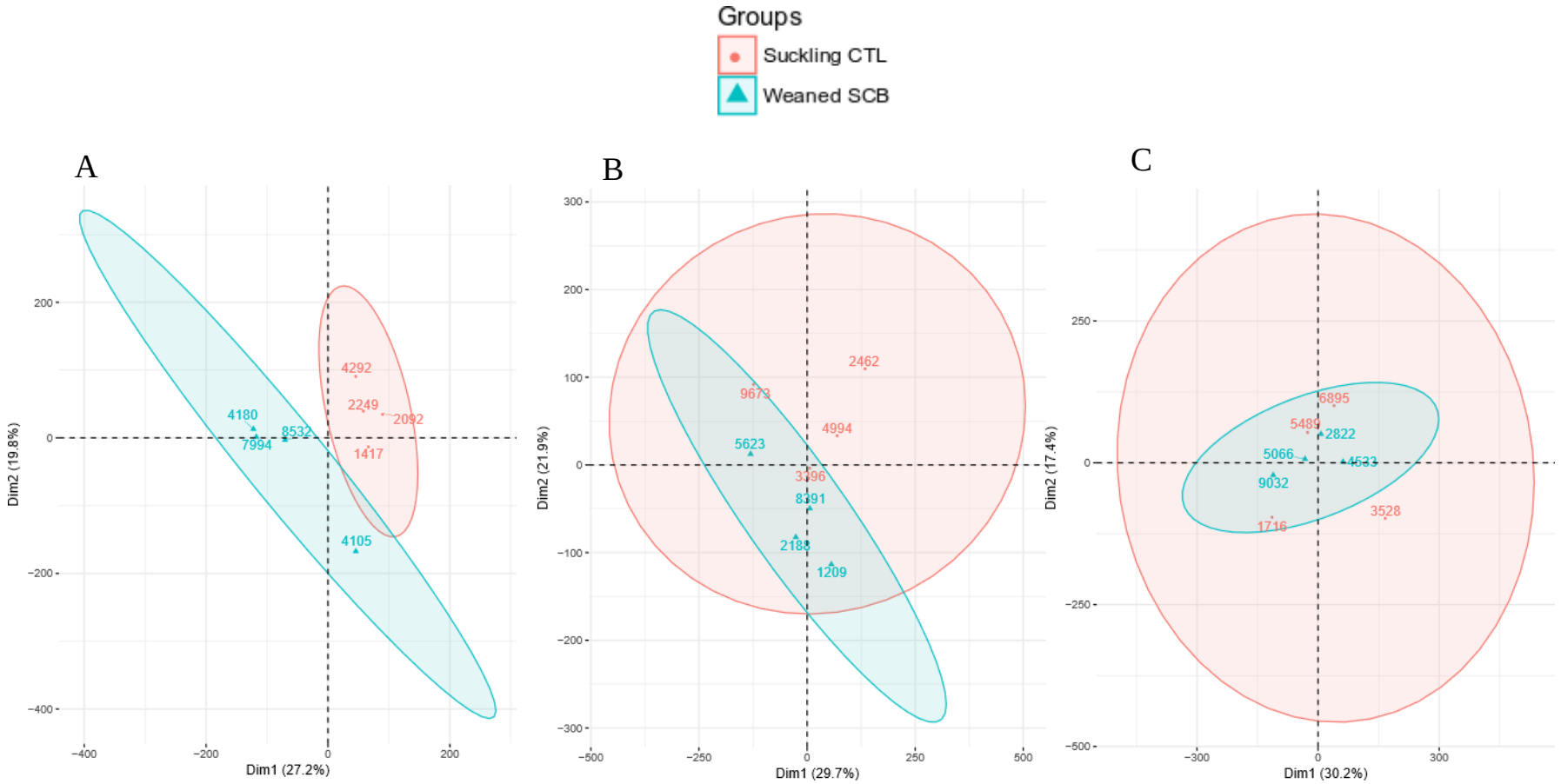


Figure 6-1: PCA to compare the global expression pattern of suckling pig colon samples with and without SCB supplementation at 22, 25 and 35 days of age. Plot A indicates 22 days of age, plot B indicates 25 days of age and plot C indicates 35 days of age. Samples from suckling control pigs are indicated in red, the corresponding samples from SCB supplemented weaned pigs are indicated in blue. Principal component analysis was applied to TPM information obtained from Kallisto mapping. X and Y axis show principal component 1 and principal component 2 respectively (percentage of variance indicated on each plot). Prediction ellipses are such that with probability 0.95, a new observation from the same group will fall inside the ellipse

6.2.2 Overview of Differential Transcript Expression Between Colon Tissue Extracted from Suckling Control and SCB Supplemented Weaned Pigs.

The pattern of differential expression between suckling control and SCB supplemented weaned animals over the three time points, was found to be similar to that found when comparing suckling control to weaned control (Figure 6-2). The greatest number of differentially expressed transcripts was identified between 22-day old animals, with a total of 341 transcripts identified (95 upregulated and 246 downregulated, see additional file 10). A reduced but substantial number of differentially expressed transcripts were identified in 25-day old animals, with 127 significantly differentially expressed, of which 43 were upregulated and 84 downregulated in the SCB supplemented weaned cohort (Additional file 11). As seen in all other comparisons, the fewest significantly differentially expressed transcripts were identified at the final comparison in samples collected from 35-day old animals. In this instance, seven transcripts were differentially expressed (Additional file 12), with four upregulated and three downregulated in the SCB supplemented weaned cohort (Figure 6-3). Eleven differentially expressed transcripts were shared between the comparisons of 22 and

25-day old animals, this was the only crossover observed between comparisons (Additional file 12).

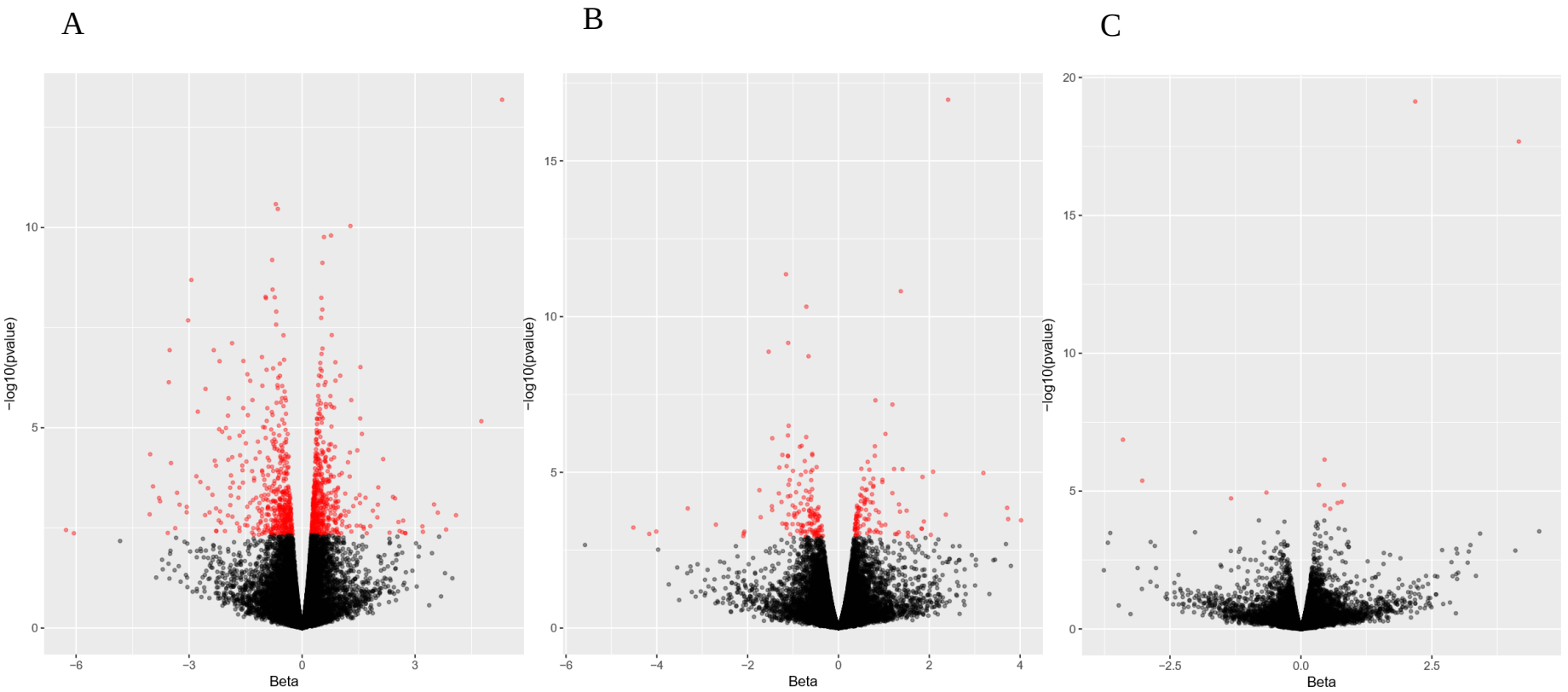


Figure 6-2: Volcano plots to show differential expression of transcripts in the colon of suckling pigs in response to SCB supplementation. -log10 *p*-value plotted against beta value. Beta value is an estimator of fold change used in the model applied by Sleuth. Transcripts with a Benjamini-Hochberg false detection rate corrected *p*-value <0.1 are indicated in red. A, differentially expressed transcripts at 22 days of age. B, differentially expressed transcripts at 25 days of age. C, differentially expressed transcripts at 35 days of age.

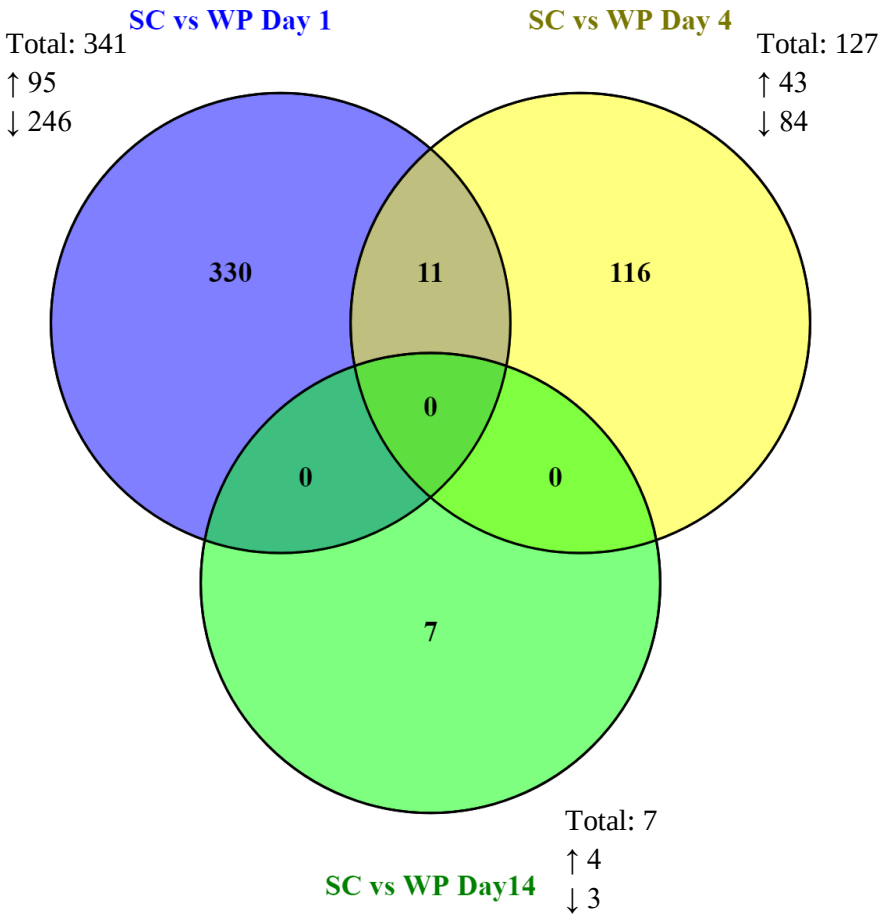


Figure 6-3: Venn diagram to demonstrate differential expression observed between suckling control pigs with and SCB supplemented weaned pigs at 22, 25 and 35 days of age. SC vs WP, suckling control vs Weaned + Probiotic (SCB). Day one, 22 days of age. Day four, 25 days of age, Day 14, 35 days of age. Total transcripts, up (↑) and down (↓) regulated transcripts are indicated. All transcripts Log_2 FC ≥ 1 or ≤ -1, $q < 0.1$

6.2.3 Comparison of the Transcriptional Effect of Weaning (Suckling Control vs Weaned Control) and Weaning with SCB Supplemented Weaned Animals (Suckling Control vs Weaned SCB).

Transcripts significantly differentially expressed during weaning without intervention (suckling control vs weaned control), were compared to those observed when the weaned cohort was SCB supplemented (suckling control vs weaned SCB) (Figure 6-4). This comparison found that 97 differentially expressed transcripts were shared between the analyses of samples collected from 22-day old animals (one-day post weaning), with 256 exclusive to the weaning without SCB analysis and 244 exclusive to the suckling control vs weaned SCB comparison.

In 25-day old animals (four days post weaning), the two analyses shared 11 transcripts, with 67 exclusive to suckling control vs weaned control and 116 transcripts exclusive to suckling control vs weaned SCB. Finally, amongst 35-day old animals, two transcripts were shared between suckling control vs weaned control and suckling control vs weaned SCB comparisons. A single transcript was exclusive to the former and five to the latter.

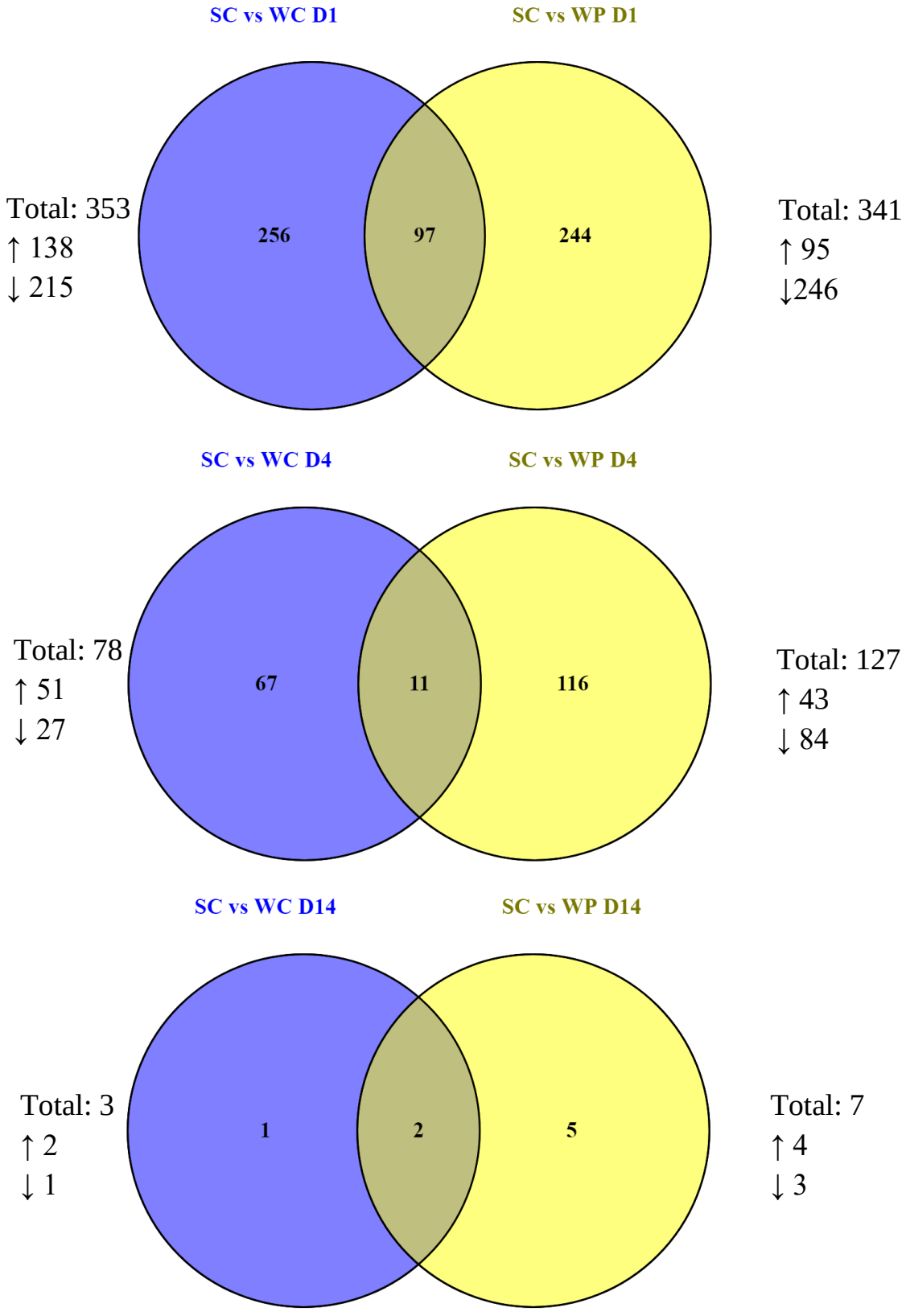


Figure 6-4: Venn Diagrams to show differentially expressed transcripts shared between (suckling control vs weaned control) and (suckling control vs weaned SCB). SC vs WC, suckling control vs weaned control. SC vs WP, suckling control vs Weaned + Probiotic (SCB). Day one, 22 days of age. Day four, 25 days of age, Day 14, 35 days of age. Total transcripts, up (↑) and down (↓) regulated transcripts are indicated. All transcripts Log2 FC ≥ 1 or ≤ -1, $q < 0.1$. Transcript Ensembl identifiers can be found in additional file 13.

6.2.4 Gene Ontology Analysis of Genes Exclusive to the Suckling Control vs SCB Supplemented Weaned Comparison

Genes which were differentially expressed only in the suckling control vs SCB supplemented weaned comparison were subject to GO analysis as these were the genes affected by probiotic supplementation. These genes were selected as the transcriptional activity of these genes may be attributed to the activity of SCB rather than weaning. As with previous comparisons, too few genes were identified as differentially expressed between 35-day old animals for this analysis to be appropriate.

6.2.4.1 Biological Process Gene Ontology Analysis of Differentially Expressed Genes Exclusive to the Suckling Control vs SCB Supplemented Weaned Comparison at One-Day Post-Weaning (22 days of age)

Six biological process GO terms were significantly enriched amongst upregulated genes ($q < 0.05$), all of which were enriched by two genes. These included *regulation of thyroid hormone generation* (2/2 genes); *hydrogen peroxide metabolic process* (2/4 genes); *urea cycle* (2/6 genes); *ERK1 and ERK2 cascade* (2/21 genes); *cellular response to drug*

(2/38 genes) and *regulation of inflammatory response* (2/47 genes) (Figure 6-5A).

Three of these GO terms were enriched by the same two genes. *Regulation of thyroid hormone generation* (2/2 genes); *hydrogen peroxide metabolic process* (2/4 genes) and *inflammatory response* (2/47 genes) were all enriched by the upregulation of dual oxidase maturation factor 1 and 2 (*DUOXA1* & *DUOXA2*). *ERK1 and ERK2 cascade* and *cellular response to drug* were both enriched by metallothionein 3 *(MT3*), with the former also enriched by mitogen-activated protein kinase kinase 2 *(MAP2K2)* and the latter by metallothionein 2A *(MT2A).* Finally, *urea cycle* was enriched by arginase 2 *(ARG2)* and arginosuccinate synthetase 1 *(ASS1).*

A total of 13 biological processes were significantly enriched amongst downregulated genes exclusive to the suckling control vs SCB supplemented weaned comparison (Figure 6-5B). The biological process with the lowest fast detection rate corrected *p*-value was *B cell receptor signalling pathway* (5/29 genes). The downregulated genes causing this enrichment were: cluster of differentiation 19 (*CD19*); myocyte-specific enhancer factor 2C (*MEF2C*); cluster of differentiation 79B (*CD79B*) and tyrosine protein kinase (*BLK*). All these genes were also identified as

down-regulated in the colon of SCB supplemented suckling pigs (Section 5.2.1). This analysis also highlighted *positive regulation of intracellular signal transduction* (2/5 genes), to be enriched by downregulation of tumour necrosis superfamily member 11 (*TNFSF11*) and fibroblast growth factor 11 (*FGF11*); *leukocyte chemotaxis*, enriched by C-X-C chemokine receptor 5 (*CXCR5*) and cannabinoid receptor 2 (*CNR2*) and enrichment of *regulation of synaptic transmission*, glutamatergic (3/18 genes) by myocyte-specific enhancer factor 2C (*MEF2C*) and serine peptidase inhibitor E2 (*SERPINE2*). A number of these genes were also identified as differentially expressed in colon samples between suckling control and SCB supplemented suckling animals; these common genes included: *MEF2C*, *SERPINE1*, *CNR2* and *CXCR5*. This suggests a common differential gene expression between these two comparisons. Information on all biological process terms enriched in both up and downregulated genes can be found in Appendix 20.

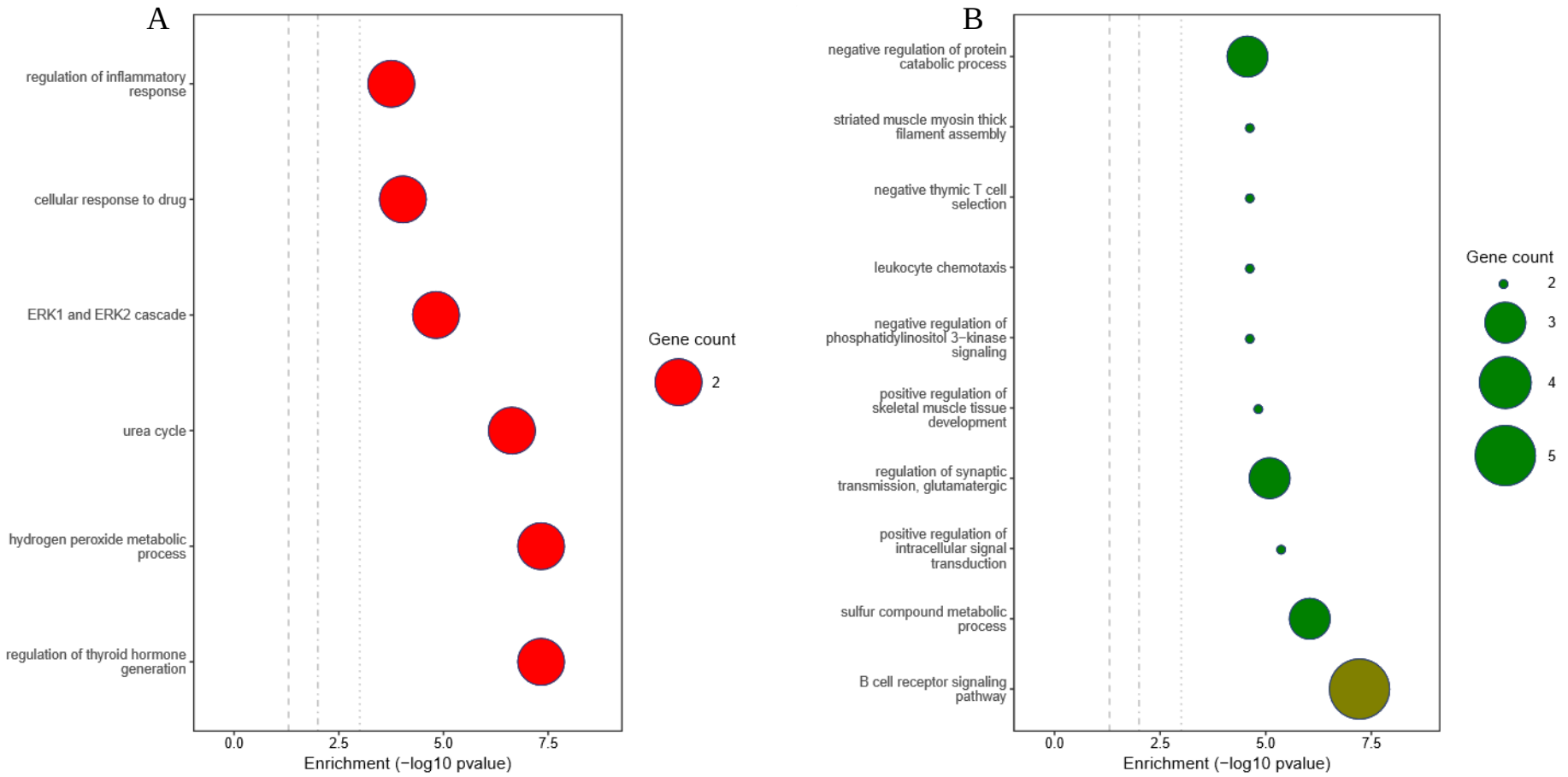


Figure 6-5: Enrichment of biological process terms in up and downregulated genes exclusive to the suckling control vs SCB supplemented weaned comparison when compared to differential gene expression observed between suckling control and weaned control samples at one day post-weaning. A, biological process enrichment of upregulated genes. B, biological process enrichment of downregulated genes. Top 10 most significantly enriched terms displayed where available. All terms shown contain equal to or greater than two differentially expressed genes and are significantly enriched ($q \leq 0.05$). Information on all significantly enriched terms including gene names and identifiers can be found in Appendix 20.

6.2.4.2 Biological Process GO Analysis of Differentially Expressed Genes Exclusive to the Suckling Control vs SCB Supplemented Weaned Comparison at Four Days Post Weaning (25 days of age)

Three biological process GO terms were significantly enriched amongst upregulated genes exclusive to the suckling control vs SCB supplemented weaned comparison at four days post weaning (25-day old animals) (Figure 6-6A). These were peptide cross-linking (2/18 genes) long-term synaptic potentiation (2/29 genes) and blood coagulation (2/33 genes). Four upregulated genes were responsible for this enrichment: transglutaminase 1 (*TGM1*); coagulation factor XIII A chain (*F13A1*); Serine peptidase inhibitor E1 (*SERPINE1*) and glial fibrillary acidic protein (*GFAP*). A full breakdown of GO enrichment can be found in Appendix 21.

Biological process enrichment of downregulated genes identified 13 significantly enriched terms (Figure 6-6B), however, the eight most significantly enriched terms were all enriched by combinations of five homeobox genes: D10, D9, D3, B3 and A10 (*HOXD10*, *HOXD9*, *HOXD3*, *HOXB3* and *HOXA10* respectively). All information on this gene ontology analysis can be found in Appendix 21.

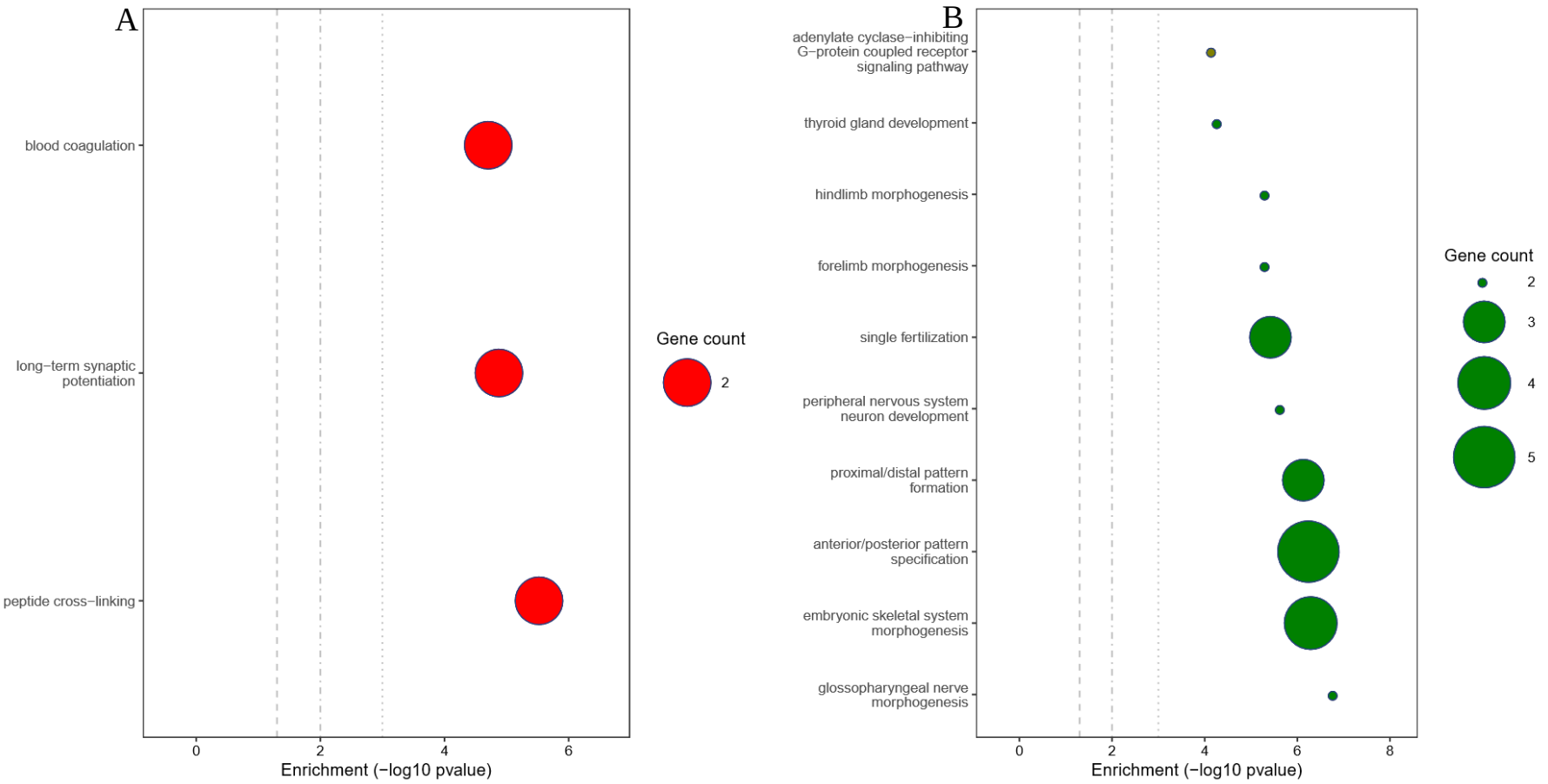


Figure 6-6: Enrichment of biological process terms in up and downregulated genes exclusive to the suckling control vs SCB supplemented weaned comparison when compared to differential gene expression observed between suckling control and weaned control samples at four days post-weaning. A, biological process enrichment of upregulated genes. B, biological process enrichment of downregulated genes. Top 10 most significantly enriched terms displayed where available. All terms shown contain equal to or greater than two differentially expressed genes and are significantly enriched ($q \leq 0.05$). Information on all significantly enriched terms including gene names and identifiers can be found in Appendix 21.

6.2.5 Comparison of Differentially Expressed Gene Sets to Identify a Common Effect of *Saccharomyces cerevisiae boulardii*

As some of the differentially expressed genes described in the previous section also appeared in the comparison of suckling control and SCB supplemented suckling samples. A comparison of all genes differentially expressed between control and SCB supplemented samples was conducted to identify any central effect of the probiotic. This included transcripts exclusively differentially expressed when in the suckling control animals to SCB supplemented weaned animals when compared to differentially expressed transcripts in the suckling control vs weaned control comparison. These differentially expressed transcripts may be attributed to SCB supplementation rather than weaning. This comparison also included differentially expressed transcripts identified in the comparisons of suckling control vs SCB supplemented suckling animals and weaned control vs SCB supplemented weaned animals. As all these transcript sets represent transcriptional differences attributed to SCB, shared transcripts may indicate a central transcriptional effect of oral SCB supplementation.

In the comparison of differentially expressed transcripts identified in 22-day old pigs, one-day post weaning, 86 differentially expressed

transcripts were shared between those from the suckling control vs SCB supplemented weaned comparison and the suckling control vs SCB supplemented suckling comparison. The single differentially expressed transcript identified when comparing weaned control samples to SCB supplemented samples was not differentially expressed in either of the other comparisons (Figure 6-7).

The comparison of SCB associated differential expression in 25-day old animals, four days post weaning, identified 12 transcripts shared between the weaned control vs SCB supplemented weaned comparison and those from the suckling control vs SCB supplemented weaned comparison which could be attributed to SCB (Figure 6-8). No other differentially expressed transcripts were shared between comparisons. No transcripts were shared between any comparisons between 35-day old animals, 14 days post weaning (Figure 6-9).

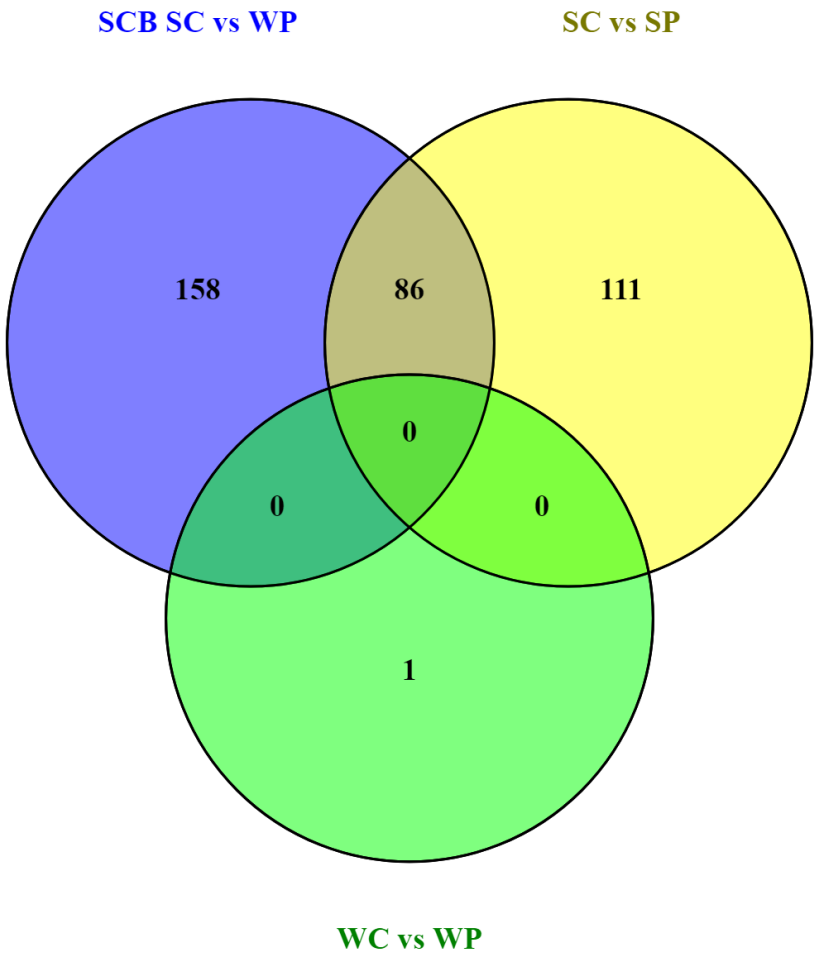


Figure 6-7: Comparison of differentially expressed transcripts to identify a common effect of oral SCB supplementation in the colon of 22 day old pigs. SCB SC vs WP, transcriptional differences exclusive to the SC vs WP comparison when compared to SC vs WP (therefore transcription attributed to SCB rather than weaning). SC, suckling control. SP, suckling probiotic (SCB supplemented). WC, weaned control. WP, weaned probiotic (SCB supplemented). Only differentially expressed transcripts shown ($q < 0.1$, Log2 FC ≥ 1 or ≤ -1). Transcript Ensembl identifiers can be found in Additional file 14.

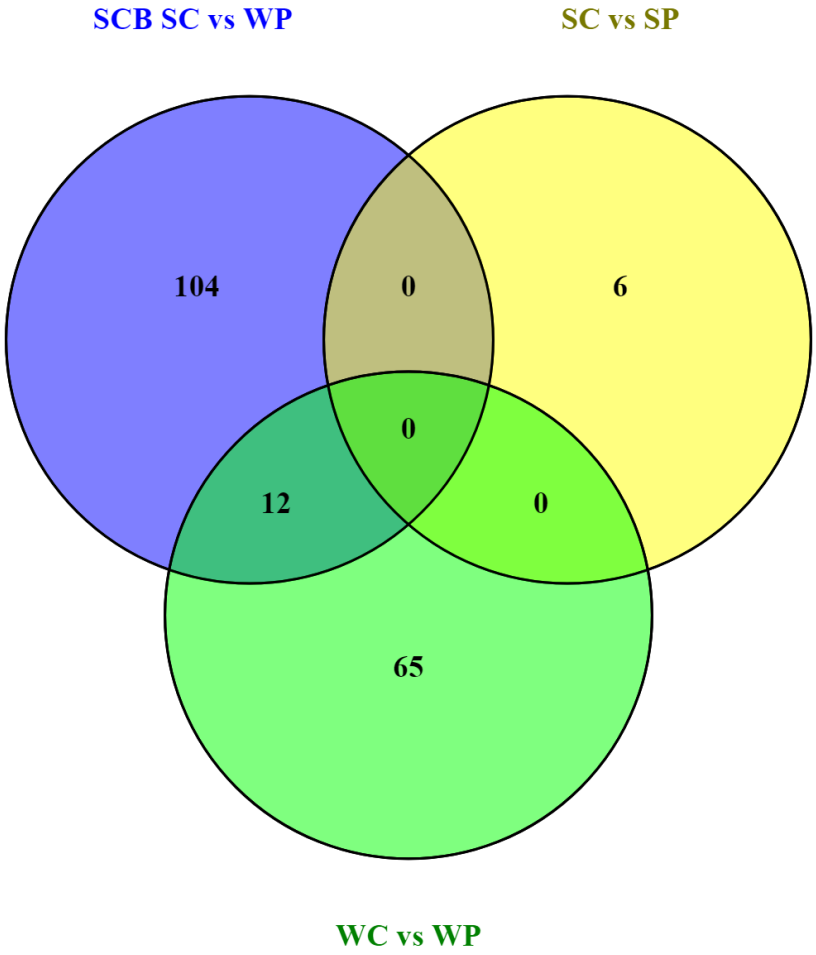


Figure 6-8: Comparison of differentially expressed transcripts to identify a common effect of oral SCB supplementation in the colon of 25 day old pigs. SCB SC vs WP, transcriptional differences exclusive to the SC vs WP comparison when compared to SC vs WP (therefore transcription attributed to SCB rather than weaning). SC, suckling control. SP, suckling probiotic (SCB supplemented). WC, weaned control. WP, weaned probiotic (SCB supplemented). Only differentially expressed transcripts shown ($q < 0.1$, Log2 FC ≥ 1 or ≤ -1). Transcript Ensembl identifiers can be found in Additional file 15.

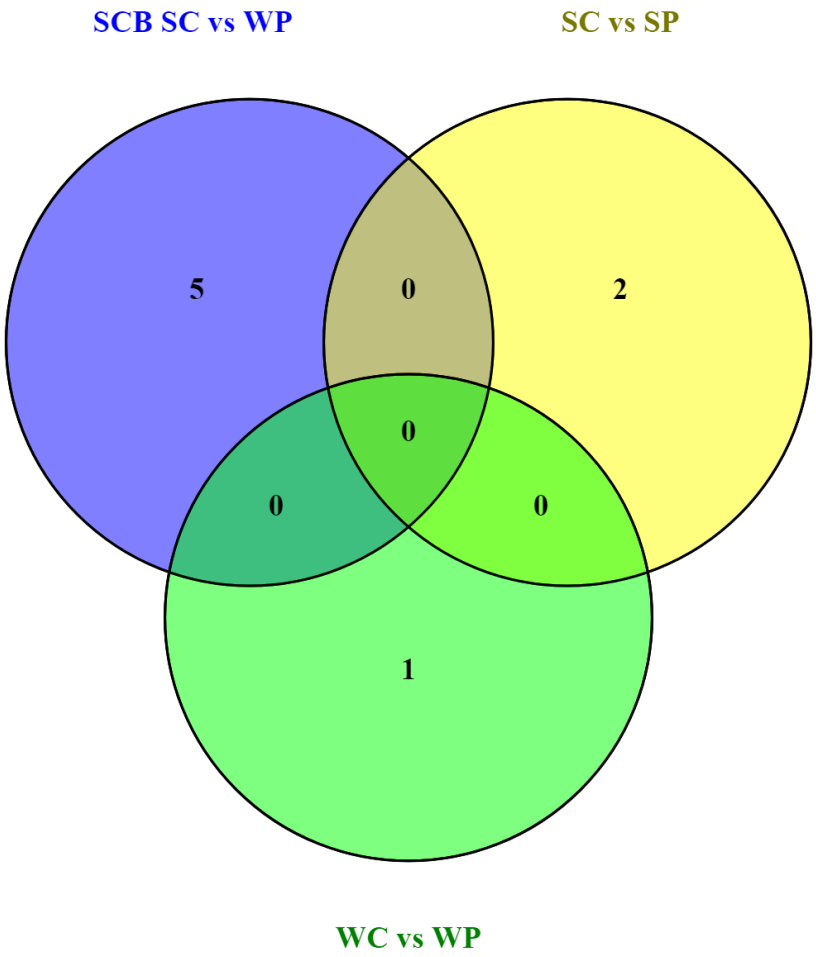


Figure 6-9: Comparison of differentially expressed transcripts to identify a common effect of oral SCB supplementation in the colon of 25 day old pigs. SCB SC vs WP, transcriptional differences exclusive to the SC vs WP comparison when compared to SC vs WP (therefore transcription attributed to SCB rather than weaning). SC, suckling control. SP, suckling probiotic (SCB supplemented). WC, weaned control. WP, weaned probiotic (SCB supplemented). Only differentially expressed transcripts shown ($q < 0.1$, Log2 FC ≥ 1 or ≤ -1). Transcript Ensembl identifiers can be found in Additional file 16.

6.2.6 Comparison of Expression Values for Differentially Expressed Transcripts Across all Samples

As no universal effect of oral SCB supplementation could be identified, all differentially expressed transcripts ($q \leq 0.1$, Log_2 FC ≥ 1 or ≤ -1) across all comparisons (SC vs WP, SC vs SP, WC vs WP, SC vs WP and SP vs WP), were collated and analysed using principal component analysis and heatmaps. This approach allowed observation as to whether expression across all of these differentially expressed features could differentiate between treatments. The final comparison of suckling vs weaned where both have been supplemented with SCB is not discussed elsewhere as this information is not pertinent to either the transcriptional effect of weaning without probiotic intervention or the identification of the transcriptional effect of SCB supplementation. However differential expression information can be found in additional files 17-19).

6.2.6.1 Comparison of Expression Value Profiles for all Differentially Expressed Transcripts identified between Colon Samples Collected from 22 Day Old Pigs

Principal component analysis (PCA) conducted on TPM values for the 662 transcripts differentially expressed in at least one comparison (q ≤0.1, Log_2 FC ≥ 1 or ≤ -1) of 22-day old pig colon samples identified clustering based on treatment, although some overlap in 95% confidence intervals was seen between all groups. However, SCB supplemented suckling and weaned samples overlapped almost completely, suggesting that the expression pattern over these genes was similar between these cohorts. A tight clustering of suckling control sample suggested that the expression pattern in these samples was distinct from the other cohorts (Figure 6-10).

The heatmap displaying this same data confirmed these observations, with two distinct sample clusters identified (Figure 6-11). The first, containing the suckling control samples in addition to sample 4105 of the SCB supplemented weaned cohort; sample 7980 of the SCB supplemented suckling cohort and sample 9223 of the weaned control group. This is reflected in the PCA plot, as points representing these

three samples are situated closest to the suckling control grouping. TPM information used can be found in additional file 20.

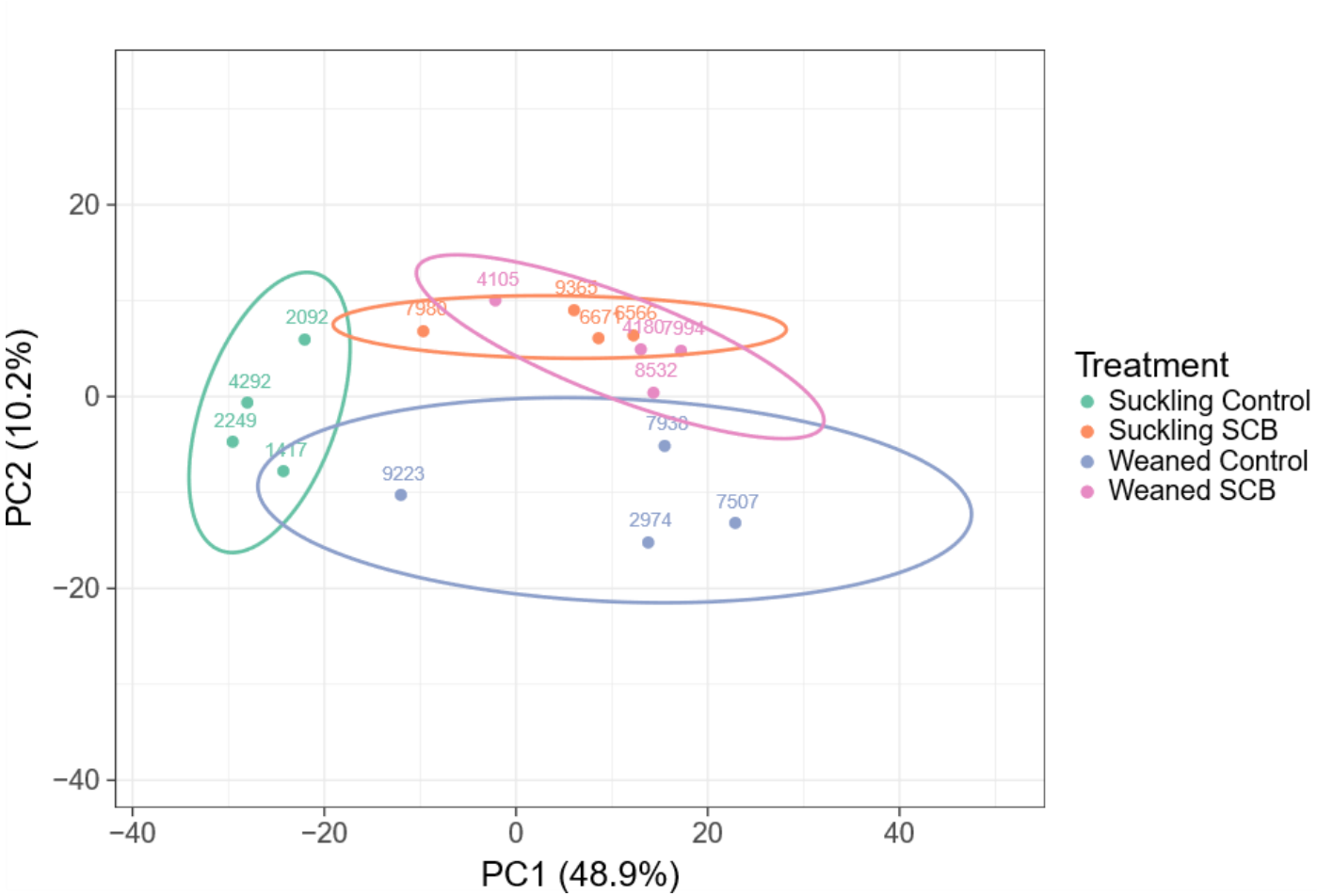


Figure 6-10: PCA to explain the relationship of sample expression patterns across all differentially expressed transcripts identified between 22 day old pig colon samples. Unit variance scaling is applied to rows; SVD with imputation is used to calculate principal components. X and Y axis show principal component 1 and principal component 2 that explain 48.9% and 10.2% of the total variance, respectively. Prediction ellipses are such that with probability 0.95, a new observation from the same group will fall inside the ellipse. N = 16 data points.

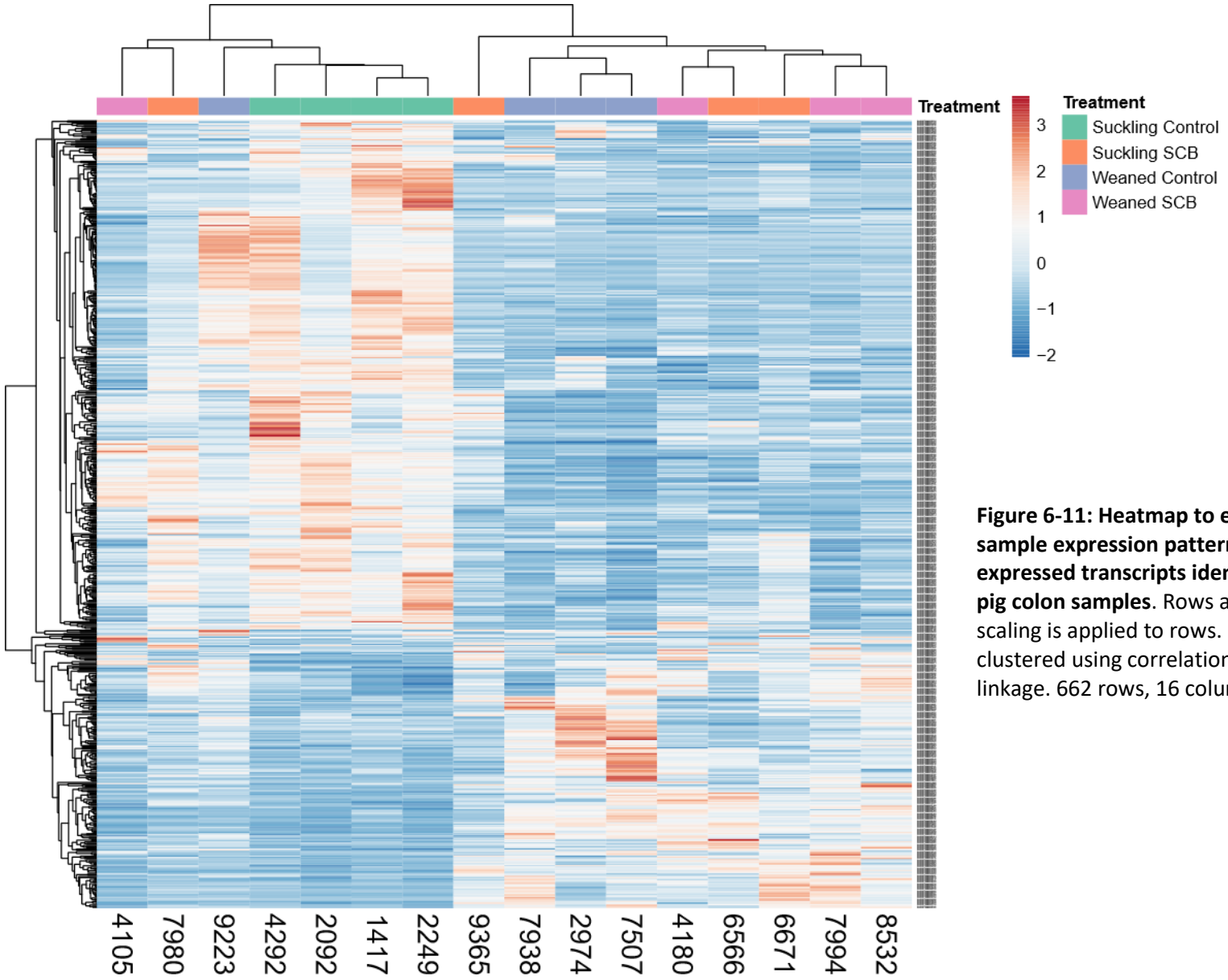


Figure 6-11: Heatmap to explain the relationship of sample expression patterns across all differentially expressed transcripts identified between 22 day old pig colon samples. Rows are centered; unit variance scaling is applied to rows. Both rows and columns are clustered using correlation distance and average linkage. 662 rows, 16 columns.

6.2.6.2 Comparison of Expression Value Profiles for all Differentially Expressed Transcripts identified in all Comparisons Between Colon Samples Collected from 25-day old pigs

PCA analysis conducted on TPM values for the 355 transcripts identified as differentially expressed in at least one comparison of colon samples from 25-day old pigs again identified separate groups based on treatment. Although 95% confidence ellipses for the treatments did overlap in some instances, separate and distinct groups consisting of weaned control and SCB supplemented weaned samples were identified. However, this analysis found that both suckling cohorts overlapped, suggesting that the expression patterns of these two cohorts were similar (Figure 6-12).

The same information visualised using a heatmap identified a separation based on weaning status. Clustering of suckling samples found no clear distinction between those from SCB supplemented animals and their control counterparts. However, a distinct separation is apparent between samples collected from weaned control and SCB supplemented weaned pigs (Figure 6-13). TPM expression values used in this analysis can be found in additional file 21.

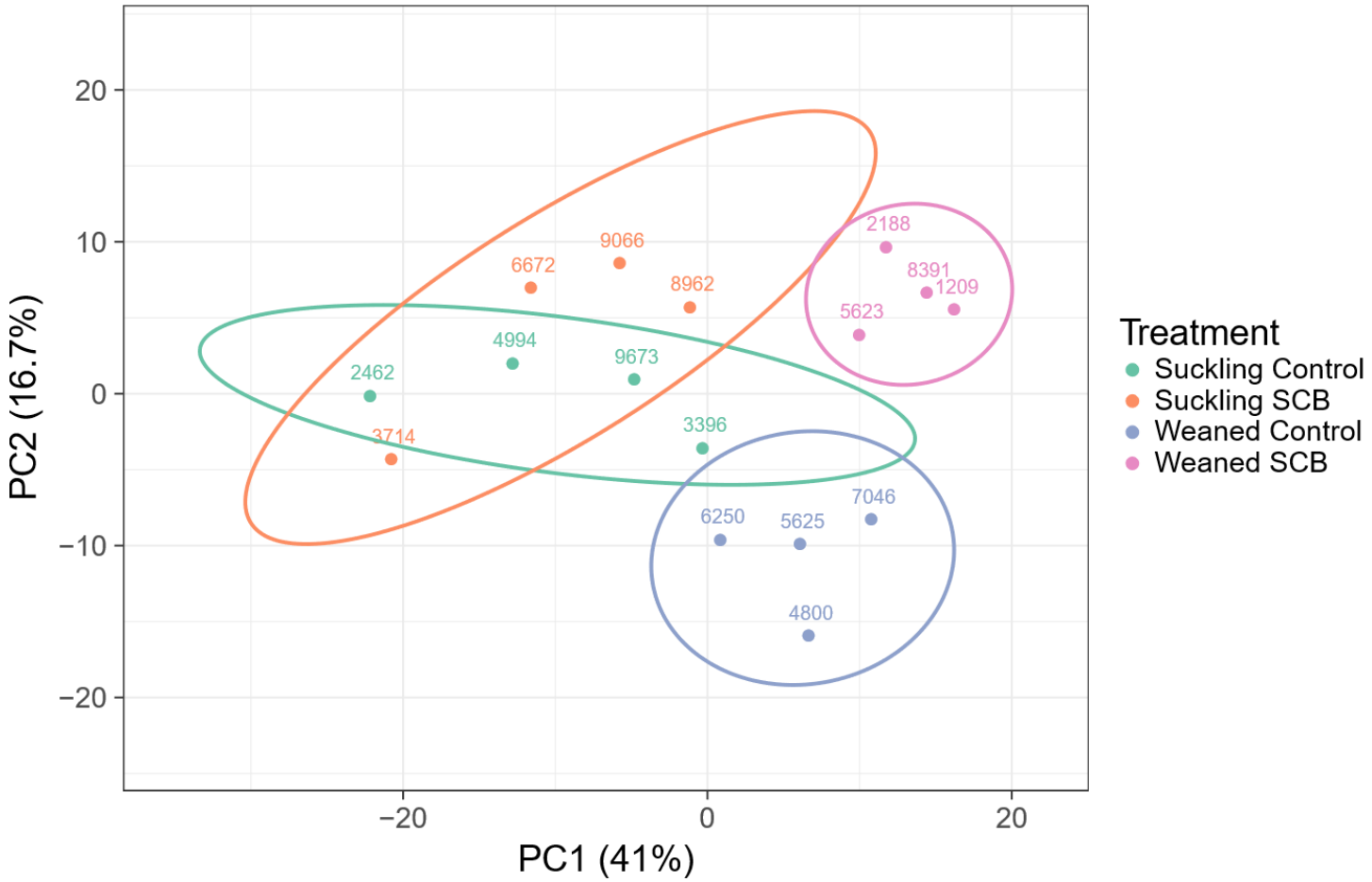


Figure 6-12: PCA to explain the relationship of sample expression patterns across all differentially expressed transcripts identified between 25 day old pig colon samples. Unit variance scaling is applied to rows; SVD with imputation is used to calculate principal components. X and Y axis show principal component 1 and principal component 2 that explain 41% and 16.7% of the total variance, respectively. Prediction ellipses are such that with probability 0.95, a new observation from the same group will fall inside the ellipse. N = 16 data points

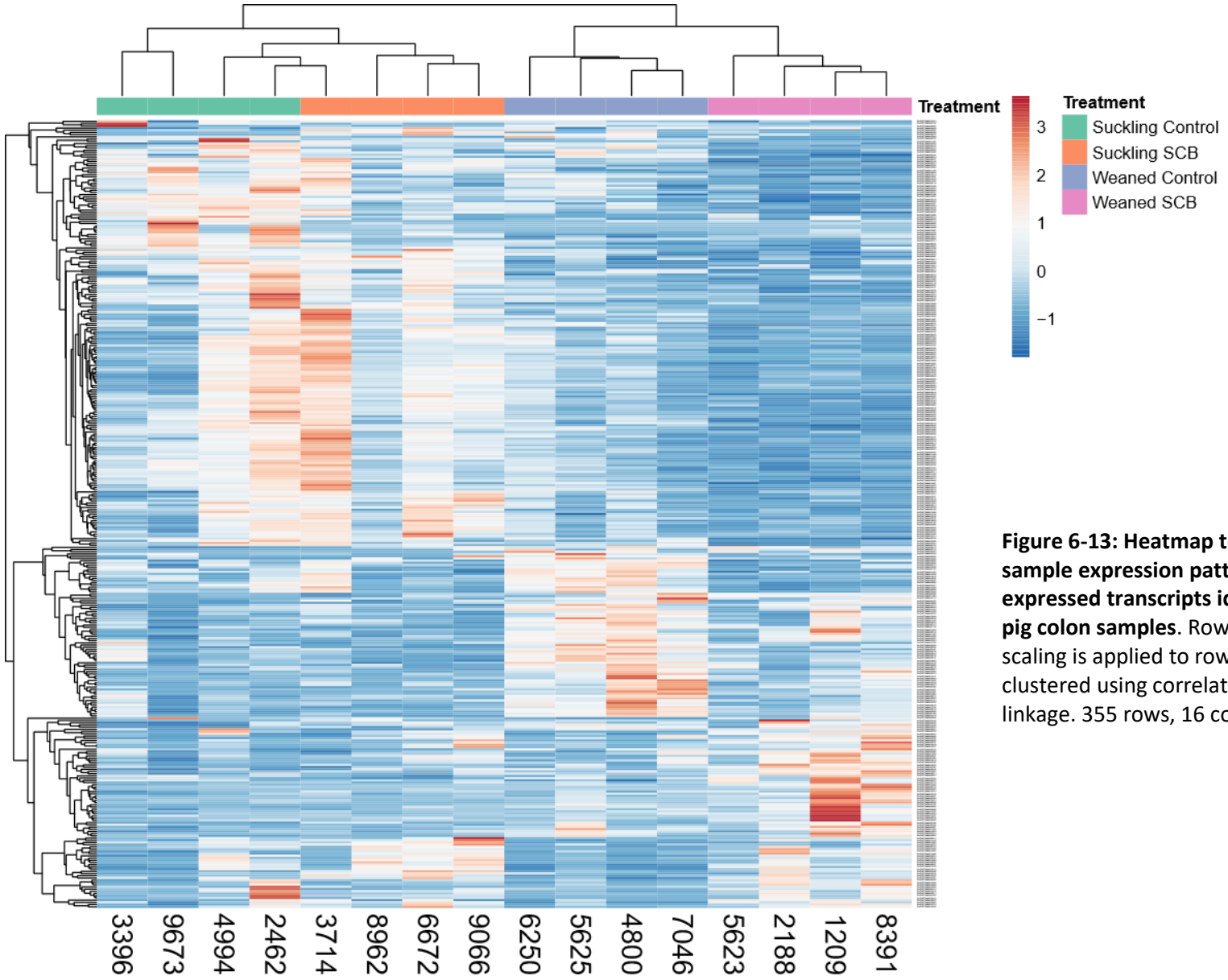


Figure 6-13: Heatmap to explain the relationship of sample expression patterns across all differentially expressed transcripts identified between 25 day old pig colon samples. Rows are centered; unit variance scaling is applied to rows. Both rows and columns are clustered using correlation distance and average linkage. 355 rows, 16 columns.

6.2.6.3 Comparison of Expression Value Profiles for all Differentially Expressed Transcripts Identified in all Comparisons Between Colon Samples Collected from 35-Day Old Pigs

Only a total of 74 transcripts were differentially expressed in comparisons between colon samples from 35-day old pigs. PCA analysis conducted on the TPM values obtained for these transcripts identified no clear distinction between treatments (Figure 6-14). The heatmap displaying these values (Figure 6-15) also failed to distinguish samples based on treatment. TPM values used in this analysis can be found in additional file 22.

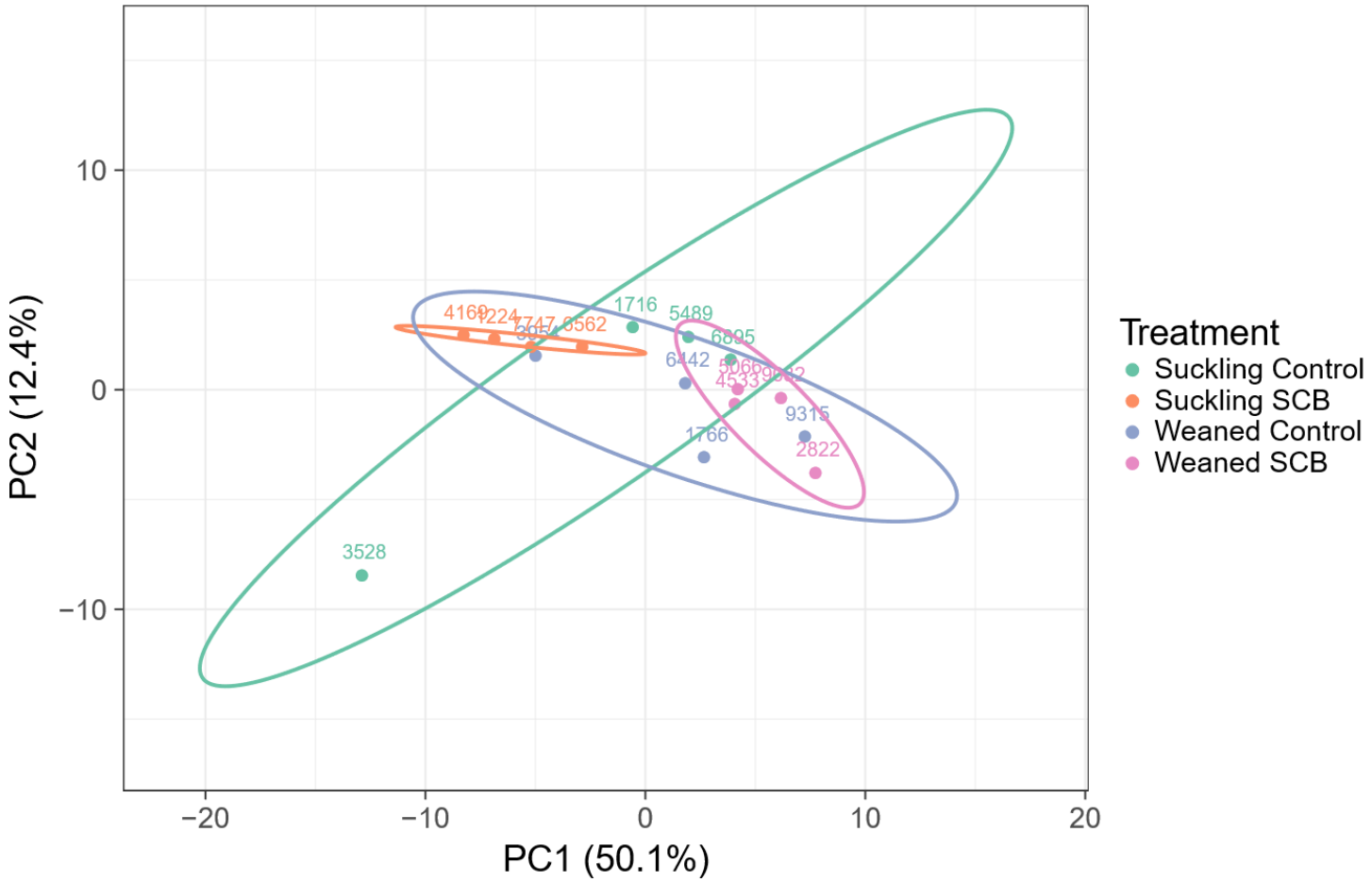


Figure 6-14: PCA to explain the relationship of sample expression patterns across all differentially expressed transcripts identified between 35-day old pig colon samples. Unit variance scaling is applied to rows; SVD with imputation is used to calculate principal components. X and Y axis show principal component 1 and principal component 2 that explain 50.1% and 12.4% of the total variance, respectively. Prediction ellipses are such that with probability 0.95, a new observation from the same group will fall inside the ellipse. N = 16 data points.

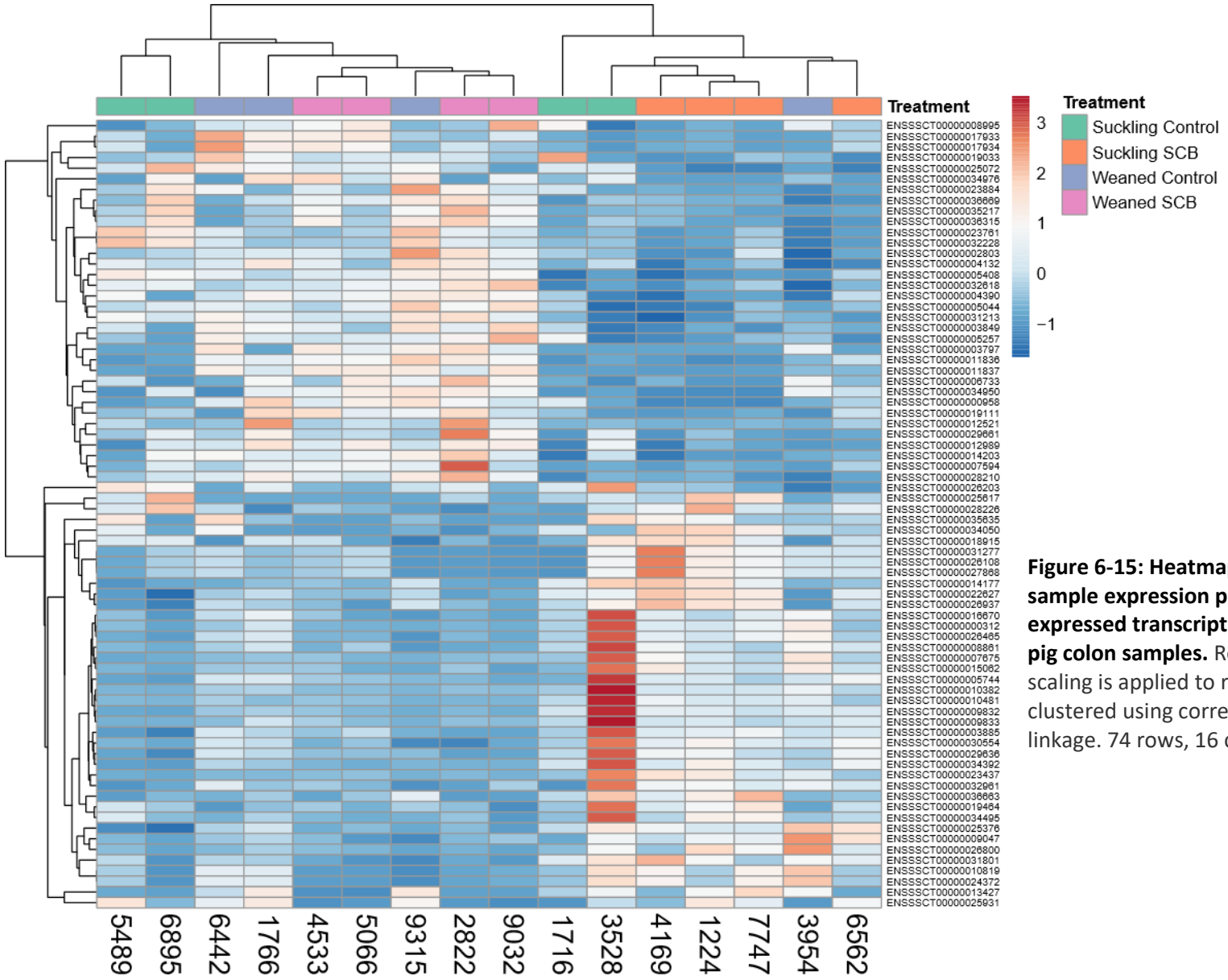


Figure 6-15: Heatmap to explain the relationship of sample expression patterns across all differentially expressed transcripts identified between 35-day old pig colon samples. Rows are centered; unit variance scaling is applied to rows. Both rows and columns are clustered using correlation distance and average linkage. 74 rows, 16 columns.

6.3 Discussion

Expression profiles of suckling control colon samples and SCB supplemented weaned samples were compared to identify differential expression at one, four and 14 days post-weaning when the weaned pigs had been orally supplemented with SCB from 7 days of age. The number of differentially expressed transcripts at each of the three post-weaning time points was like that observed when comparing suckling control to weaned control (weaning without SCB treatment). The maximal number of differentially expressed transcripts were identified one-day post-weaning, fewer identified at four days post-weaning and the fewest identified at 14 days after weaning.

However, when the differentially expressed transcripts identified in these two analyses were compared, 97 transcripts were shared by both analyses at one-day post-weaning whereas eleven and two transcripts were shared at four and 14 days post-weaning respectively. These may represent a common transcriptional effect of weaning on the colon. As this chapter concerns the transcriptional effect of SCB, the 244, 166 and five transcripts exclusive to the suckling control vs SCB supplemented weaned comparison at the three time points respectively were of

interest as the transcriptional activity of these transcripts could be attributed to the presence of SCB in the colon.

GO analysis of the 244 transcripts exclusively differentially expressed in the suckling control vs SCB weaned comparison at 1-day post weaning highlighted the downregulation of several genes also downregulated in the comparison between suckling control and SCB suckling samples. These genes included: cluster of differentiation 19 (*CD19*); myocyte-specific enhancer factor 2C (*MEF2C*); cluster of differentiation 79B (*CD79B*) and tyrosine protein kinase (*BLK*), all of which are involved in B-cell receptor signalling. The same analysis of the 166 transcripts exclusive to the suckling control vs SCB weaned comparison at four days post weaning highlighted some of the same genes identified in the comparison of weaned control vs SCB weaned, e.g. *SERPINE1*.

As similarities were observed with the comparisons of suckling control vs SCB suckling and weaned control vs SCB weaned, all three groups of transcripts were compared to identify transcripts which were differentially expressed in all analyses, as this may constitute a central transcriptional effect of oral SCB supplementation on the colon. The result of this was that at none of the three time points were any transcripts differentially expressed in all three comparisons, indicating

that there is no universal transcriptional effect of oral *Saccharomyces cerevisiae boulardii* supplementation in the colon. However, the 86 shared between suckling control vs SCB weaned and suckling control vs SCB suckling at one-day post weaning and the twelve shared between suckling control vs SCB weaned and weaned control vs SCB weaned at four days post weaning may warrant further investigation.

As no universal transcriptional effect of probiotic *Saccharomyces cerevisiae boulardii* in the colon could be identified, all differentially expressed transcripts ($q \leq 0.1$, log2 FC ≥ 2) from all comparisons were collated (SC vs WC, SC vs WP, SC vs SP, WC vs WP, SC vs SP). The TPM expression values for these transcripts in all samples were compared to observe whether the expression of these transcripts across all samples could distinguish between treatments. Viewing expression information in this manner would overcome the disadvantages of pairwise comparison by combining information from all samples at a given time point.

The greatest number of differentially expressed transcripts were detected the five comparisons of 22-day old animals (one-day post-weaning) with a combined total of 662 transcripts. Principal component analysis (PCA) conducted on expression values for these transcripts

identified a separate grouping of suckling control and weaned control samples, whereas samples from SCB supplemented weaned and suckling samples grouped together (Figure 6-10). Heatmap visualisation of these expression values identified two sample clusters, with the first containing all suckling control samples in addition to sample 9223 from the weaned control cohort; sample 7980 from the SCB supplemented suckling cohort and sample 4105 from the SCB supplemented weaned cohort. The second cluster contained all other samples. When this is considered in the context of the PCA analysis, these three samples are responsible for drawing their respective groups closer to that of the suckling control samples. Without these three samples, a very close clustering of both SCB supplemented suckling and SCB supplemented weaned samples would be apparent, with separate and distinct clusters of suckling and weaned control samples.

The reason for the distinct expression profile of these transcripts in these three samples is unclear. However, in the case of both sample 9223 (weaned control) and sample 4105 (SCB supplemented weaned), the similarities to the suckling control cohort may result from a lack of consumption of solid feed considering that samples were collected only 24 hours after removal from the sow. Whereas other weaned pigs have

commenced solid feed consumption (Pie *et al.*, 2004; Bauer *et al.*, 2011; Chen *et al.*, 2013; Liu *et al.*, 2016a). Although as no information is available concerning feed consumption in these animals, this is unconfirmed.

The cause of the distinct profile of sample 7980 of the SCB supplemented suckling cohort is unclear, as this animal had continued access to the sow's milk, discounting any effect of solid feed consumption.

Overall, the effect of oral supplementation of pigs with *Saccharomyces cerevisiae boulardii* from seven days of age has the effect of normalising the expression of these 622 transcripts in the colon of 22-day old pigs (one-day post weaning). Thereby making expression in expression in weaned and suckling animals more alike each other than corresponding suckling control and weaned control samples.

In the five comparisons of 25-day old pigs, a combined total of 355 transcripts were differentially expressed. PCA conducted on the TPM expression values for these 355 transcripts over all samples identified separate clusters of weaned control and SCB supplemented weaned control samples. All suckling samples clustered together. Heatmap visualisation of these expression values and hierarchical clustering

identified two distinct clusters of weaned and suckling samples. SCB supplemented suckling and suckling control samples were intermingled within the suckling cluster. However, a distinct differentiation was observed between SCB supplemented weaned and weaned control samples. The reduction in the number of differentially expressed transcripts, coupled with the clear clustering of samples based on weaning status suggests that four days post-weaning is a time point where recovery from weaning stress is in progress. The clear distinction observed between SCB supplemented weaned and weaned control samples, which is not observed between their suckling equivalents suggests a different and more pronounced effect of SCB in weaned animals than suckling animals at this stage.

In the comparisons of 35-day old animals, only 74 transcripts were differentially expressed. However, PCA analysis showed a tight clustering of all samples and heatmap visualisation and hierarchical clustering could not distinguish between treatments. This information combined suggests that differential expression at this time point is not weaning or SCB related. Therefore the transcriptional effect of weaning in the colon is concluded by this point (Moeser *et al.*, 2007a; Moeser *et al.*, 2017).

6.4 Conclusion

No universal transcriptional effect of oral SCB supplementation could be identified. However, a global view is taken of expression of all transcripts identified as differentially expressed in pairwise comparisons suggests that SCB supplementation may act to normalise expression in 22-day old animals (one-day post weaning).

7 General Discussion

In this concluding chapter, the key findings of this work will be discussed in the context of the current literature. Also discussed will be the strengths and limitations of this study, and a view is given to potential future directions to continue this line of study.

7.1 Results Summary

Comparison of the findings of the current study with existing literature is difficult due to several factors. The age at which pigs are weaned in a commercial environment and in weaning studies varies from 14 to 35 days of age (Pie *et al.*, 2004; Li *et al.*, 2016a; Turpin *et al.*, 2016; Moeser *et al.*, 2017). This affects intestinal permeability, with animals weaned at 28 days of age exhibiting lower intestinal permeability than those weaned at 21 days of age when measured 24 hours after weaning (Moeser *et al.*, 2017). This is attributed to the natural maturation of the epithelial barrier in young pigs which is initially permeable. However, the epithelial barrier usually matures within the first two to three weeks of postnatal life characterised by a decline in intestinal permeability (Catassi *et al.*, 1995; De Quelen *et al.*, 2011). Weaning earlier than in

natural conditions, 10-12 weeks of age, interferes with this period of maturation by depriving the weaned animals of milk-derived immunoglobulins, cytokines and peptides which suppress neonatal inflammatory cytokine expression (Newburg and Walker, 2007). As this process is gradual, direct comparison of findings in animals weaned at different ages is confounded.

A second confounding factor is that very little of the research conducted to investigate the effects of weaning focuses on the colon. The majority of research into the transcriptional effects of weaning on the gastrointestinal tract of pigs, focuses on the small intestine (Wiese *et al.*, 2003; Pie *et al.*, 2004; Smith *et al.*, 2010; Hu *et al.*, 2013; He *et al.*, 2017; Radloff *et al.*, 2017). This is perhaps surprising as weaning related elevated levels of circulating corticotrophin-releasing factor (CRF), a stress marker, have been demonstrated to cause increases in colonic motility, permeability and ion secretion (Moeser *et al.*, 2007a).

The key findings regarding weaning without SCB supplementation relate to increased transcription of proinflammatory cytokines *IL1B2* (FC = 2.957) and *IL1A* (FC = 2.63), as well as increased transcription of the pro-apoptotic cytokine TRAIL (*TNFSF10*, FC = 5.57) in weaned pigs one-day post-weaning. Increased mRNA expression of *IL1B2* has previously

been identified in the proximal colon of pigs weaned at 28 days of age, for the first two days post-weaning. *IL1B2* mRNA was also elevated during this period in the proximal, mid and distal small intestine (Pie *et al.*, 2004). The authors attribute this increased expression in all intestinal segments investigated to general stress associated with weaning rather than to specific stimulation. This finding is also mirrored by plasma concentration of IL-1 in pigs weaned at 21 days of age (McCracken *et al.*, 1995).

A study utilising a DNA microarray approach to weaning in ileal samples collected from weaned and suckling pigs five days after weaning, weaning at 28 days of age, has many parallels to the differential expression noted in the current study, including increased expression of *TNFSF10* (Bomba *et al.,* 2014). As this study detailed the transcriptional activity in the ileum at five days post weaning, it could be reasonably expected that the findings would most closely match the findings of the element of the current study detailing four days post-weaning. Indeed, this study identified increased expression of farsenoid X receptor (*NR1H4*) and apolipoprotein A-1 (*APOA1*) whereas in the current study, the former and apolipoprotein C-3 (*APOC3*) were upregulated.

The final time point surveyed for transcriptional activity was 14 days post-weaning, where the fewest differences were observed between weaned and suckling pigs. This point coincides with the culmination of intestinal permeability decline after weaning related increases, representing the natural time course for post-weaning colonic barrier function repair (Moeser *et al.*, 2007a; Peace *et al.*, 2011).

Overall, weaning prompts a nonspecific increase in immune-related transcription in the colon, which has ceased by 14 days post weaning.

Interpretation of the transcriptional effects of SCB in the porcine colon in the context of current literature is particularly difficult as most of the studies on the effect of probiotics use bacterial preparations, rather than yeast. Comparing the effects of a bacterial probiotic to a yeast probiotic is inappropriate as these organisms belong to entirely different kingdoms, therefore have different cell wall components and modes of action (Czerucka *et al.*, 2007). This combined with the lack of studies detailing the effects on the colon specifically, makes a comparison to existing knowledge difficult.

The key overall finding is that SCB supplementation has a markedly different effect on weaned animals than what was apparent in suckling animals. The most transcriptional differences noted in 22-day old

suckling animals. Conversely, the time point at which supplementation had the greatest effect on weaned animals was four days post-weaning, 25 days of age. This is consistent with existing literature where SCB has a lesser effect on healthy intestine than in inflammatory conditions such as Crohn's disease, a finding the authors attribute to reduced contact between the probiotic and immune cells (Hudson *et al.*, 2016).

Key SCB related transcriptional changes in the colon of weaned animals at four days post-weaning included increased expression of *IL10* (FC = 2.88), *CCL19* (FC = 5), *CCL22* (FC = 2.54), *TIMP1* (FC= 2.46) and *SERPINE1* (FC = 3.15).

Increased expression of the anti-inflammatory cytokine *IL10* in response to SCB supplementation has been previously reported, with authors suggesting that this upregulation may inhibit intestinal injury in a mouse model of IBS (Yanaba *et al.*, 2011; Brun *et al.*, 2017). However, SCB was found to not affect *CCL19* and *CCL22* expression in mesenteric lymph nodes (Dalmasso *et al.*, 2006). Expression of the receptor for these molecules, *CCR7*, was also found to be upregulated by SCB at four days post-weaning. This contrasts with published findings where SCB supernatant reduced the proportion of CCR7 positive dendritic cells after naïve human dendritic cells were stimulated with

lipopolysaccharide (Thomas *et al.*, 2009). Although, as the current study does not include a challenge element, this is not directly comparable. It does however, demonstrate the interaction between SCB supernatant products and dendritic cells. In the context of weaning, a reduction in the maturation of dendritic cells and subsequent migration to secondary lymphoid organs would be detrimental to the establishment of immune tolerance to the new food and environmental antigens to which pigs are exposed after weaning (Forster *et al.*, 2008). As expression of *CCR7* and its two ligands: *CCL19* and *CCL22* are increased in colon tissue by SCB supplementation, this is an area which merits further study to understand the action of SCB in the weaned pig.

Finally, although increased transcription of protease inhibitors *SERPINE1* and *TIMP1* is not a previously reported effect of SCB supplementation, increased expression of these may act to inhibit weaning associated extracellular matrix breakdown by matrix metalloproteases (McCracken *et al.*, 1999). Further investigation would be required to identify a link between this transcriptional activity and mucosal barrier integrity during weaning.

As no universal effect of SCB supplementation on transcription in the colon could be identified, it may be that the effects vary based on the

physiological status of the host, perhaps dictating the interaction of the probiotic with immune cells (Hudson *et al.*, 2016). This would further explain differences between the findings of the current study and existing literature detailing the effect of SCB in challenge models.

In summary, oral SCB supplementation may be beneficial in weaned pigs as it may promote an anti-inflammatory response by increasing *IL10* transcription as well as having effects on dendritic cell trafficking and maturation and reducing extracellular matrix breakdown. Although the effects of supplementation in suckling pigs is less clear, it appears to have the effect of normalising the expression pattern of the subset of transcripts identified as differentially expressed in all comparisons of 22-day old animals, making the expression pattern of these transcripts more like their SCB supplemented weaned counterparts than suckling control samples.

7.2 Limitations of the Current Study

A fundamental limitation of this study is that no physical differences were identified between weaned and suckling colon samples, such as differences in transepithelial resistance (Moeser *et al.*, 2007b; Moeser *et al.*, 2017). In fact, the only indication of stress identified was elevated

serum cortisol levels (Le Bon, 2012b), when elevated CRF has been demonstrated to be a more reliable indicator of weaning related intestinal barrier dysfunction (Moeser *et al.*, 2007a; Overman *et al.*, 2012).

A lack of pilot studies compounded this. Although the probiotic dose was optimised in previous experimentation, leading to 5.5 ± 0.23 Log_{10} CFU g^{-1} colon contents at one day post weaning and 4.2 ± 0.41 Log_{10} CFU g^{-1} at 14 days post weaning (Le Bon, 2012b), no effect of this supplementation was identified. A pilot study should have been conducted whereby the permeability of colon samples collected from weaned and suckling animals, with and without probiotic supplementation, one day after weaning was compared using Ussing chamber experiments. Such a pilot study with four animals per cohort would have given insight into weaning related alterations in colon permeability and any effect on this permeability brought about by SCB supplementation. If this pilot study reveals a beneficial effect of probiotic supplementation on weaning related increases in intestinal permeability, the probiotic dose could be varied as a continuation of this pilot study to determine a minimum dosage sufficient to ameliorate weaning related changes in colon permeability. This would have also

given some justification for the large-scale employment of RNA-seq in the full trial.

A limitation of the sample collection technique employed was that whole colon tissue contains a mixed population of cell types which may vary from sample to sample. An alternative method would be to use a laser microdissection system to allow isolation of only epithelial cells from a sample. This methodology would require freshly frozen mucosa samples to be cut into 18 µm sections and mounted onto pre-cooled RNAse and DNAse free membrane slides before tissue is dehydrated in a decreasing series of graded alcohols (95, 75 and 50 %). The tissue would then be stained by dipping slides for 15 seconds in 1 % cresyl violet acetate followed by post staining fixation of the slides in an increasing series of graded alcohols (50, 75, 95 and 100 %). Once this process is complete, stained tissue sections can be microdissected to select areas of epithelial cells to capture 100,000-250,000 cells using an instrument such as a Microbeam LMPC system (Carl Zeiss MicroImaging, Munich, Germany). Although this method of collection would result in a reduced total RNA yield per sample, it would ensure that all RNA used in the study was extracted from epithelial cells (Funke, 2011; Kummari *et al.*, 2015).

A limitation of the trial design is that the treatments were not sex-matched (Appendix 4), with some groups comprising entirely of male pigs, e.g. the 22-day old suckling control cohort, and others of varying proportions of males and females. This is a limiting factor as sex-linked differences in gut gene expression have been identified, including an upregulation in gene expression related to immune function in human women in the absence of disease or pathology (Sankaran-Walters *et al.*, 2013). Sex-linked differences in gene expression have also been noted in pigs (Zhang *et al.*, 2013; Howard *et al.*, 2015). Indeed, sex-linked differences have been noted in the enteric nervous system of early weaned pigs (Medland *et al.*, 2016). As the effect of sex imbalance on gene expression cannot be estimated, this is a confounding factor. Another limitation of the trial design is the lack of monitoring of feed consumption, although this is practically difficult, the inclusion of this information would have aided in the understanding of the dietary composition of both suckling and weaned pigs.

Another limitation is the power of the trial, with only four samples per treatment per time point. Although tools for RNA sample size calculation exist, they vary widely in answers given and require prior knowledge of expected results, for example the number of features

expected to be differentially expressed (Hart *et al.*, 2013; Ching *et al.*, 2014; Poplawski and Binder, 2017). It is however clear that four samples per treatment is not sufficient to identify the subtler changes in expression. This was addressed in the current study by only considering transcripts with greater than two-fold change in expression, however, to reliably identify features with greater than 0.5 fold change, 12 samples per treatment would be required (Schurch *et al.*, 2016). The inclusion of subtler differential gene expression would provide a more complete picture of the transcriptional changes in the colon in response to weaning and probiotic SCB supplementation. Although the biological relevance of small fold changes on an individual gene or transcript may be negligible, this information may improve GO and network analyses and therefore understanding of the processes and functions affected by the treatments. A separate limitation of the analysis methodology is that no minimum cut-off was applied to TPM values, filtering low expression features, as these can introduce noisy and misleading fold change values (Sha *et al.*, 2015).

As a transcriptomic approach was taken to this study, a primary limitation is that only transcription was monitored. Therefore further

work would be required to determine if detected changes in transcription translate to equivalent changes at the protein level.

7.3 Future Perspectives

In addition to protein level validation of some of the findings, future work could explore a number of different avenues.

Initially, two other animal trials following the same experimental design were conducted. Including colon samples from these trials in the RNA-seq analysis would increase the sample number to twelve per treatment at each time point, allowing a more robust RNA-seq analysis which could include features differentially expressed with a lower fold change cut-off.

This could then be coupled with an investigation of stress marker transcription in the hypothalamus and pituitary gland collected from animals slaughtered in one of these trials. Transcription of markers such as corticotropin-releasing factor in the hypothalamus and pro-opiomelanocortin in the pituitary gland could provide greater insight into the stress experienced during weaning (Hay *et al.*, 2001).

These studies could also be utilised to evaluate the influence of weaning and SCB supplementation on the intestinal microbiota by conducting 16S bacterial metagenomics on the colon luminal contents collected as part of these trials (Schloss *et al.*, 2009). This continuation is ongoing within the research team and will provide an understanding of the bacteria exposed to the colon, and how these change over the course of weaning and resulting from SCB supplementation.

If another animal trial were to be conducted, the focus would be on the initial period after weaning, as few transcriptional differences were identified two weeks after weaning. It has been suggested that the intestinal morphology, such as villus height, is in flux until the fifth-day post weaning (Campbell *et al.*, 2013). Therefore, the first five days post weaning would be a suitable scope for the study. A study which included the transcriptomic analysis of colon tissue from 12 pigs per treatment at each of these five days, with tissue collected for Ussing chamber transepithelial resistance experiments, would provide an excellent survey of the transcriptional changes underlying proposed alterations in gut morphology. An even balance of male and female pigs in these groups would balance any sex-linked differences in gene

expression and solid feed consumption collected so that the effect of this factor on expression could be investigated.

Alternatively, another animal trial could be conducted with the exclusive aim of identifying the transcriptional effect of weaning at different ages on the porcine colon. In this instance, animals would be weaned at a range of ages to cover the range of commercial weaning ages (e.g. 21, 25, 30 and 35 days of age). Samples would then be collected post mortem one day after weaning. After Ussing chamber experiments to quantify colon permeability, RNA-seq analysis comparing samples from these weaned animals and suckling counterparts would then function as a survey to view a timeline of weaning related transcription in the colon. Existing research suggests that later weaning would reduce the transcriptional differences observed between weaned and suckling animals (Wang *et al.*, 2008; Campbell *et al.*, 2013; Moeser *et al.*, 2017). However, as this approach has not been adopted on colon samples, such a study would add new knowledge to the field.

This study could then be expanded to include probiotic supplementation, once a suitable weaning age had been ascertained, i.e a balance between early weaning and colon disruption. This would

reduce the complexity of comparisons as only the effect of probiotic supplementation on weaned animals would be surveyed.

As previously mentioned, any further RNA-seq study should include 12 experimental replicates to ensure robust statistical analysis (Schurch *et al.*, 2016). To this end, 12 pigs would be weaned at each age and compared to 12 suckling pigs of the same age.

7.4 Conclusion

This transcriptomic study has identified a number of interesting transcriptional effects of weaning and oral *Saccharomyces cerevisiae boulardii* supplementation in the porcine colon. These findings suggest that SCB supplementation of the weaned pig may, despite having limited effects on the colon of weaned animals immediately after weaning, act to dampen the duration of the weaning related proinflammatory immune response. However, further work would be required to validate these findings on the protein and functional levels.

References

ABDULKADIR, B., NELSON, A., SKEATH, T., MARRS, E. C., PERRY, J. D., CUMMINGS, S. P., EMBLETON, N. D., BERRINGTON, J. E. & STEWART, C. J. 2016. Routine Use of Probiotics in Preterm Infants: Longitudinal Impact on the Microbiome and Metabolome. *Neonatology,* 109**,** 239-47.

ABERNATHY, J. & OVERTURF, K. 2016. Comparison of Ribosomal RNA Removal Methods for Transcriptome Sequencing Workflows in Teleost Fish. *Anim Biotechnol,* 27**,** 60-5.

ADACHI, Y., OKAZAKI, M., OHNO, N. & YADOMAE, T. 1994. Enhancement of cytokine production by macrophages stimulated with (1-->3)-beta-D-glucan, grifolan (GRN), isolated from Grifola frondosa. *Biol Pharm Bull,* 17**,** 1554-60.

ADDELMAN, S. 1969. Generalized Randomized Block Design. *American Statistician,* 23**,** 35-&.

ADESSI, C., MATTON, G., AYALA, G., TURCATTI, G., MERMOD, J. J., MAYER, P. & KAWASHIMA, E. 2000. Solid phase DNA amplification: characterisation of primer attachment and amplification mechanisms. *Nucleic Acids Res,* 28**,** E87.

AGGARWAL, B. B., GUPTA, S. C. & KIM, J. H. 2012. Historical perspectives on tumor necrosis factor and its superfamily: 25 years later, a golden journey. *Blood,* 119**,** 651-65.

AHMED, I., ROY, B. C., KHAN, S. A., SEPTER, S. & UMAR, S. 2016. Microbiome, Metabolome and Inflammatory Bowel Disease. *Microorganisms,* 4.

ALDINI, R., RODA, A., MONTAGNANI, M. & RODA, E. 1995. Bile acid structure and intestinal absorption in the animal model. *Ital J Gastroenterol,* 27**,** 141-4.

ALEXOPOULOU, L., HOLT, A. C., MEDZHITOV, R. & FLAVELL, R. A. 2001. Recognition of double-stranded RNA and activation of NF-kappaB by Toll-like receptor 3. *Nature,* 413**,** 732-8.

ALLEN, A., HUTTON, D. A., LEONARD, A. J., PEARSON, J. P. & SELLERS, L. A. 1986. The role of mucus in the protection of the gastroduodenal mucosa. *Scand J Gastroenterol Suppl,* 125**,** 71-8.

ALSMARK, C., FOSTER, P. G., SICHERITZ-PONTEN, T., NAKJANG, S., MARTIN EMBLEY, T. & HIRT, R. P. 2013. Patterns of prokaryotic lateral gene transfers affecting parasitic microbial eukaryotes. *Genome Biol,* 14**,** R19.

AMASHEH, S., BARMEYER, C., KOCH, C. S., TAVALALI, S., MANKERTZ, J., EPPLE, H. J., GEHRING, M. M., FLORIAN, P., KROESEN, A. J., ZEITZ, M., FROMM, M. & SCHULZKE, J.

D. 2004. Cytokine-dependent transcriptional down-regulation of epithelial sodium channel in ulcerative colitis. *Gastroenterology*, 126**,** 1711-20.

ANDERS, S. & HUBER, W. 2010. Differential expression analysis for sequence count data. *Genome Biol,* 11**,** R106.

ANDREWS, S. 2010. FastQC A Quality Control tool for High Throughput Sequence Data. *http://www.bioinformatics.babraham.ac.uk/projects/fastqc/*.

AREND, W. P., MALYAK, M., GUTHRIDGE, C. J. & GABAY, C. 1998. Interleukin-1 receptor antagonist: role in biology. *Annu Rev Immunol,* 16**,** 27-55.

AREND, W. P., PALMER, G. & GABAY, C. 2008. IL-1, IL-18, and IL-33 families of cytokines. *Immunol Rev*, 223**,** 20-38.

ASHBURNER, M., BALL, C. A., BLAKE, J. A., BOTSTEIN, D., BUTLER, H., CHERRY, J. M., DAVIS, A. P., DOLINSKI, K., DWIGHT, S. S., EPPIG, J. T., HARRIS, M. A., HILL, D. P., ISSEL-TARVER, L., KASARSKIS, A., LEWIS, S., MATESE, J. C., RICHARDSON, J. E., RINGWALD, M., RUBIN, G. M. & SHERLOCK, G. 2000. Gene ontology: tool for the unification of biology. The Gene Ontology Consortium. *Nat Genet*, 25**,** 25-9.

ASHWELL, J. D., LU, F. W. & VACCHIO, M. S. 2000. Glucocorticoids in T cell development and function*. *Annu Rev Immunol*, 18**,** 309-45.

ASTRUP, E., RANHEIM, T., DAMAS, J. K., DAVI, G., SANTILLI, F., JENSENIUS, M., VITALE, G., AUKRUST, P., OLANO, J. P. & OTTERDAL, K. 2014. Increased expression of the homeostatic chemokines CCL19 and CCL21 in clinical and experimental Rickettsia conorii infection. *BMC Infect Dis*, 14**,** 70.

AUDHYA, T., HOLLANDER, C. S., SCHLESINGER, D. H. & HUTCHINSON, B. 1989. Structural characterization and localization of corticotropin-releasing factor in testis. *Biochim Biophys Acta*, 995**,** 10-6.

AYUSO, M., FERNANDEZ, A., NUNEZ, Y., BENITEZ, R., ISABEL, B., BARRAGAN, C., FERNANDEZ, A. I., REY, A. I., MEDRANO, J. F., CANOVAS, A., GONZALEZ-BULNES, A., LOPEZ-BOTE, C. & OVILO, C. 2015. Comparative Analysis of Muscle Transcriptome between Pig Genotypes Identifies Genes and Regulatory Mechanisms Associated to Growth, Fatness and Metabolism. *PLoS One*, 10**,** e0145162.

BADIA, R., ZANELLO, G., CHEVALEYRE, C., LIZARDO, R., MEURENS, F., MARTINEZ, P., BRUFAU, J. & SALMON, H. 2012. Effect of Saccharomyces cerevisiae var. Boulardii and beta-galactomannan oligosaccharide on porcine intestinal epithelial and

dendritic cells challenged in vitro with Escherichia coli F4 (K88). *Vet Res,* 43**,** 4.

BAILEY, M., HAVERSON, K., INMAN, C., HARRIS, C., JONES, P., CORFIELD, G., MILLER, B. & STOKES, C. 2005. The development of the mucosal immune system pre- and post-weaning: balancing regulatory and effector function. *Proc Nutr Soc,* 64**,** 451-7.

BAJOU, K., LEWALLE, J. M., MARTINEZ, C. R., SORIA, C., LU, H., NOEL, A. & FOIDART, J. M. 2002. Human breast adenocarcinoma cell lines promote angiogenesis by providing cells with uPA-PAI-1 and by enhancing their expression. *Int J Cancer,* 100**,** 501-6.

BALASUBRAMANIAN, B., LI, T. & KIM, I. H. 2016. Effects of supplementing growing-finishing pig diets with Bacillus spp. probiotic on growth performance and meat-carcass grade qualitytraits. *Revista Brasileira de Zootecnia,* 45**,** 93-100.

BALE, T. L., CONTARINO, A., SMITH, G. W., CHAN, R., GOLD, L. H., SAWCHENKO, P. E., KOOB, G. F., VALE, W. W. & LEE, K. F. 2000. Mice deficient for corticotropin-releasing hormone receptor-2 display anxiety-like behaviour and are hypersensitive to stress. *Nat Genet,* 24**,** 410-4.

BALE, T. L., PICETTI, R., CONTARINO, A., KOOB, G. F., VALE, W. W. & LEE, K. F. 2002. Mice deficient for both corticotropin-releasing factor receptor 1 (CRFR1) and CRFR2 have an impaired stress response and display sexually dichotomous anxiety-like behavior. *J Neurosci,* 22**,** 193-9.

BALE, T. L. & VALE, W. W. 2004. CRF and CRF receptors: role in stress responsivity and other behaviors. *Annu Rev Pharmacol Toxicol,* 44**,** 525-57.

BAPTISTA, A. P., OLIVIER, B. J., GOVERSE, G., GREUTER, M., KNIPPENBERG, M., KUSSER, K., DOMINGUES, R. G., VEIGA-FERNANDES, H., LUSTER, A. D., LUGERING, A., RANDALL, T. D., CUPEDO, T. & MEBIUS, R. E. 2013. Colonic patch and colonic SILT development are independent and differentially regulated events. *Mucosal Immunol,* 6**,** 511-21.

BARBARA, G., STANGHELLINI, V., DE GIORGIO, R., CREMON, C., COTTRELL, G. S., SANTINI, D., PASQUINELLI, G., MORSELLI-LABATE, A. M., GRADY, E. F., BUNNETT, N. W., COLLINS, S. M. & CORINALDESI, R. 2004. Activated mast cells in proximity to colonic nerves correlate with abdominal pain in irritable bowel syndrome. *Gastroenterology,* 126**,** 693-702.

BARBARESCHI, M., GASPARINI, G., MORELLI, L., FORTI, S. & DALLA PALMA, P. 1995. Novel methods for the determination

of the angiogenic activity of human tumors. *Breast Cancer Res Treat,* 36**,** 181-92.

BARC, M. C., CHARRIN-SARNEL, C., ROCHET, V., BOURLIOUX, F., SANDRE, C., BOUREAU, H., DORE, J. & COLLIGNON, A. 2008. Molecular analysis of the digestive microbiota in a gnotobiotic mouse model during antibiotic treatment: Influence of Saccharomyces boulardii. *Anaerobe,* 14**,** 229-33.

BARMAN, N. N., BIANCHI, A. T., ZWART, R. J., PABST, R. & ROTHKOTTER, H. J. 1997. Jejunal and ileal Peyer's patches in pigs differ in their postnatal development. *Anat Embryol (Berl),* 195**,** 41-50.

BARREAU, F., CARTIER, C., LEVEQUE, M., FERRIER, L., MORIEZ, R., LAROUTE, V., ROSZTOCZY, A., FIORAMONTI, J. & BUENO, L. 2007. Pathways involved in gut mucosal barrier dysfunction induced in adult rats by maternal deprivation: corticotrophin-releasing factor and nerve growth factor interplay. *J Physiol,* 580**,** 347-56.

BATES, J. M., MITTGE, E., KUHLMAN, J., BADEN, K. N., CHEESMAN, S. E. & GUILLEMIN, K. 2006. Distinct signals from the microbiota promote different aspects of zebrafish gut differentiation. *Dev Biol,* 297**,** 374-86.

BATISTA, T. M., MARQUES, E. T., JR., FRANCO, G. R. & DOURADINHA, B. 2014. Draft Genome Sequence of the Probiotic Yeast Saccharomyces cerevisiae var. boulardii Strain ATCC MYA-796. *Genome Announc,* 2.

BAUER, B. K., ISOM, S. C., SPATE, L. D., WHITWORTH, K. M., SPOLLEN, W. G., BLAKE, S. M., SPRINGER, G. K., MURPHY, C. N. & PRATHER, R. S. 2010. Transcriptional profiling by deep sequencing identifies differences in mRNA transcript abundance in in vivo-derived versus in vitro-cultured porcine blastocyst stage embryos. *Biol Reprod,* 83**,** 791-8.

BAUER, E., METZLER-ZEBELI, B. U., VERSTEGEN, M. W. & MOSENTHIN, R. 2011. Intestinal gene expression in pigs: effects of reduced feed intake during weaning and potential impact of dietary components. *Nutr Res Rev,* 24**,** 155-75.

BAZAN, J. F., BACON, K. B., HARDIMAN, G., WANG, W., SOO, K., ROSSI, D., GREAVES, D. R., ZLOTNIK, A. & SCHALL, T. J. 1997. A new class of membrane-bound chemokine with a CX3C motif. *Nature,* 385**,** 640-4.

BEGUE, B., WAJANT, H., BAMBOU, J. C., DUBUQUOY, L., SIEGMUND, D., BEAULIEU, J. F., CANIONI, D., BERREBI, D., BROUSSE, N., DESREUMAUX, P., SCHMITZ, J., LENTZE, M. J., GOULET, O., CERF-BENSUSSAN, N. & RUEMMELE,

F. M. 2006. Implication of TNF-related apoptosis-inducing ligand in inflammatory intestinal epithelial lesions. *Gastroenterology,* 130**,** 1962-74.

BENJAMINI, Y. & HOCHBERG, Y. 1995. Controlling the False Discovery Rate: A Practical and Powerful Approach to Multiple Testing. *Journal of the Royal Statistical Society. Series B (Methodological),* 57**,** 289-300.

BENTLEY, D. R. 2006. Whole-genome re-sequencing. *Curr Opin Genet Dev,* 16**,** 545-52.

BERCIK, P., PARK, A. J., SINCLAIR, D., KHOSHDEL, A., LU, J., HUANG, X., DENG, Y., BLENNERHASSETT, P. A., FAHNESTOCK, M., MOINE, D., BERGER, B., HUIZINGA, J. D., KUNZE, W., MCLEAN, P. G., BERGONZELLI, G. E., COLLINS, S. M. & VERDU, E. F. 2011. The anxiolytic effect of Bifidobacterium longum NCC3001 involves vagal pathways for gut-brain communication. *Neurogastroenterol Motil,* 23**,** 1132-9.

BERG, R., BERNASCONI, P., FOWLER, D. & GAUTREAUX, M. 1993. Inhibition of Candida albicans translocation from the gastrointestinal tract of mice by oral administration of Saccharomyces boulardii. *J Infect Dis,* 168**,** 1314-8.

BERIN, M. C., DWINELL, M. B., ECKMANN, L. & KAGNOFF, M. F. 2001. Production of MDC/CCL22 by human intestinal epithelial cells. *Am J Physiol Gastrointest Liver Physiol,* 280**,** G1217-26.

BERTELSEN, R. J., JENSEN, E. T. & RINGEL-KULKA, T. 2016. Use of probiotics and prebiotics in infant feeding. *Best Pract Res Clin Gastroenterol,* 30**,** 39-48.

BESEDOVSKY, H., DEL REY, A., SORKIN, E. & DINARELLO, C. A. 1986. Immunoregulatory feedback between interleukin-1 and glucocorticoid hormones. *Science,* 233**,** 652-4.

BEVERLEY, P. C. 1997. Vaccine immunity. *Immunol Today,* 18**,** 413-5.

BICKSTON, S. J. & COMINELLI, F. 2000. Recombinant interleukin 10 for the treatment of active Crohn's disease: lessons in biologic therapy. *Gastroenterology,* 119**,** 1781-3.

BILEZIKJIAN, L. M. & VALE, W. W. 1983. Glucocorticoids inhibit corticotropin-releasing factor-induced production of adenosine 3',5'-monophosphate in cultured anterior pituitary cells. *Endocrinology,* 113**,** 657-62.

BIRCHENOUGH, G. M., JOHANSSON, M. E., GUSTAFSSON, J. K., BERGSTROM, J. H. & HANSSON, G. C. 2015. New developments in goblet cell mucus secretion and function. *Mucosal Immunol,* 8**,** 712-9.

BIRNBAUMER, M. 2000. Vasopressin receptors. *Trends Endocrinol Metab,* 11**,** 406-10.

BISCHOFF, L., ALVAREZ, S., DAI, D. L., SOUKHATCHEVA, G., ORBAN, P. C. & VERCHERE, C. B. 2015. Cellular mechanisms of CCL22-mediated attenuation of autoimmune diabetes. *J Immunol,* 194**,** 3054-64.

BLACK, R. A., RAUCH, C. T., KOZLOSKY, C. J., PESCHON, J. J., SLACK, J. L., WOLFSON, M. F., CASTNER, B. J., STOCKING, K. L., REDDY, P., SRINIVASAN, S., NELSON, N., BOIANI, N., SCHOOLEY, K. A., GERHART, M., DAVIS, R., FITZNER, J. N., JOHNSON, R. S., PAXTON, R. J., MARCH, C. J. & CERRETTI, D. P. 1997. A metalloproteinase disintegrin that releases tumour-necrosis factor-alpha from cells. *Nature,* 385**,** 729-33.

BLECHA, F., POLLMANN, D. S. & NICHOLS, D. A. 1983. Weaning pigs at an early age decreases cellular immunity. *J Anim Sci,* 56**,** 396-400.

BLIKSLAGER, A. T., ROBERTS, M. C., RHOADS, J. M. & ARGENZIO, R. A. 1997. Is reperfusion injury an important cause of mucosal damage after porcine intestinal ischemia? *Surgery,* 121**,** 526-34.

BLOOM, P. D. & BOEDEKER, E. C. 1996. Mucosal immune responses to intestinal bacterial pathogens. *Semin Gastrointest Dis,* 7**,** 151-66.

BOECKXSTAENS, G. 2015. Mast cells and inflammatory bowel disease. *Curr Opin Pharmacol,* 25**,** 45-9.

BOES, M. 2000. Role of natural and immune IgM antibodies in immune responses. *Mol Immunol,* 37**,** 1141-9.

BOLGER, M. S., ROSS, D. S., JIANG, H., FRANK, M. M., GHIO, A. J., SCHWARTZ, D. A. & WRIGHT, J. R. 2007. Complement levels and activity in the normal and LPS-injured lung. *Am J Physiol Lung Cell Mol Physiol,* 292**,** L748-59.

BOMBA, L., MINUTI, A., MOISA, S. J., TREVISI, E., EUFEMI, E., LIZIER, M., CHEGDANI, F., LUCCHINI, F., RZEPUS, M., PRANDINI, A., ROSSI, F., MAZZA, R., BERTONI, G., LOOR, J. J. & AJMONE-MARSAN, P. 2014. Gut response induced by weaning in piglet features marked changes in immune and inflammatory response. *Funct Integr Genomics,* 14**,** 657-71.

BORASCHI, D., LUCCHESI, D., HAINZL, S., LEITNER, M., MAIER, E., MANGELBERGER, D., OOSTINGH, G. J., PFALLER, T., PIXNER, C., POSSELT, G., ITALIANI, P., NOLD, M. F., NOLD-PETRY, C. A., BUFLER, P. & DINARELLO, C. A. 2011. IL-37: a new anti-inflammatory cytokine of the IL-1 family. *Eur Cytokine Netw,* 22**,** 127-47.

BORODY, T., FISCHER, M., MITCHELL, S. & CAMPBELL, J. 2015. Fecal microbiota transplantation in gastrointestinal disease: 2015 update and the road ahead. *Expert Rev Gastroenterol Hepatol,* 9**,** 1379-91.

BOUDRY, G., LALLES, J. P., MALBERT, C. H., BOBILLIER, E. & SEVE, B. 2002. Diet-related adaptation of the small intestine at weaning in pigs is functional rather than structural. *J Pediatr Gastroenterol Nutr,* 34**,** 180-7.

BOUDRY, G., PERON, V., LE HUEROU-LURON, I., LALLES, J. P. & SEVE, B. 2004. Weaning induces both transient and long-lasting modifications of absorptive, secretory, and barrier properties of piglet intestine. *J Nutr,* 134**,** 2256-62.

BOYER, P. E., D'COSTA, S., EDWARDS, L. L., MILLOWAY, M., SUSICK, E., BORST, L. B., THAKUR, S., CAMPBELL, J. M., CRENSHAW, J. D., POLO, J. & MOESER, A. J. 2015. Early-life dietary spray-dried plasma influences immunological and intestinal injury responses to later-life Salmonella typhimurium challenge. *Br J Nutr,* 113**,** 783-93.

BRADDING, P. 2009. Human lung mast cell heterogeneity. *Thorax,* 64**,** 278-80.

BRANDT-BOHNE, U., KEENE, D. R., WHITE, F. A. & KOCH, M. 2007. MEGF9: a novel transmembrane protein with a strong and developmentally regulated expression in the nervous system. *Biochem J,* 401**,** 447-57.

BRAY, N. L., PIMENTEL, H., MELSTED, P. & PACHTER, L. 2016. Near-optimal probabilistic RNA-seq quantification. *Nat Biotechnol,* 34**,** 525-7.

BROUSSEAU, J. P., TALBOT, G., BEAUDOIN, F., LAUZON, K., ROY, D. & LESSARD, M. 2015. Effects of probiotics Pediococcus acidilactici strain MA18/5M and Saccharomyces cerevisiae subsp. boulardii strain SB-CNCM I-1079 on fecal and intestinal microbiota of nursing and weanling piglets. *J Anim Sci,* 93**,** 5313-26.

BRUBAKER, S. W., BONHAM, K. S., ZANONI, I. & KAGAN, J. C. 2015. Innate immune pattern recognition: a cell biological perspective. *Annu Rev Immunol,* 33**,** 257-90.

BRUGMANN, S. A. & WELLS, J. M. 2013. Building additional complexity to in vitro-derived intestinal tissues. *Stem Cell Res Ther,* 4 Suppl 1**,** S1.

BRUHN, T. O., ENGELAND, W. C., ANTHONY, E. L., GANN, D. S. & JACKSON, I. M. 1987. Corticotropin-releasing factor in the adrenal medulla. *Ann N Y Acad Sci,* 512**,** 115-28.

BRUN, P., SCARPA, M., MARCHIORI, C., SARASIN, G., CAPUTI, V., PORZIONATO, A., GIRON, M. C., PALU, G. & CASTAGLIUOLO, I. 2017. Saccharomyces boulardii CNCM I-745 supplementation reduces gastrointestinal dysfunction in an animal model of IBS. *PLoS One,* 12**,** e0181863.

BUCKLEY, M. M., O'HALLORAN, K. D., RAE, M. G., DINAN, T. G. & O'MALLEY, D. 2014. Modulation of enteric neurons by interleukin-6 and corticotropin-releasing factor contributes to visceral hypersensitivity and altered colonic motility in a rat model of irritable bowel syndrome. *J Physiol,* 592**,** 5235-50.

BUENO, L. & FIORAMONTI, J. 1986. Effects of corticotropin-releasing factor, corticotropin and cortisol on gastrointestinal motility in dogs. *Peptides,* 7**,** 73-7.

BUHNER, S., LI, Q., VIGNALI, S., BARBARA, G., DE GIORGIO, R., STANGHELLINI, V., CREMON, C., ZELLER, F., LANGER, R., DANIEL, H., MICHEL, K. & SCHEMANN, M. 2009. Activation of human enteric neurons by supernatants of colonic biopsy specimens from patients with irritable bowel syndrome. *Gastroenterology,* 137**,** 1425-34.

BUHNER, S. & SCHEMANN, M. 2012. Mast cell-nerve axis with a focus on the human gut. *Biochim Biophys Acta,* 1822**,** 85-92.

BURGESS, D. J. 2016. Gene expression: A space for transcriptomics. *Nat Rev Genet,* 17**,** 436-7.

BURKEY, T. E., SKJOLAAS, K. A., DRITZ, S. S. & MINTON, J. E. 2007. Expression of Toll-like receptors, interleukin 8, macrophage migration inhibitory factor, and osteopontin in tissues from pigs challenged with Salmonella enterica serovar Typhimurium or serovar Choleraesuis. *Vet Immunol Immunopathol,* 115**,** 309-19.

BURKEY, T. E., SKJOLAAS, K. A. & MINTON, J. E. 2009. Board-invited review: porcine mucosal immunity of the gastrointestinal tract. *J Anim Sci,* 87**,** 1493-501.

BUTLER, J. E., LAGER, K. M., SPLICHAL, I., FRANCIS, D., KACSKOVICS, I., SINKORA, M., WERTZ, N., SUN, J., ZHAO, Y., BROWN, W. R., DEWALD, R., DIERKS, S., MUYLDERMANS, S., LUNNEY, J. K., MCCRAY, P. B., ROGERS, C. S., WELSH, M. J., NAVARRO, P., KLOBASA, F., HABE, F. & RAMSOONDAR, J. 2009. The piglet as a model for B cell and immune system development. *Vet Immunol Immunopathol,* 128**,** 147-70.

BUTLER, J. E., WEBER, P., SINKORA, M., SUN, J., FORD, S. J. & CHRISTENSON, R. K. 2000. Antibody repertoire development in fetal and neonatal piglets. II. Characterization of heavy chain

complementarity-determining region 3 diversity in the developing fetus. *J Immunol,* 165**,** 6999-7010.

BUTS, J. P., BERNASCONI, P., VAERMAN, J. P. & DIVE, C. 1990. Stimulation of secretory IgA and secretory component of immunoglobulins in small intestine of rats treated with Saccharomyces boulardii. *Dig Dis Sci,* 35**,** 251-6.

BUTS, J. P., DEKEYSER, N., STILMANT, C., DELEM, E., SMETS, F. & SOKAL, E. 2006. Saccharomyces boulardii produces in rat small intestine a novel protein phosphatase that inhibits Escherichia coli endotoxin by dephosphorylation. *Pediatr Res,* 60**,** 24-9.

CAIRNS, J. A. & WALLS, A. F. 1997. Mast cell tryptase stimulates the synthesis of type I collagen in human lung fibroblasts. *J Clin Invest,* 99**,** 1313-21.

CAMPBELL, J. M., CRENSHAW, J. D. & POLO, J. 2013. The biological stress of early weaned piglets. *J Anim Sci Biotechnol,* 4**,** 19.

CARAMORI, G. & ADCOCK, I. 2005. Anti-inflammatory mechanisms of glucocorticoids targeting granulocytes. *Curr Drug Targets Inflamm Allergy,* 4**,** 455-63.

CARDOSO, T. F., CANOVAS, A., CANELA-XANDRI, O., GONZALEZ-PRENDES, R., AMILLS, M. & QUINTANILLA, R. 2017a. RNA-seq based detection of differentially expressed genes in the skeletal muscle of Duroc pigs with distinct lipid profiles. *Sci Rep,* 7**,** 40005.

CARDOSO, T. F., QUINTANILLA, R., TIBAU, J., GIL, M., MARMOL-SANCHEZ, E., GONZALEZ-RODRIGUEZ, O., GONZALEZ-PRENDES, R. & AMILLS, M. 2017b. Nutrient supply affects the mRNA expression profile of the porcine skeletal muscle. *BMC Genomics,* 18**,** 603.

CARNEIRO, M. O., RUSS, C., ROSS, M. G., GABRIEL, S. B., NUSBAUM, C. & DEPRISTO, M. A. 2012. Pacific biosciences sequencing technology for genotyping and variation discovery in human data. *BMC Genomics,* 13**,** 375.

CASEY, P. G., GARDINER, G. E., CASEY, G., BRADSHAW, B., LAWLOR, P. G., LYNCH, P. B., LEONARD, F. C., STANTON, C., ROSS, R. P., FITZGERALD, G. F. & HILL, C. 2007. A five-strain probiotic combination reduces pathogen shedding and alleviates disease signs in pigs challenged with Salmonella enterica Serovar Typhimurium. *Appl Environ Microbiol,* 73**,** 1858-63.

CASTAGLIUOLO, I., RIEGLER, M. F., VALENICK, L., LAMONT, J. T. & POTHOULAKIS, C. 1999. Saccharomyces boulardii

protease inhibits the effects of Clostridium difficile toxins A and B in human colonic mucosa. *Infect Immun,* 67**,** 302-7.

CASTILLO, M., MARTIN-ORUE, S. M., NOFRARIAS, M., MANZANILLA, E. G. & GASA, J. 2007. Changes in caecal microbiota and mucosal morphology of weaned pigs. *Vet Microbiol,* 124**,** 239-47.

CATASSI, C., BONUCCI, A., COPPA, G. V., CARLUCCI, A. & GIORGI, P. L. 1995. Intestinal permeability changes during the first month: effect of natural versus artificial feeding. *J Pediatr Gastroenterol Nutr,* 21**,** 383-6.

CAVACINI, L. A., KUHRT, D., DUVAL, M., MAYER, K. & POSNER, M. R. 2003. Binding and neutralization activity of human IgG1 and IgG3 from serum of HIV-infected individuals. *AIDS Res Hum Retroviruses,* 19**,** 785-92.

CHANG, C. P., PEARSE, R. V., 2ND, O'CONNELL, S. & ROSENFELD, M. G. 1993. Identification of a seven transmembrane helix receptor for corticotropin-releasing factor and sauvagine in mammalian brain. *Neuron,* 11**,** 1187-95.

CHATZAKI, E., CROWE, P. D., WANG, L., MILLION, M., TACHE, Y. & GRIGORIADIS, D. E. 2004. CRF receptor type 1 and 2 expression and anatomical distribution in the rat colon. *J Neurochem,* 90**,** 309-16.

CHE, L., CHEN, H., YU, B., HE, J., ZHENG, P., MAO, X., YU, J., HUANG, Z. & CHEN, D. 2014. Long-term intake of pea fiber affects colonic barrier function, bacterial and transcriptional profile in pig model. *Nutr Cancer,* 66**,** 388-99.

CHEN, C., AI, H., REN, J., LI, W., LI, P., QIAO, R., OUYANG, J., YANG, M., MA, J. & HUANG, L. 2011. A global view of porcine transcriptome in three tissues from a full-sib pair with extreme phenotypes in growth and fat deposition by paired-end RNA sequencing. *BMC Genomics,* 12**,** 448.

CHEN, G., SHAW, M. H., KIM, Y. G. & NUNEZ, G. 2009. NOD-like receptors: role in innate immunity and inflammatory disease. *Annu Rev Pathol,* 4**,** 365-98.

CHEN, H., MAO, X., HE, J., YU, B., HUANG, Z., YU, J., ZHENG, P. & CHEN, D. 2013. Dietary fibre affects intestinal mucosal barrier function and regulates intestinal bacteria in weaning piglets. *Br J Nutr,* 110**,** 1837-48.

CHEN, P., BOWMAN, A. B., MUKHOPADHYAY, S. & ASCHNER, M. 2015. SLC30A10: A novel manganese transporter. *Worm,* 4**,** e1042648.

CHEN, R., LEWIS, K. A., PERRIN, M. H. & VALE, W. W. 1993. Expression cloning of a human corticotropin-releasing-factor receptor. *Proc Natl Acad Sci U S A,* 90**,** 8967-71.

CHING, T., HUANG, S. & GARMIRE, L. X. 2014. Power analysis and sample size estimation for RNA-Seq differential expression. *RNA,* 20**,** 1684-96.

CLARKE, C. J., HALES, A., HUNT, A. & FOXWELL, B. M. 1998. IL-10-mediated suppression of TNF-alpha production is independent of its ability to inhibit NF kappa B activity. *Eur J Immunol,* 28**,** 1719-26.

COLLIER, C. T., CARROLL, J. A., BALLOU, M. A., STARKEY, J. D. & SPARKS, J. C. 2011. Oral administration of Saccharomyces cerevisiae boulardii reduces mortality associated with immune and cortisol responses to Escherichia coli endotoxin in pigs. *J Anim Sci,* 89**,** 52-8.

COMPEAU, P. E., PEVZNER, P. A. & TESLER, G. 2011. How to apply de Bruijn graphs to genome assembly. *Nat Biotechnol,* 29**,** 987-91.

CONESA, A., MADRIGAL, P., TARAZONA, S., GOMEZ-CABRERO, D., CERVERA, A., MCPHERSON, A., SZCZESNIAK, M. W., GAFFNEY, D. J., ELO, L. L., ZHANG, X. & MORTAZAVI, A. 2016. A survey of best practices for RNA-seq data analysis. *Genome Biol,* 17**,** 13.

CONSTANTIN, G., MAJEED, M., GIAGULLI, C., PICCIO, L., KIM, J. Y., BUTCHER, E. C. & LAUDANNA, C. 2000. Chemokines trigger immediate beta2 integrin affinity and mobility changes: differential regulation and roles in lymphocyte arrest under flow. *Immunity,* 13**,** 759-69.

CONSTANTINO, J., GOMES, C., FALCAO, A., NEVES, B. M. & CRUZ, M. T. 2017. Dendritic cell-based immunotherapy: a basic review and recent advances. *Immunol Res*.

COOMBES, J. L. & POWRIE, F. 2008. Dendritic cells in intestinal immune regulation. *Nat Rev Immunol,* 8**,** 435-46.

COSTE, S. C., KESTERSON, R. A., HELDWEIN, K. A., STEVENS, S. L., HEARD, A. D., HOLLIS, J. H., MURRAY, S. E., HILL, J. K., PANTELY, G. A., HOHIMER, A. R., HATTON, D. C., PHILLIPS, T. J., FINN, D. A., LOW, M. J., RITTENBERG, M. B., STENZEL, P. & STENZEL-POORE, M. P. 2000. Abnormal adaptations to stress and impaired cardiovascular function in mice lacking corticotropin-releasing hormone receptor-2. *Nat Genet,* 24**,** 403-9.

COUPER, K. N., BLOUNT, D. G. & RILEY, E. M. 2008. IL-10: the master regulator of immunity to infection. *J Immunol,* 180**,** 5771-7.

CRAWFORD, M. & DAGNINO, L. 2017. Scaffolding proteins in the development and maintenance of the epidermal permeability barrier. *Tissue Barriers***,** e1341969.

CRISP, S. J., KULLMANN, D. M. & VINCENT, A. 2016. Autoimmune synaptopathies. *Nat Rev Neurosci,* 17**,** 103-17.

CRIVELLATO, E. & RIBATTI, D. 2010. The mast cell: an evolutionary perspective. *Biol Rev Camb Philos Soc,* 85**,** 347-60.

CULLEN, M. J., LING, N., FOSTER, A. C. & PELLEYMOUNTER, M. A. 2001. Urocortin, corticotropin releasing factor-2 receptors and energy balance. *Endocrinology,* 142**,** 992-9.

CZERUCKA, D., DAHAN, S., MOGRABI, B., ROSSI, B. & RAMPAL, P. 2000. Saccharomyces boulardii preserves the barrier function and modulates the signal transduction pathway induced in enteropathogenic Escherichia coli-infected T84 cells. *Infect Immun,* 68**,** 5998-6004.

CZERUCKA, D., PICHE, T. & RAMPAL, P. 2007. Review article: yeast as probiotics -- Saccharomyces boulardii. *Aliment Pharmacol Ther,* 26**,** 767-78.

CZERUCKA, D., ROUX, I. & RAMPAL, P. 1994. Saccharomyces boulardii inhibits secretagogue-mediated adenosine 3',5'-cyclic monophosphate induction in intestinal cells. *Gastroenterology,* 106**,** 65-72.

D'ARGENIO, V. & SALVATORE, F. 2015. The role of the gut microbiome in the healthy adult status. *Clin Chim Acta,* 451**,** 97-102.

DA SILVA, E. Z., JAMUR, M. C. & OLIVER, C. 2014. Mast cell function: a new vision of an old cell. *J Histochem Cytochem,* 62**,** 698-738.

DAHAN, S., DALMASSO, G., IMBERT, V., PEYRON, J. F., RAMPAL, P. & CZERUCKA, D. 2003. Saccharomyces boulardii interferes with enterohemorrhagic Escherichia coli-induced signaling pathways in T84 cells. *Infect Immun,* 71**,** 766-73.

DALLMAN, M. F., AKANA, S. F., CASCIO, C. S., DARLINGTON, D. N., JACOBSON, L. & LEVIN, N. 1987. Regulation of ACTH secretion: variations on a theme of B. *Recent Prog Horm Res,* 43**,** 113-73.

DALMASSO, G., COTTREZ, F., IMBERT, V., LAGADEC, P., PEYRON, J. F., RAMPAL, P., CZERUCKA, D., GROUX, H., FOUSSAT, A. & BRUN, V. 2006. Saccharomyces boulardii

inhibits inflammatory bowel disease by trapping T cells in mesenteric lymph nodes. *Gastroenterology,* 131**,** 1812-25.

DAUDELIN, J. F., LESSARD, M., BEAUDOIN, F., NADEAU, E., BISSONNETTE, N., BOUTIN, Y., BROUSSEAU, J. P., LAUZON, K. & FAIRBROTHER, J. M. 2011. Administration of probiotics influences F4 (K88)-positive enterotoxigenic Escherichia coli attachment and intestinal cytokine expression in weaned pigs. *Vet Res,* 42**,** 69.

DAUTZENBERG, F. M. & HAUGER, R. L. 2002. The CRF peptide family and their receptors: yet more partners discovered. *Trends Pharmacol Sci,* 23**,** 71-7.

DAUTZENBERG, F. M., KILPATRICK, G. J., HAUGER, R. L. & MOREAU, J. 2001. Molecular biology of the CRH receptors-- in the mood. *Peptides,* 22**,** 753-60.

DAYNES, R. A., ARANEO, B. A., DOWELL, T. A., HUANG, K. & DUDLEY, D. 1990. Regulation of murine lymphokine production in vivo. III. The lymphoid tissue microenvironment exerts regulatory influences over T helper cell function. *J Exp Med,* 171**,** 979-96.

DE QUELEN, F., CHEVALIER, J., ROLLI-DERKINDEREN, M., MOUROT, J., NEUNLIST, M. & BOUDRY, G. 2011. n-3 polyunsaturated fatty acids in the maternal diet modify the postnatal development of nervous regulation of intestinal permeability in piglets. *J Physiol,* 589**,** 4341-52.

DEL COCO, V. F., SPARO, M. D., SIDOTI, A., SANTIN, M., BASUALDO, J. A. & CORDOBA, M. A. 2016. Effects of Enterococcus faecalis CECT 7121 on Cryptosporidium parvum infection in mice. *Parasitol Res*.

DERETIC, V., SAITOH, T. & AKIRA, S. 2013. Autophagy in infection, inflammation and immunity. *Nat Rev Immunol,* 13**,** 722-37.

DICKENSHEETS, H. L., FREEMAN, S. L., SMITH, M. F. & DONNELLY, R. P. 1997. Interleukin-10 upregulates tumor necrosis factor receptor type-II (p75) gene expression in endotoxin-stimulated human monocytes. *Blood,* 90**,** 4162-71.

DINAN, T. G. & CRYAN, J. F. 2016. Microbes, Immunity and Behaviour: Psychoneuroimmunology Meets the Microbiome. *Neuropsychopharmacology*.

DINARELLO, C. A. 2009. Immunological and inflammatory functions of the interleukin-1 family. *Annu Rev Immunol,* 27**,** 519-50.

DING, L., YANG, L., WANG, Z. & HUANG, W. 2015. Bile acid nuclear receptor FXR and digestive system diseases. *Acta Pharm Sin B,* 5**,** 135-44.

DING, P. H. & JIN, L. J. 2014. The role of lipopolysaccharide-binding protein in innate immunity: a revisit and its relevance to oral/periodontal health. *J Periodontal Res,* 49**,** 1-9.

DO, C. H. 2012. Estimation of weaning age effects on growth performance in berkshire pigs. *Asian-Australas J Anim Sci,* 25**,** 151-62.

DO NASCIMENTO, N. C., GUIMARAES, A. M. S., DOS SANTOS, A. P., CHU, Y., MARQUES, L. M. & MESSICK, J. B. 2018. RNA-Seq based transcriptome of whole blood from immunocompetent pigs (Sus scrofa) experimentally infected with Mycoplasma suis strain Illinois. *Vet Res,* 49**,** 49.

DOBSON, A., COTTER, P. D., ROSS, R. P. & HILL, C. 2012. Bacteriocin production: a probiotic trait? *Appl Environ Microbiol,* 78**,** 1-6.

DOCKE, W. D., RANDOW, F., SYRBE, U., KRAUSCH, D., ASADULLAH, K., REINKE, P., VOLK, H. D. & KOX, W. 1997. Monocyte deactivation in septic patients: restoration by IFN-gamma treatment. *Nat Med,* 3**,** 678-81.

DRUMMOND, R. A. & BROWN, G. D. 2011. The role of Dectin-1 in the host defence against fungal infections. *Curr Opin Microbiol,* 14**,** 392-9.

DUMBELL, R., MATVEEVA, O. & OSTER, H. 2016. Circadian Clocks, Stress, and Immunity. *Front Endocrinol (Lausanne),* 7**,** 37.

DUNNE, C. 2001. Adaptation of bacteria to the intestinal niche: probiotics and gut disorder. *Inflamm Bowel Dis,* 7**,** 136-45.

EKKEL, E. D., DIELEMAN, S. J., SCHOUTEN, W. G., PORTELA, A., CORNELISSEN, G., TIELEN, M. J. & HALBERG, F. 1996. The circadian rhythm of cortisol in the saliva of young pigs. *Physiol Behav,* 60**,** 985-9.

ELHUSSEIN MOHAMED, O. Y., ELAZOMI, A., MOHAMED, M. S. & ABDALLA, F. B. 2016. Local elevation of CCL22: A new trend in immunotherapy (skin model). *Journal of Cellular Immunotherapy,* 2**,** 79-84.

ESTEVE-CODINA, A., KOFLER, R., PALMIERI, N., BUSSOTTI, G., NOTREDAME, C. & PEREZ-ENCISO, M. 2011. Exploring the gonad transcriptome of two extreme male pigs with RNA-seq. *BMC Genomics,* 12**,** 552.

EVRENSEL, A. & CEYLAN, M. E. 2015. The Gut-Brain Axis: The Missing Link in Depression. *Clin Psychopharmacol Neurosci,* 13**,** 239-44.

FARMER, C. & QUESNEL, H. 2009. Nutritional, hormonal, and environmental effects on colostrum in sows. *J Anim Sci,* 87**,** 56-64.

FAWZY, A., ARPADI, S., KANKASA, C., SINKALA, M., MWIYA, M., THEA, D. M., ALDROVANDI, G. M. & KUHN, L. 2011. Early weaning increases diarrhea morbidity and mortality among uninfected children born to HIV-infected mothers in Zambia. *J Infect Dis,* 203**,** 1222-30.

FINE, A. & GOLDSTEIN, R. H. 1987. The effect of transforming growth factor-beta on cell proliferation and collagen formation by lung fibroblasts. *J Biol Chem,* 262**,** 3897-902.

FINOTELLO, F. & DI CAMILLO, B. 2015. Measuring differential gene expression with RNA-seq: challenges and strategies for data analysis. *Brief Funct Genomics,* 14**,** 130-42.

FLORI, L., GAO, Y., LALOE, D., LEMONNIER, G., LEPLAT, J. J., TEILLAUD, A., COSSALTER, A. M., LAFFITTE, J., PINTON, P., DE VAUREIX, C., BOUFFAUD, M., MERCAT, M. J., LEFEVRE, F., OSWALD, I. P., BIDANEL, J. P. & ROGEL-GAILLARD, C. 2011. Immunity traits in pigs: substantial genetic variation and limited covariation. *PLoS One,* 6**,** e22717.

FORSTER, R., DAVALOS-MISSLITZ, A. C. & ROT, A. 2008. CCR7 and its ligands: balancing immunity and tolerance. *Nat Rev Immunol,* 8**,** 362-71.

FOSTER, J. A. & MCVEY NEUFELD, K. A. 2013. Gut-brain axis: how the microbiome influences anxiety and depression. *Trends Neurosci,* 36**,** 305-12.

FRAZEE, A. C., PERTEA, G., JAFFE, A. E., LANGMEAD, B., SALZBERG, S. L. & LEEK, J. T. 2015. Ballgown bridges the gap between transcriptome assembly and expression analysis. *Nat Biotechnol,* 33**,** 243-6.

FREEMAN, T. C., IVENS, A., BAILLIE, J. K., BERALDI, D., BARNETT, M. W., DORWARD, D., DOWNING, A., FAIRBAIRN, L., KAPETANOVIC, R., RAZA, S., TOMOIU, A., ALBERIO, R., WU, C., SU, A. I., SUMMERS, K. M., TUGGLE, C. K., ARCHIBALD, A. L. & HUME, D. A. 2012. A gene expression atlas of the domestic pig. *BMC Biol,* 10**,** 90.

FRESE, S. A., PARKER, K., CALVERT, C. C. & MILLS, D. A. 2015. Diet shapes the gut microbiome of pigs during nursing and weaning. *Microbiome,* 3**,** 28.

FRIEDMANN, E., HAUBEN, E., MAYLANDT, K., SCHLEEGER, S., VREUGDE, S., LICHTENTHALER, S. F., KUHN, P. H., STAUFFER, D., ROVELLI, G. & MARTOGLIO, B. 2006. SPPL2a and SPPL2b promote intramembrane proteolysis of

TNFalpha in activated dendritic cells to trigger IL-12 production. *Nat Cell Biol,* 8**,** 843-8.

FROSALI, S., PAGLIARI, D., GAMBASSI, G., LANDOLFI, R., PANDOLFI, F. & CIANCI, R. 2015. How the Intricate Interaction among Toll-Like Receptors, Microbiota, and Intestinal Immunity Can Influence Gastrointestinal Pathology. *J Immunol Res,* 2015**,** 489821.

FUNKE, B. 2011. Laser microdissection of intestinal epithelial cells and downstream analysis. *Methods Mol Biol,* 755**,** 189-96.

FURUSE, M., FUJITA, K., HIIRAGI, T., FUJIMOTO, K. & TSUKITA, S. 1998. Claudin-1 and -2: novel integral membrane proteins localizing at tight junctions with no sequence similarity to occludin. *J Cell Biol,* 141**,** 1539-50.

FURUSE, M., HIRASE, T., ITOH, M., NAGAFUCHI, A., YONEMURA, S., TSUKITA, S. & TSUKITA, S. 1993. Occludin: a novel integral membrane protein localizing at tight junctions. *J Cell Biol,* 123**,** 1777-88.

GADALETA, R. M., VAN MIL, S. W., OLDENBURG, B., SIERSEMA, P. D., KLOMP, L. W. & VAN ERPECUM, K. J. 2010. Bile acids and their nuclear receptor FXR: Relevance for hepatobiliary and gastrointestinal disease. *Biochim Biophys Acta,* 1801**,** 683-92.

GALLAGHER, N. L., GILES, L. R. & WYNN, P. C. 2002. The development of a circadian pattern of salivary cortisol secretion in the neonatal piglet. *Biol Neonate,* 81**,** 113-8.

GALLI, S. J. & TSAI, M. 2012. IgE and mast cells in allergic disease. *Nat Med,* 18**,** 693-704.

GAMBLE, K. L., BERRY, R., FRANK, S. J. & YOUNG, M. E. 2014. Circadian clock control of endocrine factors. *Nat Rev Endocrinol,* 10**,** 466-75.

GANTNER, B. N., SIMMONS, R. M., CANAVERA, S. J., AKIRA, S. & UNDERHILL, D. M. 2003. Collaborative induction of inflammatory responses by dectin-1 and Toll-like receptor 2. *J Exp Med,* 197**,** 1107-17.

GAREAU, M. G., SHERMAN, P. M. & WALKER, W. A. 2010. Probiotics and the gut microbiota in intestinal health and disease. *Nat Rev Gastroenterol Hepatol,* 7**,** 503-14.

GATTO, M., IACCARINO, L., GHIRARDELLO, A., BASSI, N., PONTISSO, P., PUNZI, L., SHOENFELD, Y. & DORIA, A. 2013. Serpins, immunity and autoimmunity: old molecules, new functions. *Clin Rev Allergy Immunol,* 45**,** 267-80.

GEDEK, B. R. 1999. Adherence of Escherichia coli serogroup O 157 and the Salmonella typhimurium mutant DT 104 to the surface of Saccharomyces boulardii. *Mycoses,* 42**,** 261-4.

GEIJTENBEEK, T. B. & GRINGHUIS, S. I. 2009. Signalling through C-type lectin receptors: shaping immune responses. *Nat Rev Immunol,* 9**,** 465-79.

GEISBERGER, R., LAMERS, M. & ACHATZ, G. 2006. The riddle of the dual expression of IgM and IgD. *Immunology,* 118**,** 429-37.

GEORGE, A. 1996. Generation of gamma interferon responses in murine Peyer's patches following oral immunization. *Infect Immun,* 64**,** 4606-11.

GEWOLB, I. H., SCHWALBE, R. S., TACIAK, V. L., HARRISON, T. S. & PANIGRAHI, P. 1999. Stool microflora in extremely low birthweight infants. *Arch Dis Child Fetal Neonatal Ed,* 80**,** F167-73.

GILFILLAN, A. M. & BEAVEN, M. A. 2011. Regulation of mast cell responses in health and disease. *Crit Rev Immunol,* 31**,** 475-529.

GINSBERG, H. N., LE, N. A., GOLDBERG, I. J., GIBSON, J. C., RUBINSTEIN, A., WANG-IVERSON, P., NORUM, R. & BROWN, W. V. 1986. Apolipoprotein B metabolism in subjects with deficiency of apolipoproteins CIII and AI. Evidence that apolipoprotein CIII inhibits catabolism of triglyceride-rich lipoproteins by lipoprotein lipase in vivo. *J Clin Invest,* 78**,** 1287-95.

GOHEL, M. K., PRAJAPATI, J. B., MUDGAL, S. V., PANDYA, H. V., SINGH, U. S., TRIVEDI, S. S., PHATAK, A. G. & PATEL, R. M. 2016. Effect of Probiotic Dietary Intervention on Calcium and Haematological Parameters in Geriatrics. *J Clin Diagn Res,* 10**,** LC05-9.

GOLI, Y. D. & MONIRI, R. 2016. Efficacy of probiotics as an adjuvant agent in eradication of Helicobacter pylori infection and associated side effects. *Benef Microbes***,** 1-10.

GONZALEZ-MARISCAL, L., BETANZOS, A., NAVA, P. & JARAMILLO, B. E. 2003. Tight junction proteins. *Prog Biophys Mol Biol,* 81**,** 1-44.

GONZALEZ, L. M., MOESER, A. J. & BLIKSLAGER, A. T. 2015. Porcine models of digestive disease: the future of large animal translational research. *Transl Res,* 166**,** 12-27.

GOODWIN, S., MCPHERSON, J. D. & MCCOMBIE, W. R. 2016. Coming of age: ten years of next-generation sequencing technologies. *Nat Rev Genet,* 17**,** 333-51.

GOROSPE, J. R., NISHIKAWA, B. K. & HOFFMAN, E. P. 1996. Recruitment of mast cells to muscle after mild damage. *J Neurol Sci,* 135**,** 10-7.

GOSALBEZ, L. & RAMON, D. 2015. Probiotics in transition: novel strategies. *Trends Biotechnol,* 33**,** 195-6.

GRENHAM, S., CLARKE, G., CRYAN, J. F. & DINAN, T. G. 2011. Brain-gut-microbe communication in health and disease. *Front Physiol,* 2**,** 94.

GRESSE, R., CHAUCHEYRAS-DURAND, F., FLEURY, M. A., VAN DE WIELE, T., FORANO, E. & BLANQUET-DIOT, S. 2017. Gut Microbiota Dysbiosis in Postweaning Piglets: Understanding the Keys to Health. *Trends Microbiol,* 25**,** 851-873.

GROER, M. W., LUCIANO, A. A., DISHAW, L. J., ASHMEADE, T. L., MILLER, E. & GILBERT, J. A. 2014. Development of the preterm infant gut microbiome: a research priority. *Microbiome,* 2**,** 38.

GROSCHWITZ, K. R. & HOGAN, S. P. 2009. Intestinal barrier function: molecular regulation and disease pathogenesis. *J Allergy Clin Immunol,* 124**,** 3-20; quiz 21-2.

GRUBER, B. L., KEW, R. R., JELASKA, A., MARCHESE, M. J., GARLICK, J., REN, S., SCHWARTZ, L. B. & KORN, J. H. 1997. Human mast cells activate fibroblasts: tryptase is a fibrogenic factor stimulating collagen messenger ribonucleic acid synthesis and fibroblast chemotaxis. *J Immunol,* 158**,** 2310-7.

GUE, M., FIORAMONTI, J., FREXINOS, J., ALVINERIE, M. & BUENO, L. 1987. Influence of acoustic stress by noise on gastrointestinal motility in dogs. *Dig Dis Sci,* 32**,** 1411-7.

GUE, M., JUNIEN, J. L. & BUENO, L. 1991. Conditioned emotional response in rats enhances colonic motility through the central release of corticotropin-releasing factor. *Gastroenterology,* 100**,** 964-70.

GUNAWAN, A., SAHADEVAN, S., NEUHOFF, C., GROSSE-BRINKHAUS, C., GAD, A., FRIEDEN, L., TESFAYE, D., THOLEN, E., LOOFT, C., UDDIN, M. J., SCHELLANDER, K. & CINAR, M. U. 2013. RNA deep sequencing reveals novel candidate genes and polymorphisms in boar testis and liver tissues with divergent androstenone levels. *PLoS One,* 8**,** e63259.

GUPTA, S. 2002. Tumor necrosis factor-alpha-induced apoptosis in T cells from aged humans: a role of TNFR-I and downstream signaling molecules. *Exp Gerontol,* 37**,** 293-9.

HALL, D. A., BERESFORD, I. J., BROWNING, C. & GILES, H. 1999. Signalling by CXC-chemokine receptors 1 and 2 expressed in CHO cells: a comparison of calcium mobilization, inhibition of

adenylyl cyclase and stimulation of GTPgammaS binding induced by IL-8 and GROalpha. *Br J Pharmacol,* 126**,** 810-8.

HAMILTON, M. J., FREI, S. M. & STEVENS, R. L. 2014. The multifaceted mast cell in inflammatory bowel disease. *Inflamm Bowel Dis,* 20**,** 2364-78.

HAMMON, H. M., FRIETEN, D., GERBERT, C., KOCH, C., DUSEL, G., WEIKARD, R. & KUHN, C. 2018. Different milk diets have substantial effects on the jejunal mucosal immune system of pre-weaning calves, as demonstrated by whole transcriptome sequencing. *Sci Rep,* 8**,** 1693.

HAMMOND, M. E., LAPOINTE, G. R., FEUCHT, P. H., HILT, S., GALLEGOS, C. A., GORDON, C. A., GIEDLIN, M. A., MULLENBACH, G. & TEKAMP-OLSON, P. 1995. IL-8 induces neutrophil chemotaxis predominantly via type I IL-8 receptors. *J Immunol,* 155**,** 1428-33.

HANCOX, L. R., LE BON, M., RICHARDS, P. J., GUILLOU, D., DODD, C. E. & MELLITS, K. H. 2015. Effect of a single dose of Saccharomyces cerevisiae var. boulardii on the occurrence of porcine neonatal diarrhoea. *Animal,* 9**,** 1756-9.

HANSEN, K. D., BRENNER, S. E. & DUDOIT, S. 2010. Biases in Illumina transcriptome sequencing caused by random hexamer priming. *Nucleic Acids Res,* 38**,** e131.

HARDCASTLE, T. J. & KELLY, K. A. 2010. baySeq: empirical Bayesian methods for identifying differential expression in sequence count data. *BMC Bioinformatics,* 11**,** 422.

HARDIN, J. A. 2005. Dendritic cells: potential triggers of autoimmunity and targets for therapy. *Ann Rheum Dis,* 64 Suppl 4**,** iv86-90.

HART, S. N., THERNEAU, T. M., ZHANG, Y., POLAND, G. A. & KOCHER, J. P. 2013. Calculating sample size estimates for RNA sequencing data. *J Comput Biol,* 20**,** 970-8.

HAUGSTETTER, J., BLICHER, T. & ELLGAARD, L. 2005. Identification and characterization of a novel thioredoxin-related transmembrane protein of the endoplasmic reticulum. *J Biol Chem,* 280**,** 8371-80.

HAY, M., ORGEUR, P., LEVY, F., LE DIVIDICH, J., CONCORDET, D., NOWAK, R., SCHAAL, B. & MORMEDE, P. 2001. Neuroendocrine consequences of very early weaning in swine. *Physiol Behav,* 72**,** 263-9.

HAYAKAWA, T., MASUDA, T., KUROSAWA, D. & TSUKAHARA, T. 2016. Dietary administration of probiotics to sows and/or their neonates improves the reproductive performance, incidence of post-weaning diarrhea and histopathological parameters in the intestine of weaned piglets. *Anim Sci J,* 87**,** 1501-1510.

HAYASHI, F., SMITH, K. D., OZINSKY, A., HAWN, T. R., YI, E. C., GOODLETT, D. R., ENG, J. K., AKIRA, S., UNDERHILL, D. M. & ADEREM, A. 2001. The innate immune response to bacterial flagellin is mediated by Toll-like receptor 5. *Nature,* 410**,** 1099-103.

HE, L., ZHOU, X., HUANG, N., LI, H., CUI, Z., TIAN, J., JIANG, Q., LIU, S., WU, J., LI, T., YAO, K. & YIN, Y. 2017. Administration of alpha-ketoglutarate improves epithelial restitution under stress injury in early-weaning piglets. *Oncotarget,* 8**,** 91965-91978.

HEGARTY, J. W., GUINANE, C. M., ROSS, R. P., HILL, C. & COTTER, P. D. 2016. Bacteriocin production: a relatively unharnessed probiotic trait? *F1000Res,* 5**,** 2587.

HEIL, F., AHMAD-NEJAD, P., HEMMI, H., HOCHREIN, H., AMPENBERGER, F., GELLERT, T., DIETRICH, H., LIPFORD, G., TAKEDA, K., AKIRA, S., WAGNER, H. & BAUER, S. 2003. The Toll-like receptor 7 (TLR7)-specific stimulus loxoribine uncovers a strong relationship within the TLR7, 8 and 9 subfamily. *Eur J Immunol,* 33**,** 2987-97.

HERFARTH, H. & SCHOLMERICH, J. 2002. IL-10 therapy in Crohn's disease: at the crossroads. Treatment of Crohn's disease with the anti-inflammatory cytokine interleukin 10. *Gut,* 50**,** 146-7.

HERICH, R., LEVKUT, M., BOMBA, A., GANCARCIKOVA, S. & NEMCOVA, R. 2004. Differences in the development of the small intestine between gnotobiotic and conventionally bred piglets. *Berl Munch Tierarztl Wochenschr,* 117**,** 46-51.

HICKSON, M. 2011. Probiotics in the prevention of antibiotic-associated diarrhoea and Clostridium difficile infection. *Therap Adv Gastroenterol,* 4**,** 185-97.

HILL, D. A. & ARTIS, D. 2010. Intestinal bacteria and the regulation of immune cell homeostasis. *Annu Rev Immunol,* 28**,** 623-67.

HOLGATE, S. T. 2008. Pathogenesis of asthma. *Clin Exp Allergy,* 38**,** 872-97.

HOLT, P. R. & DUBOIS, R. N., JR. 1991. In vivo immediate early gene expression induced in intestinal and colonic mucosa by feeding. *FEBS Lett,* 287**,** 102-4.

HONG, G., ZHANG, W., LI, H., SHEN, X. & GUO, Z. 2014. Separate enrichment analysis of pathways for up- and downregulated genes. *J R Soc Interface,* 11**,** 20130950.

HOOPER, L. V., MIDTVEDT, T. & GORDON, J. I. 2002. How host-microbial interactions shape the nutrient environment of the mammalian intestine. *Annu Rev Nutr,* 22**,** 283-307.

HOWARD, J. T., O'NAN, A. T., MALTECCA, C., BAYNES, R. E. & ASHWELL, M. S. 2015. Differential Gene Expression across

Breed and Sex in Commercial Pigs Administered Fenbendazole and Flunixin Meglumine. *PLoS One,* 10**,** e0137830.

HOWELL, J. C. & WELLS, J. M. 2011. Generating intestinal tissue from stem cells: potential for research and therapy. *Regen Med,* 6**,** 743-55.

HRDLICKOVA, R., TOLOUE, M. & TIAN, B. 2016. RNA-Seq methods for transcriptome analysis. *Wiley Interdiscip Rev RNA.*

HSU, S. Y. & HSUEH, A. J. 2001. Human stresscopin and stresscopin-related peptide are selective ligands for the type 2 corticotropin-releasing hormone receptor. *Nat Med,* 7**,** 605-11.

HU, C. H., XIAO, K., LUAN, Z. S. & SONG, J. 2013. Early weaning increases intestinal permeability, alters expression of cytokine and tight junction proteins, and activates mitogen-activated protein kinases in pigs. *J Anim Sci,* 91**,** 1094-101.

HU, J., YANG, D., CHEN, W., LI, C., WANG, Y., ZENG, Y. & WANG, H. 2016. Whole Blood Transcriptome Sequencing Reveals Gene Expression Differences between Dapulian and Landrace Piglets. *Biomed Res Int,* 2016**,** 7907980.

HUANG, Y., GAUVREAU, H. & HARDING, J. 2012. Diagnostic investigation of porcine periweaning failure-to-thrive syndrome: lack of compelling evidence linking to common porcine pathogens. *J Vet Diagn Invest,* 24**,** 96-106.

HUDSON, L. E., MCDERMOTT, C. D., STEWART, T. P., HUDSON, W. H., RIOS, D., FASKEN, M. B., CORBETT, A. H. & LAMB, T. J. 2016. Characterization of the Probiotic Yeast Saccharomyces boulardii in the Healthy Mucosal Immune System. *PLoS One,* 11**,** e0153351.

HUNGIN, A. P., MULLIGAN, C., POT, B., WHORWELL, P., AGREUS, L., FRACASSO, P., LIONIS, C., MENDIVE, J., PHILIPPART DE FOY, J. M., RUBIN, G., WINCHESTER, C., DE WIT, N. & EUROPEAN SOCIETY FOR PRIMARY CARE, G. 2013. Systematic review: probiotics in the management of lower gastrointestinal symptoms in clinical practice -- an evidence-based international guide. *Aliment Pharmacol Ther,* 38**,** 864-86.

IDDAMALGODA, A., LE, Q. T., ITO, K., TANAKA, K., KOJIMA, H. & KIDO, H. 2008. Mast cell tryptase and photoaging: possible involvement in the degradation of extra cellular matrix and basement membrane proteins. *Arch Dermatol Res,* 300 Suppl 1**,** S69-76.

IKENOUCHI, J., FURUSE, M., FURUSE, K., SASAKI, H., TSUKITA, S. & TSUKITA, S. 2005. Tricellulin constitutes a novel barrier at tricellular contacts of epithelial cells. *J Cell Biol,* 171**,** 939-45.

INDIAN COUNCIL OF MEDICAL RESEARCH TASK, F., CO-ORDINATING UNIT, I. & CO-ORDINATING UNIT, D. B. T. 2011. ICMR-DBT guidelines for evaluation of probiotics in food. *Indian J Med Res,* 134**,** 22-5.

INOUE, R., TSUKAHARA, T., NAKATANI, M., OKUTANI, M., NISHIBAYASHI, R., OGAWA, S., HARAYAMA, T., NAGINO, T., HATANAKA, H., FUKUTA, K., ROMERO-PEREZ, G. A., USHIDA, K. & KELLY, D. 2015. Weaning Markedly Affects Transcriptome Profiles and Peyer's Patch Development in Piglet Ileum. *Front Immunol,* 6**,** 630.

IWAKI, S., TKACZYK, C., SATTERTHWAITE, A. B., HALCOMB, K., BEAVEN, M. A., METCALFE, D. D. & GILFILLAN, A. M. 2005. Btk plays a crucial role in the amplification of Fc epsilonRI-mediated mast cell activation by kit. *J Biol Chem,* 280**,** 40261-70.

IWASAKI, A. & KELSALL, B. L. 2000. Localization of distinct Peyer's patch dendritic cell subsets and their recruitment by chemokines macrophage inflammatory protein (MIP)-3alpha, MIP-3beta, and secondary lymphoid organ chemokine. *J Exp Med,* 191**,** 1381-94.

IWASAKI, A. & KELSALL, B. L. 2001. Unique functions of CD11b+, CD8 alpha+, and double-negative Peyer's patch dendritic cells. *J Immunol,* 166**,** 4884-90.

JACKSON, J. R., HURLEY, W. L., EASTER, R. A., JENSEN, A. H. & ODLE, J. 1995. Effects of induced or delayed parturition and supplemental dietary fat on colostrum and milk composition in sows. *J Anim Sci,* 73**,** 1906-13.

JAHNEL, J., FICKERT, P., HAUER, A. C., HOGENAUER, C., AVIAN, A. & TRAUNER, M. 2014. Inflammatory bowel disease alters intestinal bile acid transporter expression. *Drug Metab Dispos,* 42**,** 1423-31.

JAKAITIS, B. M. & DENNING, P. W. 2014. Commensal and probiotic bacteria may prevent NEC by maturing intestinal host defenses. *Pathophysiology,* 21**,** 47-54.

JANEWAY, C. A. T., P.; WALPORT, M. 2001. Immunobiology: The Immune System in Health and Disease. New York: Garland Science.

JAWHARA, S., HABIB, K., MAGGIOTTO, F., PIGNEDE, G., VANDEKERCKOVE, P., MAES, E., DUBUQUOY, L., FONTAINE, T., GUERARDEL, Y. & POULAIN, D. 2012. Modulation of intestinal inflammation by yeasts and cell wall extracts: strain dependence and unexpected anti-inflammatory role of glucan fractions. *PLoS One,* 7**,** e40648.

JENSEN, P. & RECÉN, B. 1989. When to wean — Observations from free-ranging domestic pigs. *Applied Animal Behaviour Science,* 23**,** 49-60.

JONES, B. L. & KEARNS, G. L. 2011. Histamine: new thoughts about a familiar mediator. *Clin Pharmacol Ther,* 89**,** 189-97.

JORGENSEN, A. B., FRIKKE-SCHMIDT, R., NORDESTGAARD, B. G. & TYBJAERG-HANSEN, A. 2014. Loss-of-function mutations in APOC3 and risk of ischemic vascular disease. *N Engl J Med,* 371**,** 32-41.

JUNG, C., HUGOT, J. P. & BARREAU, F. 2010. Peyer's Patches: The Immune Sensors of the Intestine. *Int J Inflam,* 2010**,** 823710.

JUNG, K., KIM, J. H., CHEONG, H. S., SHIN, E., KIM, S. H., HWANG, J. Y., LEE, E., YOON, M. O., KIM, S. H., SIO, C. A., SHIN, H. D. & JUNG, S. E. 2015. Gene expression profile of necrotizing enterocolitis model in neonatal mice. *Int J Surg,* 23**,** 28-34.

JUNG, W. Y., KWON, S. G., SON, M., CHO, E. S., LEE, Y., KIM, J. H., KIM, B. W., PARK, D. H., HWANG, J. H., KIM, T. W., PARK, H. C., PARK, B. Y., CHOI, J. S., CHO, K. K., CHUNG, K. H., SONG, Y. M., KIM, I. S., JIN, S. K., KIM, D. H., LEE, S. W., LEE, K. W., BANG, W. Y. & KIM, C. W. 2012. RNA-Seq approach for genetic improvement of meat quality in pig and evolutionary insight into the substrate specificity of animal carbonyl reductases. *PLoS One,* 7**,** e42198.

KALSBEEK, A., VAN HEERIKHUIZE, J. J., WORTEL, J. & BUIJS, R. M. 1996. A diurnal rhythm of stimulatory input to the hypothalamo-pituitary-adrenal system as revealed by timed intrahypothalamic administration of the vasopressin V1 antagonist. *J Neurosci,* 16**,** 5555-65.

KAPLAN, J. L., SHI, H. N. & WALKER, W. A. 2011. The role of microbes in developmental immunologic programming. *Pediatr Res,* 69**,** 465-72.

KAPSORITAKIS, A. N., KAPSORITAKI, A. I., DAVIDI, I. P., LOTIS, V. D., MANOLAKIS, A. C., MYLONIS, P. I., THEODORIDOU, A. T., GERMENIS, A. E. & POTAMIANOS, S. P. 2008. Imbalance of tissue inhibitors of metalloproteinases (TIMP) - 1 and - 4 serum levels, in patients with inflammatory bowel disease. *BMC Gastroenterol,* 8**,** 55.

KAREM, K. L., KANANGAT, S. & ROUSE, B. T. 1996. Cytokine expression in the gut associated lymphoid tissue after oral administration of attenuated Salmonella vaccine strains. *Vaccine,* 14**,** 1495-502.

KARLIS, J., PENTTILA, I., TRAN, T. B., JONES, B., NOBBS, S., ZOLA, H. & FLESCH, I. E. 2004. Characterization of colonic and mesenteric lymph node dendritic cell subpopulations in a murine adoptive transfer model of inflammatory bowel disease. *Inflamm Bowel Dis,* 10**,** 834-47.

KATO-KATAOKA, A., NISHIDA, K., TAKADA, M., KAWAI, M., KIKUCHI-HAYAKAWA, H., SUDA, K., ISHIKAWA, H., GONDO, Y., SHIMIZU, K., MATSUKI, T., KUSHIRO, A., HOSHI, R., WATANABE, O., IGARASHI, T., MIYAZAKI, K., KUWANO, Y. & ROKUTAN, K. 2016. Fermented Milk Containing Lactobacillus casei Strain Shirota Preserves the Diversity of the Gut Microbiota and Relieves Abdominal Dysfunction in Healthy Medical Students Exposed to Academic Stress. *Appl Environ Microbiol,* 82**,** 3649-58.

KAWAI, T., TAKEUCHI, O., FUJITA, T., INOUE, J., MUHLRADT, P. F., SATO, S., HOSHINO, K. & AKIRA, S. 2001. Lipopolysaccharide stimulates the MyD88-independent pathway and results in activation of IFN-regulatory factor 3 and the expression of a subset of lipopolysaccharide-inducible genes. *J Immunol,* 167**,** 5887-94.

KAWAKAMI, Y. 2016. Introduction: Cancer Immunology Special Issue-Immunopathology. *Int Immunol,* 28**,** 371.

KELLY, J. R., KENNEDY, P. J., CRYAN, J. F., DINAN, T. G., CLARKE, G. & HYLAND, N. P. 2015. Breaking down the barriers: the gut microbiome, intestinal permeability and stress-related psychiatric disorders. *Front Cell Neurosci,* 9**,** 392.

KELNER, G. S., KENNEDY, J., BACON, K. B., KLEYENSTEUBER, S., LARGAESPADA, D. A., JENKINS, N. A., COPELAND, N. G., BAZAN, J. F., MOORE, K. W., SCHALL, T. J. & ET AL. 1994. Lymphotactin: a cytokine that represents a new class of chemokine. *Science,* 266**,** 1395-9.

KENNEDY, M. K., WILLIS, C. R. & ARMITAGE, R. J. 2006. Deciphering CD30 ligand biology and its role in humoral immunity. *Immunology,* 118**,** 143-52.

KENNY, M., SMIDT, H., MENGHERI, E. & MILLER, B. 2011. Probiotics - do they have a role in the pig industry? *Animal,* 5**,** 462-70.

KHATRI, I., AKHTAR, A., KAUR, K., TOMAR, R., PRASAD, G. S., RAMYA, T. N. & SUBRAMANIAN, S. 2013. Gleaning evolutionary insights from the genome sequence of a probiotic yeast Saccharomyces boulardii. *Gut Pathog,* 5**,** 30.

KHATRI, I., TOMAR, R., GANESAN, K., PRASAD, G. S. & SUBRAMANIAN, S. 2017. Complete genome sequence and

comparative genomics of the probiotic yeast Saccharomyces boulardii. *Sci Rep,* 7**,** 371.

KHOA, D. V. & WIMMERS, K. 2015. Genetic Association of the Porcine C9 Complement Component with Hemolytic Complement Activity. *Asian-Australas J Anim Sci,* 28**,** 1354-61.

KIHARA, N., FUJIMURA, M., YAMAMOTO, I., ITOH, E., INUI, A. & FUJIMIYA, M. 2001. Effects of central and peripheral urocortin on fed and fasted gastroduodenal motor activity in conscious rats. *Am J Physiol Gastrointest Liver Physiol,* 280**,** G406-19.

KIM, D., LANGMEAD, B. & SALZBERG, S. L. 2015. HISAT: a fast spliced aligner with low memory requirements. *Nat Methods,* 12**,** 357-60.

KIM, Y. B. 1975. Developmental immunity in the piglet. *Birth Defects Orig Artic Ser,* 11**,** 549-57.

KING'ORI, A. M. 2012. The Pre-Weaning Piglet: Colostrum and Milk Intake: a Review. *J Anim Prod Adv,* 2**,** 277-283.

KINNEBREW, M. A. & PAMER, E. G. 2012. Innate immune signaling in defense against intestinal microbes. *Immunol Rev,* 245**,** 113-31.

KISHIMOTO, T., PEARSE, R. V., 2ND, LIN, C. R. & ROSENFELD, M. G. 1995. A sauvagine/corticotropin-releasing factor receptor expressed in heart and skeletal muscle. *Proc Natl Acad Sci U S A,* 92**,** 1108-12.

KISHIMOTO, T., RADULOVIC, J., RADULOVIC, M., LIN, C. R., SCHRICK, C., HOOSHMAND, F., HERMANSON, O., ROSENFELD, M. G. & SPIESS, J. 2000. Deletion of crhr2 reveals an anxiolytic role for corticotropin-releasing hormone receptor-2. *Nat Genet,* 24**,** 415-9.

KLEIJ, H. P. & BIENENSTOCK, J. 2005. Significance of Conversation between Mast Cells and Nerves. *Allergy Asthma Clin Immunol,* 1**,** 65-80.

KLOBASA, F. & BUTLER, J. E. 1987. Absolute and relative concentrations of immunoglobulins G, M, and A, and albumin in the lacteal secretion of sows of different lactation numbers. *Am J Vet Res,* 48**,** 176-82.

KOIZUMI, N., MOROZUMI, A., IMAMURA, M., TANAKA, E., IWAHANA, H. & SATO, R. 1997. Lipopolysaccharide-binding proteins and their involvement in the bacterial clearance from the hemolymph of the silkworm Bombyx mori. *Eur J Biochem,* 248**,** 217-24.

KOLIARAKI, V., PALLANGYO, C. K., GRETEN, F. R. & KOLLIAS, G. 2017. Mesenchymal Cells in Colon Cancer. *Gastroenterology,* 152**,** 964-979.

KOPP-HOOLIHAN, L. 2001. Prophylactic and therapeutic uses of probiotics: a review. *J Am Diet Assoc,* 101**,** 229-38; quiz 239-41.

KRISTENSEN, N. B., BRYRUP, T., ALLIN, K. H., NIELSEN, T., HANSEN, T. H. & PEDERSEN, O. 2016. Alterations in fecal microbiota composition by probiotic supplementation in healthy adults: a systematic review of randomized controlled trials. *Genome Med,* 8**,** 52.

KROGER, S., PIEPER, R., SCHWELBERGER, H. G., WANG, J., VILLODRE TUDELA, C., ASCHENBACH, J. R., VAN KESSEL, A. G. & ZENTEK, J. 2013. Diets high in heat-treated soybean meal reduce the histamine-induced epithelial response in the colon of weaned piglets and increase epithelial catabolism of histamine. *PLoS One,* 8**,** e80612.

KUJAWA-SZEWIECZEK, A., ADAMCZAK, M., KWIECIEN, K., DUDZICZ, S., GAZDA, M. & WIECEK, A. 2015. The Effect of Lactobacillus plantarum 299v on the Incidence of Clostridium difficile Infection in High Risk Patients Treated with Antibiotics. *Nutrients,* 7**,** 10179-88.

KUKURBA, K. R. & MONTGOMERY, S. B. 2015. RNA Sequencing and Analysis. *Cold Spring Harb Protoc,* 2015**,** 951-69.

KUMAR, H., KAWAI, T. & AKIRA, S. 2011. Pathogen recognition by the innate immune system. *Int Rev Immunol,* 30**,** 16-34.

KUMMARI, E., GUO-ROSS, S. X. & EELLS, J. B. 2015. Laser capture microdissection--a demonstration of the isolation of individual dopamine neurons and the entire ventral tegmental area. *J Vis Exp***,** e52336.

KUVAEVA, I. B., ZAKHAROVA, N. V., ORLOVA, N. G. & VESELOVA, O. L. 1980. [Functional state of the immunological system and of the gastrointestinal tract in children with a food allergy]. *Vopr Pitan***,** 33-40.

KWAK, J. Y., MAMURA, M., BARLIC-DICEN, J. & GRAGE-GRIEBENOW, E. 2014. Pathophysiological roles of cytokine-chemokine immune network. *J Immunol Res,* 2014**,** 615130.

KYRIAKIS, S. C., GEORGOULAKIS, I., SPAIS, A., ALEXOPOULOS, C., MILIOTIS, C. C. & KRITAS, S. K. 2003. Evaluation of Toyocerin, a Probiotic Containing Bacillus toyoi Spores, on Health Status and Productivity of Weaned, Growing and Finishing Pigs. *Asian-Australas J Anim Sci,* 16**,** 1326-1331.

KYROVA, K., STEPANOVA, H., RYCHLIK, I., POLANSKY, O., LEVA, L., SEKELOVA, Z., FALDYNA, M. & VOLF, J. 2014. The response of porcine monocyte derived macrophages and dendritic cells to Salmonella Typhimurium and lipopolysaccharide. *BMC Vet Res,* 10**,** 244.

LAMKANFI, M. & DIXIT, V. M. 2014. Mechanisms and functions of inflammasomes. *Cell,* 157**,** 1013-22.

LAN, R. X., LEE, S. I. & KIM, I. H. 2016. Effects of multistrain probiotics on growth performance, nutrient digestibility, blood profiles, faecal microbial shedding, faecal score and noxious gas emission in weaning pigs. *J Anim Physiol Anim Nutr (Berl),* 100**,** 1130-1138.

LANG, R., PATEL, D., MORRIS, J. J., RUTSCHMAN, R. L. & MURRAY, P. J. 2002. Shaping gene expression in activated and resting primary macrophages by IL-10. *J Immunol,* 169**,** 2253-63.

LANTIER, L., LACROIX-LAMANDE, S., POTIRON, L., METTON, C., DROUET, F., GUESDON, W., GNAHOUI-DAVID, A., LE VERN, Y., DERIAUD, E., FENIS, A., RABOT, S., DESCAMPS, A., WERTS, C. & LAURENT, F. 2013. Intestinal CD103+ dendritic cells are key players in the innate immune control of Cryptosporidium parvum infection in neonatal mice. *PLoS Pathog,* 9**,** e1003801.

LARSEN, P. E. & DAI, Y. 2015. Metabolome of human gut microbiome is predictive of host dysbiosis. *Gigascience,* 4**,** 42.

LAU, C. S. & CHAMBERLAIN, R. S. 2016. Probiotics are effective at preventing Clostridium difficile-associated diarrhea: a systematic review and meta-analysis. *Int J Gen Med,* 9**,** 27-37.

LAW, C. W., CHEN, Y., SHI, W. & SMYTH, G. K. 2014. voom: Precision weights unlock linear model analysis tools for RNA-seq read counts. *Genome Biol,* 15**,** R29.

LE BON, M. 2012a. *Effect of Probiotic Supplementation on Immunomodulation in Pig.* University of Nottingham.

LE BON, M. 2012b. *Effect of Probiotic Supplementation on Immunomodulation in Pig.* PhD, University of Nottingham.

LÊ, S., JOSSE, J. & HUSSON, F. 2008. FactoMineR: An R Package for Multivariate Analysis. *2008,* 25**,** 18.

LEE DO, Y., KIM, E. & CHOI, M. H. 2015. Technical and clinical aspects of cortisol as a biochemical marker of chronic stress. *BMB Rep,* 48**,** 209-16.

LEE, S. H. 2015. Intestinal permeability regulation by tight junction: implication on inflammatory bowel diseases. *Intest Res,* 13**,** 11-8.

LEIBBRANDT, V. D., EWAN, R. C., SPEER, V. C. & ZIMMERMAN, D. R. 1975. Effect of Weaning and Age at Weaning on Baby Pig Performance. *Journal of Animal Science,* 40**,** 1077-1080.

LENG, N., DAWSON, J. A., THOMSON, J. A., RUOTTI, V., RISSMAN, A. I., SMITS, B. M., HAAG, J. D., GOULD, M. N., STEWART, R. M. & KENDZIORSKI, C. 2013. EBSeq: an

empirical Bayes hierarchical model for inference in RNA-seq experiments. *Bioinformatics,* 29**,** 1035-43.
LENTSCH, A. B., CZERMAK, B. J., JORDAN, J. A. & WARD, P. A. 1999. Regulation of acute lung inflammatory injury by endogenous IL-13. *J Immunol,* 162**,** 1071-6.
LENZ, H. J., BURLAGE, M., RAEDLER, A. & GRETEN, H. 1988a. Central nervous system effects of corticotropin-releasing factor on gastrointestinal transit in the rat. *Gastroenterology,* 94**,** 598-602.
LENZ, H. J., RAEDLER, A., GRETEN, H., VALE, W. W. & RIVIER, J. E. 1988b. Stress-induced gastrointestinal secretory and motor responses in rats are mediated by endogenous corticotropin-releasing factor. *Gastroenterology,* 95**,** 1510-7.
LETTERIO, J. J. & ROBERTS, A. B. 1997. TGF-beta: a critical modulator of immune cell function. *Clin Immunol Immunopathol,* 84**,** 244-50.
LEVI-SCHAFFER, F. & KUPIETZKY, A. 1990. Mast cells enhance migration and proliferation of fibroblasts into an in vitro wound. *Exp Cell Res,* 188**,** 42-9.
LEVY, S. E. & MYERS, R. M. 2016. Advancements in Next-Generation Sequencing. *Annu Rev Genomics Hum Genet*.
LEWIS, A. & SOUTHERN, L. 2000. *Swine Nutrition*, CRC Press.
LEWIS, K., LI, C., PERRIN, M. H., BLOUNT, A., KUNITAKE, K., DONALDSON, C., VAUGHAN, J., REYES, T. M., GULYAS, J., FISCHER, W., BILEZIKJIAN, L., RIVIER, J., SAWCHENKO, P. E. & VALE, W. W. 2001. Identification of urocortin III, an additional member of the corticotropin-releasing factor (CRF) family with high affinity for the CRF2 receptor. *Proc Natl Acad Sci U S A,* 98**,** 7570-5.
LI, H., HANDSAKER, B., WYSOKER, A., FENNELL, T., RUAN, J., HOMER, N., MARTH, G., ABECASIS, G., DURBIN, R. & GENOME PROJECT DATA PROCESSING, S. 2009. The Sequence Alignment/Map format and SAMtools. *Bioinformatics,* 25**,** 2078-9.
LI, H. & HOMER, N. 2010. A survey of sequence alignment algorithms for next-generation sequencing. *Brief Bioinform,* 11**,** 473-83.
LI, J. & TIBSHIRANI, R. 2013. Finding consistent patterns: a nonparametric approach for identifying differential expression in RNA-Seq data. *Stat Methods Med Res,* 22**,** 519-36.
LI, J., WITTEN, D. M., JOHNSTONE, I. M. & TIBSHIRANI, R. 2012. Normalization, testing, and false discovery rate estimation for RNA-sequencing data. *Biostatistics,* 13**,** 523-38.

LI, L. A., YANG, J. J., LI, Y., LV, L., XIE, J. J., DU, G. M., JIN, T. M., QIN, S. Y. & JIAO, X. L. 2016a. Effect of weaning age on cortisol release in piglets. *Genet Mol Res,* 15.

LI, M. C. & HE, S. H. 2004. IL-10 and its related cytokines for treatment of inflammatory bowel disease. *World J Gastroenterol,* 10**,** 620-5.

LI, Q. & ZHAO, C. 2015. [An in vitro study on substance P-stimulated neuro-immune mechanism of mast cell degranulation]. *Lin Chung Er Bi Yan Hou Tou Jing Wai Ke Za Zhi,* 29**,** 1118-20.

LI, S., FEI, G., FANG, X., YANG, X., SUN, X., QIAN, J., WOOD, J. D. & KE, M. 2016b. Changes in Enteric Neurons of Small Intestine in a Rat Model of Irritable Bowel Syndrome with Diarrhea. *J Neurogastroenterol Motil,* 22**,** 310-20.

LI, W. R., SHI, Q. S., DAI, H. Q., LIANG, Q., XIE, X. B., HUANG, X. M., ZHAO, G. Z. & ZHANG, L. X. 2016c. Antifungal activity, kinetics and molecular mechanism of action of garlic oil against Candida albicans. *Sci Rep,* 6**,** 22805.

LI, Y., LIU, H., WANG, P., WANG, L., SUN, Y., LIU, G., ZHANG, P., KANG, L., JIANG, S. & JIANG, Y. 2016d. RNA-Seq Analysis Reveals Genes Underlying Different Disease Responses to Porcine Circovirus Type 2 in Pigs. *PLoS One,* 11**,** e0155502.

LI, Y., SONG, Z., KERR, K. A. & MOESER, A. J. 2017. Chronic social stress in pigs impairs intestinal barrier and nutrient transporter function, and alters neuro-immune mediator and receptor expression. *PLoS One,* 12**,** e0171617.

LIGUMSKY, M., SIMON, P. L., KARMELI, F. & RACHMILEWITZ, D. 1990. Role of interleukin 1 in inflammatory bowel disease--enhanced production during active disease. *Gut,* 31**,** 686-9.

LIN, H. K., GODIWALLA, S. Y., PALMER, B., FRIMBERGER, D., YANG, Q., MADIHALLY, S. V., FUNG, K. M. & KROPP, B. P. 2014. Understanding roles of porcine small intestinal submucosa in urinary bladder regeneration: identification of variable regenerative characteristics of small intestinal submucosa. *Tissue Eng Part B Rev,* 20**,** 73-83.

LIU, H., NGUYEN, Y. T., NETTLETON, D., DEKKERS, J. C. & TUGGLE, C. K. 2016a. Post-weaning blood transcriptomic differences between Yorkshire pigs divergently selected for residual feed intake. *BMC Genomics,* 17**,** 73.

LIU, Q., ZHU, X., XU, L., FU, Y. & GARVEY, W. T. 2013. 6-Mercaptopurine augments glucose transport activity in skeletal muscle cells in part via a mechanism dependent upon orphan nuclear receptor NR4A3. *Am J Physiol Endocrinol Metab,* 305**,** E1081-92.

LIU, S., GAO, X., GAO, N., WANG, X., FANG, X., HU, H. Z., WANG, G. D., XIA, Y. & WOOD, J. D. 2005. Expression of type 1 corticotropin-releasing factor receptor in the guinea pig enteric nervous system. *J Comp Neurol,* 481**,** 284-98.

LIU, Y., BEYER, A. & AEBERSOLD, R. 2016b. On the Dependency of Cellular Protein Levels on mRNA Abundance. *Cell,* 165**,** 535-50.

LOBERT, V. H., BRECH, A., PEDERSEN, N. M., WESCHE, J., OPPELT, A., MALEROD, L. & STENMARK, H. 2010. Ubiquitination of alpha 5 beta 1 integrin controls fibroblast migration through lysosomal degradation of fibronectin-integrin complexes. *Dev Cell,* 19**,** 148-59.

LOVE, M. I., HUBER, W. & ANDERS, S. 2014. Moderated estimation of fold change and dispersion for RNA-seq data with DESeq2. *Genome Biol,* 15**,** 550.

LOWE, R., SHIRLEY, N., BLEACKLEY, M., DOLAN, S. & SHAFEE, T. 2017. Transcriptomics technologies. *PLoS Comput Biol,* 13**,** e1005457.

LU, S., HUFFMAN, M., YAO, Y., MANSBACH, C. M., 2ND, CHENG, X., MENG, S. & BLACK, D. D. 2002. Regulation of MTP expression in developing swine. *J Lipid Res,* 43**,** 1303-11.

LUND, J., SATO, A., AKIRA, S., MEDZHITOV, R. & IWASAKI, A. 2003. Toll-like receptor 9-mediated recognition of Herpes simplex virus-2 by plasmacytoid dendritic cells. *J Exp Med,* 198**,** 513-20.

MACH, N., BERRI, M., ESQUERRE, D., CHEVALEYRE, C., LEMONNIER, G., BILLON, Y., LEPAGE, P., OSWALD, I. P., DORE, J., ROGEL-GAILLARD, C. & ESTELLE, J. 2014. Extensive expression differences along porcine small intestine evidenced by transcriptome sequencing. *PLoS One,* 9**,** e88515.

MACKAY, C. R. 1993. Immunological memory. *Adv Immunol,* 53**,** 217-65.

MACMANES, M. D. 2014. On the optimal trimming of high-throughput mRNA sequence data. *Front Genet,* 5**,** 13.

MARDIS, E. R. 2017. DNA sequencing technologies: 2006-2016. *Nat Protoc,* 12**,** 213-218.

MARGUERAT, S. & BAHLER, J. 2010. RNA-seq: from technology to biology. *Cell Mol Life Sci,* 67**,** 569-79.

MARKOWSKA-DANIEL, I., POMORSKA-MOL, M. & PEJSAK, Z. 2010. Dynamic changes of immunoglobulin concentrations in pig colostrum and serum around parturition. *Pol J Vet Sci,* 13**,** 21-7.

MARON, D. F., SMITH, T. J. S. & NACHMAN, K. E. 2013. Restrictions on antimicrobial use in food animal production: an international regulatory and economic survey. *Global Health,* 9**,** 48.

MARTIN-PADURA, I., LOSTAGLIO, S., SCHNEEMANN, M., WILLIAMS, L., ROMANO, M., FRUSCELLA, P., PANZERI, C., STOPPACCIARO, A., RUCO, L., VILLA, A., SIMMONS, D. & DEJANA, E. 1998. Junctional adhesion molecule, a novel member of the immunoglobulin superfamily that distributes at intercellular junctions and modulates monocyte transmigration. *J Cell Biol,* 142**,** 117-27.

MARTIN, M. 2011. Cutadapt removes adapter sequences from high-throughput sequencing reads. *2011*, 17.

MARTINEZ-MIRO, S., TECLES, F., RAMON, M., ESCRIBANO, D., HERNANDEZ, F., MADRID, J., ORENGO, J., MARTINEZ-SUBIELA, S., MANTECA, X. & CERON, J. J. 2016. Causes, consequences and biomarkers of stress in swine: an update. *BMC Vet Res,* 12**,** 171.

MARTINEZ, V., RIVIER, J., WANG, L. & TACHE, Y. 1997. Central injection of a new corticotropin-releasing factor (CRF) antagonist, astressin, blocks CRF- and stress-related alterations of gastric and colonic motor function. *J Pharmacol Exp Ther,* 280**,** 754-60.

MARTINEZ, V. & TACHE, Y. 2006. CRF1 receptors as a therapeutic target for irritable bowel syndrome. *Curr Pharm Des,* 12**,** 4071-88.

MARTINEZ, V., WANG, L., RIVIER, J., GRIGORIADIS, D. & TACHE, Y. 2004. Central CRF, urocortins and stress increase colonic transit via CRF1 receptors while activation of CRF2 receptors delays gastric transit in mice. *J Physiol,* 556**,** 221-34.

MATSUDA, H., KAWAKITA, K., KISO, Y., NAKANO, T. & KITAMURA, Y. 1989. Substance P induces granulocyte infiltration through degranulation of mast cells. *J Immunol,* 142**,** 927-31.

MATTOLI, S., ACKERMAN, V., VITTORI, E. & MARINI, M. 1995. Mast cell chemotactic activity of RANTES. *Biochem Biophys Res Commun,* 209**,** 316-21.

MAZIADE, P. J., PEREIRA, P. & GOLDSTEIN, E. J. 2015. A Decade of Experience in Primary Prevention of Clostridium difficile Infection at a Community Hospital Using the Probiotic Combination Lactobacillus acidophilus CL1285, Lactobacillus casei LBC80R, and Lactobacillus rhamnosus CLR2 (Bio-K+). *Clin Infect Dis,* 60 Suppl 2**,** S144-7.

MCCRACKEN, B. A., GASKINS, H. R., RUWE-KAISER, P. J., KLASING, K. C. & JEWELL, D. E. 1995. Diet-dependent and diet-independent metabolic responses underlie growth stasis of pigs at weaning. *J Nutr,* 125**,** 2838-45.

MCCRACKEN, B. A., SPURLOCK, M. E., ROOS, M. A., ZUCKERMANN, F. A. & GASKINS, H. R. 1999. Weaning anorexia may contribute to local inflammation in the piglet small intestine. *J Nutr,* 129**,** 613-9.

MCFARLAND, L. V. 2014. Use of probiotics to correct dysbiosis of normal microbiota following disease or disruptive events: a systematic review. *BMJ Open,* 4**,** e005047.

MCKAIG, B. C., MCWILLIAMS, D., WATSON, S. A. & MAHIDA, Y. R. 2003. Expression and regulation of tissue inhibitor of metalloproteinase-1 and matrix metalloproteinases by intestinal myofibroblasts in inflammatory bowel disease. *Am J Pathol,* 162**,** 1355-60.

MCLAMB, B. L., GIBSON, A. J., OVERMAN, E. L., STAHL, C. & MOESER, A. J. 2013. Early weaning stress in pigs impairs innate mucosal immune responses to enterotoxigenic E. coli challenge and exacerbates intestinal injury and clinical disease. *PLoS One,* 8**,** e59838.

MCNEIL, H. P., ADACHI, R. & STEVENS, R. L. 2007. Mast cell-restricted tryptases: structure and function in inflammation and pathogen defense. *J Biol Chem,* 282**,** 20785-9.

MEDEIROS, N. I., MATTOS, R. T., MENEZES, C. A., FARES, R. C. G., TALVANI, A., DUTRA, W. O., RIOS-SANTOS, F., CORREA-OLIVEIRA, R. & GOMES, J. A. S. 2017. IL-10 and TGF-beta unbalanced levels in neutrophils contribute to increase inflammatory cytokine expression in childhood obesity. *Eur J Nutr*.

MEDLAND, J. E., POHL, C. S., EDWARDS, L. L., FRANDSEN, S., BAGLEY, K., LI, Y. & MOESER, A. J. 2016. Early life adversity in piglets induces long-term upregulation of the enteric cholinergic nervous system and heightened, sex-specific secretomotor neuron responses. *Neurogastroenterol Motil,* 28**,** 1317-29.

MENCHETTI, L., TRAINA, G., TOMASELLO, G., CASAGRANDE-PROIETTI, P., LEONARDI, L., BARBATO, O. & BRECCHIA, G. 2016. Potential benefits of colostrum in gastrointestinal diseases. *Front Biosci (Schol Ed),* 8**,** 331-51.

MEREU, A., TEDO, G., MOESER, A. J., RIMBACH, G. & IPHARRAGUERRE, I. R. 2015. Cromolyn-mediated improvement of intestinal barrier function is associated with enhanced piglet performance after weaning. *BMC Vet Res,* 11**,** 274.

MERLOT, E., QUESNEL, H. & PRUNIER, A. 2013. Prenatal stress, immunity and neonatal health in farm animal species. *Animal,* 7**,** 2016-25.

MESSINA, V., BUCCIONE, C., MAROTTA, G., ZICCHEDDU, G., SIGNORE, M., MATTIA, G., PUGLISI, R., SACCHETTI, B., BIANCONE, L. & VALTIERI, M. 2017. Gut Mesenchymal Stromal Cells in Immunity. *Stem Cells Int,* 2017**,** 8482326.

METSALU, T. & VILO, J. 2015. ClustVis: a web tool for visualizing clustering of multivariate data using Principal Component Analysis and heatmap. *Nucleic Acids Res,* 43**,** W566-70.

METZLER-ZEBELI, B. U., MANN, E., ERTL, R., SCHMITZ-ESSER, S., WAGNER, M., KLEIN, D., RITZMANN, M. & ZEBELI, Q. 2015. Dietary calcium concentration and cereals differentially affect mineral balance and tight junction proteins expression in jejunum of weaned pigs. *Br J Nutr,* 113**,** 1019-31.

MILLER, E. J., COHEN, A. B., NAGAO, S., GRIFFITH, D., MAUNDER, R. J., MARTIN, T. R., WEINER-KRONISH, J. P., STICHERLING, M., CHRISTOPHERS, E. & MATTHAY, M. A. 1992. Elevated levels of NAP-1/interleukin-8 are present in the airspaces of patients with the adult respiratory distress syndrome and are associated with increased mortality. *Am Rev Respir Dis,* 146**,** 427-32.

MILLET, S. & MAERTENS, L. 2011. The European ban on antibiotic growth promoters in animal feed: from challenges to opportunities. *Vet J,* 187**,** 143-4.

MISCHKE, M. & PLOSCH, T. 2013. More than just a gut instinct-the potential interplay between a baby's nutrition, its gut microbiome, and the epigenome. *Am J Physiol Regul Integr Comp Physiol,* 304**,** R1065-9.

MITTAL, R. K. 2016. Regulation and dysregulation of esophageal peristalsis by the integrated function of circular and longitudinal muscle layers in health and disease. *Am J Physiol Gastrointest Liver Physiol,* 311**,** G431-43.

MIYATA, K., ITO, H. & FUKUDO, S. 1998. Involvement of the 5-HT3 receptor in CRH-induce defecation in rats. *Am J Physiol,* 274**,** G827-31.

MODICA, S., GOFFLOT, F., MURZILLI, S., D'ORAZIO, A., SALVATORE, L., PELLEGRINI, F., NICOLUCCI, A., TOGNONI, G., COPETTI, M., VALANZANO, R., VESCHI, S., MARIANI-COSTANTINI, R., PALASCIANO, G., SCHOONJANS, K., AUWERX, J. & MOSCHETTA, A. 2010. The intestinal nuclear receptor signature with epithelial localization patterns and expression modulation in tumors. *Gastroenterology,* 138**,** 636-48, 648 e1-12.

MOESER, A. J., BORST, L. B., OVERMAN, B. L. & PITTMAN, J. S. 2012. Defects in small intestinal epithelial barrier function and

morphology associated with peri-weaning failure to thrive syndrome (PFTS) in swine. *Res Vet Sci,* 93**,** 975-82.

MOESER, A. J., KLOK, C. V., RYAN, K. A., WOOTEN, J. G., LITTLE, D., COOK, V. L. & BLIKSLAGER, A. T. 2007a. Stress signaling pathways activated by weaning mediate intestinal dysfunction in the pig. *Am J Physiol Gastrointest Liver Physiol,* 292**,** G173-81.

MOESER, A. J., POHL, C. S. & RAJPUT, M. 2017. Weaning stress and gastrointestinal barrier development: Implications for lifelong gut health in pigs. *Animal Nutrition*.

MOESER, A. J., RYAN, K. A., NIGHOT, P. K. & BLIKSLAGER, A. T. 2007b. Gastrointestinal dysfunction induced by early weaning is attenuated by delayed weaning and mast cell blockade in pigs. *Am J Physiol Gastrointest Liver Physiol,* 293**,** G413-21.

MONNIKES, H., TEBBE, J., BAUER, C., LAUER, G. & ARNOLD, R. 1996. Microinfusion of corticotropin-releasing factor into the locus coeruleus/subcoeruleus nuclei inhibits gastric acid secretion via spinal pathways in the rat. *Brain Res,* 728**,** 157-65.

MOON, H. W. 1972. Vacuolated villous epithelium of the small intestine of young pigs. *Vet Pathol,* 9**,** 3-21.

MOOS, W. H., FALLER, D. V., HARPP, D. N., KANARA, I., PERNOKAS, J., POWERS, W. R. & STELIOU, K. 2016. Microbiota and Neurological Disorders: A Gut Feeling. *Biores Open Access,* 5**,** 137-45.

MORE, M. I. & SWIDSINSKI, A. 2015. Saccharomyces boulardii CNCM I-745 supports regeneration of the intestinal microbiota after diarrheic dysbiosis - a review. *Clin Exp Gastroenterol,* 8**,** 237-55.

MORELLI, L. 2008. Postnatal development of intestinal microflora as influenced by infant nutrition. *J Nutr,* 138**,** 1791S-1795S.

MOSENTHIN , R. 1998. Physiology of Small and Large Intestine of Swine. *AJAS,* 11**,** 608-619.

MOTOURI, M., MATSUYAMA, H., YAMAMURA, J., TANAKA, M., AOE, S., IWANAGA, T. & KAWAKAMI, H. 2003. Milk sphingomyelin accelerates enzymatic and morphological maturation of the intestine in artificially reared rats. *J Pediatr Gastroenterol Nutr,* 36**,** 241-7.

MOUSSAOUI, N., JACOBS, J. P., LARAUCHE, M., BIRAUD, M., MILLION, M., MAYER, E. & TACHE, Y. 2017. Chronic Early-life Stress in Rat Pups Alters Basal Corticosterone, Intestinal Permeability, and Fecal Microbiota at Weaning: Influence of Sex. *J Neurogastroenterol Motil,* 23**,** 135-143.

MUCKSOVA, J., BABICEK, K. & POSPISIL, M. 2001. Particulate 1,3-beta-D-glucan, carboxymethylglucan and sulfoethylglucan--influence of their oral or intraperitoneal administration on immunological respondence of mice. *Folia Microbiol (Praha),* 46**,** 559-63.

MUMY, K. L., CHEN, X., KELLY, C. P. & MCCORMICK, B. A. 2008. Saccharomyces boulardii interferes with Shigella pathogenesis by postinvasion signaling events. *Am J Physiol Gastrointest Liver Physiol,* 294**,** G599-609.

MURPHY, K., TRAVERS, P. & WALPORT, M. 2007. *Janeway's Immunobiology,* New York and London, Garland Science.

MUTOH, M., NIHO, N., KOMIYA, M., TAKAHASHI, M., OHTSUBO, R., NAKATOGAWA, K., UEDA, K., SUGIMURA, T. & WAKABAYASHI, K. 2008. Plasminogen activator inhibitor-1 (Pai-1) blockers suppress intestinal polyp formation in Min mice. *Carcinogenesis,* 29**,** 824-9.

NAGAOKA, M., YASHIRO, T., UCHIDA, Y., ANDO, T., HARA, M., ARAI, H., OGAWA, H., OKUMURA, K., KASAKURA, K. & NISHIYAMA, C. 2017. The Orphan Nuclear Receptor NR4A3 Is Involved in the Function of Dendritic Cells. *J Immunol,* 199**,** 2958-2967.

NANDURI, B., PENDARVIS, K., SHACK, L. A., KUMAR, R., CLYMER, J. W., KORVICK, D. L. & BURGESS, S. C. 2013. Ultrasonic incisions produce less inflammatory mediator response during early healing than electrosurgical incisions. *PLoS One,* 8**,** e73032.

NEU, J. 2007. Perinatal and neonatal manipulation of the intestinal microbiome: a note of caution. *Nutr Rev,* 65**,** 282-5.

NEUFELD, K. M., LUCZYNSKI, P., ORIACH, C. S., DINAN, T. G. & CRYAN, J. F. 2016. What's bugging your teen?-The microbiota and adolescent mental health. *Neurosci Biobehav Rev*.

NEWBURG, D. S. & WALKER, W. A. 2007. Protection of the neonate by the innate immune system of developing gut and of human milk. *Pediatr Res,* 61**,** 2-8.

NGUYEN, M., LEURIDAN, E., ZHANG, T., DE WIT, D., WILLEMS, F., VAN DAMME, P., GOLDMAN, M. & GORIELY, S. 2010. Acquisition of adult-like TLR4 and TLR9 responses during the first year of life. *PLoS One,* 5**,** e10407.

NIESS, J. H., BRAND, S., GU, X., LANDSMAN, L., JUNG, S., MCCORMICK, B. A., VYAS, J. M., BOES, M., PLOEGH, H. L., FOX, J. G., LITTMAN, D. R. & REINECKER, H. C. 2005. CX3CR1-mediated dendritic cell access to the intestinal lumen and bacterial clearance. *Science,* 307**,** 254-8.

NIJMEIJER, R. M., GADALETA, R. M., VAN MIL, S. W., VAN BODEGRAVEN, A. A., CRUSIUS, J. B., DIJKSTRA, G., HOMMES, D. W., DE JONG, D. J., STOKKERS, P. C., VERSPAGET, H. W., WEERSMA, R. K., VAN DER WOUDE, C. J., STAPELBROEK, J. M., SCHIPPER, M. E., WIJMENGA, C., VAN ERPECUM, K. J., OLDENBURG, B. & DUTCH INITIATIVE ON CROHN, C. 2011. Farnesoid X receptor (FXR) activation and FXR genetic variation in inflammatory bowel disease. *PLoS One,* 6**,** e23745.

NISHIDA, N., YANO, H., NISHIDA, T., KAMURA, T. & KOJIRO, M. 2006. Angiogenesis in cancer. *Vasc Health Risk Manag,* 2**,** 213-9.

NOGALLER, A. M. & ABDEEVA, O. V. 1991. [Allergy and the endocrine system of the gastrointestinal tract]. *Klin Med (Mosk),* 69**,** 17-23.

NOOR, S. & WILSON, E. H. 2012. Role of C-C chemokine receptor type 7 and its ligands during neuroinflammation. *J Neuroinflammation,* 9**,** 77.

O'CONNOR, A. M., SARGEANT, J. M., GARDNER, I. A., DICKSON, J. S., TORRENCE, M. E., DEWEY, C. E., DOHOO, I. R., EVANS, R. B., GRAY, J. T., GREINER, M., KEEFE, G., LEFEBVRE, S. L., MORLEY, P. S., RAMIREZ, A., SISCHO, W., SMITH, D. R., SNEDEKER, K., SOFOS, J., WARD, M. P. & WILLS, R. 2010. The REFLECT statement: methods and processes of creating reporting guidelines for randomized controlled trials for livestock and food safety by modifying the CONSORT statement. *Zoonoses and public health,* 57**,** 95-104.

O'MALLEY, D. 2015. Immunomodulation of enteric neural function in irritable bowel syndrome. *World J Gastroenterol,* 21**,** 7362-6.

O'NEILL, L. A. 2008. The interleukin-1 receptor/Toll-like receptor superfamily: 10 years of progress. *Immunol Rev,* 226**,** 10-8.

O'NEILL, L. A. & BOWIE, A. G. 2007. The family of five: TIR-domain-containing adaptors in Toll-like receptor signalling. *Nat Rev Immunol,* 7**,** 353-64.

OAKES, P. W., PATEL, D. C., MORIN, N. A., ZITTERBART, D. P., FABRY, B., REICHNER, J. S. & TANG, J. X. 2009. Neutrophil morphology and migration are affected by substrate elasticity. *Blood,* 114**,** 1387-95.

OEZTUERK, H., SCHROEDER, B., BEYERBACH, M. & BREVES, G. 2005. Influence of living and autoclaved yeasts of Saccharomyces boulardii on in vitro ruminal microbial metabolism. *J Dairy Sci,* 88**,** 2594-600.

OLIVEROS, J. C. 2007-2015. Venny. An interactive tool for comparing lists with Venn's diagrams.

OOSTING, M., CHENG, S. C., BOLSCHER, J. M., VESTERING-STENGER, R., PLANTINGA, T. S., VERSCHUEREN, I. C., ARTS, P., GARRITSEN, A., VAN EENENNAAM, H., STURM, P., KULLBERG, B. J., HOISCHEN, A., ADEMA, G. J., VAN DER MEER, J. W., NETEA, M. G. & JOOSTEN, L. A. 2014. Human TLR10 is an anti-inflammatory pattern-recognition receptor. *Proc Natl Acad Sci U S A,* 111**,** E4478-84.

OPAL, S. M. & DEPALO, V. A. 2000. Anti-inflammatory cytokines. *Chest,* 117**,** 1162-72.

OPAL, S. M., WHERRY, J. C. & GRINT, P. 1998. Interleukin-10: potential benefits and possible risks in clinical infectious diseases. *Clin Infect Dis,* 27**,** 1497-507.

ORIENTE, A., FEDARKO, N. S., PACOCHA, S. E., HUANG, S. K., LICHTENSTEIN, L. M. & ESSAYAN, D. M. 2000. Interleukin-13 modulates collagen homeostasis in human skin and keloid fibroblasts. *J Pharmacol Exp Ther,* 292**,** 988-94.

OTTO, A., MACHARIA, R., MATSAKAS, A., VALASEK, P., MANKOO, B. S. & PATEL, K. 2010. A hypoplastic model of skeletal muscle development displaying reduced foetal myoblast cell numbers, increased oxidative myofibres and improved specific tension capacity. *Dev Biol,* 343**,** 51-62.

OUCHIDA, R., MORI, H., HASE, K., TAKATSU, H., KUROSAKI, T., TOKUHISA, T., OHNO, H. & WANG, J. Y. 2012. Critical role of the IgM Fc receptor in IgM homeostasis, B-cell survival, and humoral immune responses. *Proc Natl Acad Sci U S A,* 109**,** E2699-706.

OVERED-SAYER, C., RAPLEY, L., MUSTELIN, T. & CLARKE, D. L. 2013. Are mast cells instrumental for fibrotic diseases? *Front Pharmacol,* 4**,** 174.

OVERMAN, E. L., RIVIER, J. E. & MOESER, A. J. 2012. CRF induces intestinal epithelial barrier injury via the release of mast cell proteases and TNF-alpha. *PLoS One,* 7**,** e39935.

PABST, R., GEIST, M., ROTHKOTTER, H. J. & FRITZ, F. J. 1988. Postnatal development and lymphocyte production of jejunal and ileal Peyer's patches in normal and gnotobiotic pigs. *Immunology,* 64**,** 539-44.

PAKDAMAN, M. N., UDANI, J. K., MOLINA, J. P. & SHAHANI, M. 2016. The effects of the DDS-1 strain of lactobacillus on symptomatic relief for lactose intolerance - a randomized, double-blind, placebo-controlled, crossover clinical trial. *Nutr J,* 15**,** 56.

PALM, N. W. & MEDZHITOV, R. 2009. Pattern recognition receptors and control of adaptive immunity. *Immunol Rev,* 227**,** 221-33.

PAMER, E. G. 2007. Immune responses to commensal and environmental microbes. *Nat Immunol,* 8**,** 1173-8.

PAPADIMITRIOU, K., ZOUMPOPOULOU, G., FOLIGNE, B., ALEXANDRAKI, V., KAZOU, M., POT, B. & TSAKALIDOU, E. 2015. Discovering probiotic microorganisms: in vitro, in vivo, genetic and omics approaches. *Front Microbiol,* 6**,** 58.

PARK, K., MIKULSKI, Z., SEO, G. Y., ANDREYEV, A. Y., MARCOVECCHIO, P., BLATCHLEY, A., KRONENBERG, M. & HEDRICK, C. C. 2016. The transcription factor NR4A3 controls CD103+ dendritic cell migration. *J Clin Invest,* 126**,** 4603-4615.

PATTERSON, J. K., LEI, X. G. & MILLER, D. D. 2008. The pig as an experimental model for elucidating the mechanisms governing dietary influence on mineral absorption. *Exp Biol Med (Maywood),* 233**,** 651-64.

PEACE, R. M., CAMPBELL, J., POLO, J., CRENSHAW, J., RUSSELL, L. & MOESER, A. 2011. Spray-dried porcine plasma influences intestinal barrier function, inflammation, and diarrhea in weaned pigs. *J Nutr,* 141**,** 1312-7.

PEREIRA, F. C. & BERRY, D. 2017. Microbial nutrient niches in the gut. *Environ Microbiol,* 19**,** 1366-1378.

PERRIN, M., DONALDSON, C., CHEN, R., BLOUNT, A., BERGGREN, T., BILEZIKJIAN, L., SAWCHENKO, P. & VALE, W. 1995. Identification of a second corticotropin-releasing factor receptor gene and characterization of a cDNA expressed in heart. *Proc Natl Acad Sci U S A,* 92**,** 2969-73.

PERRIN, M. H. & VALE, W. W. 1999. Corticotropin releasing factor receptors and their ligand family. *Ann N Y Acad Sci,* 885**,** 312-28.

PERTEA, M., KIM, D., PERTEA, G. M., LEEK, J. T. & SALZBERG, S. L. 2016. Transcript-level expression analysis of RNA-seq experiments with HISAT, StringTie and Ballgown. *Nat Protoc,* 11**,** 1650-67.

PERTEA, M., PERTEA, G. M., ANTONESCU, C. M., CHANG, T. C., MENDELL, J. T. & SALZBERG, S. L. 2015. StringTie enables improved reconstruction of a transcriptome from RNA-seq reads. *Nat Biotechnol,* 33**,** 290-5.

PEVZNER, V., WOLF, I., BURGSTAHLER, R., FORSTER, R. & LIPP, M. 1999. Regulation of expression of chemokine receptor BLR1/CXCR5 during B cell maturation. *Curr Top Microbiol Immunol,* 246**,** 79-84; discussion 85.

PIE, S., LALLES, J. P., BLAZY, F., LAFFITTE, J., SEVE, B. & OSWALD, I. P. 2004. Weaning is associated with an upregulation

of expression of inflammatory cytokines in the intestine of piglets. *J Nutr,* 134**,** 641-7.

PIMENTEL, H., BRAY, N. L., PUENTE, S., MELSTED, P. & PACHTER, L. 2017. Differential analysis of RNA-seq incorporating quantification uncertainty. *Nat Methods,* 14**,** 687-690.

PINCHUK, I. V., MIFFLIN, R. C., SAADA, J. I. & POWELL, D. W. 2010. Intestinal mesenchymal cells. *Curr Gastroenterol Rep,* 12**,** 310-8.

POHL, C. S., MEDLAND, J. E., MACKEY, E., EDWARDS, L. L., BAGLEY, K. D., DEWILDE, M. P., WILLIAMS, K. J. & MOESER, A. J. 2017. Early weaning stress induces chronic functional diarrhea, intestinal barrier defects, and increased mast cell activity in a porcine model of early life adversity. *Neurogastroenterol Motil*.

POPLAWSKI, A. & BINDER, H. 2017. Feasibility of sample size calculation for RNA-seq studies. *Brief Bioinform*.

POSTLETHWAITE, A. E., KESKI-OJA, J., MOSES, H. L. & KANG, A. H. 1987. Stimulation of the chemotactic migration of human fibroblasts by transforming growth factor beta. *J Exp Med,* 165**,** 251-6.

POWELL, J. 1998. Enhanced concatemer cloning-a modification to the SAGE (Serial Analysis of Gene Expression) technique. *Nucleic Acids Res,* 26**,** 3445-6.

PUIG-OLIVERAS, A., RAMAYO-CALDAS, Y., COROMINAS, J., ESTELLE, J., PEREZ-MONTARELO, D., HUDSON, N. J., CASELLAS, J., FOLCH, J. M. & BALLESTER, M. 2014. Differences in muscle transcriptome among pigs phenotypically extreme for fatty acid composition. *PLoS One,* 9**,** e99720.

QU, C., BRINCK-JENSEN, N. S., ZANG, M. & CHEN, K. 2014. Monocyte-derived dendritic cells: targets as potent antigen-presenting cells for the design of vaccines against infectious diseases. *Int J Infect Dis,* 19**,** 1-5.

QUIGLEY, E. M. 2013. Gut bacteria in health and disease. *Gastroenterol Hepatol (N Y),* 9**,** 560-9.

RADLOFF, J., ZAKRZEWSKI, S. S., PIEPER, R., MARKOV, A. G. & AMASHEH, S. 2017. Porcine milk induces a strengthening of barrier function in porcine jejunal epithelium in vitro. *Ann N Y Acad Sci,* 1397**,** 110-118.

RAJPUT, I. R., LI, L. Y., XIN, X., WU, B. B., JUAN, Z. L., CUI, Z. W., YU, D. Y. & LI, W. F. 2013. Effect of Saccharomyces boulardii and Bacillus subtilis B10 on intestinal ultrastructure modulation

and mucosal immunity development mechanism in broiler chickens. *Poult Sci,* 92**,** 956-65.

RAMAYO-CALDAS, Y., MACH, N., ESTEVE-CODINA, A., COROMINAS, J., CASTELLO, A., BALLESTER, M., ESTELLE, J., IBANEZ-ESCRICHE, N., FERNANDEZ, A. I., PEREZ-ENCISO, M. & FOLCH, J. M. 2012. Liver transcriptome profile in pigs with extreme phenotypes of intramuscular fatty acid composition. *BMC Genomics,* 13**,** 547.

RAO, J. N. & WANG, J. Y. 2010. *Regulation of Gastrointestinal Mucosal Growth.* San Rafael (CA).

RAO, R. K. & SAMAK, G. 2013. Protection and Restitution of Gut Barrier by Probiotics: Nutritional and Clinical Implications. *Curr Nutr Food Sci,* 9**,** 99-107.

REBOLDI, A. & CYSTER, J. G. 2016. Peyer's patches: organizing B-cell responses at the intestinal frontier. *Immunol Rev,* 271**,** 230-45.

REDDY, K. E., JEONG, J. Y., LEE, Y., LEE, H. J., KIM, M. S., KIM, D. W., JUNG, H. J., CHOE, C., OH, Y. K. & LEE, S. D. 2017. Deoxynivalenol- and zearalenone-contaminated feeds alter gene expression profiles in the livers of piglets. *Asian-Australas J Anim Sci*.

REINER, A., YEKUTIELI, D. & BENJAMINI, Y. 2003. Identifying differentially expressed genes using false discovery rate controlling procedures. *Bioinformatics,* 19**,** 368-75.

RESCIGNO, M., URBANO, M., VALZASINA, B., FRANCOLINI, M., ROTTA, G., BONASIO, R., GRANUCCI, F., KRAEHENBUHL, J. P. & RICCIARDI-CASTAGNOLI, P. 2001. Dendritic cells express tight junction proteins and penetrate gut epithelial monolayers to sample bacteria. *Nat Immunol,* 2**,** 361-7.

REYES, T. M., LEWIS, K., PERRIN, M. H., KUNITAKE, K. S., VAUGHAN, J., ARIAS, C. A., HOGENESCH, J. B., GULYAS, J., RIVIER, J., VALE, W. W. & SAWCHENKO, P. E. 2001. Urocortin II: a member of the corticotropin-releasing factor (CRF) neuropeptide family that is selectively bound by type 2 CRF receptors. *Proc Natl Acad Sci U S A,* 98**,** 2843-8.

RHEN, T. & CIDLOWSKI, J. A. 2005. Antiinflammatory action of glucocorticoids--new mechanisms for old drugs. *N Engl J Med,* 353**,** 1711-23.

RHOUMA, M., FAIRBROTHER, J. M., BEAUDRY, F. & LETELLIER, A. 2017. Post weaning diarrhea in pigs: risk factors and non-colistin-based control strategies. *Acta Vet Scand,* 59**,** 31.

RICHARDS, A., MUEHLBAUER, A. L., ALAZIZI, A., BURNS, M. B., GOULD, T. J., CASCARDO, C., PIQUE-REGI, R.,

BLEKHMAN, R. & LUCA, F. 2017. Variation in gut microbiota composition impacts host gene expression. *bioRxiv*.

RIERA ROMO, M., PEREZ-MARTINEZ, D. & CASTILLO FERRER, C. 2016. Innate immunity in vertebrates: an overview. *Immunology,* 148**,** 125-39.

RIGOTHIER, M. C., MACCARIO, J. & GAYRAL, P. 1994. Inhibitory activity of saccharomyces yeasts on the adhesion of Entamoeba histolytica trophozoites to human erythrocytes in vitro. *Parasitol Res,* 80**,** 10-5.

RIPERT, G., RACEDO, S. M., ELIE, A. M., JACQUOT, C., BRESSOLLIER, P. & URDACI, M. C. 2016. Secreted Compounds of the Probiotic Bacillus clausii Strain O/C Inhibit the Cytotoxic Effects Induced by Clostridium difficile and Bacillus cereus Toxins. *Antimicrob Agents Chemother,* 60**,** 3445-54.

RIVIER, C. & VALE, W. 1983. Modulation of stress-induced ACTH release by corticotropin-releasing factor, catecholamines and vasopressin. *Nature,* 305**,** 325-7.

ROBINSON, M. D., MCCARTHY, D. J. & SMYTH, G. K. 2010. edgeR: a Bioconductor package for differential expression analysis of digital gene expression data. *Bioinformatics,* 26**,** 139-40.

RODINO-JANEIRO, B. K., ALONSO-COTONER, C., PIGRAU, M., LOBO, B., VICARIO, M. & SANTOS, J. 2015. Role of Corticotropin-releasing Factor in Gastrointestinal Permeability. *J Neurogastroenterol Motil,* 21**,** 33-50.

RODRIGUES, A. C., CARA, D. C., FRETEZ, S. H., CUNHA, F. Q., VIEIRA, E. C., NICOLI, J. R. & VIEIRA, L. Q. 2000. Saccharomyces boulardii stimulates sIgA production and the phagocytic system of gnotobiotic mice. *J Appl Microbiol,* 89**,** 404-14.

ROGIER, E. W., FRANTZ, A. L., BRUNO, M. E., WEDLUND, L., COHEN, D. A., STROMBERG, A. J. & KAETZEL, C. S. 2014. Secretory antibodies in breast milk promote long-term intestinal homeostasis by regulating the gut microbiota and host gene expression. *Proc Natl Acad Sci U S A,* 111**,** 3074-9.

ROLHION, N. & CHASSAING, B. 2016. When pathogenic bacteria meet the intestinal microbiota. *Philos Trans R Soc Lond B Biol Sci,* 371.

ROOS, A., ESSERS, M., VAN GIJLSWIJK-JANSSEN, D., BOVIN, N. V. & DAHA, M. R. 2001. Both IgG and IgM anti-pig antibodies induce complement activation and cytotoxicity. *Xenotransplantation,* 8**,** 3-14.

ROTHE, J., GEHR, G., LOETSCHER, H. & LESSLAUER, W. 1992. Tumor necrosis factor receptors--structure and function. *Immunol Res,* 11**,** 81-90.

ROUND, J. L. & MAZMANIAN, S. K. 2009. The gut microbiota shapes intestinal immune responses during health and disease. *Nat Rev Immunol,* 9**,** 313-23.

SAITO, A., OKAZAKI, H., SUGAWARA, I., YAMAMOTO, K. & TAKIZAWA, H. 2003. Potential action of IL-4 and IL-13 as fibrogenic factors on lung fibroblasts in vitro. *Int Arch Allergy Immunol,* 132**,** 168-76.

SAKATA, T., KOJIMA, T., FUJIEDA, M., TAKAHASHI, M. & MICHIBATA, T. 2003. Influences of probiotic bacteria on organic acid production by pig caecal bacteria in vitro. *Proc Nutr Soc,* 62**,** 73-80.

SALARIA, S., CHANA, G., CALDARA, F., FELTRIN, E., ALTIERI, M., FAGGIONI, F., DOMENICI, E., MERLO-PICH, E. & EVERALL, I. P. 2006. Microarray analysis of cultured human brain aggregates following cortisol exposure: implications for cellular functions relevant to mood disorders. *Neurobiol Dis,* 23**,** 630-6.

SALAZAR-GONZALEZ, R. M., NIESS, J. H., ZAMMIT, D. J., RAVINDRAN, R., SRINIVASAN, A., MAXWELL, J. R., STOKLASEK, T., YADAV, R., WILLIAMS, I. R., GU, X., MCCORMICK, B. A., PAZOS, M. A., VELLA, A. T., LEFRANCOIS, L., REINECKER, H. C. & MCSORLEY, S. J. 2006. CCR6-mediated dendritic cell activation of pathogen-specific T cells in Peyer's patches. *Immunity,* 24**,** 623-32.

SAMONIS, G., FALAGAS, M. E., LIONAKIS, S., NTAOUKAKIS, M., KOFTERIDIS, D. P., NTALAS, I. & MARAKI, S. 2011. Saccharomyces boulardii and Candida albicans experimental colonization of the murine gut. *Med Mycol,* 49**,** 395-9.

SANDERS, M. E., AKKERMANS, L. M., HALLER, D., HAMMERMAN, C., HEIMBACH, J., HORMANNSPERGER, G., HUYS, G., LEVY, D. D., LUTGENDORFF, F., MACK, D., PHOTHIRATH, P., SOLANO-AGUILAR, G. & VAUGHAN, E. 2010. Safety assessment of probiotics for human use. *Gut Microbes,* 1**,** 164-85.

SANGILD, P. T. 2003. Uptake of colostral immunoglobulins by the compromised newborn farm animal. *Acta Vet Scand Suppl,* 98**,** 105-22.

SANKARAN-WALTERS, S., MACAL, M., GRISHINA, I., NAGY, L., GOULART, L., COOLIDGE, K., LI, J., FENTON, A., WILLIAMS, T., MILLER, M. K., FLAMM, J., PRINDIVILLE,

T., GEORGE, M. & DANDEKAR, S. 2013. Sex differences matter in the gut: effect on mucosal immune activation and inflammation. *Biol Sex Differ,* 4**,** 10.

SANTOCCHI, E., GUIDUCCI, L., FULCERI, F., BILLECI, L., BUZZIGOLI, E., APICELLA, F., CALDERONI, S., GROSSI, E., MORALES, M. A. & MURATORI, F. 2016. Gut to brain interaction in Autism Spectrum Disorders: a randomized controlled trial on the role of probiotics on clinical, biochemical and neurophysiological parameters. *BMC Psychiatry,* 16**,** 183.

SANTOS, J., BENJAMIN, M., YANG, P. C., PRIOR, T. & PERDUE, M. H. 2000. Chronic stress impairs rat growth and jejunal epithelial barrier function: role of mast cells. *Am J Physiol Gastrointest Liver Physiol,* 278**,** G847-54.

SANTOS, J., SAUNDERS, P. R., HANSSEN, N. P., YANG, P. C., YATES, D., GROOT, J. A. & PERDUE, M. H. 1999. Corticotropin-releasing hormone mimics stress-induced colonic epithelial pathophysiology in the rat. *Am J Physiol,* 277**,** G391-9.

SANTOS, J., YANG, P. C., SODERHOLM, J. D., BENJAMIN, M. & PERDUE, M. H. 2001. Role of mast cells in chronic stress induced colonic epithelial barrier dysfunction in the rat. *Gut,* 48**,** 630-6.

SANTOS, J., YATES, D., GUILARTE, M., VICARIO, M., ALONSO, C. & PERDUE, M. H. 2008. Stress neuropeptides evoke epithelial responses via mast cell activation in the rat colon. *Psychoneuroendocrinology,* 33**,** 1248-56.

SARMA, J. V. & WARD, P. A. 2011. The complement system. *Cell Tissue Res,* 343**,** 227-35.

SATO, A. & IWASAKI, A. 2005. Peyer's patch dendritic cells as regulators of mucosal adaptive immunity. *Cell Mol Life Sci,* 62**,** 1333-8.

SAUNDERS, P. R., SANTOS, J., HANSSEN, N. P., YATES, D., GROOT, J. A. & PERDUE, M. H. 2002. Physical and psychological stress in rats enhances colonic epithelial permeability via peripheral CRH. *Dig Dis Sci,* 47**,** 208-15.

SAUTRON, V., TERENINA, E., GRESS, L., LIPPI, Y., BILLON, Y., LARZUL, C., LIAUBET, L., VILLA-VIALANEIX, N. & MORMEDE, P. 2015. Time course of the response to ACTH in pig: biological and transcriptomic study. *BMC Genomics,* 16**,** 961.

SAWCHENKO, P. E., IMAKI, T., POTTER, E., KOVACS, K., IMAKI, J. & VALE, W. 1993. The functional neuroanatomy of corticotropin-releasing factor. *Ciba Found Symp,* 172**,** 5-21; discussion 21-9.

SCANZANO, A. & COSENTINO, M. 2015. Adrenergic regulation of innate immunity: a review. *Front Pharmacol,* 6**,** 171.

SCHARF, O., GOLDING, H., KING, L. R., ELLER, N., FRAZIER, D., GOLDING, B. & SCOTT, D. E. 2001. Immunoglobulin G3 from polyclonal human immunodeficiency virus (HIV) immune globulin is more potent than other subclasses in neutralizing HIV type 1. *J Virol,* 75**,** 6558-65.

SCHLOSS, P. D., WESTCOTT, S. L., RYABIN, T., HALL, J. R., HARTMANN, M., HOLLISTER, E. B., LESNIEWSKI, R. A., OAKLEY, B. B., PARKS, D. H., ROBINSON, C. J., SAHL, J. W., STRES, B., THALLINGER, G. G., VAN HORN, D. J. & WEBER, C. F. 2009. Introducing mothur: open-source, platform-independent, community-supported software for describing and comparing microbial communities. *Appl Environ Microbiol,* 75**,** 7537-41.

SCHNEIDER, S. M., GIRARD-PIPAU, F., FILIPPI, J., HEBUTERNE, X., MOYSE, D., HINOJOSA, G. C., POMPEI, A. & RAMPAL, P. 2005. Effects of Saccharomyces boulardii on fecal short-chain fatty acids and microflora in patients on long-term total enteral nutrition. *World J Gastroenterol,* 11**,** 6165-9.

SCHROEDER, H. W., JR. & CAVACINI, L. 2010. Structure and function of immunoglobulins. *J Allergy Clin Immunol,* 125**,** S41-52.

SCHURCH, N. J., SCHOFIELD, P., GIERLINSKI, M., COLE, C., SHERSTNEV, A., SINGH, V., WROBEL, N., GHARBI, K., SIMPSON, G. G., OWEN-HUGHES, T., BLAXTER, M. & BARTON, G. J. 2016. Erratum: How many biological replicates are needed in an RNA-seq experiment and which differential expression tool should you use? *RNA,* 22**,** 1641.

SCHWARTZ, L. B. 1994. Tryptase: a clinical indicator of mast cell-dependent events. *Allergy Proc,* 15**,** 119-23.

SELMIN, O. I., FANG, C., LYON, A. M., DOETSCHMAN, T. C., THOMPSON, P. A., MARTINEZ, J. D., SMITH, J. W., LANCE, P. M. & ROMAGNOLO, D. F. 2016. Inactivation of Adenomatous Polyposis Coli Reduces Bile Acid/Farnesoid X Receptor Expression through Fxr gene CpG Methylation in Mouse Colon Tumors and Human Colon Cancer Cells. *J Nutr,* 146**,** 236-42.

SENBANJO, L. T. & CHELLAIAH, M. A. 2017. CD44: A Multifunctional Cell Surface Adhesion Receptor Is a Regulator of Progression and Metastasis of Cancer Cells. *Front Cell Dev Biol,* 5**,** 18.

SHA, Y., PHAN, J. H. & WANG, M. D. 2015. Effect of low-expression gene filtering on detection of differentially expressed genes in RNA-seq data. *Conf Proc IEEE Eng Med Biol Soc,* 2015**,** 6461-4.

SHI, L. H., BALAKRISHNAN, K., THIAGARAJAH, K., MOHD ISMAIL, N. I. & YIN, O. S. 2016. Beneficial Properties of Probiotics. *Trop Life Sci Res,* 27**,** 73-90.

SHIOTA, N., NISHIKORI, Y., KAKIZOE, E., SHIMOURA, K., NIIBAYASHI, T., SHIMBORI, C., TANAKA, T. & OKUNISHI, H. 2010. Pathophysiological role of skin mast cells in wound healing after scald injury: study with mast cell-deficient W/W(V) mice. *Int Arch Allergy Immunol,* 151**,** 80-8.

SHUI, Y., GUAN, Z. B. & ZHANG, S. Q. 2008. Molecular characterization of cytokine TWEAK and its receptor Fn14 in pig (Sus scrofa). *Vet Immunol Immunopathol,* 126**,** 396-402.

SINGER, M. & SANSONETTI, P. J. 2004. IL-8 is a key chemokine regulating neutrophil recruitment in a new mouse model of Shigella-induced colitis. *J Immunol,* 173**,** 4197-206.

SINKORA, J., REHAKOVA, Z., SINKORA, M., CUKROWSKA, B. & TLASKALOVA-HOGENOVA, H. 2002. Early development of immune system in pigs. *Vet Immunol Immunopathol,* 87**,** 301-6.

SINKORA, M., SUN, J. & BUTLER, J. E. 2000. Antibody repertoire development in fetal and neonatal piglets. V. VDJ gene chimeras resembling gene conversion products are generated at high frequency by PCR in vitro. *Mol Immunol,* 37**,** 1025-34.

SLEBIODA, T. J. & KMIEC, Z. 2014. Tumour necrosis factor superfamily members in the pathogenesis of inflammatory bowel disease. *Mediators Inflamm,* 2014**,** 325129.

SMITH, C. A., FARRAH, T. & GOODWIN, R. G. 1994. The TNF receptor superfamily of cellular and viral proteins: activation, costimulation, and death. *Cell,* 76**,** 959-62.

SMITH, F., CLARK, J. E., OVERMAN, B. L., TOZEL, C. C., HUANG, J. H., RIVIER, J. E., BLIKSLAGER, A. T. & MOESER, A. J. 2010. Early weaning stress impairs development of mucosal barrier function in the porcine intestine. *Am J Physiol Gastrointest Liver Physiol,* 298**,** G352-63.

SMITH, S. M. & VALE, W. W. 2006. The role of the hypothalamic-pituitary-adrenal axis in neuroendocrine responses to stress. *Dialogues Clin Neurosci,* 8**,** 383-95.

SOCHA-BANASIAK, A., PIERZYNOWSKI, S., WOLINSKI, J., GRUJIC, D., BORYCZKA, M., GRZESIAK, P., SZCZUREK, P., CZKWIANIANC, E., WESTROM, B. & GONCHAROVA, K. 2017. The pig as a model for premature infants - the importance of

immunoglobulin supplementation for growth and development. *J Biol Regul Homeost Agents,* 31**,** 87-92.

SODERHOLM, J. D., YANG, P. C., CEPONIS, P., VOHRA, A., RIDDELL, R., SHERMAN, P. M. & PERDUE, M. H. 2002a. Chronic stress induces mast cell-dependent bacterial adherence and initiates mucosal inflammation in rat intestine. *Gastroenterology,* 123**,** 1099-108.

SODERHOLM, J. D., YATES, D. A., GAREAU, M. G., YANG, P. C., MACQUEEN, G. & PERDUE, M. H. 2002b. Neonatal maternal separation predisposes adult rats to colonic barrier dysfunction in response to mild stress. *Am J Physiol Gastrointest Liver Physiol,* 283**,** G1257-63.

SODHI, S. S., SONG, K. D., GHOSH, M., SHARMA, N., LEE, S. J., KIM, J. H., KIM, N., MONGRE, R. K., ADHIKARI, P., KIM, J. Y., HONG, S. P., OH, S. J. & JEONG, D. K. 2014. Comparative transcriptomic analysis by RNA-seq to discern differential expression of genes in liver and muscle tissues of adult Berkshire and Jeju Native Pig. *Gene,* 546**,** 233-42.

SOHN, K. & UNDERWOOD, M. A. 2017. Prenatal and postnatal administration of prebiotics and probiotics. *Semin Fetal Neonatal Med*.

SOLLNER, J. F., LEPARC, G., HILDEBRANDT, T., KLEIN, H., THOMAS, L., STUPKA, E. & SIMON, E. 2017. An RNA-Seq atlas of gene expression in mouse and rat normal tissues. *Sci Data,* 4**,** 170185.

SONCK, E., STUYVEN, E., GODDEERIS, B. & COX, E. 2010. The effect of beta-glucans on porcine leukocytes. *Vet Immunol Immunopathol,* 135**,** 199-207.

STALLMACH, A., VON LAMPE, B., MATTHES, H., BORNHOFT, G. & RIECKEN, E. O. 1992. Diminished expression of integrin adhesion molecules on human colonic epithelial cells during the benign to malign tumour transformation. *Gut,* 33**,** 342-6.

STEAD, R. H., DIXON, M. F., BRAMWELL, N. H., RIDDELL, R. H. & BIENENSTOCK, J. 1989. Mast cells are closely apposed to nerves in the human gastrointestinal mucosa. *Gastroenterology,* 97**,** 575-85.

STENGEL, A. & TACHE, Y. 2010. Corticotropin-releasing factor signaling and visceral response to stress. *Exp Biol Med (Maywood),* 235**,** 1168-78.

STENZEL, P., KESTERSON, R., YEUNG, W., CONE, R. D., RITTENBERG, M. B. & STENZEL-POORE, M. P. 1995. Identification of a novel murine receptor for corticotropin-

releasing hormone expressed in the heart. *Mol Endocrinol,* 9**,** 637-45.

STEVENS, C. E., ARGENZIO, R. A. & ROBERTS, M. C. 1986. Comparative physiology of the mammalian colon and suggestions for animal models of human disorders. *Clin Gastroenterol,* 15**,** 763-85.

STEVENS, R. L. & ADACHI, R. 2007. Protease-proteoglycan complexes of mouse and human mast cells and importance of their beta-tryptase-heparin complexes in inflammation and innate immunity. *Immunol Rev,* 217**,** 155-67.

STOKES, C. R. 2017. The development and role of microbial-host interactions in gut mucosal immune development. *J Anim Sci Biotechnol,* 8**,** 12.

STOW, J. L., LOW, P. C., OFFENHAUSER, C. & SANGERMANI, D. 2009. Cytokine secretion in macrophages and other cells: pathways and mediators. *Immunobiology,* 214**,** 601-12.

STROUD, M. J., KAMMERER, R. A. & BALLESTREM, C. 2011. Characterization of G2L3 (GAS2-like 3), a new microtubule- and actin-binding protein related to spectraplakins. *J Biol Chem,* 286**,** 24987-95.

STUBBE, H., BERDOZ, J., KRAEHENBUHL, J. P. & CORTHESY, B. 2000. Polymeric IgA is superior to monomeric IgA and IgG carrying the same variable domain in preventing Clostridium difficile toxin A damaging of T84 monolayers. *J Immunol,* 164**,** 1952-60.

SU, D. L., LU, Z. M., SHEN, M. N., LI, X. & SUN, L. Y. 2012. Roles of pro- and anti-inflammatory cytokines in the pathogenesis of SLE. *J Biomed Biotechnol,* 2012**,** 347141.

SUGIHARA, T., KOBORI, A., IMAEDA, H., TSUJIKAWA, T., AMAGASE, K., TAKEUCHI, K., FUJIYAMA, Y. & ANDOH, A. 2010. The increased mucosal mRNA expressions of complement C3 and interleukin-17 in inflammatory bowel disease. *Clin Exp Immunol,* 160**,** 386-93.

SUMMERFIELD, A. & MCCULLOUGH, K. C. 2009. The porcine dendritic cell family. *Dev Comp Immunol,* 33**,** 299-309.

SUO, C., YIN, Y., WANG, X., LOU, X., SONG, D., WANG, X. & GU, Q. 2012. Effects of lactobacillus plantarum ZJ316 on pig growth and pork quality. *BMC Vet Res,* 8**,** 89.

SWIDSINSKI, A., LOENING-BAUCKE, V. & HERBER, A. 2009. Mucosal flora in Crohn's disease and ulcerative colitis - an overview. *J Physiol Pharmacol,* 60 Suppl 6**,** 61-71.

SZEKY, A., RATZ, F., TUBOLY, S. & NAGY, G. 1979. Absorption of colostral immunoglobulins in suckling piglets. *Acta Microbiol Acad Sci Hung,* 26**,** 99-110.

TACHE, Y. & BONAZ, B. 2007. Corticotropin-releasing factor receptors and stress-related alterations of gut motor function. *J Clin Invest,* 117**,** 33-40.

TACHE, Y., LARAUCHE, M., YUAN, P. Q. & MILLION, M. 2017. Brain and gut CRF signaling: biological actions and role in the gastrointestinal tract. *Curr Mol Pharmacol*.

TACHE, Y. & PERDUE, M. H. 2004. Role of peripheral CRF signalling pathways in stress-related alterations of gut motility and mucosal function. *Neurogastroenterol Motil,* 16 Suppl 1**,** 137-42.

TAKADA, M., NISHIDA, K., KATAOKA-KATO, A., GONDO, Y., ISHIKAWA, H., SUDA, K., KAWAI, M., HOSHI, R., WATANABE, O., IGARASHI, T., KUWANO, Y., MIYAZAKI, K. & ROKUTAN, K. 2016. Probiotic Lactobacillus casei strain Shirota relieves stress-associated symptoms by modulating the gut-brain interaction in human and animal models. *Neurogastroenterol Motil*.

TAKEDA, K. & AKIRA, S. 2005. Toll-like receptors in innate immunity. *Int Immunol,* 17**,** 1-14.

TARTAGLIA, L. A. & GOEDDEL, D. V. 1992. Two TNF receptors. *Immunol Today,* 13**,** 151-3.

TASTEYRE, A., BARC, M. C., KARJALAINEN, T., BOURLIOUX, P. & COLLIGNON, A. 2002. Inhibition of in vitro cell adherence of Clostridium difficile by Saccharomyces boulardii. *Microb Pathog,* 32**,** 219-25.

TCHOUGOUNOVA, E., LUNDEQUIST, A., FAJARDO, I., WINBERG, J. O., ABRINK, M. & PEJLER, G. 2005. A key role for mast cell chymase in the activation of pro-matrix metalloprotease-9 and pro-matrix metalloprotease-2. *J Biol Chem,* 280**,** 9291-6.

THACKER, P. A. 2013. Alternatives to antibiotics as growth promoters for use in swine production: a review. *J Anim Sci Biotechnol,* 4**,** 35.

THAPA, B. R. 2005. Health factors in colostrum. *Indian J Pediatr,* 72**,** 579-81.

THOMAS, S., PRZESDZING, I., METZKE, D., SCHMITZ, J., RADBRUCH, A. & BAUMGART, D. C. 2009. Saccharomyces boulardii inhibits lipopolysaccharide-induced activation of human dendritic cells and T cell proliferation. *Clin Exp Immunol,* 156**,** 78-87.

TIAGO, F. C., MARTINS, F. S., SOUZA, E. L., PIMENTA, P. F., ARAUJO, H. R., CASTRO, I. M., BRANDAO, R. L. & NICOLI, J. R. 2012. Adhesion to the yeast cell surface as a mechanism for trapping pathogenic bacteria by Saccharomyces probiotics. *J Med Microbiol,* 61**,** 1194-207.

TOHNO, M., SHIMOSATO, T., MOUE, M., ASO, H., WATANABE, K., KAWAI, Y., YAMAGUCHI, T., SAITO, T. & KITAZAWA, H. 2006. Toll-like receptor 2 and 9 are expressed and functional in gut-associated lymphoid tissues of presuckling newborn swine. *Vet Res,* 37**,** 791-812.

TOMAS, C., NEWTON, J. & WATSON, S. 2013. A review of hypothalamic-pituitary-adrenal axis function in chronic fatigue syndrome. *ISRN Neurosci,* 2013**,** 784520.

TRACEY, D., KLARESKOG, L., SASSO, E. H., SALFELD, J. G. & TAK, P. P. 2008. Tumor necrosis factor antagonist mechanisms of action: a comprehensive review. *Pharmacol Ther,* 117**,** 244-79.

TRAPNELL, C., ROBERTS, A., GOFF, L., PERTEA, G., KIM, D., KELLEY, D. R., PIMENTEL, H., SALZBERG, S. L., RINN, J. L. & PACHTER, L. 2012. Differential gene and transcript expression analysis of RNA-seq experiments with TopHat and Cufflinks. *Nat Protoc,* 7**,** 562-78.

TRAUTMANN, A., TOKSOY, A., ENGELHARDT, E., BROCKER, E. B. & GILLITZER, R. 2000. Mast cell involvement in normal human skin wound healing: expression of monocyte chemoattractant protein-1 is correlated with recruitment of mast cells which synthesize interleukin-4 in vivo. *J Pathol,* 190**,** 100-6.

TURNBULL, A. V. & RIVIER, C. L. 1999. Regulation of the hypothalamic-pituitary-adrenal axis by cytokines: actions and mechanisms of action. *Physiol Rev,* 79**,** 1-71.

TURNER, M. D., NEDJAI, B., HURST, T. & PENNINGTON, D. J. 2014. Cytokines and chemokines: At the crossroads of cell signalling and inflammatory disease. *Biochim Biophys Acta,* 1843**,** 2563-2582.

TURPIN, D. L., LANGENDIJK, P., CHEN, T. Y. & PLUSKE, J. R. 2016. Intermittent Suckling in Combination with an Older Weaning Age Improves Growth, Feed Intake and Aspects of Gastrointestinal Tract Carbohydrate Absorption in Pigs after Weaning. *Animals (Basel),* 6.

UBEROS, J., AGUILERA-RODRIGUEZ, E., JEREZ-CALERO, A., MOLINA-OYA, M., MOLINA-CARBALLO, A. & NARBONA-LOPEZ, E. 2017. Probiotics to prevent necrotising enterocolitis and nosocomial infection in very low birth weight preterm infants. *Br J Nutr,* 117**,** 994-1000.

UCHIDA, K. & KAMIKAWA, Y. 2007. Muscularis mucosae - the forgotten sibling. *J Smooth Muscle Res,* 43**,** 157-77.

UEMATSU, S., SATO, S., YAMAMOTO, M., HIROTANI, T., KATO, H., TAKESHITA, F., MATSUDA, M., COBAN, C., ISHII, K. J., KAWAI, T., TAKEUCHI, O. & AKIRA, S. 2005. Interleukin-1 receptor-associated kinase-1 plays an essential role for Toll-like receptor (TLR)7- and TLR9-mediated interferon-{alpha} induction. *J Exp Med,* 201**,** 915-23.

UENISHI, H. & SHINKAI, H. 2009. Porcine Toll-like receptors: the front line of pathogen monitoring and possible implications for disease resistance. *Dev Comp Immunol,* 33**,** 353-61.

ULRICH-LAI, Y. M. & HERMAN, J. P. 2009. Neural regulation of endocrine and autonomic stress responses. *Nat Rev Neurosci,* 10**,** 397-409.

UPHAM, J. W., RATE, A., ROWE, J., KUSEL, M., SLY, P. D. & HOLT, P. G. 2006. Dendritic cell immaturity during infancy restricts the capacity to express vaccine-specific T-cell memory. *Infect Immun,* 74**,** 1106-12.

VALDES-VARELA, L., HERNANDEZ-BARRANCO, A. M., RUAS-MADIEDO, P. & GUEIMONDE, M. 2016. Effect of Bifidobacterium upon Clostridium difficile Growth and Toxicity When Co-cultured in Different Prebiotic Substrates. *Front Microbiol,* 7**,** 738.

VALE, W., SPIESS, J., RIVIER, C. & RIVIER, J. 1981. Characterization of a 41-residue ovine hypothalamic peptide that stimulates secretion of corticotropin and beta-endorphin. *Science,* 213**,** 1394-7.

VAN DER KLEIJ, H. P., MA, D., REDEGELD, F. A., KRANEVELD, A. D., NIJKAMP, F. P. & BIENENSTOCK, J. 2003. Functional expression of neurokinin 1 receptors on mast cells induced by IL-4 and stem cell factor. *J Immunol,* 171**,** 2074-9.

VAN DER MEER, M. J., SWEEP, C. G., RIJNKELS, C. E., PESMAN, G. J., TILDERS, F. J., KLOPPENBORG, P. W. & HERMUS, A. R. 1996. Acute stimulation of the hypothalamic-pituitary-adrenal axis by IL-1 beta, TNF alpha and IL-6: a dose response study. *J Endocrinol Invest,* 19**,** 175-82.

VAN ERK, M. J., TEULING, E., STAAL, Y. C., HUYBERS, S., VAN BLADEREN, P. J., AARTS, J. M. & VAN OMMEN, B. 2004. Time- and dose-dependent effects of curcumin on gene expression in human colon cancer cells. *J Carcinog,* 3**,** 8.

VANDEVYVER, S., DEJAGER, L., TUCKERMANN, J. & LIBERT, C. 2013. New insights into the anti-inflammatory mechanisms of

glucocorticoids: an emerging role for glucocorticoid-receptor-mediated transactivation. *Endocrinology,* 154**,** 993-1007.

VARNER, J. A., EMERSON, D. A. & JULIANO, R. L. 1995. Integrin alpha 5 beta 1 expression negatively regulates cell growth: reversal by attachment to fibronectin. *Mol Biol Cell,* 6**,** 725-40.

VAUGHAN, J., DONALDSON, C., BITTENCOURT, J., PERRIN, M. H., LEWIS, K., SUTTON, S., CHAN, R., TURNBULL, A. V., LOVEJOY, D., RIVIER, C. & ET AL. 1995. Urocortin, a mammalian neuropeptide related to fish urotensin I and to corticotropin-releasing factor. *Nature,* 378**,** 287-92.

VEERAPPAN, A., O'CONNOR, N. J., BRAZIN, J., REID, A. C., JUNG, A., MCGEE, D., SUMMERS, B., BRANCH-ELLIMAN, D., STILES, B., WORGALL, S., KANER, R. J. & SILVER, R. B. 2013. Mast cells: a pivotal role in pulmonary fibrosis. *DNA Cell Biol,* 32**,** 206-18.

VELCULESCU, V. E., ZHANG, L., VOGELSTEIN, B. & KINZLER, K. W. 1995. Serial analysis of gene expression. *Science,* 270**,** 484-7.

VENUGOPALAN, V., SHRINER, K. A. & WONG-BERINGER, A. 2010. Regulatory oversight and safety of probiotic use. *Emerg Infect Dis,* 16**,** 1661-5.

VIGHI, G., MARCUCCI, F., SENSI, L., DI CARA, G. & FRATI, F. 2008. Allergy and the gastrointestinal system. *Clin Exp Immunol,* 153 Suppl 1**,** 3-6.

VITA, N., LAURENT, P., LEFORT, S., CHALON, P., LELIAS, J. M., KAGHAD, M., LE FUR, G., CAPUT, D. & FERRARA, P. 1993. Primary structure and functional expression of mouse pituitary and human brain corticotrophin releasing factor receptors. *FEBS Lett,* 335**,** 1-5.

VOLAREVIC, V., AL-QAHTANI, A., ARSENIJEVIC, N., PAJOVIC, S. & LUKIC, M. L. 2010. Interleukin-1 receptor antagonist (IL-1Ra) and IL-1Ra producing mesenchymal stem cells as modulators of diabetogenesis. *Autoimmunity,* 43**,** 255-63.

VON LAMPE, B., BARTHEL, B., COUPLAND, S. E., RIECKEN, E. O. & ROSEWICZ, S. 2000. Differential expression of matrix metalloproteinases and their tissue inhibitors in colon mucosa of patients with inflammatory bowel disease. *Gut,* 47**,** 63-73.

WALSH, A. M., SWEENEY, T., O'SHEA, C. J., DOYLE, D. N. & O'DOHERTY, J. V. 2012. Effects of supplementing dietary laminarin and fucoidan on intestinal morphology and the immune gene expression in the weaned pig. *J Anim Sci,* 90 Suppl 4**,** 284-6.

WANG, J., CHEN, L., LI, P., LI, X., ZHOU, H., WANG, F., LI, D., YIN, Y. & WU, G. 2008. Gene expression is altered in piglet

small intestine by weaning and dietary glutamine supplementation. *J Nutr,* 138**,** 1025-32.

WANG, K., WEI, G. & LIU, D. 2012. CD19: a biomarker for B cell development, lymphoma diagnosis and therapy. *Exp Hematol Oncol,* 1**,** 36.

WANG, L., FENG, Z., WANG, X., WANG, X. & ZHANG, X. 2010. DEGseq: an R package for identifying differentially expressed genes from RNA-seq data. *Bioinformatics,* 26**,** 136-8.

WANG, X. W. & WANG, J. X. 2013. Pattern recognition receptors acting in innate immune system of shrimp against pathogen infections. *Fish Shellfish Immunol,* 34**,** 981-9.

WANG, Y., XUE, S., LIU, X., LIU, H., HU, T., QIU, X., ZHANG, J. & LEI, M. 2016. Analyses of Long Non-Coding RNA and mRNA profiling using RNA sequencing during the pre-implantation phases in pig endometrium. *Sci Rep,* 6**,** 20238.

WANG, Z., GERSTEIN, M. & SNYDER, M. 2009. RNA-Seq: a revolutionary tool for transcriptomics. *Nat Rev Genet,* 10**,** 57-63.

WARRINGTON, R., WATSON, W., KIM, H. L. & ANTONETTI, F. R. 2011. An introduction to immunology and immunopathology. *Allergy Asthma Clin Immunol,* 7 Suppl 1**,** S1.

WATTS, A. G. 2005. Glucocorticoid regulation of peptide genes in neuroendocrine CRH neurons: a complexity beyond negative feedback. *Front Neuroendocrinol,* 26**,** 109-30.

WEBER, N., NIELSEN, J. P., JAKOBSEN, A. S., PEDERSEN, L. L., HANSEN, C. F. & PEDERSEN, K. S. 2015. Occurrence of diarrhoea and intestinal pathogens in non-medicated nursery pigs. *Acta Vet Scand,* 57**,** 64.

WEBSTER, J. I. & STERNBERG, E. M. 2004. Role of the hypothalamic-pituitary-adrenal axis, glucocorticoids and glucocorticoid receptors in toxic sequelae of exposure to bacterial and viral products. *J Endocrinol,* 181**,** 207-21.

WEINER, H. L. 2001. Induction and mechanism of action of transforming growth factor-beta-secreting Th3 regulatory cells. *Immunol Rev,* 182**,** 207-14.

WEIR, T. L., MANTER, D. K., SHEFLIN, A. M., BARNETT, B. A., HEUBERGER, A. L. & RYAN, E. P. 2013. Stool microbiome and metabolome differences between colorectal cancer patients and healthy adults. *PLoS One,* 8**,** e70803.

WELLER, K., FOITZIK, K., PAUS, R., SYSKA, W. & MAURER, M. 2006. Mast cells are required for normal healing of skin wounds in mice. *FASEB J,* 20**,** 2366-8.

WENG, M. & WALKER, W. A. 2013. The role of gut microbiota in programming the immune phenotype. *J Dev Orig Health Dis,* 4**,** 203-14.

WEST, C., STANISZ, A. M., WONG, A. & KUNZE, W. A. 2016. Effects of Saccharomyces cerevisiae or boulardii yeasts on acute stress induced intestinal dysmotility. *World J Gastroenterol,* 22**,** 10532-10544.

WESTENDORP, R. G., LANGERMANS, J. A., HUIZINGA, T. W., ELOUALI, A. H., VERWEIJ, C. L., BOOMSMA, D. I. & VANDENBROUCKE, J. P. 1997. Genetic influence on cytokine production and fatal meningococcal disease. *Lancet,* 349**,** 170-3.

WESTROM, B. R., OHLSSON, B. G., SVENDSEN, J., TAGESSON, C. & KARLSSON, B. W. 1985. Intestinal transmission of macromolecules (BSA and FITC-dextran) in the neonatal pig: enhancing effect of colostrum, proteins and proteinase inhibitors. *Biol Neonate,* 47**,** 359-66.

WHITE, O., DUNNING, T., SUTTON, G., ADAMS, M., VENTER, J. C. & FIELDS, C. 1993. A quality control algorithm for DNA sequencing projects. *Nucleic Acids Res,* 21**,** 3829-38.

WICK, G., GRUNDTMAN, C., MAYERL, C., WIMPISSINGER, T. F., FEICHTINGER, J., ZELGER, B., SGONC, R. & WOLFRAM, D. 2013. The immunology of fibrosis. *Annu Rev Immunol,* 31**,** 107-35.

WIESE, F., SIMON, O. & WEYRAUCH, K. D. 2003. Morphology of the small intestine of weaned piglets and a novel method for morphometric evaluation. *Anat Histol Embryol,* 32**,** 102-9.

WILKINS, T. & SEQUOIA, J. 2017. Probiotics for Gastrointestinal Conditions: A Summary of the Evidence. *Am Fam Physician,* 96**,** 170-178.

WILLIAMS, C. L., PETERSON, J. M., VILLAR, R. G. & BURKS, T. F. 1987. Corticotropin-releasing factor directly mediates colonic responses to stress. *Am J Physiol,* 253**,** G582-6.

WILLIAMS, C. L., VILLAR, R. G., PETERSON, J. M. & BURKS, T. F. 1988. Stress-induced changes in intestinal transit in the rat: a model for irritable bowel syndrome. *Gastroenterology,* 94**,** 611-21.

WILLIAMS, C. R., BACCARELLA, A., PARRISH, J. Z. & KIM, C. C. 2016. Trimming of sequence reads alters RNA-Seq gene expression estimates. *BMC Bioinformatics,* 17**,** 103.

WILLING, B. P. & VAN KESSEL, A. G. 2007. Enterocyte proliferation and apoptosis in the caudal small intestine is influenced by the composition of colonizing commensal bacteria in the neonatal gnotobiotic pig. *J Anim Sci,* 85**,** 3256-66.

WITTMANN, T., CRENNER, F., ANGEL, F., HANUSZ, L., RINGWALD, C. & GRENIER, J. F. 1990. Long-duration stress. Immediate and late effects on small and large bowel motility in rat. *Dig Dis Sci,* 35**,** 495-500.

WOOF, J. M. & MESTECKY, J. 2005. Mucosal immunoglobulins. *Immunol Rev,* 206**,** 64-82.

WOUTERS, M. M., VICARIO, M. & SANTOS, J. 2016. The role of mast cells in functional GI disorders. *Gut,* 65**,** 155-68.

XIE, Y., MATSUMOTO, H., NALBANTOGLU, I., KERR, T. A., LUO, J., RUBIN, D. C., KENNEDY, S. & DAVIDSON, N. O. 2013. Intestine-Specific Mttp Deletion Increases the Severity of Experimental Colitis and Leads to Greater Tumor Burden in a Model of Colitis Associated Cancer. *PLoS One,* 8**,** e67819.

YAN, Y. H., YU, F., ZENG, C., CAO, L. H., ZHANG, Z. & XU, Q. A. 2016. CCL17 combined with CCL19 as a nasal adjuvant enhances the immunogenicity of an anti-caries DNA vaccine in rodents. *Acta Pharmacol Sin,* 37**,** 1229-36.

YANABA, K., YOSHIZAKI, A., ASANO, Y., KADONO, T., TEDDER, T. F. & SATO, S. 2011. IL-10-producing regulatory B10 cells inhibit intestinal injury in a mouse model. *Am J Pathol,* 178**,** 735-43.

YAO, Y., LU, S., HUANG, Y., BEEMAN-BLACK, C. C., LU, R., PAN, X., HUSSAIN, M. M. & BLACK, D. D. 2011. Regulation of microsomal triglyceride transfer protein by apolipoprotein A-IV in newborn swine intestinal epithelial cells. *Am J Physiol Gastrointest Liver Physiol,* 300**,** G357-63.

YU, Y., LIU, Z. Q., LIU, X. Y., YANG, L., GENG, X. R., YANG, G., LIU, Z. G., ZHENG, P. Y. & YANG, P. C. 2013. Stress-Derived Corticotropin Releasing Factor Breaches Epithelial Endotoxin Tolerance. *PLoS One,* 8**,** e65760.

YUAN LU, Y. S., WESLEY WARREN AND RONALD WALTER 2016. *Next Generation Sequencing - Advances, Applications and Challenges,* InTech.

YUAN, P. Q., WU, S. V., WANG, L. & TACHE, Y. 2010. Corticotropin releasing factor in the rat colon: expression, localization and upregulation by endotoxin. *Peptides,* 31**,** 322-31.

ZACCHETTI, G., DUBOULE, D. & ZAKANY, J. 2007. Hox gene function in vertebrate gut morphogenesis: the case of the caecum. *Development,* 134**,** 3967-73.

ZAMPELI, E. & TILIGADA, E. 2009. The role of histamine H4 receptor in immune and inflammatory disorders. *Br J Pharmacol,* 157**,** 24-33.

ZANELLO, G., MEURENS, F., BERRI, M., CHEVALEYRE, C., MELO, S., AUCLAIR, E. & SALMON, H. 2011. Saccharomyces cerevisiae decreases inflammatory responses induced by F4+ enterotoxigenic Escherichia coli in porcine intestinal epithelial cells. *Vet Immunol Immunopathol,* 141**,** 133-8.

ZHANG, C., YU, M., YANG, Y., MU, C., SU, Y. & ZHU, W. 2017. Differential effect of early antibiotic intervention on bacterial fermentation patterns and mucosal gene expression in the colon of pigs under diets with different protein levels. *Appl Microbiol Biotechnol,* 101**,** 2493-2505.

ZHANG, J., ZHOU, C., MA, J., CHEN, L., JIANG, A., ZHU, L., SHUAI, S., WANG, J., LI, M. & LI, X. 2013. Breed, sex and anatomical location-specific gene expression profiling of the porcine skeletal muscles. *BMC Genet,* 14**,** 53.

ZHANG, Q., GOU, W., WANG, X., ZHANG, Y., MA, J., ZHANG, H., ZHANG, Y. & ZHANG, H. 2016. Genome Resequencing Identifies Unique Adaptations of Tibetan Chickens to Hypoxia and High-Dose Ultraviolet Radiation in High-Altitude Environments. *Genome Biol Evol,* 8**,** 765-76.

ZHANG, Y., CHENG, Y., HANSEN, G. H., NIELS-CHRISTIANSEN, L. L., KOENTGEN, F., OHLSSON, L., NILSSON, A. & DUAN, R. D. 2011. Crucial role of alkaline sphingomyelinase in sphingomyelin digestion: a study on enzyme knockout mice. *J Lipid Res,* 52**,** 771-81.

ZHAO, S. 2014. Assessment of the impact of using a reference transcriptome in mapping short RNA-Seq reads. *PLoS One,* 9**,** e101374.

Appendix 1: Creep Feed Composition

BOCM PAULS LTD, VALLEY LANE, WHERSTEAD, IP9 2AX P03903 STIMMULATE ONE A complementary feedingstuff for suckling pigs under 3 weeks of age, and a complete feedingstuff for weaned pigs from 3 to 6 weeks of age.

OIL	7.50 %	VITAMIN A -retinol 15000 iu/kg
PROTEIN	21.25 %	VITAMIN D3-cholecalciferol 2000 iu/kg
FIBRE	2.00 %	VITAMIN E.alpha-tocopherol acetate 300 iu/kg
ASH	5.00 %	SODIUM SELENITE-selenium 0.50 mg/kg
LYSINE	1.70 %	COPPER SULPHATE-copper 170 mg/kg
MOISTURE	13.80 %	

DO NOT FEED TO ANIMALS OTHER THAN PIGS, ESP. SHEEP. SHEEP SHOULD NOT HAVE ACCESS TO EFFLUENT FROM TREATED PIGS.

Contains the following ingredients in descending order by weight:

40-25% inclusion: WHEAT, WHEAT COOKED

25-10% inclusion: WHEY POWDER

10-0% inclusion: SOYA BEAN (HEAT TREATED)(GM*2), MILK PRODUCTS & BY PRODUCTS, BAKERY BY-PRODUCT, HIPRO SOYA(GM*2), FISH MEAL, VEGETABLE OILS(GM*2), LT FISH MEAL, VITS/MINS, LYSINE, SUGAR, CALCIUM CARBONATE, MONO CALCIUM PHOSPHATE, METHYL-HYDROXY-ANALOGUE, THREONINE

THIS FEEDINGSTUFF CONTAINS FISHMEAL-CANNOT BE FED TO RUMINANT ANIMALS "(GM*2) Produced from genetically modified material"

Contains Natuphos 5000G (EC No.1600 in CAT.N of Dir.70/524/EEC) to provide 3-Phytase (EC 3.1.3.8) at 500 FTU/kg

Contains permitted antioxidant: ethoxyquin, butylated hydroxy-anisole (BHA),citric & phosporic acid & mono/diglycerides of edible fatty acids

Contains permitted preservatives: formic acid, lactic acid, phosphoric acid, citric acid, acetic acid

Contains additives: Na-K salts of edible fatty acids - E 470

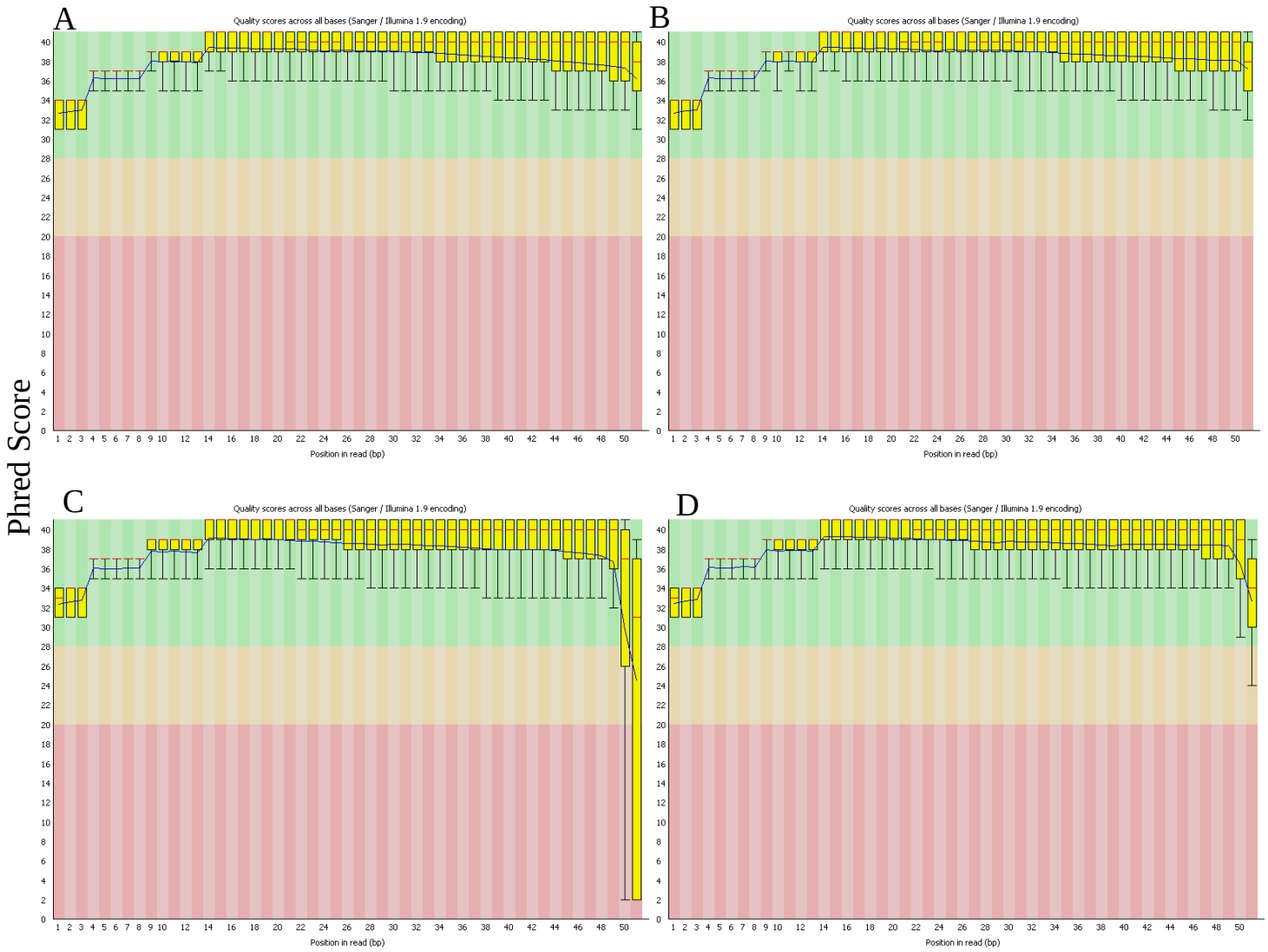
Contains: DL-hydroxy-4-methylmercaptobutyric acid 2100 mg/kg Monomer acid: min 65%, Total acids: min 85%

Contains permitted emulsifier: E484 Contains Belfeed (EC No.51 in CAT.N of Dir.70/524/EEC) to provide: Endo-1,4-beta-xylanase (EC 3.2.1.8) 10 IU/kg NET WEIGHT: see bag/bulk delivery order. The stated vitamin levels will be retained until:(See Best Before) Feeding instructions and further information available from your supplier. Store in cool dry conditions. ---------- SEQ No #SSSSSS BEST BEFORE !DD.MM.YY VER No 9278 VMR Est.App.No.aGB2018667 UFAS-Compound Feeds 41 31/12/10 ----------

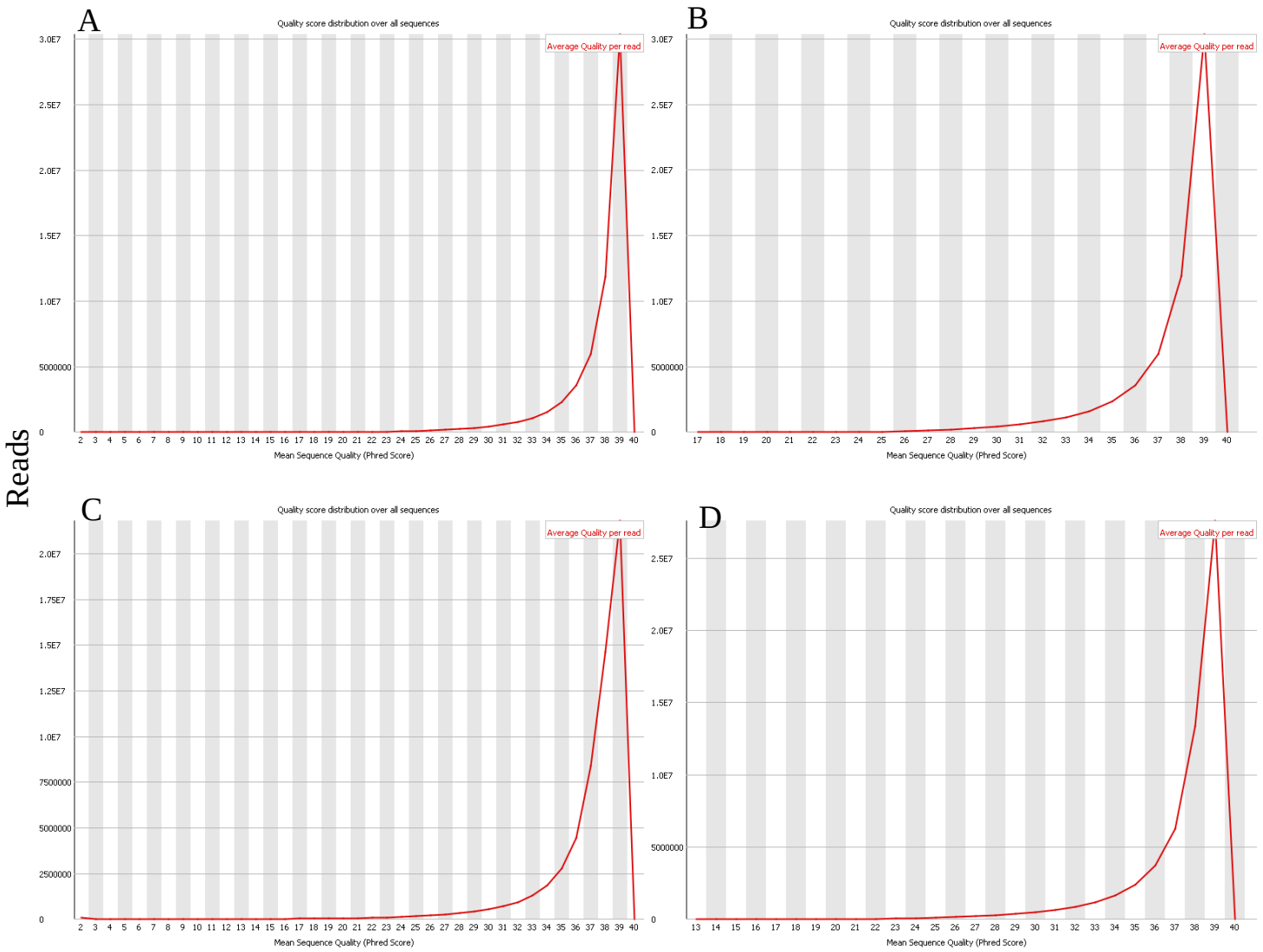
Appendix 2: Sample Concentration and Sequencing Information

Flowcell ID	Lane	Species	Sample ID	User Description	RNA concentration [ng/ml	RNA Integrity Number (RIN)	Index Sequence	Library Concentration (ng.	Insert Size (bp)	Sample Total Reads (50bp)	Sample Total Yield in Mbp (50bp)	Sample Total Reads (100bp)	Sample Total Yield in Mbp (100bp)	Sample Total Reads (ALL)	Sample Total Yield in Mbp (ALL)
COROUACXX	1	pig	797_179	7507	459	9.6	TTAGGC	57.66	174	93,314,948	4759	0	0	93,314,948	4759
COROUACXX	1	pig	797_177	8532	630	8.7	ATCACG	67.34	179	77,945,336	3975	22,860,336	2309	100,805,672	6284
COROUACXX	1	pig	797_178	9223	465	9	CGATGT	74.03	183	124,993,526	6375	0	0	124,993,526	6375
COROUACXX	2	pig	797_182	1417	992	9.6	GCCAAT	44.25	175	101,153,470	5159	0	0	101,153,470	5159
COROUACXX	2	pig	797_181	2092	529	9.7	ACAGTG	28.73	175	98,640,240	5031	0	0	98,640,240	5031
COROUACXX	2	pig	797_180	2974	1040	8.6	TGACCA	81.5	172	109,016,648	5560	0	0	109,016,648	5560
COROUACXX	3	pig	797_183	2249	266	6.8	CAGATC	61.07	179	122,492,444	6247	0	0	122,492,444	6247
COROUACXX	3	pig	797_185	4180	593	9.2	GATCAG	84.31	166	65,430,716	3337	36,463,486	3683	101,894,202	7020
COROUACXX	3	pig	797_184	4292	250	9.1	ACTTGA	59.07	180	107,966,394	5506	0	0	107,966,394	5506
COROUACXX	4	pig	797_186	4105	428	8.5	TAGCTT	60.31	171	94,755,536	4833	0	0	94,755,536	4833
COROUACXX	4	pig	797_187	7994	809	9.7	GGCTAC	58.44	169	119,972,944	6119	0	0	119,972,944	6119
COROUACXX	4	pig	797_188	9365	192	9.9	CTTGTA	59.7	176	73,450,270	3746	31,330,806	3164	104,781,076	6910
COROUACXX	5	pig	797_189	6671	816	8.8	AGTCAA	59.56	172	115,931,908	5913	0	0	115,931,908	5913
COROUACXX	5	pig	797_190	7938	300	7.9	AGTTCC	37.2	172	112,475,418	5736	0	0	112,475,418	5736
COROUACXX	5	pig	797_191	7980	650	9.3	ATGTCA	59.19	170	101,400,148	5171	0	0	101,400,148	5171
COROUACXX	6	pig	797_194	3954	184	8.4	GTGAAA	50.62	174	76,426,054	3898	22,906,586	2314	99,332,640	6212
COROUACXX	6	pig	797_193	6442	646	9.5	GTCCGC	42.23	176	133,593,626	6813	0	0	133,593,626	6813
COROUACXX	6	pig	797_192	6566	854	9.6	CCGTCC	48.97	176	88,186,828	4498	15,877,334	1604	104,064,162	6102
COROUACXX	7	pig	797_197	1716	458	9.3	CGTACG	59.95	180	105,480,316	5379	0	0	105,480,316	5379
COROUACXX	7	pig	797_196	1766	572	7.4	GTTTCG	62.78	168	101,408,474	5172	0	0	101,408,474	5172
COROUACXX	7	pig	797_195	9315	302	9.2	GTGGCC	89.07	176	118,626,560	6050	0	0	118,626,560	6050
COROUACXX	8	pig	797_198	3528	804	7.4	GAGTGG	73.06	171	84,166,312	4292	13,635,476	1377	97,801,788	5669
COROUACXX	8	pig	797_199	5489	562	7.8	ACTGAT	82.11	165	93,696,242	4779	0	0	93,696,242	4779
COROUACXX	8	pig	797_200	6895	910	7.7	ATTCCT	83.17	165	110,244,074	5622	0	0	110,244,074	5622
D0H7HACXX	1	pig	797_153	4800	518	7.7	ATCACG	51.13	174	87,439,854	4372	16,146,504	1631	103,586,358	6003
D0H7HACXX	1	pig	797_154	5625	163	8.7	CGATGT	48.52	174	102,507,156	5125	0	0	102,507,156	5125
D0H7HACXX	1	pig	797_155	6250	117	8.2	TTAGGC	65.44	171	66,120,234	3306	41,409,718	4182	107,529,952	7488
D0H7HACXX	2	pig	797_158	1209	1047	9.6	GCCAAT	35.93	170	73,182,106	3659	32,884,432	3321	106,066,538	6980
D0H7HACXX	2	pig	797_157	5623	482	9.3	ACAGTG	53.87	180	104,375,700	5219	0	0	104,375,700	5219
D0H7HACXX	2	pig	797_156	7046	745	9.7	TGACCA	48.18	169	90,653,232	4533	0	0	90,653,232	4533
D0H7HACXX	3	pig	797_160	2188	650	9.2	ACTTGA	46.35	169	77,132,486	3857	22,622,656	2285	99,755,142	6142
D0H7HACXX	3	pig	797_159	8391	609	9.2	CAGATC	63.14	169	89,649,378	4482	15,699,074	1586	105,348,452	6068
D0H7HACXX	3	pig	797_161	8962	1032	9.1	GATCAG	56.39	167	60,328,772	3016	45,230,166	4568	105,558,938	7584
D0H7HACXX	4	pig	797_164	3714	490	9.3	CTTGTA	40.7	162	66,226,012	3311	41,470,018	4188	107,696,030	7499
D0H7HACXX	4	pig	797_162	6672	368	9.5	TAGCTT	22.95	179	83,549,034	4177	17,370,602	1754	100,919,636	5931
D0H7HACXX	4	pig	797_163	9066	195	8.8	GGCTAC	56.88	170	87,919,052	4396	15,168,698	1532	103,087,750	5928
D0H7HACXX	5	pig	797_165	2462	578	7.9	AGTCAA	42.3	168	99,960,764	4998	0	0	99,960,764	4998
D0H7HACXX	5	pig	797_167	3396	548	9.5	ATGTCA	38.77	180	94,141,250	4707	0	0	94,141,250	4707
D0H7HACXX	5	pig	797_166	9673	977	8	AGTTCC	42.54	180	105,427,694	5271	0	0	105,427,694	5271
D0H7HACXX	6	pig	797_169	4533	69	8.5	GTCCGC	40.45	174	120,218,622	6011	0	0	120,218,622	6011
D0H7HACXX	6	pig	797_168	4994	556	9.1	CCGTCC	36.89	181	92,739,100	4637	0	0	92,739,100	4637
D0H7HACXX	6	pig	797_170	9032	292	9.1	GTGAAA	45.03	177	87,488,408	4374	15,443,028	1560	102,931,436	5934
D0H7HACXX	7	pig	797_172	1224	224	9	GTTTCG	44.63	170	91,460,396	4573	0	0	91,460,396	4573
D0H7HACXX	7	pig	797_171	4169	386	9.3	GTGGCC	37.03	171	86,288,242	4314	16,259,360	1642	102,547,602	5956
D0H7HACXX	7	pig	797_173	7747	1413	9.6	CGTACG	47.66	177	76,383,314	3819	22,036,690	2226	98,420,004	6045
D0H7HACXX	8	pig	797_176	2822	572	9.1	ATTCCT	47.78	169	86,802,950	4340	15,115,182	1527	101,918,132	5867
D0H7HACXX	8	pig	797_175	5066	191	9.1	ACTGAT	47.79	173	94,645,792	4732	0	0	94,645,792	4732
D0H7HACXX	8	pig	797_174	6562	839	9.3	GAGTGG	45.73	179	61,586,964	3079	48,995,738	4949	110,582,702	8028
Mean					**557.75**	**8.89**		**53.97**	**173.27**	**94,104,061**	**4,755.79**	**24,206,850**	**2,444.89**	**104,706,684**	**5,826.67**
SD					**291.89**	**0.72**		**14.77**	**4.89**	**17,413,247**	**901.12**	**10,240,449**	**1,034.12**	**9,022,281**	**845.92**
Pairs										**47,052,031**		**12,103,425**		**52,353,342**	

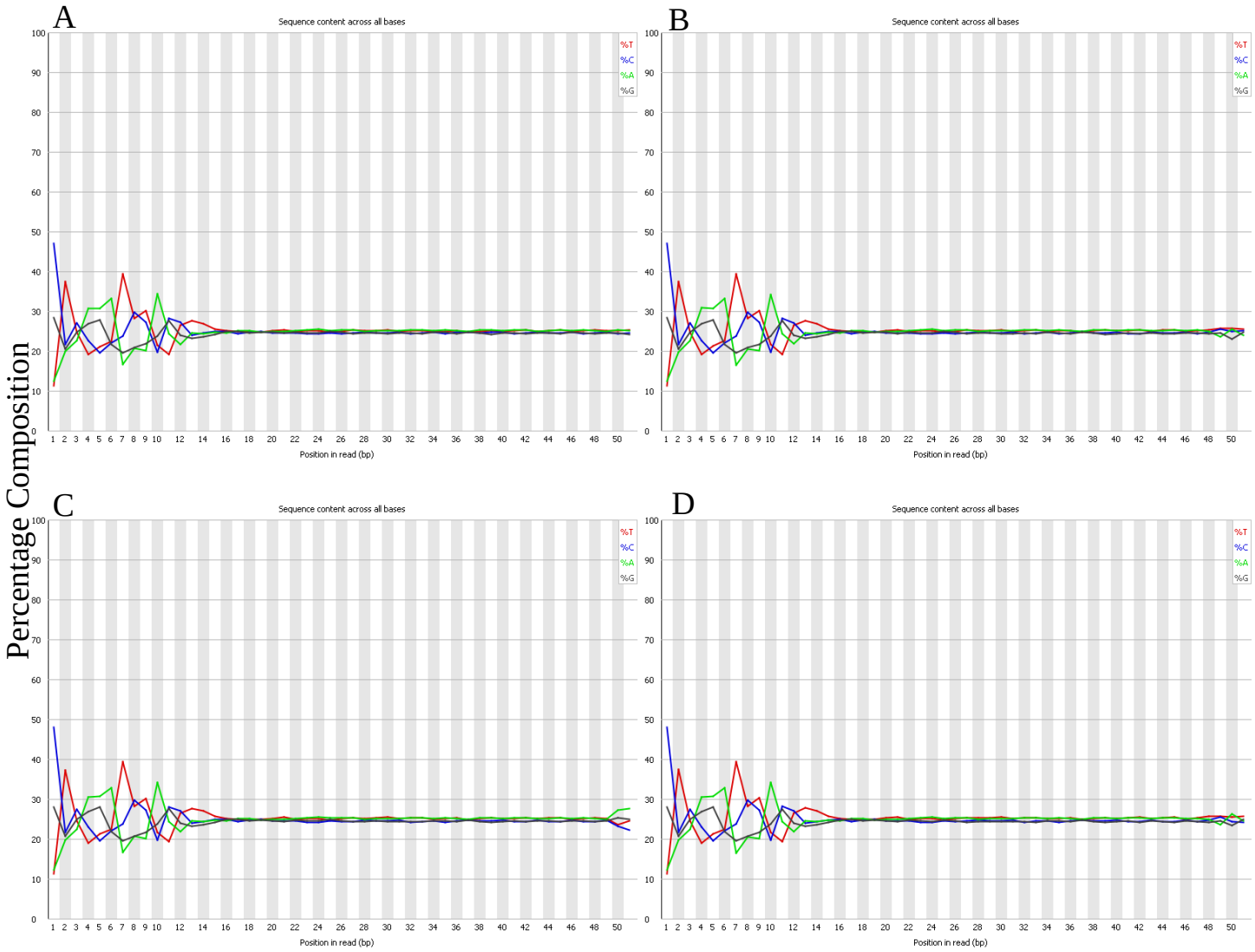
Appendix 3: Benchmarking of 50 and 100bp Reads



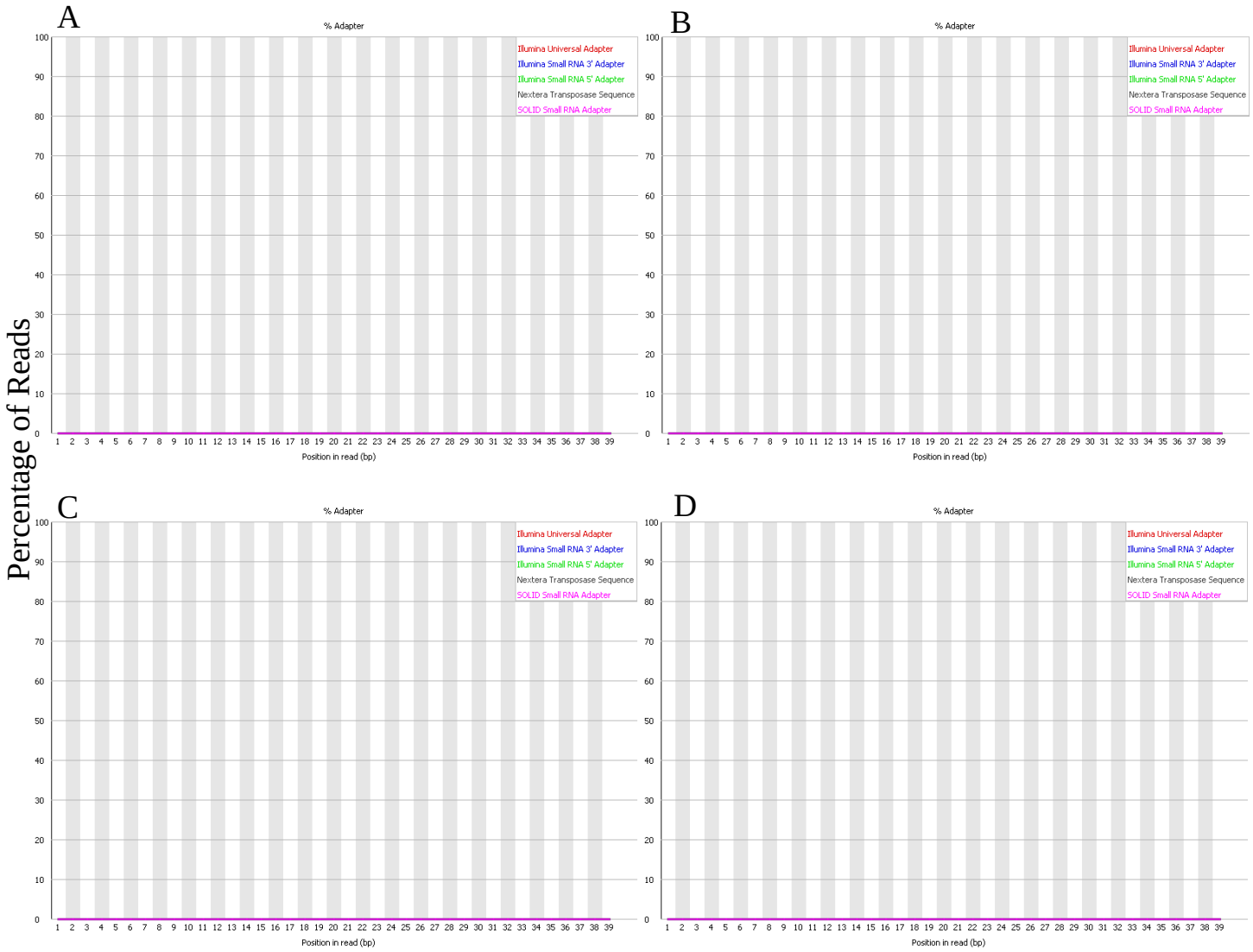
Per base quality. Sample 7994 (50bp reads) A, read 1 before filtering, B, Read 1 after filtering. C, Read 2 before filtering. D, read 2 after filtering.



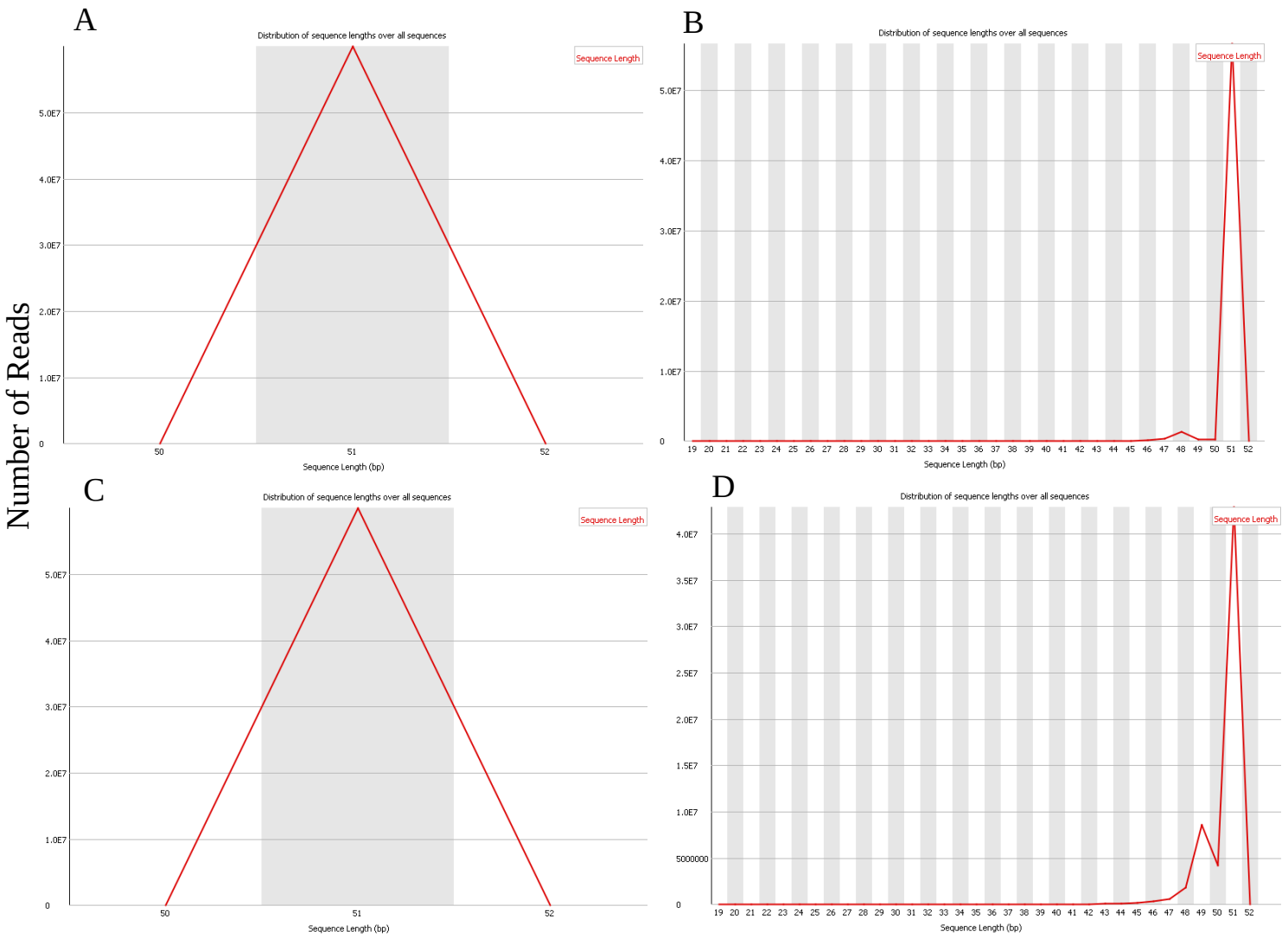
Per sequence quality. Sample 7994 (50bp reads) A, read 1 before filtering, B, Read 1 after filtering. C, Read 2 before filtering. D, read 2 after filtering.



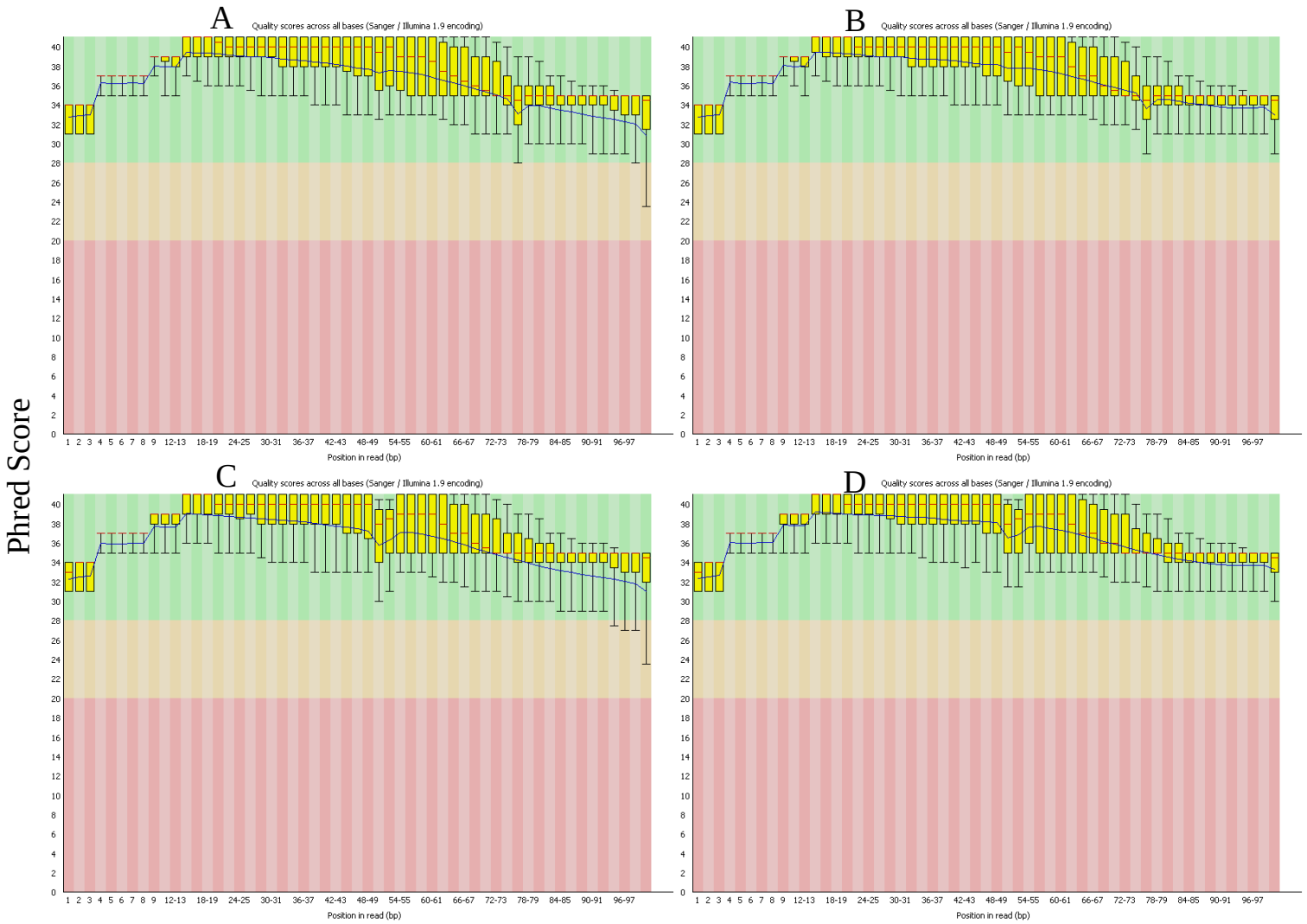
Per base sequence composition. Sample 7994 (50bp reads) A, read 1 before filtering, B, Read 1 after filtering. C, Read 2 before filtering. D, read 2 after filtering.



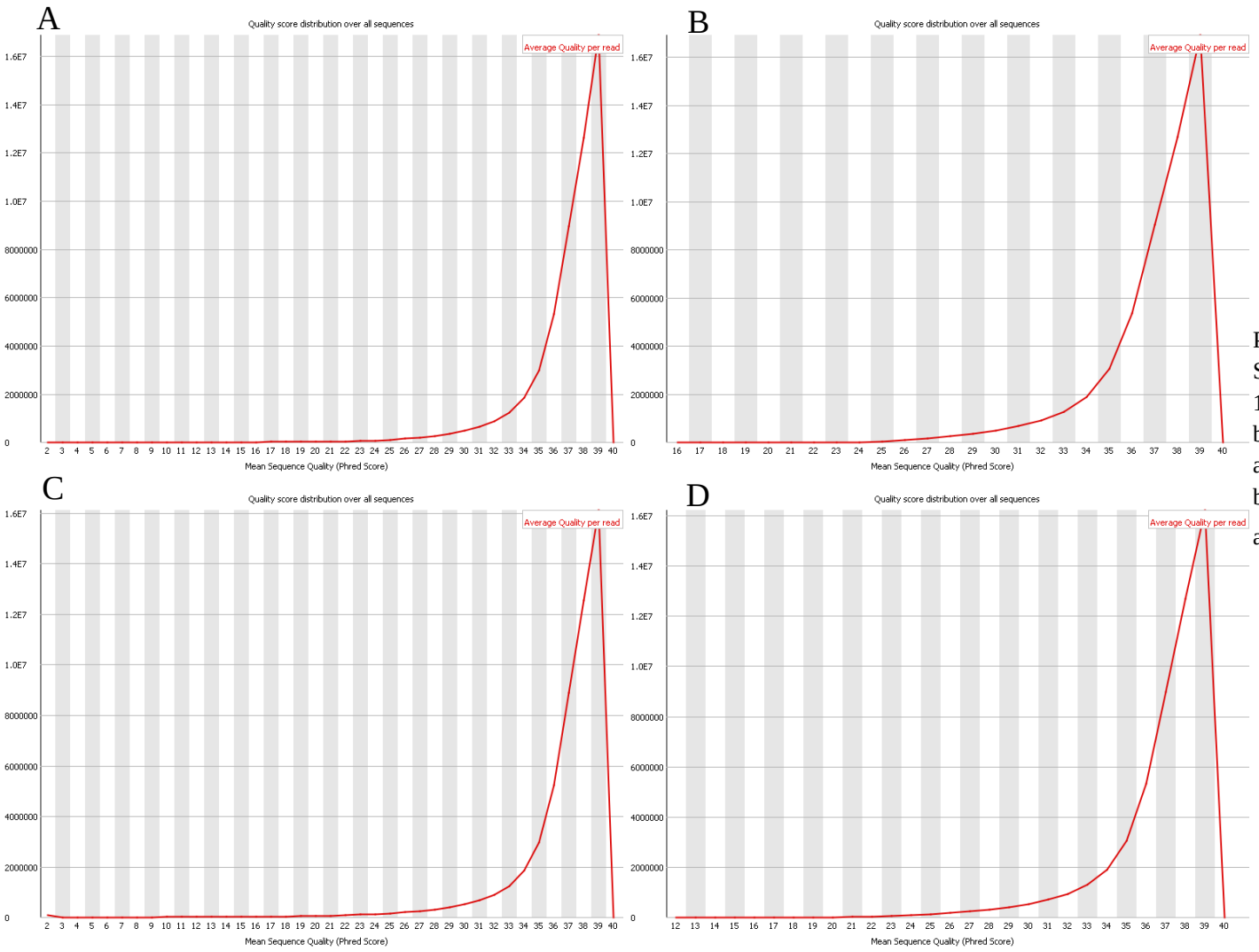
Adapter contamination. Sample 7994 (50bp reads) A, read 1 before filtering, B, Read 1 after filtering. C, Read 2 before filtering. D, read 2 after filtering.



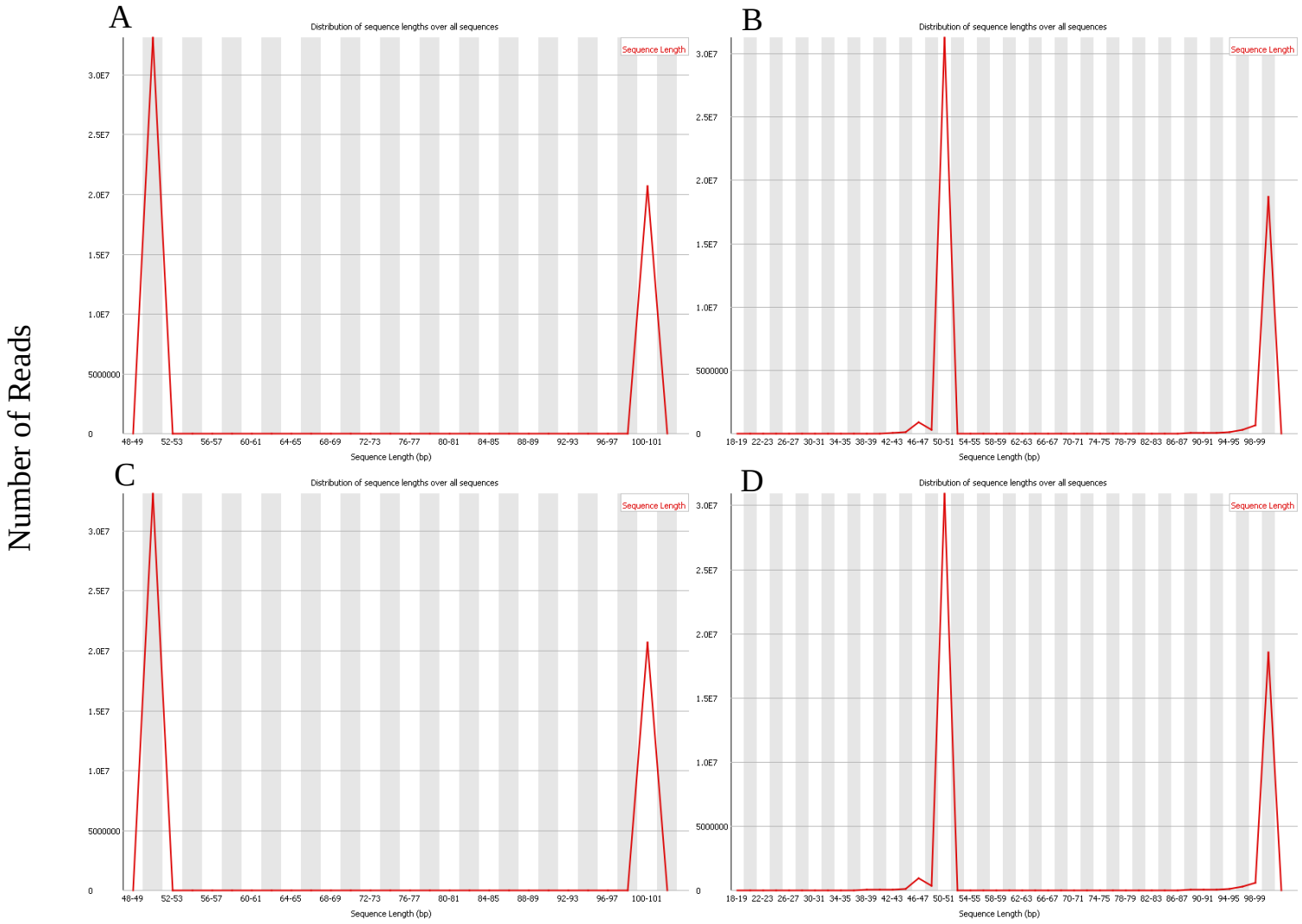
Sequence length distribution. Sample 7994 (50bp reads) A, read 1 before filtering, B, Read 1 after filtering. C, Read 2 before filtering. D, read 2 after filtering.



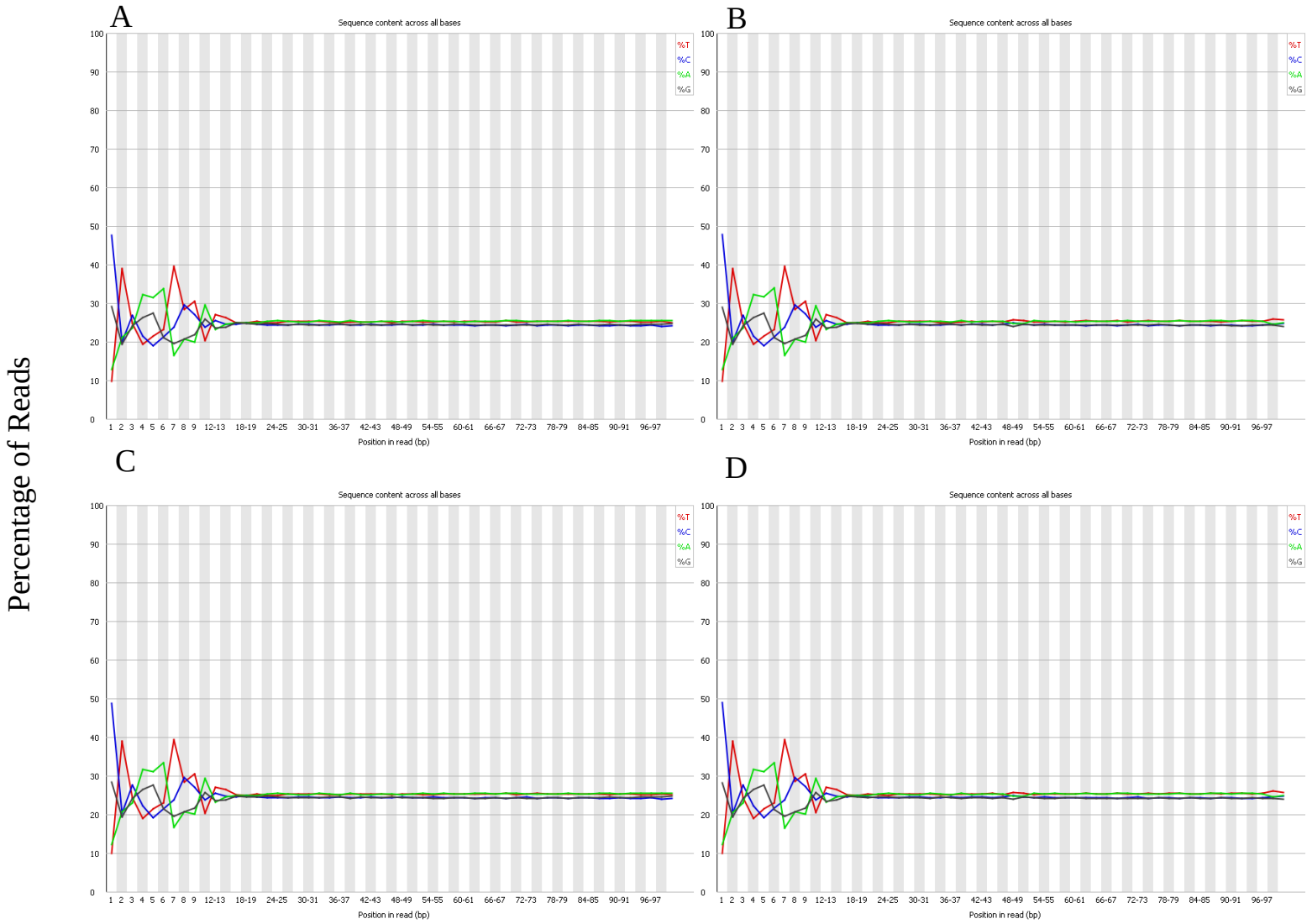
Per base quality. Sample 6250 (50 and 100bp reads) A, read 1 before filtering, B, Read 1 after filtering. C, Read 2 before filtering. D, read 2 after filtering.



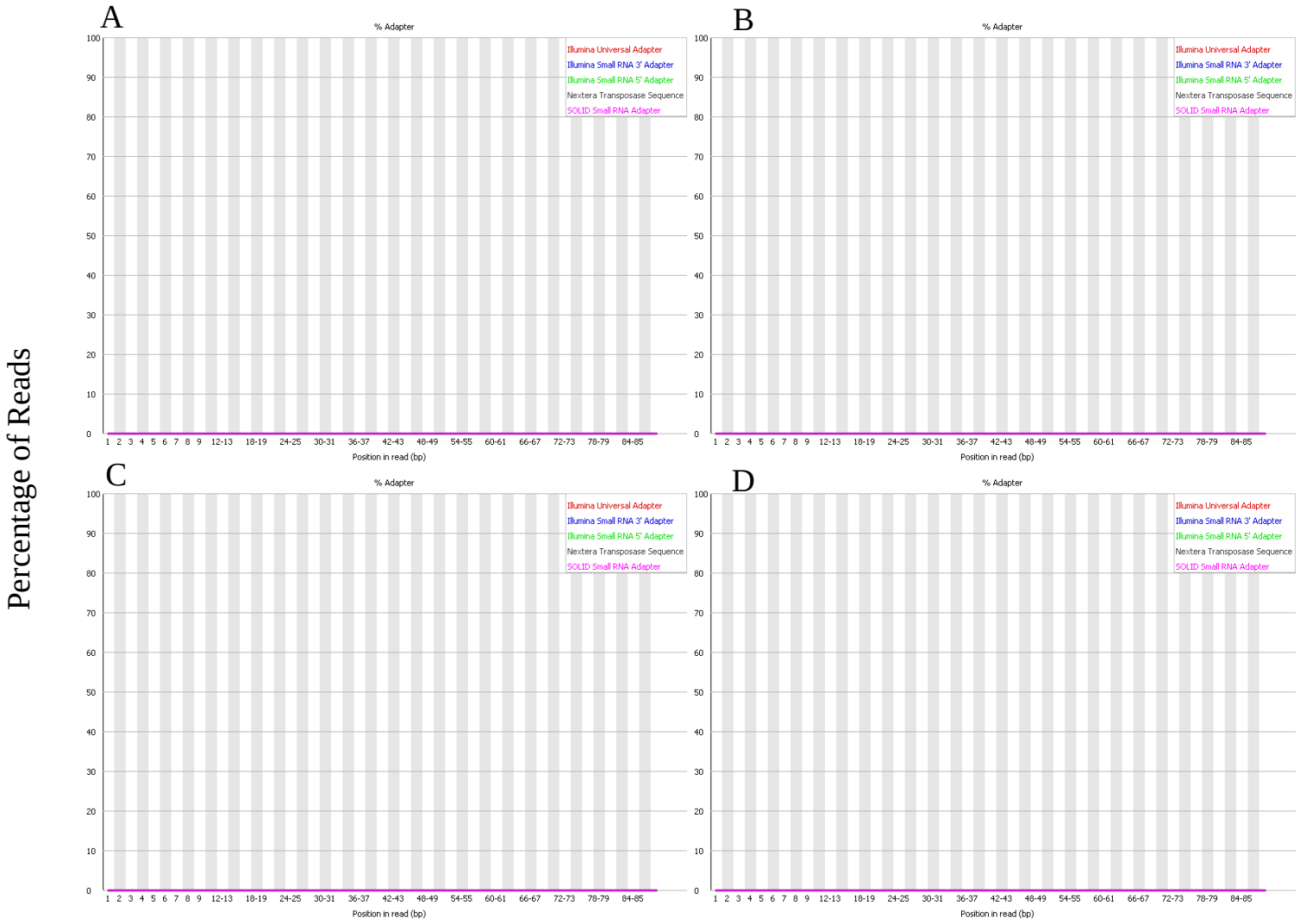
Per sequence quality. Sample 6250 (50 and 100bp reads) A, read 1 before filtering, B, Read 1 after filtering. C, Read 2 before filtering. D, read 2 after filtering.



Sequence length distribution. Sample 6250 (50 and 100bp reads) A, read 1 before filtering, B, Read 1 after filtering. C, Read 2 before filtering. D, read 2 after filtering



Base composition. Sample 6250 (50 and 100bp reads) A, read 1 before filtering, B, Read 1 after filtering. C, Read 2 before filtering. D, read 2 after filtering.



Adaptor contamination. Sample 6250 (50 and 100bp reads) A, read 1 before filtering, B, Read 1 after filtering. C, Read 2 before filtering. D, read 2 after filtering

Appendix 4: Sample Treatment Information

ID	sex	Days Post wing	probiotic / control	Weaned / Unweaned	Weight at Slaughter (kg)
1417	m	1	c	u	7.5
2092	m	1	c	u	7.5
2249	m	1	c	u	7.5
4292	m	1	c	u	8.5
2462	m	4	c	u	11
3396	f	4	c	u	9
4994	m	4	c	u	9.5
9673	m	4	c	u	9
1716	f	14	c	u	13
3528	f	14	c	u	16.5
5489	m	14	c	u	12
6895	f	14	c	u	13
6566	f	1	p	u	6
6671	f	1	p	u	7
7980	f	1	p	u	7
9365	m	1	p	u	7.5
3714	m	4	p	u	8
6672	m	4	p	u	9.5
8962	m	4	p	u	8
9066	f	4	p	u	7
1224	f	14	p	u	12.5
4169	m	14	p	u	13.5
6562	f	14	p	u	9
7747	f	14	p	u	15
2974	f	1	c	w	7.5
7507	f	1	c	w	7
7938	m	1	c	w	5
9223	f	1	c	w	7.5
4800	m	4	c	w	9
5625	m	4	c	w	6.5
6250	f	4	c	w	6.5
7046	m	4	c	w	7
1766	m	14	c	w	14.5
3954	m	14	c	w	10.5
6442	f	14	c	w	14
9315	m	14	c	w	13.5
4105	m	1	p	w	7
4180	f	1	p	w	7
7994	f	1	p	w	8.5
8532	f	1	p	w	6.5
1209	m	4	p	w	6.5
2188	m	4	p	w	9
5623	m	4	p	w	6.5
8391	m	4	p	w	9.5
2822	m	14	p	w	14.5
4533	f	14	p	w	10.5
5066	f	14	p	w	12
9032	f	14	p	w	15.5

Appendix 5: Read Usage Numbers and Percentages

HiSat2

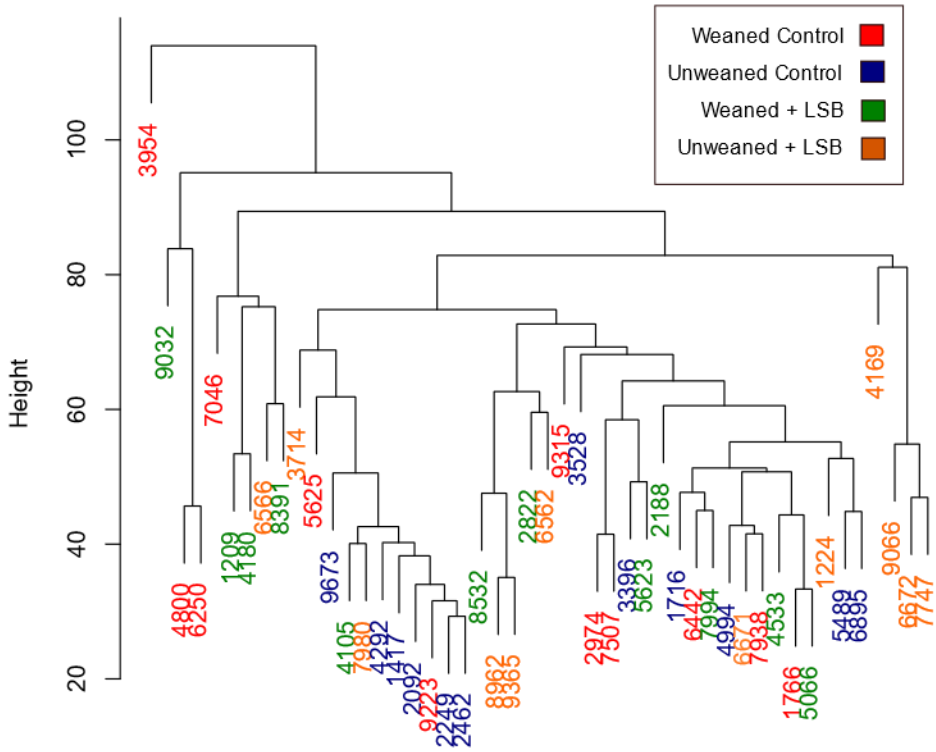
Sample ID	Raw Reads	Trimmed Reads	Unmapped Reads	Mapped Reads	Trimmed Reads %	Unmapped Reads %	Mapped Reads %
1209	53033269	234227	8175538	44623504	0.44	15.42	84.14
1224	45730198	243319	8094350	37392529	0.53	17.70	81.77
1417	50576735	344958	8467638	41764139	0.68	16.74	82.58
1716	52740158	350395	8662421	43727342	0.66	16.42	82.91
1766	50704237	327666	8479125	41897446	0.65	16.72	82.63
2092	49320120	407130	8297151	40615839	0.83	16.82	82.35
2188	49877571	264331	7674074	41939166	0.53	15.39	84.08
2249	61246222	455725	9506317	51284180	0.74	15.52	83.73
2462	49980382	292538	8138088	41549756	0.59	16.28	83.13
2822	50959066	262771	8503025	42193270	0.52	16.69	82.80
2974	54508324	591657	9174429	44742238	1.09	16.83	82.08
3396	47070625	379914	7924082	38766629	0.81	16.83	82.36
3528	48900894	309824	8086089	40504981	0.63	16.54	82.83
3714	53848015	316957	8482029	45049029	0.59	15.75	83.66
3954	49666320	397499	7302490	41966331	0.80	14.70	84.50
4105	47377768	328369	8387899	38661500	0.69	17.70	81.60
4169	51273801	312594	8100756	42860451	0.61	15.80	83.59
4180	50947101	429393	7897778	42619930	0.84	15.50	83.66
4292	53983197	393391	9027036	44562770	0.73	16.72	82.55
4533	60109311	377253	9427566	50304492	0.63	15.68	83.69
4800	51793179	240694	8596634	42955851	0.46	16.60	82.94
4994	46369550	235060	7799783	38334707	0.51	16.82	82.67
5066	47322896	225780	7979044	39118072	0.48	16.86	82.66
5489	46848121	291031	7834297	38722793	0.62	16.72	82.66
5623	52187850	321645	8715184	43151021	0.62	16.70	82.68
5625	51253578	260521	8517478	42475579	0.51	16.62	82.87
6250	53764976	292789	8066375	45405812	0.54	15.00	84.45
6442	66796813	456798	11183935	55156080	0.68	16.74	82.57
6562	55291351	315953	8764192	46211206	0.57	15.85	83.58
6566	52032081	328631	8253723	43449727	0.63	15.86	83.51
6671	57965954	421136	9411433	48133385	0.73	16.24	83.04
6672	50459818	245828	7824926	42389064	0.49	15.51	84.01
6895	55122037	373315	8500861	46247861	0.68	15.42	83.90
7046	45326616	426159	7524690	37375767	0.94	16.60	82.46
7507	46657474	327084	7047156	39283234	0.70	15.10	84.19
7747	49210002	261602	7694866	41253534	0.53	15.64	83.83
7938	56237709	363065	9235428	46639216	0.65	16.42	82.93
7980	50700074	471639	8258493	41969942	0.93	16.29	82.78
7994	59986472	335013	8686023	50965436	0.56	14.48	84.96
8391	52674226	270999	8137533	44265694	0.51	15.45	84.04
8532	50402836	342906	8040527	42019403	0.68	15.95	83.37
8962	52779469	382946	8209514	44187009	0.73	15.55	83.72
9032	51465718	392548	7822802	43250368	0.76	15.20	84.04
9066	51543875	192218	7408875	43942782	0.37	14.37	85.25
9223	62496763	484938	10403694	51608131	0.78	16.65	82.58
9315	59313280	418679	9853274	49041327	0.71	16.61	82.68
9365	52390538	352425	8421458	43616655	0.67	16.07	83.25
9673	52713847	317733	7709830	44686284	0.60	14.63	84.77
average	52,353,342.02	341,021.79	8,410,623.10	43,601,697.13	0.65	16.08	83.27
stdev	4,511,140.42	79,345.66	769,488.77	3,838,314.40	0.14	0.78	0.82

Kallisto

Sample ID	Raw P reads	Trimmed Reads	Unmapped reads	Mapped Reads	Trimmed Reads %	Unmapped Reads %	Mapped Reads %
1209	53033269	234227	19760558	33038484	0.44%	37.26%	62.30%
1224	45730198	243319	17690061	27796818	0.53%	38.68%	60.78%
1417	50576735	344958	19850393	30381384	0.68%	39.25%	60.07%
1716	52740158	350395	19285586	33104177	0.66%	36.57%	62.77%
1766	50704237	327666	19154864	31221707	0.65%	37.78%	61.58%
2092	49320120	407130	20047898	28865092	0.83%	40.65%	58.53%
2188	49877571	264331	18068602	31544638	0.53%	36.23%	63.24%
2249	61246222	455725	23081259	37709238	0.74%	37.69%	61.57%
2462	49980382	292538	20303736	29384108	0.59%	40.62%	58.79%
2822	50959066	262771	20065388	30630907	0.52%	39.38%	60.11%
2974	54508324	591657	21484988	32431679	1.09%	39.42%	59.50%
3396	47070625	379914	17625918	29064793	0.81%	37.45%	61.75%
3528	48900894	309824	19793565	28797505	0.63%	40.48%	58.89%
3714	53848015	316957	21909069	31621989	0.59%	40.69%	58.72%
3954	49666320	397499	17853077	31415744	0.80%	35.95%	63.25%
4105	47377768	328369	19856054	27193345	0.69%	41.91%	57.40%
4169	51273801	312594	19486930	31474277	0.61%	38.01%	61.38%
4180	50947101	429393	18419995	32097713	0.84%	36.16%	63.00%
4292	53983197	393391	21468047	32121759	0.73%	39.77%	59.50%
4533	60109311	377253	23543578	36188480	0.63%	39.17%	60.20%
4800	51793179	240694	19365357	32187128	0.46%	37.39%	62.15%
4994	46369550	235060	18011552	28122938	0.51%	38.84%	60.65%
5066	47322896	225780	18133778	28963338	0.48%	38.32%	61.20%
5489	46848121	291031	17749458	28807632	0.62%	37.89%	61.49%
5623	52187850	321645	18810626	33055579	0.62%	36.04%	63.34%
5625	51253578	260521	20581285	30411772	0.51%	40.16%	59.34%
6250	53764976	292789	20461874	33010313	0.54%	38.06%	61.40%
6442	66796813	456798	27167485	39172530	0.68%	40.67%	58.64%
6562	55291351	315953	21610572	33364826	0.57%	39.08%	60.34%
6566	52032081	328631	18811319	32892131	0.63%	36.15%	63.22%
6671	57965954	421136	21645821	35898997	0.73%	37.34%	61.93%
6672	50459818	245828	19601776	30612214	0.49%	38.85%	60.67%
6895	55122037	373315	21661470	33087252	0.68%	39.30%	60.03%
7046	45326616	426159	16619205	28281252	0.94%	36.67%	62.39%
7507	46657474	327084	17380799	28949591	0.70%	37.25%	62.05%
7747	49210002	261602	18916196	30032204	0.53%	38.44%	61.03%
7938	56237709	363065	21808464	34066180	0.65%	38.78%	60.58%
7980	50700074	471639	22386996	27841439	0.93%	44.16%	54.91%
7994	59986472	335013	24363088	35288371	0.56%	40.61%	58.83%
8391	52674226	270999	19880378	32522849	0.51%	37.74%	61.74%
8532	50402836	342906	20085463	29974467	0.68%	39.85%	59.47%
8962	52779469	382946	19790593	32605930	0.73%	37.50%	61.78%
9032	51465718	392548	18740583	32332587	0.76%	36.41%	62.82%
9066	51543875	192218	19801298	31550359	0.37%	38.42%	61.21%
9223	62496763	484938	25586660	36425165	0.78%	40.94%	58.28%
9315	59313280	418679	23703210	35191391	0.71%	39.96%	59.33%
9365	52390538	352425	20314597	31723516	0.67%	38.78%	60.55%
9673	52713847	317733	20196133	32199981	0.60%	38.31%	61.08%
Average	52353342.02	341021.7917	20,248,658	31,763,662	0.65%	38.65%	60.70%
stdev	4511140.415	79345.66307	2,144,403	2,654,475	0.14%	1.70%	1.72%

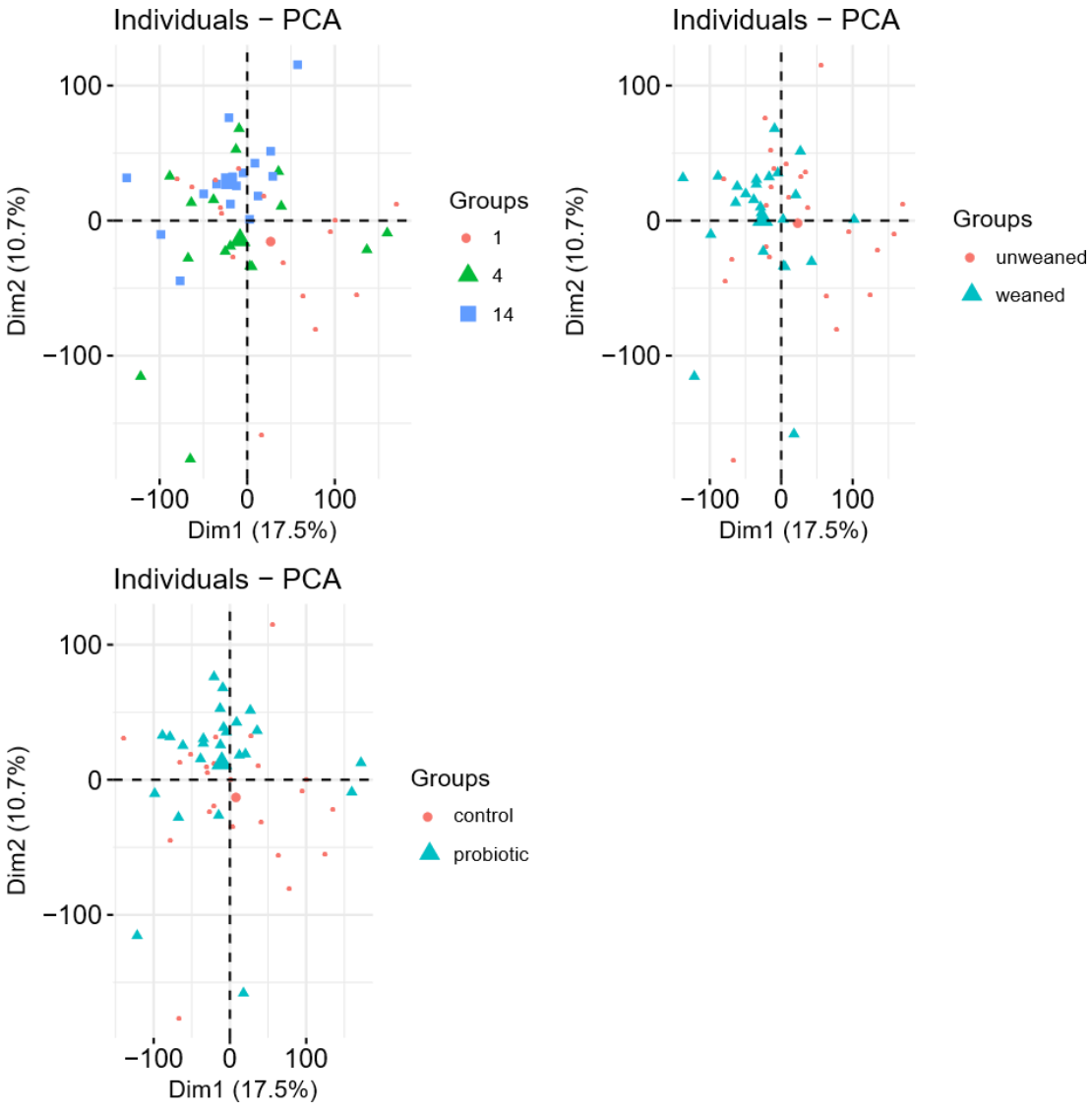
Appendix 6: Hierarchical clustering of FPKM

Profiles Without FPKM Cutoff

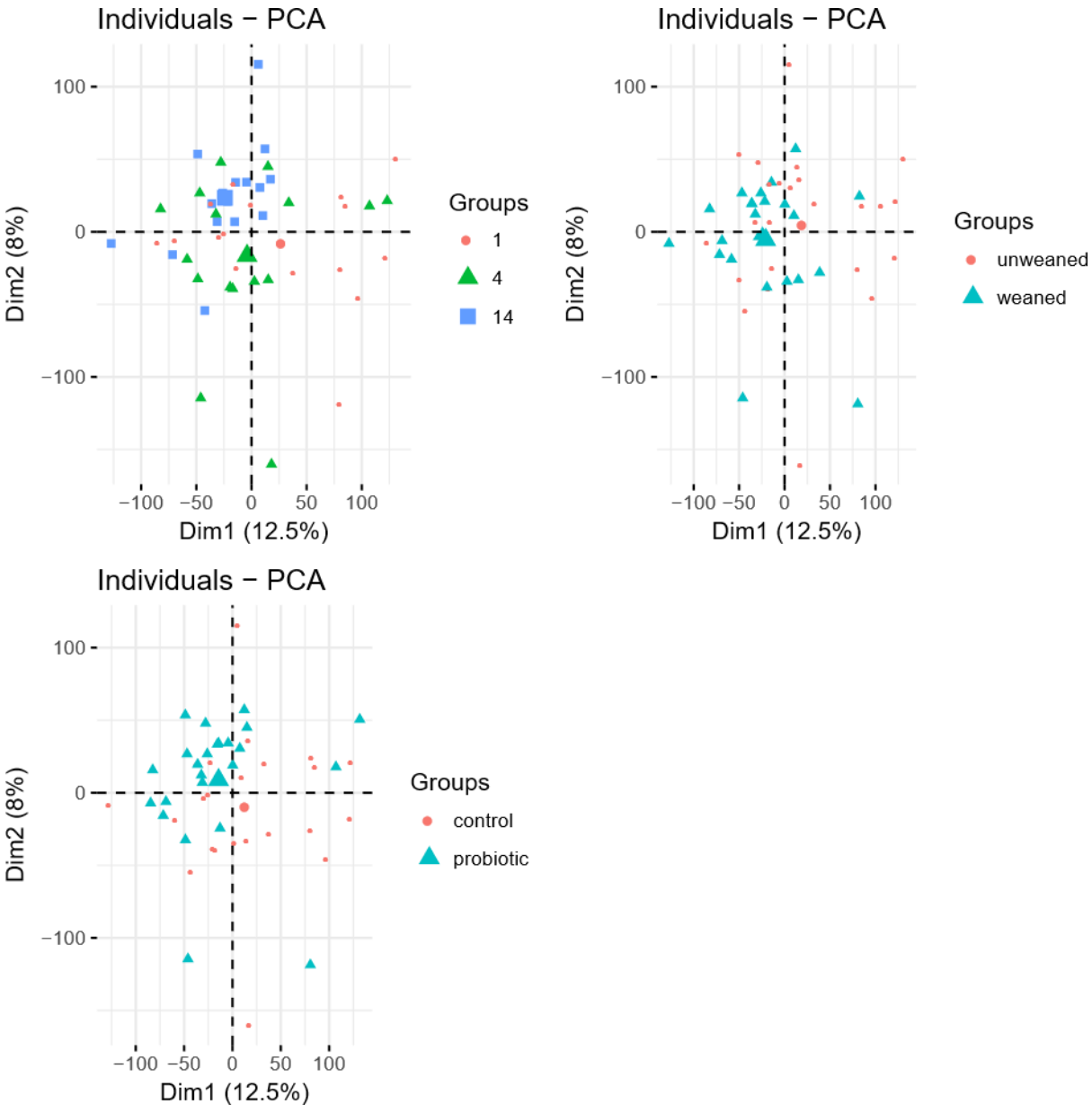


Appendix 7: PCA Plots Comparing Transcript Expression Profiles Between Treatments when Applying HiSat2 and Kallisto Mapping Methodologies.

Kallisto



HiSat2


Individuals − PCA
Dim2 (8%)
Dim1 (12.5%)
100
0
−100
−100 −50 0 50 100
Groups
1
4
14
Individuals − PCA
Dim2 (8%)
Dim1 (12.5%)
Groups
unweaned
weaned
Individuals − PCA
Dim2 (8%)
Dim1 (12.5%)
Groups
control
probiotic

Appendix 8: Biological Process Gene Ontology Terms Enriched in Genes Up and Downregulated by Weaning at One Day Post-Weaning

Enriched in upregulated genes							
GO ID	GO Gene Count	Gene IDs	Gene Names	Gene Count	Gene Ontology Name	p value	q value
GO:0010828	3	ENSSSCG00000005385 ENSSSCG00000013551	NR4A3 C3	2	positive regulation of glucose transport	4.57E-07	0.0001999
GO:0098869	44	ENSSSCG00000000843 ENSSSCG00000004675 ENSSSCG00000004678 ENSSSCG00000022742 ENSSSCG00000008214	TXNRD1 DUOX1 DUOX2 FABP1 PRDX6	5	cellular oxidant detoxification	1.08E-06	0.0004724
GO:0001660	4	ENSSSCG00000008088 ENSSSCG00000008090	IL1B2 IL1A	2	fever generation	1.82E-06	0.0007949
GO:0003081	4	ENSSSCG00000009132 ENSSSCG00000012485	ENPEP NOX1	2	regulation of systemic arterial blood pressure by renin-angiotensin	1.82E-06	0.0007949
GO:0050665	5	ENSSSCG00000004675 ENSSSCG00000004678	DUOX1 DUOX2	2	hydrogen peroxide biosynthetic process	4.52E-06	0.0019759
GO:0010575	20	ENSSSCG00000012485 ENSSSCG00000013551 ENSSSCG00000008090	IL1A NOX1 C3	3	positive regulation of vascular endothelial growth factor production	1.53E-05	0.0066702
GO:0006955	192	ENSSSCG00000008088 ENSSSCG00000016856 ENSSSCG00000020906 ENSSSCG00000003437 ENSSSCG00000009881 ENSSSCG00000016859	TNFRSF8 IL1B2 IL1A OAS2 C9 C7 TNFSF10	8	immune response	1.90E-05	0.0082875

		ENSSSCG00000020750 ENSSSCG00000008090					
GO:0010951	80	ENSSSCG00000004890 ENSSSCG00000004889 ENSSSCG00000013551 ENSSSCG00000002479 ENSSSCG00000004894	SERPINA11 SERPINB10 SERPINB2 SERPINB5 C3	5	negative regulation of endopeptidase activity	3.66E-05	0.0160068
GO:0071398	9	ENSSSCG00000000875 ENSSSCG00000015334	NR1H4 PDK4	2	cellular response to fatty acid	3.71E-05	0.0162236
GO:0045778	10	ENSSSCG00000030095 ENSSSCG00000016113	BMPR2 ZBTB16	2	positive regulation of ossification	5.27E-05	0.023045
GO:0001707	31	ENSSSCG00000005385 ENSSSCG00000000843 ENSSSCG00000016113	TXNRD1 NR4A3 BMPR2	3	mesoderm formation	9.28E-05	0.0405456
GO:0061036	12	ENSSSCG00000030095 ENSSSCG00000016113	BMPR2 ZBTB16	2	positive regulation of cartilage development	9.56E-05	0.041771
Enriched in downregulated genes							
GO ID	GO Gene Count	Gene IDs	Gene Names	Gene count	Gene Ontology Name	p value	q value
GO:0030326	47	ENSSSCG00000025578 ENSSSCG00000015815 ENSSSCG00000008991 ENSSSCG00000023261 ENSSSCG00000015979 ENSSSCG00000015981	FRAS1 FGFR1 HOXD13 HOXD10 GDF5 ALDH1A2	6	embryonic limb morphogenesis	1.93E-06	0.0013146
GO:0001757	3	ENSSSCG00000015357 ENSSSCG00000017376	MEOX2 MEOX1	2	somite specification	2.00E-06	0.001361
GO:0006814	61	ENSSSCG00000003882 ENSSSCG00000014896 ENSSSCG00000028923 ENSSSCG00000017282 ENSSSCG00000011676 ENSSSCG00000027024	SLC5A9 SCN4A ASIC3 SCNN1B	6	sodium ion transport	1.15E-05	0.0078492

GO:0060527	5	ENSSSCG00000025822 ENSSSCG00000015979	HOXD13 SFRP1	2	prostate epithelial cord arborization involved in prostate glandular acinus morphogenesis	1.96E-05	0.013356
GO:0060687	6	ENSSSCG00000025822 ENSSSCG00000015979	HOXD13 SFRP1	2	regulation of branching involved in prostate gland morphogenesis	3.89E-05	0.0264623
GO:0097485	6	ENSSSCG00000016230 ENSSSCG00000011872	SEMA5B EPHA4	2	neuron projection guidance	3.89E-05	0.0264623
GO:0061053	16	ENSSSCG00000015357 ENSSSCG00000016018 ENSSSCG00000017376	MEOX2 FRZB MEOX1	3	somite development	4.03E-05	0.0274364
GO:0006810	533	ENSSSCG00000009929 ENSSSCG00000011784 ENSSSCG00000001753 ENSSSCG00000022536 ENSSSCG00000004827 ENSSSCG00000003882 ENSSSCG00000014896 ENSSSCG00000028923 ENSSSCG00000028112 ENSSSCG00000017282 ENSSSCG00000013512 ENSSSCG00000011664 ENSSSCG00000011676 ENSSSCG00000006890 ENSSSCG00000013833 ENSSSCG00000027024 ENSSSCG00000000871 ENSSSCG00000009665	CHRNB4 SLC5A9 GABRA5 ABCA4 TRPV4 RBP1 PLIN4 SLC1A6 SCN4A SLC37A2 ASIC3 CLIC3 SCNN1B	18	transport	4.98E-05	0.0338585
GO:0042573	7	ENSSSCG00000025578 ENSSSCG00000011664	RBP1 ALDH1A2	2	retinoic acid metabolic process	6.75E-05	0.0458761
GO:0050891	7	ENSSSCG00000009929 ENSSSCG00000028923	TRPV4 SCNN1B	2	multicellular organismal water homeostasis	6.75E-05	0.0458761

Appendix 9: Cellular Component Gene Ontology Terms Enriched in Genes Up and Downregulated by Weaning at One Day Post-Weaning

Gene Ontologies Enriched in Upregulated genes							
GO ID	GO gene count	Gene IDs		Gene count	GO Name	p value	q value
GO:0071438	5	ENSSSCG00000015896 ENSSSCG00000012485	NOX1 FAP	2	invadopodium membrane	4.52E-06	0.00036173
GO:0005579	6	ENSSSCG00000016856 ENSSSCG00000016859	C7 C9	2	membrane attack complex	8.99E-06	0.00071934
GO:0005615	966	ENSSSCG00000008088 ENSSSCG00000009444 ENSSSCG00000004890 ENSSSCG00000016856 ENSSSCG00000020906 ENSSSCG00000015896 ENSSSCG00000022742 ENSSSCG00000015657 ENSSSCG00000004889 ENSSSCG00000008963 ENSSSCG00000013551 ENSSSCG00000002479 ENSSSCG00000016113 ENSSSCG00000020750 ENSSSCG00000006796 ENSSSCG00000004894 ENSSSCG00000008090 ENSSSCG00000015662	SERPINA11 SERPINA10 SERPINB2 SERPINB5 CHI3L2 IL1B2 AREG OLFM4 C3 PIGR FAP BMPR2 C9 TNFSF10 PRDX6	18	extracellular space	0.00016599	0.01327902
Gene Ontologies Enriched in Downregulated genes							

GO ID	GO gene count	GOI.gene_ids		Gene count	GO Name	p value	q value
		ENSSSCG00000014983 ENSSSCG00000026425 ENSSSCG00000015285 ENSSSCG00000009361 ENSSSCG00000025822 ENSSSCG00000023806 ENSSSCG00000012766 ENSSSCG00000000759 ENSSSCG00000006478 ENSSSCG00000012680	CTGF HAPLN2 POSTN GPC3 BGN MMP20 LRRN2 LRRN1		proteinaceous		
GO:0005578	167	ENSSSCG00000004192	SFRP1 ADAMTSL2	11	extracellular matrix	1.46E-06	0.00014308
		ENSSSCG00000000261 ENSSSCG00000025414 ENSSSCG00000016018 ENSSSCG00000010400 ENSSSCG00000020657 ENSSSCG00000014983 ENSSSCG00000010479 ENSSSCG00000026425 ENSSSCG00000008054 ENSSSCG00000013512 ENSSSCG00000012766 ENSSSCG00000000759 ENSSSCG00000030843 ENSSSCG00000001570 ENSSSCG00000000151 ENSSSCG00000011596 ENSSSCG00000003963 ENSSSCG00000006610 ENSSSCG00000023261 ENSSSCG00000015234	IGFBP6 PI16 CTGF S100A11 NTN3 RBP4 TRH BGN PLIN4 MMP20 KIRREL3 FRZB BCAM				
GO:0005576	670	ENSSSCG00000004192	GDF5 PYY ADAMTSL2 APLN	21	extracellular region	4.32E-05	0.00423247

GO:0005890	10	ENSSSCG00000014896 ENSSSCG00000011676	ATP1B2	2	sodium:potassium-exchanging ATPase complex	0.00022489	0.02203924
GO:0031012	251	ENSSSCG00000007358 ENSSSCG00000020657 ENSSSCG00000014983 ENSSSCG00000006474 ENSSSCG00000009361 ENSSSCG00000013762 ENSSSCG00000008991 ENSSSCG00000025822 ENSSSCG00000010728 ENSSSCG00000012766	NES EMLIN3 FRAS1 POSTN CPXM2 BGN PODNL1 MMP20 BCAM SFRP1	10	extracellular matrix	0.00036605	0.03587319

Appendix 10: Molecular Function Gene Ontology Terms Enriched in Genes Up and Downregulated by Weaning at One Day Post-Weaning

Gene Ontologies Enriched in upregulated genes							
GO ID	GO Gene count	Gene IDs	Gene Names	Gene Count	GO Name	p value	q value
GO:0016174	5	ENSSSCG00000004675 ENSSSCG00000004678	DUOX1 DUOX2	2	NAD(P)H oxidase activity	4.52E-06	0.00076
GO:0004601	16	ENSSSCG00000004675 ENSSSCG00000004678 ENSSSCG00000022742	DUOX1 DUOX2 PRDX6	3	peroxidase activity	5.87E-06	0.000987
GO:0005149	6	ENSSSCG00000008088 ENSSSCG00000008090	IL1B2 IL1A	2	interleukin-1 receptor binding	8.99E-06	0.001511
GO:0004675	13	ENSSSCG00000015873 ENSSSCG00000016113	ACVR1C BMPR2	2	transmembrane receptor protein serine/threonine kinase activity	0.000124	0.020758
GO:0004702	13	ENSSSCG00000015873 ENSSSCG00000016113	ACVR1C BMPR2	2	signal transducer, downstream of receptor, with serine/threonine kinase activity	0.000124	0.020758

GO:0004867	63	ENSSSCG00000004890 ENSSSCG00000004889 ENSSSCG00000002479 ENSSSCG00000004894	SERPINA11 SERPINA10 SERPINB2 SERPINB5	4	serine-type endopeptidase inhibitor activity	0.000128	0.0215
GO:0016209	16	ENSSSCG00000022742 ENSSSCG00000008214	FABP1 PRDX6	2	antioxidant activity	0.000238	0.039957
Gene ontologies Enriched in downregulated genes							
GO ID	GO Gene count	Gene IDs	Gene Names	Gene Count	GO Name	p value	q value
GO:0015280	6	ENSSSCG00000028923 ENSSSCG00000027024	ASIC3 SCNN1B	2	ligand-gated sodium channel activity	3.89E-05	0.009145
GO:0005272	20	ENSSSCG00000028923 ENSSSCG00000017282 ENSSSCG00000027024	SCNA2 ASIC3 SCNN1B	3	sodium channel activity	0.000103	0.024257
GO:0005230	39	ENSSSCG00000011784 ENSSSCG00000001753 ENSSSCG00000004827 ENSSSCG00000009665	CHRNB4 GABRA5 CHRNA2	4	extracellular ligand-gated ion channel activity	0.000126	0.02958
GO:0015464	9	ENSSSCG00000001753 ENSSSCG00000009665	CHRNB4 CHRNA2	2	acetylcholine receptor activity	0.000159	0.037343

Appendix 11: Biological Process Gene Ontology Terms Enriched in Genes Up and Downregulated by Weaning at Four Days Post-Weaning

Gene Ontologies Enriched in Upregulated genes							
GO ID	GO Gene Count	Gene IDs	Gene Names	Gene Count	GO Name	p value	q value
GO:0045765	21	ENSSSCG00000027130 ENSSSCG00000000293	ITGA5 TNFRSF12A	2	regulation of angiogenesis	2.49E-05	0.005086
GO:0030522	25	ENSSSCG00000005385 ENSSSCG00000000875	NR1H4 NR4A3	2	intracellular receptor signaling pathway	4.28E-05	0.008727
Gene Ontologies Enriched in Downregulated genes							
GO ID	GO Gene Count	Gene IDs	Gene Names	Gene Count	GO Name	p value	q value
GO:0042157	17	ENSSSCG00000009179 ENSSSCG00000015069	MTTP APOC3	2	lipoprotein metabolic process	2.23E-06	0.000223
GO:0006641	27	ENSSSCG00000009179 ENSSSCG00000015069	MTTP APOC3	2	triglyceride metabolic process	9.48E-06	0.000948
GO:0042632	43	ENSSSCG00000009179 ENSSSCG00000015069	MTTP APOC3	2	cholesterol homeostasis	3.94E-05	0.003936
GO:0006869	47	ENSSSCG00000009179 ENSSSCG00000015069	MTTP APOC3	2	lipid transport	5.15E-05	0.005151

Appendix 12: Cellular Component Gene Ontology Terms Enriched in Genes Up and Downregulated by Weaning at Four Days Post-Weaning

Gene Ontologies enriched in downregulated genes							
GO ID	GO Gene Count	Gene IDs	Gene Names	Gene Count	GO Name	p value	q value
GO:0045177	66	ENSSSCG00000015896 ENSSSCG00000009132	ENPEP FAP	2	apical part of cell	0.000143	0.004276

Appendix 13: Molecular Function Gene Ontology Terms Enriched in Genes Up and Downregulated by Weaning at Four Days Post-Weaning

Gene ontologies enriched in upregulated genes							
GO ID	GO Gene Count	Gene IDs	Gene Names	Gene Count	GO Name	p value	q value
GO:0004879	30	ENSSSCG00000005385 ENSSSCG00000000875	NR1H4 NR4A3	2	nuclear receptor activity	7.48E-05	0.005834
GO:0003707	49	ENSSSCG00000005385 ENSSSCG00000000875	NR1H4 NR4A3	2	steroid hormone receptor activity	0.000327	0.025524
Gene ontologies enriched in downregulated genes							
GO ID	GO Gene Count	Gene IDs	Gene Names	Gene Count	GO Name	p value	q value
GO:0030170	45	ENSSSCG00000013283 ENSSSCG00000004644	HDC ACCSL	2	pyridoxal phosphate binding	4.52E-05	0.002213
GO:0003824	363	ENSSSCG00000006001 ENSSSCG00000013283 ENSSSCG00000016720 ENSSSCG00000004644	HDC ENPP2 ACCSL PGAM2	4	catalytic activity	0.000211	0.010317

Appendix 14: Biological Process Gene Ontology Terms Enriched in Genes Differentially Expressed in Suckling Pigs by SCB Supplementation at 22 Days of Age

Gene ontologies enriched in upregulated genes							
GO ID	GO Gene Count	Gene IDs	Gene Names	Gene Count	GO Name	p value	q value
GO:0071222	73	ENSSSCG00000028758 ENSSSCG00000009100 ENSSSCG00000008953 ENSSSCG00000009469	CXCL8 TNIP3 ACOD1 LBP	4	cellular response to lipopolysaccharide	1.50E-07	2.54E-05
GO:0090023	21	ENSSSCG00000028758 ENSSSCG00000008953	CXCL8 LBP	2	positive regulation of neutrophil chemotaxis	6.08E-06	0.001028134
GO:0006302	52	ENSSSCG00000006127 ENSSSCG00000011876	NBN DTX3L	2	double-strand break repair	9.75E-05	0.016478403
GO:0045087	162	ENSSSCG00000016856 ENSSSCG00000001234 ENSSSCG00000028758	TRIM10 C9 LBP	3	innate immune response	0.00016605	0.028062237
Gene ontologies enriched in downregulated genes							
GO ID	GO Gene Count	Gene IDs	Gene Names	Gene Count	GO Name	p value	q value

GO:0050853	29	ENSSSCG00000014149 ENSSSCG00000017283 ENSSSCG00000027568 ENSSSCG00000007807	CD19 MEF2C CD79B BLK	4	B cell receptor signaling pathway	6.25E-07	0.000306468
GO:0030595	8	ENSSSCG00000027849 ENSSSCG00000015098	CXCR5 CNR2	2	leukocyte chemotaxis	1.03E-05	0.005063972
GO:0071688	8	ENSSSCG00000015747 ENSSSCG00000013236	MYBPC3	2	striated muscle myosin thick filament assembly	1.03E-05	0.005063972
GO:1902166	8	ENSSSCG00000004699 ENSSSCG00000013297	ELL3 CD44	2	negative regulation of intrinsic apoptotic signaling pathway in response to DNA damage by p53 class mediator	1.03E-05	0.005063972
GO:0050710	9	ENSSSCG00000024644 ENSSSCG00000001131	CIDEA	2	negative regulation of cytokine secretion	1.54E-05	0.007564007
GO:0090150	9	ENSSSCG00000028911 ENSSSCG00000005352	FRMPD1 COLQ	2	establishment of protein localization to membrane	1.54E-05	0.007564007
GO:0010043	10	ENSSSCG00000026386 ENSSSCG00000009827	HVCN1 SLC30A2	2	response to zinc ion	2.20E-05	0.010760284
GO:0071277	33	ENSSSCG00000014149 ENSSSCG00000017923 ENSSSCG00000013023	RASGRP2 MEF2C ALOX15	3	cellular response to calcium ion	3.81E-05	0.018653196
GO:0048535	14	ENSSSCG00000001405 ENSSSCG00000015098	LTB CXCR5	2	lymph node development	6.55E-05	0.032094269

GO:0045663	15	ENSSSCG00000014149 ENSSSCG00000001097	RIPOR2 MEF2C	2	positive regulation of myoblast differentiation	8.15E-05	0.03994933

Appendix 15: Cellular Component Gene Ontology Terms Enriched in Genes Differentially Expressed in Suckling Pigs by SCB Supplementation at 22 Days of Age

Gene ontologies enriched in upregulated genes							
GO ID	GO Gene Count	Gene IDs	Gene Names	Gene Count	GO Name	p value	q value
GO:0072562	73	ENSSSCG00000016856 ENSSSCG00000015662	C4BPA C9	2	blood microparticle	0.00026779	0.01017589
GO:0005615	966	ENSSSCG00000004890 ENSSSCG00000016856 ENSSSCG00000028758 ENSSSCG00000015662 ENSSSCG00000008953 ENSSSCG00000009138	SERPINB2 CXCL8 CFI C4BPA C9 LBP	6	extracellular space	0.00105985	0.04027423
Gene ontologies enriched in downregulated genes							
GO ID	GO Gene Count	Gene IDs	Gene Names	Gene Count	GO Name	p value	q value

GO:0016021	3806	ENSSSCG00000006491 ENSSSCG00000026360 ENSSSCG00000001459 ENSSSCG00000027849 ENSSSCG00000039007 ENSSSCG00000000563 ENSSSCG00000021812 ENSSSCG00000020694 ENSSSCG00000020657 ENSSSCG00000001131 ENSSSCG00000007695 ENSSSCG00000004458 ENSSSCG00000017283 ENSSSCG00000026386 ENSSSCG00000009564 ENSSSCG00000003382 ENSSSCG00000029395 ENSSSCG00000006458 ENSSSCG00000009429 ENSSSCG00000016784 ENSSSCG00000017801 ENSSSCG00000013777 ENSSSCG00000028923 ENSSSCG00000017282 ENSSSCG00000013474 ENSSSCG00000027877 ENSSSCG00000009827 ENSSSCG00000030305 ENSSSCG00000013297 ENSSSCG00000005584 ENSSSCG00000020695 ENSSSCG00000015294 ENSSSCG00000011878 ENSSSCG00000028674 ENSSSCG00000001405 ENSSSCG00000005943 ENSSSCG00000025644 ENSSSCG00000027024 ENSSSCG00000006456 ENSSSCG00000022906 ENSSSCG00000007807 ENSSSCG00000007861 ENSSSCG00000015098 ENSSSCG00000015656	LRMP LTB HLA-DOB TAS1R1 TPBG CRB2 ST3GAL1 FCRL1 FCRL4 CD19 GP2 TNFSF11 TMEM255B HVCN1 CASR CD44 S1PR4 CLEC17A CXCR5 FCMR ANKH SCN4A CD79B TUSC5 BCAM DSG1 MS4A1 CLGN SLC30A2 ASIC3 CNR2 TLR10 CR2 SCNN1B TMEM25 SLC15A2 CLEC4G	44	integral component of membrane	2.27E-07	1.90E-05
GO:0005859	8	ENSSSCG00000015747 ENSSSCG00000013236	MYBPC3	2	muscle myosin complex	1.03E-05	0.00086811

GO:0016020	4910	ENSSSCG00000026360 ENSSSCG00000001459 ENSSSCG00000027849 ENSSSCG00000039007 ENSSSCG00000000563 ENSSSCG00000021812 ENSSSCG00000020694 ENSSSCG00000020657 ENSSSCG00000017923 ENSSSCG00000001131 ENSSSCG00000007695 ENSSSCG00000004458 ENSSSCG00000017283 ENSSSCG00000026386 ENSSSCG00000009564 ENSSSCG00000003382 ENSSSCG00000029395 ENSSSCG00000006458 ENSSSCG00000009429 ENSSSCG00000016784 ENSSSCG00000017801 ENSSSCG00000013777 ENSSSCG00000028923 ENSSSCG00000017282 ENSSSCG00000013474 ENSSSCG00000027877 ENSSSCG00000009827 ENSSSCG00000009668 ENSSSCG00000030305 ENSSSCG00000013297 ENSSSCG00000005584 ENSSSCG00000020695 ENSSSCG00000015294 ENSSSCG00000011878 ENSSSCG00000028674 ENSSSCG00000001834 ENSSSCG00000001405 ENSSSCG00000005943 ENSSSCG00000006289 ENSSSCG00000025644 ENSSSCG00000027024 ENSSSCG00000006456 ENSSSCG00000022906 ENSSSCG00000007807 ENSSSCG00000007861 ENSSSCG00000015098 ENSSSCG00000015656	LRMP LTB HLA-DOB MFGE8 TAS1R1 TPBG CRB2 ST3GAL1 F5 FCRL1 FCRL4 CD19 GP2 TNFSF11 TMEM255B CLU HVCN1 CASR CD44 S1PR4 CLEC17A CXCR5 FCMR ANKH SCN4A CD79B TUSC5 ALOX15 BCAM DSG1 MS4A1 CLGN SLC30A2 ASIC3 CNR2 TLR10 CR2 SCNN1B TMEM25 SLC15A2 CLEC4G	47	membrane	2.22E-05	0.00186821
GO:0009897	155	ENSSSCG00000021812 ENSSSCG00000017283 ENSSSCG00000028923 ENSSSCG00000001834 ENSSSCG00000007807 ENSSSCG00000015098	MFGE8 CD19 CXCR5 CD79B MS4A1	6	external side of plasma membrane	3.25E-05	0.00273316

			SCNN1B				
GO:0031430	15	ENSSSCG00000015747 ENSSSCG00000013236	MYBPC3	2	M band	8.15E-05	0.00684846

Appendix 16: Molecular Function Gene Ontology Terms Enriched in Genes Differentially Expressed in Suckling Pigs by SCB Supplementation at 22 Days of Age

Gene ontologies enriched in upregulated genes							
GO ID	GO Gene Count	Gene IDs	Gene Names	Gene Count	GO Name	p value	q value
GO:0003924	195	ENSSSCG00000006923 ENSSSCG00000030801 ENSSSCG00000006919	GBP2	3	GTPase activity	0.00033724	0.01989744
Gene ontologies enriched in downregulated genes							
GO ID	GO Gene Count	Gene IDs	Gene Names	Gene Count	GO Name	p value	q value
GO:0015280	6	ENSSSCG00000028923 ENSSSCG00000027024	ASIC3 SCNN1B	2	ligand-gated sodium channel activity	3.72E-06	0.00063277
GO:0005272	20	ENSSSCG00000028923 ENSSSCG00000017282 ENSSSCG00000027024	SCN4A ASIC3 SCNN1B	3	sodium channel activity	4.78E-06	0.00081178
GO:0097493	9	ENSSSCG00000015747 ENSSSCG00000013236	MYBPC3	2	structural molecule activity conferring elasticity	1.54E-05	0.00262425
GO:0051371	11	ENSSSCG00000015747 ENSSSCG00000013236	MYBPC3	2	muscle alpha-actinin binding	3.01E-05	0.00511151
GO:0023026	12	ENSSSCG00000001459 ENSSSCG00000021812	HLA-DOB MS4A1	2	MHC class II protein complex binding	3.99E-05	0.0067867
GO:0071837	12	ENSSSCG00000014149 ENSSSCG00000017376	MEF2C MEOX1	2	HMG box domain binding	3.99E-05	0.0067867

GO:0008307	20	ENSSSCG00000015747 ENSSSCG00000013236	MYBPC3	2	structural constituent of muscle	0.00020002	0.0340034

Appendix 17: Biological Process Gene Ontology Terms Enriched in Genes Differentially Expressed in Weaned Pigs by SCB Supplementation at 25 Days of Age

Gene ontologies enriched in upregulated genes							
GO ID	GO Gene Count	Gene IDs	Gene Names	Gene Count	GO Name	p value	q value
GO:0006954	147	ENSSSCG00000014369 ENSSSCG00000002821 ENSSSCG00000017466 ENSSSCG00000015476 ENSSSCG00000015652 ENSSSCG00000010966 ENSSSCG00000008957	CCL22 AMCF-II CCL19 CD14 CHI3L1 IL10 CCR7	7	inflammatory response	7.81E-11	1.74E-08
GO:0006955	192	ENSSSCG00000002821 ENSSSCG00000017466 ENSSSCG00000009542 ENSSSCG00000015652 ENSSSCG00000010966 ENSSSCG00000001405 ENSSSCG00000008957	LTB CCL22 AMCF-II TNFSF13B CCL19 IL10 CCR7	7	immune response	6.60E-10	1.47E-07
GO:0002408	3	ENSSSCG00000017466 ENSSSCG00000010966	CCL19 CCR7	2	myeloid dendritic cell chemotaxis	4.19E-09	9.34E-07

GO:0070098	46	ENSSSCG00000002821 ENSSSCG00000017466 ENSSSCG00000010966 ENSSSCG00000008957	CCL22 AMCF-II CCL19 CCR7	4	chemokine-mediated signaling pathway	1.17E-08	2.61E-06
GO:0090023	21	ENSSSCG00000017466 ENSSSCG00000010966 ENSSSCG00000008957	AMCF-II CCL19 CCR7	3	positive regulation of neutrophil chemotaxis	3.67E-08	8.19E-06
GO:0006935	64	ENSSSCG00000002821 ENSSSCG00000017466 ENSSSCG00000010966 ENSSSCG00000008957	CCL22 AMCF-II CCL19 CCR7	4	chemotaxis	6.39E-08	1.42E-05
GO:0051045	7	ENSSSCG00000012277 ENSSSCG00000015652	TIMP1 IL10	2	negative regulation of membrane protein ectodomain proteolysis	1.46E-07	3.25E-05
GO:0010469	256	ENSSSCG00000012277 ENSSSCG00000002821 ENSSSCG00000025698 ENSSSCG00000010966 ENSSSCG00000001405 ENSSSCG00000008957	LTB CCL22 AMCF-II CCL19 TIMP1 SERPINE1	6	regulation of receptor activity	1.62E-07	3.61E-05
GO:0002237	10	ENSSSCG00000014369 ENSSSCG00000015652	CD14 IL10	2	response to molecule of bacterial origin	4.99E-07	0.00011119
GO:0042832	12	ENSSSCG00000015652 ENSSSCG00000004195	ARG1 IL10	2	defense response to protozoan	9.12E-07	0.0002034
GO:0048247	15	ENSSSCG00000002821 ENSSSCG00000010966	CCL22 CCL19	2	lymphocyte chemotaxis	1.88E-06	0.00041925
GO:0002548	20	ENSSSCG00000002821 ENSSSCG00000010966	CCL22 CCL19	2	monocyte chemotaxis	4.68E-06	0.00104456

GO:0071222	73	ENSSSCG00000014369 ENSSSCG00000015652 ENSSSCG00000025698	CD14 IL10 SERPINE1	3	cellular response to lipopolysaccharide	6.29E-06	0.00140239
GO:2000352	22	ENSSSCG00000015652 ENSSSCG00000025698	IL10 SERPINE1	2	negative regulation of endothelial cell apoptotic process	6.31E-06	0.00140791
GO:0010951	80	ENSSSCG00000012277 ENSSSCG00000011451 ENSSSCG00000025698	ITIH3 TIMP1 SERPINE1	3	negative regulation of endopeptidase activity	9.06E-06	0.00202148
GO:0071346	27	ENSSSCG00000002821 ENSSSCG00000010966	CCL22 CCL19	2	cellular response to interferon-gamma	1.19E-05	0.00265919
GO:0030593	32	ENSSSCG00000002821 ENSSSCG00000010966	CCL22 CCL19	2	neutrophil chemotaxis	2.01E-05	0.00448408
GO:0071347	38	ENSSSCG00000002821 ENSSSCG00000010966	CCL22 CCL19	2	cellular response to interleukin-1	3.40E-05	0.00757549
GO:0070374	125	ENSSSCG00000002821 ENSSSCG00000015476 ENSSSCG00000010966	CCL22 CCL19 CHI3L1	3	positive regulation of ERK1 and ERK2 cascade	5.28E-05	0.01176341
GO:0060326	52	ENSSSCG00000002821 ENSSSCG00000008957	CCL22 AMCF-II	2	cell chemotaxis	8.76E-05	0.01953712
GO:0046330	53	ENSSSCG00000012485 ENSSSCG00000010966	CCL19 NOX1	2	positive regulation of JNK cascade	9.28E-05	0.02068619
GO:0050728	61	ENSSSCG00000015652 ENSSSCG00000006634	TNFAIP8L2 IL10	2	negative regulation of inflammatory response	0.00014124	0.03149753
GO:0051897	61	ENSSSCG00000015476 ENSSSCG00000010966	CCL19 CHI3L1	2	positive regulation of protein kinase B signaling	0.00014124	0.03149753
GO:0071356	66	ENSSSCG00000002821 ENSSSCG00000010966	CCL22 CCL19	2	cellular response to tumor necrosis	0.00017859	0.03982459

					factor		
Gene ontologies enriched in downregulated genes							
GO ID	GO Gene Count	Gene IDs	Gene Names	Gene Count	GO Name	p value	q value
GO:0006730	22	ENSSSCG00000004565 ENSSSCG00000016568	CA12 AHCYL2	2	one-carbon metabolic process	7.04E-06	0.00058399
GO:0007010	84	ENSSSCG00000002495 ENSSSCG00000029077 ENSSSCG00000001068	CAP2 SYNE3 TUBAL3	3	cytoskeleton organization	1.27E-05	0.00105585

Appendix 18: Cellular Component Gene Ontology Terms Enriched in Genes Differentially Expressed in Weaned Pigs by SCB Supplementation at 25 Days of Age

Gene ontologies enriched in upregulated genes							
GO ID	GO Gene Count	Gene IDs	Gene Names	Gene Count	GO Name	p value	q value
GO:0005615	966	ENSSSCG00000014369 ENSSSCG00000012277 ENSSSCG00000002821 ENSSSCG00000015476 ENSSSCG00000015652 ENSSSCG00000025698 ENSSSCG00000010966 ENSSSCG00000001405 ENSSSCG00000004195 ENSSSCG00000008957	LBT CCL22 ARG1 AMCF- 11 CCL19 TIMP1 CD14 CHI3L1 IL10 SERPINE1	10	extracellular space	1.93E-07	6.94E-06
GO:0005576	670	ENSSSCG00000012277 ENSSSCG00000002821 ENSSSCG00000015652 ENSSSCG00000000482 ENSSSCG00000025698 ENSSSCG00000010966 ENSSSCG00000011683 ENSSSCG00000008957	IL22 CCL22 AMCF-II CCL19 PCOLCE2 TIMP1 IL10 SERPINE1	8	extracellular region	8.69E-07	3.13E-05
GO:0071944	54	ENSSSCG00000016841 ENSSSCG00000013556	ADGRE1 SLC1A3	2	cell periphery	9.81E-05	0.003532

GO:0009897	155	ENSSSCG00000014369 ENSSSCG00000017466 ENSSSCG00000013556	ADGRE1 CD14 CCR7	3	external side of plasma membrane	0.000122	0.004379

Appendix 19: Molecular Function Gene Ontology Terms Enriched in Genes Differentially Expressed in Weaned Pigs by SCB Supplementation at 25 Days of Age

Gene ontologies enriched in upregulated genes							
GO ID	GO Gene Count	Gene IDs	Gene Names	Gene Count	GO Name	p value	q value
GO:0005125	141	ENSSSCG00000012277 ENSSSCG00000002821 ENSSSCG00000015652 ENSSSCG00000010966 ENSSSCG00000001405 ENSSSCG00000008957	LBT CCL22 AMCF-II CCL19 TIMP1 IL10	6	cytokine activity	2.64E-09	1.53E-07
GO:0008009	31	ENSSSCG00000002821 ENSSSCG00000010966 ENSSSCG00000008957	CCL22 AMCF-II CCL19	3	chemokine activity	1.91E-07	1.11E-05
GO:0048020	12	ENSSSCG00000002821 ENSSSCG00000010966	CCL22 CCL19	2	CCR chemokine receptor binding	9.12E-07	5.29E-05
GO:0005164	23	ENSSSCG00000009542 ENSSSCG00000001405	LTB TNFSF13B	2	tumor necrosis factor receptor binding	7.25E-06	0.00042064
GO:0004867	63	ENSSSCG00000011451 ENSSSCG00000025698	ITIH3 SERPINE1	2	serine-type endopeptidase inhibitor activity	0.0001555	0.00901897
Gene ontologies enriched in downregulated genes							

GO ID	GO Gene Count	Gene IDs	Gene Names	Gene Count	GO Name	p value	q value
GO:0005261	20	ENSSSCG00000023151 ENSSSCG00000017862	TRPV3 GRIN2C	2	cation channel activity	5.22E-06	0.00031846
GO:0044325	71	ENSSSCG00000010212 ENSSSCG00000003368	RNF207	2	ion channel binding	0.00024666	0.01504598

Appendix 20: Biological Process Gene Ontology Enrichment of Genes Exclusive to Suckling Control vs Weaned SCB Comparison when Compared to Suckling Control vs Weaned Control (1-day post weaning)

Enriched amongst upregulated genes							
GO ID	GO Gene Count	Gene IDs	Gene Names	Gene Count	GO Name	p value	q value
GO:2000609	2	ENSSSCG00000004677 ENSSSCG00000004676	DUOXA2 DUOXA1	2	regulation of thyroid hormone generation	0	0
GO:0042743	4	ENSSSCG00000004677 ENSSSCG00000004676	DUOXA2 DUOXA1	2	hydrogen peroxide metabolic process	4.67E-08	7.60E-06
GO:0000050	6	ENSSSCG00000005701 ENSSSCG00000002294	ARG2 ASS1	2	urea cycle	2.33E-07	3.79E-05
GO:0070371	21	ENSSSCG00000024305 ENSSSCG00000027127	MT3 MAP2K2	2	ERK1 and ERK2 cascade	1.51E-05	0.00246
GO:0035690	38	ENSSSCG00000024305 ENSSSCG00000030300	MT3 MT2A	2	cellular response to drug	9.31E-05	0.015183
GO:0050727	47	ENSSSCG00000004677 ENSSSCG00000004676	DUOXA2 DUOXA1	2	regulation of inflammatory response	0.000176	0.028764
Enriched amongst downregulated genes							

GO ID	GO Gene Count	Gene IDs	Gene Names	Gene Count	GO Name	p value	q value
GO:0050853	29	ENSSSCG00000014149 ENSSSCG00000017283 ENSSSCG00000027568 ENSSSCG00000010077 ENSSSCG00000007807	CD19 MEF2C CD79B BLK	5	B cell receptor signalling pathway	6.03E-08	4.52E-05
GO:0006790	11	ENSSSCG00000003721 ENSSSCG00000022031 ENSSSCG00000013273	CHST1 CHST2 CHST9	3	sulfur compound metabolic process	9.08E-07	0.00068
GO:1902533	5	ENSSSCG00000009429 ENSSSCG00000024954	TNFSF11 FGF11	2	positive regulation of intracellular signal transduction	3.92E-06	0.002937
GO:0051966	18	ENSSSCG00000014149 ENSSSCG00000022865 ENSSSCG00000016233	MEF2C SERPINE2 GRM	3	regulation of synaptic transmission, glutamatergic	8.09E-06	0.00606
GO:0048643	7	ENSSSCG00000014149 ENSSSCG00000016416	MEF2C SHH	2	positive regulation of skeletal muscle tissue development	1.36E-05	0.010169
GO:0014067	8	ENSSSCG00000001131 ENSSSCG00000016233	SERPINE2	2	negative regulation of phosphatidylinositol 3-kinase signalling	2.16E-05	0.016183
GO:0030595	8	ENSSSCG00000027849 ENSSSCG00000015098	CXCR5 CNR2	2	leukocyte chemotaxis	2.16E-05	0.016183
GO:0045060	8	ENSSSCG00000025294 ENSSSCG00000016416	SHH AIRE	2	negative thymic T cell selection	2.16E-05	0.016183
GO:0071688	8	ENSSSCG00000015747 ENSSSCG00000013236	MYBPC	2	striated muscle myosin thick filament assembly	2.16E-05	0.016183

GO:0042177	24	ENSSSCG00000023151 ENSSSCG00000016416 ENSSSCG00000016233	SERPINE2 SHH GRIN2C	3	negative regulation of protein catabolic process	2.71E-05	0.020332
GO:0050710	9	ENSSSCG00000001131 ENSSSCG00000009434	RGCC	2	negative regulation of cytokine secretion	3.22E-05	0.024143
GO:0010043	10	ENSSSCG00000026386 ENSSSCG00000009827	HVCN1 SCL30A2	2	response to zinc ion	4.58E-05	0.034304
GO:0014902	11	ENSSSCG00000014149 ENSSSCG00000016416	MEF2C SHH	2	myotube differentiation	6.26E-05	0.046912

Appendix 21: Biological Process Gene Ontology Enrichment of Genes Exclusive to Suckling Control vs Weaned SCB Comparison when Compared to Suckling Control vs Weaned Control (4 days post weaning)

Biological Processes Enriched Amongst Upregulated Genes							
GO ID	GO Gene Count	Gene IDs	Gene Names	Gene Count	GO Name	p value	q value
GO:0018149	18	ENSSSCG00000001993 ENSSSCG00000024310	TGM1 F13A1	2	peptide cross-linking	3.00E-06	0.000336
GO:0060291	29	ENSSSCG00000016233 ENSSSCG00000017343	SERPINE1 GFAP	2	long-term synaptic potentiation	1.33E-05	0.001488
GO:0007596	33	ENSSSCG00000024310 ENSSSCG00000016233	SERPINE1 F13A1	2	blood coagulation	1.98E-05	0.002212
Biological Processes Enriched Amongst Downregulated Genes							
GO ID	GO Gene Count	Gene IDs	Gene Names	Gene Count	GO Name	p value	q value

GO:0021615	4	ENSSSCG00000015985 ENSSSCG00000017534	HOXD3 HOXB3	2	glossopharyngeal nerve morphogenesis	1.57E-07	3.64E-05
GO:0048704	46	ENSSSCG00000015985 ENSSSCG00000017534 ENSSSCG00000015981 ENSSSCG00000015982	HOXD10 HOXD9 HOXD3 HOXB3	4	embryonic skeletal system morphogenesis	5.14E-07	0.000119
GO:0009952	88	ENSSSCG00000015985 ENSSSCG00000021204 ENSSSCG00000017534 ENSSSCG00000015981 ENSSSCG00000015982	HOXD10 HOXD9 HOXD3 HOXB3 HOXA10	5	anterior/posterior pattern specification	5.76E-07	0.000133
GO:0009954	21	ENSSSCG00000021204 ENSSSCG00000015981 ENSSSCG00000015982	HOXD10 HOXD9 HOXA10	3	proximal/distal pattern formation	7.42E-07	0.000171
GO:0048935	8	ENSSSCG00000015981 ENSSSCG00000015982	HOXD10 HOXD9	2	peripheral nervous system neuron development	2.18E-06	0.000504

GO:0007338	31	ENSSSCG00000021204 ENSSSCG00000015981 ENSSSCG00000015982	HOXD10 HOXD9 HOXA10	3	single fertilization	3.80E-06	0.000878
GO:0035136	10	ENSSSCG00000015981 ENSSSCG00000015982	HOXD10 HOXD9	2	forelimb morphogenesis	4.65E-06	0.001075
GO:0035137	10	ENSSSCG00000015981 ENSSSCG00000015982	HOXD10 HOXD9	2	hindlimb morphogenesis	4.65E-06	0.001075
GO:0030878	21	ENSSSCG00000015985 ENSSSCG00000017534	HOXD3 HOXB3	2	thyroid gland development	5.02E-05	0.011593
GO:0007193	23	ENSSSCG00000001242 ENSSSCG00000016599	GABBR1 GPR37	2	adenylate cyclase-inhibiting G-protein coupled receptor signaling pathway	6.65E-05	0.015361
GO:0007160	65	ENSSSCG00000015985 ENSSSCG00000020963 ENSSSCG00000016816	HOXD3 ADAMTS12 EPDR1	3	cell-matrix adhesion	7.50E-05	0.017317
GO:0061098	24	ENSSSCG00000017296 ENSSSCG00000010184	AGT ACE	2	positive regulation of protein tyrosine kinase activity	7.58E-05	0.017512

GO:0008217	31	ENSSSCG00000017296 ENSSSCG00000010184	AGT ACE	2	regulation of blood pressure	0.000165	0.038228
GO:0010951	80	ENSSSCG00000002341 ENSSSCG00000011129 ENSSSCG00000010184	PAPLN AGT ITIH5	3	negative regulation of endopeptidase activity	0.000168	0.038921